Using Ion-pairs to Modify Salbutamol Delivery to the Lungs

Dutton, Bridie Leigh

Awarding institution:
King's College London

Using Ion-pairs to Modify Salbutamol Delivery to the Lungs

Bridie Dutton

MSc.

A thesis submitted for the degree of Doctor of Philosophy

Institute of Pharmaceutical Science

King's College London

Abstract

This thesis investigates whether the formation of ion-pairs can influence the delivery of salbutamol to the airways of the lung. Presenting a drug with an excess of oppositely charged ion can force it to form an ion-pair complex, and this complex can modify a drug's dissolution or transport across epithelia without chemically altering the drug. The binding of salbutamol with pharmaceutically relevant counter ions was studied. It was found that the larger more hydrophobic counter ions bound more tightly to the drug. Only 2 of the investigated counter ions had a significant effect on the $LogD_{7.4}$ of salbutamol. Phytic acid was investigated as a novel counter ion. Generation of phytic acid derivatives was attempted via chemical synthesis however this method did not yield a pure sample. The binding of phytic acid was studied and was found to be stronger than the other investigated counter ions, although no change in the $logD_{7.4}$ of salbutamol was observed. Salbutamol ion-pair dry powders with particle size < 5 μm were generated via spray drying. Impactor testing found that the powders were in the respirable range. Stability testing after 4 weeks found that the powders containing both PVP and l-leucine were the most stable after this time. The biocompatibility of the counter ions with Calu-3 human bronchial epithelial cells was assessed and all counter ions were shown to be well tolerated. The effect of the ion-pairs on the transport of salbutamol across a monolayer of Calu-3 cells found a significant difference in the transport of the sulfate, gluconate and phytate ion-pairs when compared with salbutamol base. There was no significant difference in the dissolution of the phytate or octanoate powders when compared with the base. An in vivo bronchoprotection study of salbutamol base and phytate was performed. The work in this thesis suggests that an ion-pairing strategy is suitable for use to prolong drug action in the lung.

Research Communications

Conference Abstracts

Dutton, B.L., Woods, A., Sadler, R., Forbes, B., Jones, S. A. (2016) Ion-pairs: A Novel Formulation Strategy to Alter Drug Disposition in the Lungs. *Journal of Aerosol Medicine and Pulmonary Drug Delivery*, *29*(3), A66. Poster presentation, DDL26.

Dutton, B.L., Woods, A., Sadler, R., Fa, N., Forbes, B., Jones, S. A. (2017) Development of an Inhaled Ion-paired Salbutamol Formulation. *Journal of Aerosol Medicine and Pulmonary Drug Delivery*, *30*(4), A69. Poster presentation, DDL27.

Dutton, B.L., Woods, A., Sadler, R., Prime, D., Forbes, B., Jones, S. A. (2017) The Formulation of Respirable Powders Containing Salbutamol Ion-pairs. *Journal of Aerosol Medicine and Pulmonary Drug Delivery*, *30*(3), A118. Poster presentation, 21st ISAM Congress.

Dutton, B.L., Woods, A., Sadler, R., Prime, D., Forbes, B., Jones, S. A. (2017) The Effect of Ion-pairing on Salbutamol Biopharmaceutics. *Journal of Aerosol Medicine and Pulmonary Drug Delivery*, *30*(3), A119. Poster presentation, 21st ISAM Congress.

Acknowledgements

Firstly I would like to express my sincere gratitude to my supervisors for their continued guidance and support throughout this project. To Dr. Stuart Jones, his endless help and patience allowed me to grow as a person and scientist during my time at King's. To Prof Ben Forbes for all his wisdom, advice and encouragement. I would also like to thank Dr. Arcadia Woods, for all of her assistance during Dr. Jones' year away.

My thanks also go to GlaxoSmithKline for funding the project and Dr. Robyn Sadler, David Prime and the inhaled delivery science team at Ware for sharing their industry expertise and welcoming me during my time there. I would also like to thank the MRC for funding the project.

I would like to acknowledge Dr. Sandra Rudman for her help and unbelievable patience with the *in vivo* experiments and other researchers at IPS for always being there to offer help and guidance, especially Varsha Kanabar, Agostino Cilibrizzi, Faiza Benaouda and Ana Georgian. I would also like to express my gratitude to the technical staff for their assistance in the project, especially Steve Ingham, Dan Asker, Richard Harper, David Stanton and Helena Wong.

My sincere thanks go to my colleagues at IPS, who have become great friends and have made the last 4 years so much more enjoyable (Arcadia, Jo, Jesmine, Thais, Laura, Dona, Simon, Rob, Magda, Rich and everyone else on the 5th floor).

Finally, I would like to thank my family for their endless support, encouragement and love. I would like especially thank Joe Sullivan for all of his patience, his unwavering faith in me and for always knowing how to make me laugh. This would have been impossible without you.

Contents

List of Figures

List of Tables

List of equations

List of abbreviations

4-DMAP	4-Dimethylaminopyridine
ANOVA	Analysis of variance
CMC	Critical micelle concentration
COPD	Chronic obstructive pulmonary disease
DCM	Dichloromethane
DPPC	Dipalmitoylphosphatidylcholine
DMF	Dimethylformamide
DMSO	Dimethyl sulfoxide
DPI	Dry powder inhaler
DSC	Differential scanning calorimetry
ED	Emitted dose
EDTA	Ethylenediaminetetraacetic acid
FBS	Fetal bovine serum
FDA	US Food and Drug Administration
FPF	Fine particle fraction
FTIR	Fourier transformed infrared spectroscopy

GSD	Geometric standard deviation
HBSS	Hank's balanced salt solution
HPLC	High performance liquid chromatography
IC_{50}	Half maximal inhibitory concentration
IV	Intravenous
LPP	Large porous particles
MDI	Metered dose inhaler
MMAD	Mass median aerodynamic diameter
MTT	3-(4,5-Dimethylthiazol-2-yl)-2,5-diphenyltetrazolium bromide
MW	Molecular weight
NGI	Next generation impactor
NMR	Nuclear magnetic resonance
OCT	Organic cation transporter
PBS	Phosphate buffered saline
PCS	Photon correlation spectroscopy
PEG	Polyethylene glycol
PLGA	Poly(lactic-co-glycolic acid)

PSA	Polar surface area
PSD	Particle size distribution
p-TSA	p-Toluenesulfonic acid
PVP	Polyvinylpyrrolidone
PXRD	Powder x-ray diffraction
RL	Lung resistance
RT	Room temperature
SD	Standard deviation
SDS	Sodium dodecyl sulfate
SEM	Scanning electron microscopy
TEA	Tetraethylammonium
TER	Transepithelial electrical resistance
TFA	Trifluoroacetic acid
TLC	Thin layer chromatography
USP	US pharmacopoeia
UV	Ultraviolet spectroscopy
VMD	Volume mean diameter

Chapter 1

Introduction

1.1 Background

The pulmonary system is an attractive route of administration for both locally and systemically acting agents for several reasons. The lungs have an incredibly large surface area, up to 100 m^2 in the average human adult, and because the primary function of the lungs is gas exchange, the absorptive barrier a systemically acting drug would face in the deep lung is extremely thin in comparison with other routes of administration: the epithelium of the alveoli is only around 0.2 μm in thickness (Patton, 1996, Patton et al., 2004). Furthermore, delivering systemic drugs *via* the lung has the benefit of bypassing the hepatic first pass effect (Labiris and Dolovich, 2003a). For drugs that act in the lung, delivery directly to the site of action allows for a smaller dose to be given to achieve the same therapeutic effect as if the drug was dosed systemically which minimizes side-effects (Pilcer and Amighi, 2010b). Finally, both locally and systemically acting drugs benefit from a rapid onset of action when delivered via the lungs (Patton and Byron, 2007).

However, formulating an effective inhaled medicine also poses several problems. The lungs are well adapted to prevent unwanted and potentially harmful airborne particles from entering the body. The structure of the lungs encourages impaction of particles high in the airways where the barriers to drug absorption are more extreme and the lung contains many effective clearance mechanisms (Chow et al., 2007). Even the rapid absorption of medicines in to the blood can be thought of as a clearance mechanism (Patton and Byron, 2007). The result of this is that many inhaled drugs are only therapeutically effective for a very short amount of time, meaning that frequent dosing is required (Zeng et al., 1995). An ideal inhaled formulation should successfully navigate the anatomy of the lung and avoid the rapid clearance mechanisms to provide an extended period of action of the therapeutic

agent at an appropriate concentration, thus reducing the frequency of doses, minimizing fluctuations in drug concentration and increasing patient compliance (Beck-Broichsitter et al., 2012). To achieve this, an effective strategy to prolong drug action in the lungs is needed.

Extending the therapeutic action of a drug can be achieved by controlling the delivery in a number of ways including: decreasing the rate of dissolution; decreasing the absorption rate in to tissues; or increasing tissue retention time. Each of these changes would effectively create a drug reservoir to be drawn upon for an extended period of time. A number of strategies have been employed in an attempt to prolong drug action in the lungs. These include the use of liposomes, nanoparticles and prodrugs (Elhissi, 2017, Vaughn et al., 2006, Zeng et al., 1995). However, all of these methods face problems of their own, including poor stability and toxicity (De Jong and Borm, 2008, Loira-Pastoriza et al., 2014b) and therefore the need for an inhaled formulation with prolonged drug action has not yet been met. One strategy that has been used to control the delivery of drugs via other routes of administration is the use of ion-pairs (ElShaer et al., 2014, Megwa et al., 2000), though this method has not yet been fully explored for inhaled medicines (Patel et al., 2016). This thesis aims to explore the feasibility of using an ion-pair formulation to prolong drug action in the lungs. However, first there is a need to understand the processes which all inhaled medicines undergo upon administration.

1.2 Drug delivery to the lungs

1.2.1 Pulmonary physiology

The first barrier any inhaled formulation faces is the structure of the lung, therefore understanding of the organ's structure is vital when considering design of a new medicine. The airways of the lung are classically divided in to two sections: the conducting zone and the respiratory zone (figure 1.1). The conducting zone is made up of the nose, mouth, trachea, bronchi, and bronchioles up to the terminal bronchioles and the function of this zone is to slow and humidify the air before it reaches the respiratory zone (Smyth and Hickey, 2011). To do this the branching system undergoes 17 bifurcations, becoming increasing thinner as the respiratory zone is reached (Patton, 1996). The respiratory zone begins at the respiratory bronchioles, the first to have alveoli, and finishes at the alveolar ducts which consist of alveolar sacs (West, 2008). The function of the respiratory zone is gas exchange, and due to this the alveoli have an extremely large surface area, an average of 102 m^2, and an excellent blood supply (Patton, 1996, Smyth and Hickey, 2011).

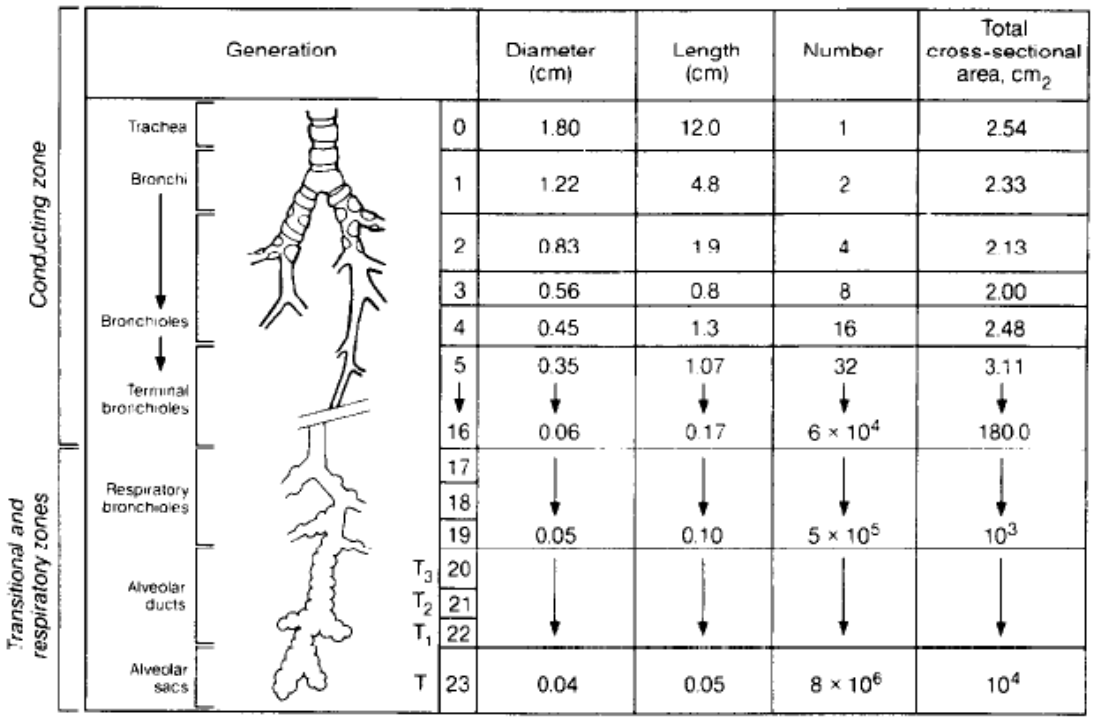

Generation		Diameter (cm)	Length (cm)	Number	Total cross-sectional area, cm_2
0		1.80	12.0	1	2.54
1		1.22	4.8	2	2.33
2		0.83	1.9	4	2.13
3		0.56	0.8	8	2.00
4		0.45	1.3	16	2.48
5 ↓ 16		0.35 ↓ 0.06	1.07 ↓ 0.17	32 ↓ 6×10^4	3.11 ↓ 180.0
17 18 19		↓ 0.05	↓ 0.10	↓ 5×10^5	↓ 10^3
20 21 22	T_3 T_2 T_1	↓	↓	↓	↓
23	T	0.04	0.05	8×10^6	10^4

Figure 1.1 - Diagram of the branching of the conducting and respiratory zones of the airways. From Patton (1996)

As the two zones of the respiratory system have different functions, the cells that line the epithelia of these zones are physically and biologically diverse. The differences in these cells can drastically affect how they interact with a pharmaceutical agent. The upper airways are lined with columnar ciliated epithelial cells which get gradually thinner as you progress further down the bifurcations (Patton and Byron, 2007). Amongst the ciliated cells are the mucus producing goblet cells, and these two types of cells together make up the mucociliary escalator, an important mechanism of clearance for the airways (figure 1.2) (Knight and Holgate, 2003). Basal cells are also present in this region. These cells provide structural support, anchoring other cells to the basement membrane, and are also thought to be progenitor cells for the ciliated and goblet cells (Knight and Holgate, 2003). The cells that make up the epithelium of the alveoli exist as a monolayer and are classified as either

Type I or Type II pneumocytes (Payne and Wellikoff, 2012). The surface area of the alveoli is predominantly Type I cells, making up around 95% of the alveolar epithelium, they are thin cells that provide a minimal barrier between the airspace and the pulmonary blood supply in order to maximize gas exchange (Castranova et al., 1988). The function of the Type II cells is lung surfactant production (Payne and Wellikoff, 2012).

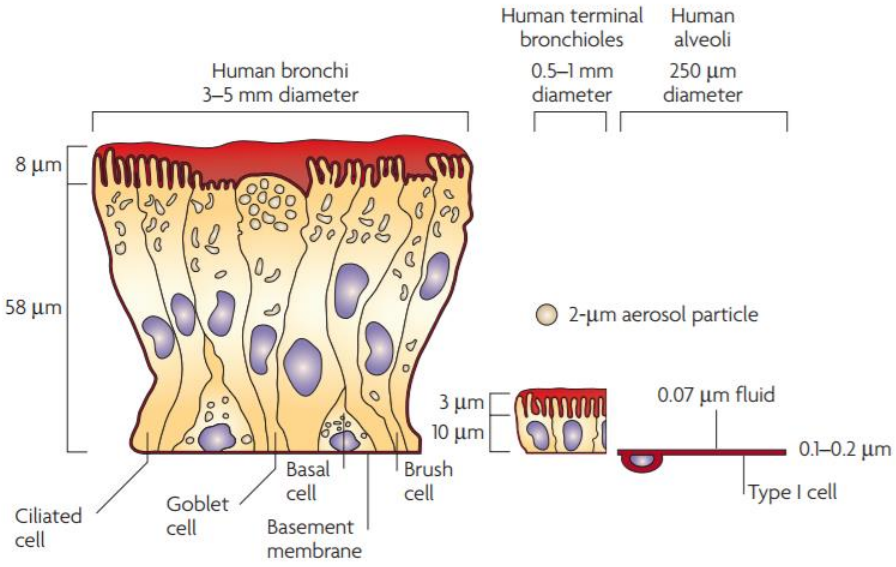

Figure 1.2 - Sizes of cells and lung surfactant found in the airways. From Patton and Byron (2007)

The composition of the lung lining fluid also changes between the conducting and respiratory zones of the lung. The conducting airways are lined with two layers: a mucus gel and periciliary sol that ranges from 5 – 100 µm in depth (Widdicombe and Widdicombe, 1995, Ng et al., 2004). The mucus contains many glycoproteins, proteins and phospholipids, and its main function is to trap inhaled material while the sol allows the beating of the cilia on the epithelial cells to move the fluid towards the mouth (Widdicombe and Widdicombe, 1995, Widdicombe, 2002). In contrast, the alveolar regions of the lung

are lined with a very thin layer, 0.1 – 0.2 μm deep, of alveolar subphase fluid and surfactant (Ng et al., 2004). The composition of surfactant comprises primarily of phospholipids (~ 90%), as well as proteins and some carbohydrates (Van Golde et al., 1988). The principal function of lung surfactant is to lower the surface tension of the air-liquid interface and help prevent the alveoli from collapsing after expiration (Van Golde et al., 1988). Lung surfactant also plays a role in response to infection, aiding in the eradication of bacteria and enhancing phagocytosis by macrophages found in the alveoli (Castranova et al., 1988).

1.2.2 Administration of medicines to the lung

With an understanding of the structure of the lungs, the next thing to consider is how an inhaled medicine will be administered as this will fundamentally influence formulation design. The three main classifications of devices used to aerosolize medicines for inhalation are nebulizers, pressurized metered dose inhalers (pMDIs) and dry powder inhalers. Each of these requires a different approach to formulation and will present different advantages and challenges for formulating an inhaled medicine with prolonged drug action.

1.2.2.1 Nebulization

Nebulizers are devices that convert a solution or suspension of a drug in to inhalable droplets that target the lower respiratory tract (Dolovich and Dhand, 2011, Myers, 2013). There are 3 categories of nebulizer depending on how they achieve aerosolization. These are jet, ultrasonic and mesh. Jet nebulizers use compressed air or oxygen to create an area of low pressure that draws the solution of drug up and causes it to form droplets as it

joins the gas stream (Labiris and Dolovich, 2003b). Ultrasonic nebulizers use an ultrasonic wave generated by a piezoelectric crystal to break up a liquid into a vapor mist (Dolovich and Dhand, 2011). Mesh nebulizers use electricity to vibrate a piezo plate and force the liquid drug through a fine mesh generating an inhalable mist (Myers, 2013). Use of all types of nebulizers requires a power source and up until fairly recently were large pieces of equipment with limited portability and long treatment times which are all disadvantages for therapies which require frequent dosing (Dolovich and Dhand, 2011). Modern nebulizers, such as the Respimat®, were created to overcome these challenges (Stein and Thiel, 2017). Minimal patient cooperation is required for effective dosing from these devices and so they are ideal for delivery to infants, the elderly or critically ill patients (Myers, 2013).

1.2.2.2 Pressurized Metered Dose Inhalers

Pressurized Metered Dose inhalers (pMDIs) are portable, cheap aerosolization devices that contain multiple doses of a medicine (Labiris and Dolovich, 2003b, Dolovich and Dhand, 2011). pMDIs use a propellant under pressure to force a reproducible dose through an atomization nozzle to achieve aerosolization (Dolovich and Dhand, 2011). Traditionally chlorofluorocarbons (CFCs) were used as propellants, until they were banned by the United Nations due to their deleterious effect on the ozone layer (Labiris and Dolovich, 2003b). They were replaced by hydrofluoralkanes (HFAs), which are non-toxic and do not affect the ozone layer, though they do have a nominal contributution to global warming (Dolovich and Dhand, 2011, Cripps et al., 2000). Although pMDIs are commonly used they are typically inefficient, only depositing between 10 – 20% of the given dose in to the lung (Lavorini and Corbetta, 2008). pMDIs dose larger particles at a high velocity

which causes a large amount of the dose to impact in the oropharyngeal region (Labiris and Dolovich, 2003b, Myers, 2013). Furthermore, they require a high degree of hand-breath coordination from the patient (Fink et al., 2013). The best technique is to release the dose at the start of a deep, slow breath and then to hold the breath for 10 seconds to allow any smaller particles to be deposited and not immediately exhaled. Accessories for pMDIs such as spacers and holding chambers can alleviate the problems associated with poor patient technique by slowing the aerosols velocity before it is inhaled, however these also reduce the portability of the devices (Labiris and Dolovich, 2003b, Myers, 2013).

1.2.2.3 Dry Powder Inhalers

Dry powder inhalers (DPI) deliver a powdered formulation, either pure drug or formed with a bulk excipient such as lactose, for inhalation (Myers, 2013). Typically DPIs are breath-actuated, powered by the patient's own inhalation, which directs air through a reservoir of particles of the drug and drives them into the airways of the patient by means of a turbulent flow that allows the particles to disperse in to a respirable size (Gac et al., 2008). There are many different types of DPI: some devices are single dose that must be reloaded by the user; some are multi-dose by the use of blister packs or a reservoir of powder. On top of the different methods of use each of the different DPI devices has a different air flow resistance, which means that they require a differing amount of inspiratory effort to achieve an optimal inhaled dose (Dekhuijzen et al., 2013). The downside of this is that an increased variability of devices and their methods of use could be confusing to patients. Furthermore, even though the higher resistance devices reportedly give greater lung deposition they might not be suitable for use with small children, the elderly, or patients with chronic obstructive pulmonary disease (COPD) due to the increased effort needed to deaggregate the powder for inhalation (Dekhuijzen et al., 2013). Depending on

the device and drug formulation DPIs can deliver anywhere between 10 – 40% of the medicine to the lungs (Islam and Cleary, 2012). Inefficiency with these devices is usually caused by the powder forming large aggregates which cannot be broken up by the turbulent air and this problem can be aggravated by increased humidity, i.e. from exhalation, in the device (Labiris and Dolovich, 2003b). The advantages of using a DPI are that they are very portable devices and because they are breath actuated they don't require the same level of coordination as an MDI would (Sou et al., 2011).

Although each of these delivery systems could be used to administer a formulation that prolongs drug action to the lungs, using a dry powder or pMDI solution could be more beneficial as the administered drug would need to dissolve in the lung lining fluid. Limiting the rate of dissolution could be a useful mechanism in creating an inhaled formulation with prolonged drug action and so administering the formulation as solid particles would be preferred.

1.2.2.4 Aerosol deposition

Regardless of the device used to administer aerosols to the lung, an understanding of the mechanisms by which particles or droplets are deposited in the lungs is essential to ensure a maximum deposition at the site of action. Factors such as the size, density, charge and morphology of particles are known to affect deposition in the lung (Heyder, 2004) and so all of these things must be taken in to account when designing an inhaled formulation. There are 5 mechanisms by which particles can deposit in the lungs: impaction, diffusion, sedimentation, electrostatic precipitation and interception; however the first 3 mechanisms are the predominant means by which therapeutic aerosols deliver drugs to the lungs (Lippmann et al., 1980). The deposition profile for varying sizes of

spherical particles of density 1 g/cm^3 is well understood and documented (figure 1.3). However drug particles for inhalation do not necessarily adhere to these characteristics and so calculation of their aerodynamic diameter is used to equate all particles (Edwards et al., 1998).

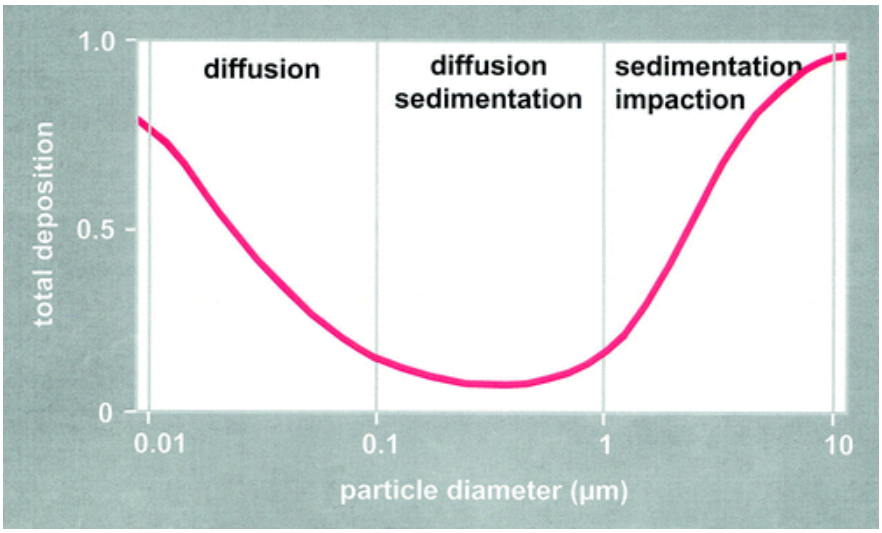

Figure 1.3 - Relationship between diameter of unit density spheres and their mechanism of deposition. From Heyder (2004)

The aerodynamic diameter is defined as the diameter of a sphere of standard density that settles at the same terminal velocity as the particle of interest (DeCarlo et al., 2004). As sedimentation and inertial impaction of a particle depend on the aerodynamic diameter, this characteristic has been used for many years to analyse where a particle is deposited in the lungs (Edwards et al., 1998). The aerodynamic diameter of a particle is given by equation 1.1.

$$d_a = d\sqrt{\rho/\rho_o} \qquad \textbf{[Equation 1.1]}$$

Where d is the geometric particle diameter, ρ is the density of the particle; ρ_o is the unit density (1 g/cm^3)

Inertial impaction occurs for particles that are travelling at a high velocity. Inhaled air changes direction with the branching of the airways, however high velocity particles tend not to be able to follow this change in direction, remaining instead on their predetermined path and impinging on the airway walls (Lippmann et al., 1980, Hickey, 2003). The occurrence of impaction increases with particle size and density, and is mainly seen in the upper airway (Bisgaard et al., 2001, Lippmann et al., 1980). Sedimentation occurs primarily in the smaller airways: the smaller bronchi; the bronchioles and alveolar spaces (Lippmann et al., 1980). This mechanism of deposition is governed by gravitational forces upon the particles when the air velocity is low (Newman, 1985). Deposition via diffusion occurs in the small airways and alveoli for particles that have a terminal velocity less than ~ 0.001 cm/s, which equates to a particle size of around 0.5 μm (Lippmann et al., 1980). Particles this small are subject to Brownian motion, collision with gas molecules in the air causing random directional changes (Bisgaard et al., 2001). However, particles of this size may also not be deposited at all and instead can be exhaled (Newman, 1985).

Control over the properties of an aerosol formulation, such as size, shape and density, is therefore essential to allow adequate deposition to the site of action for both locally systemically acting therapies.

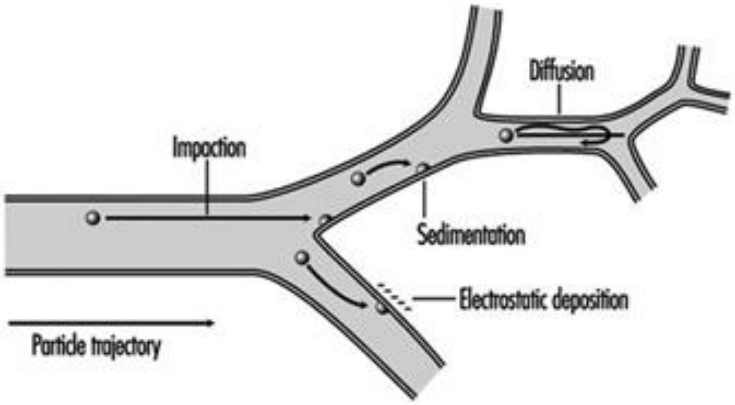

Figure 1.4 - Mechanisms of pulmonary particle deposition. From (Stellman and Office, 1998)

1.2.2.5 Dissolution

Following deposition in the lung, an inhaled particle must then be dissolved in the lung lining fluid before it can reach the pulmonary epithelium or be subject to the lungs' clearance mechanisms. The definition of dissolution is the process by which a solid substrate enters in to a solvent to yield a solution and there are many factors in the lung which could influence this (Davies and Feddah, 2003). The solubility of any drug is dependent on the structure of the drug, its formulation and physical properties, as well as the solvent in which it is to be dissolved (Olsson et al., 2011). In the lungs the site of deposition can also impact the dissolution of the drug due to the differences in the lung lining fluid (Olsson et al., 2011). The composition of the epithelial lining fluid is mainly water (96%) and so hydrophilic drugs will have rapid dissolution, the alveolar region, on the other hand, is lined with a surfactant with a high concentration of phospholipids and proteins that can increase the solubility of more hydrophobic molecules. Furthermore, smaller particles will present a greater surface area to the lung fluid, allowing for enhanced

dissolution, as will presenting the drug in a more disordered, amorphous, state (Khadka et al., 2014).

The primary reason that dissolution is thought to be rate-limiting in the lung is due to the very small volume of fluid that a particle will deposit in (Patton et al., 2010). The total volume of fluid in the lung ranges from 10 – 30 mL and at any one point its thickness can range from ~ 0.1 μm in the alveoli to a maximum of 100 μm in the upper airways (Olsson et al., 2011, Widdicombe and Widdicombe, 1995). Therefore some particles deposited in the lower airways could potentially be in fluid with a much thinner depth than their diameter (Olsson et al., 2011). There have been multiple studies that have shown the effect that altering dissolution profiles of inhaled drugs can have both *in vitro* and *in vivo* (Davies and Feddah, 2003, Yang et al., 2008a, Freiwald et al., 2005), however there have yet to be any studies that highlight the importance of dissolution in the clinic (Patton et al., 2010). Furthermore there is still discussion around an appropriate method to assess dissolution in a way that could be predictive of the situation *in vivo* (Arora et al., 2010). Pulmonary dissolution has been shown to be a rate-limiting step for some inhaled medicines (Borghardt et al., 2015), and so it is very possible that control over the rate of dissolution of an inhaled medicine could be used in a therapy that extends drug action.

1.2.2.6 Absorption

The subsequent barrier an inhaled drug particle faces is absorption across the pulmonary epithelium. The desired effect of absorption will differ depending on if the drug molecule is intended for local or systemic therapy. For systemic medicines administered *via* the lungs the absorption profile will regulate the onset and duration of action, however rapid absorption in to the blood can lead to a short duration of action for locally acting

medicines, and so for these drugs lung tissue retention may be ideal (Ehrhardt and Kim, 2007). The mechanisms by which drug molecules are absorbed are classified as either passive or active. Small hydrophobic molecules are thought to absorb in to the respiratory epithelium by transcellular diffusion, whereas hydrophilic compounds travel paracellularly, through intercellular spaces (Loira-Pastoriza et al., 2014a). Due to the difference in mechanisms, hydrophobic molecules are known to be absorbed much more rapidly than hydrophilic molecules and the absorption rate of hydrophilic compounds is inversely related to their molecular weight for molecules in the range of 60 – 75 kDa (Liu et al., 2013, Ehrhardt and Kim, 2007). It is also thought that less ionized molecules have a faster absorption rate due to having fewer interactions with proteins and lipids surrounding the intercellular pores (Liu et al., 2013). In addition to this the site of deposition of the drug affects its absorption rate. Absorption will occur much more readily in the alveolar space where the surface area is much greater and the epithelial cells are very thin (0.1 – 0.4 μm) in comparison with the tracheobronchial airways that have a smaller surface areas and columnar epithelial cells that can be up to 60 μm thick (Yang et al., 2008b). For drug molecules that are actively transported across the epithelial layers by way of transporters the absorption rate will differ depending on the expression, functionality and competition for the relevant transporters at the site of deposition (Liu et al., 2013). Macromolecules are thought to be transported across the epithelium *via* more than one route. They are thought to be able to travel through the intercellular junctions as well as being transported by transcytosis (Patton, 1996).

1.2.3 Clearance of drugs from the lung

The previous sections described an ideal situation for the administration of pulmonary medicines, in which the formulation is deposited at the correct site, dissolved if necessary and absorbed across the lung epithelium. The reality is that after deposition any inhaled particle faces one of several efficient removal mechanisms meant to protect the lungs from harmful substances (Oberdörster, 1988). In the conducting airways particles can be cleared rapidly via mucociliary clearance (Section 1.2.3.1) whereas in the lower airways clearance is slower and the work of macrophages (Section 1.2.3.2) (Stuart, 1984, Lippmann et al., 1980). Even the rapid absorption of drug molecules in to the blood can be thought of as a clearance, leading to short residence times in the lung (Section 1.2.3.4) (Patton and Byron, 2007).

1.2.3.1 Mucociliary clearance

Mucociliary clearance occurs from the trachea until the terminal bronchioles, where ciliated cells are found (Clarke and Pavia, 2015). Particles that cannot penetrate the mucus layer, and drugs that associate with mucus, that are deposited in this region are trapped and removed from the lung by the action of these cells (Edsbäcker et al., 2008). The cilia of the airways beat in a metachronal rhythm, optimizing the transport of mucus towards the mouth where it will be either swallowed or expectorated (Houtmeyers et al., 1999). The rate at which the cilia beat, and therefore the rate at which mucus is moved, increases from the distal to the proximal airways. In healthy individuals mucus moves at around 1 mm/min in the small airways, but can move as much as 2 cm/min in the trachea (Olsson et al., 2011, Edsbäcker et al., 2008). Therefore the site of deposition of particles in the conducting zone will affect their residence times in the airways. The rate of mucociliary

clearance decreases with age and can be greatly affected by diseases such as asthma, immotile cilia syndrome, bronchiectasis, and cystic fibrosis (Edsbäcker et al., 2008, Yeates et al., 1976). In diseases such as immotile cilia syndrome or bronchiectasis the reduced clearance is as a result of impaired cilia function, whereas in cystic fibrosis the increased amount and composition of the mucous impairs its removal (Houtmeyers et al., 1999). When the mucociliary escalator is damaged, cough becomes an increasingly important mechanism of clearance from the lungs. Studies have shown that in patients with COPD a significantly greater percentage of centrally deposited particles are cleared by cough in comparison with healthy individuals (60% vs 8%) (Olsson et al., 2011). An inhaled formulation that is delivered as a powder or suspension to the conducting zones of the airways would have to avoid premature removal *via* the mucociliary escalator in order to successfully extend the duration of action of the therapeutic agent.

1.2.3.2 Phagocytosis

Another mechanism by which particles are removed from the lung is phagocytic uptake by pulmonary macrophages. Macrophages are found on the alveolar surface and are able to move and engulf or lyse unwanted organisms, particles or toxic agents (Stuart, 1984). The clearance of insoluble particles *via* pulmonary macrophages is an overall slow process comprised of 2 parts. The first part is the uptake of the particle in to the cell, phagocytosis. This is a relatively rapid process, with 50 – 75% of deposited particles being phagocytosed within 2 – 3 hours and almost all within 24 hours (Geiser, 2010). Particle-bearing macrophages then move to the ciliated airways to be cleared via the mucociliary escalator, which can take anywhere from 24 hours to over a month to complete depending on the initial site of phagocytosis (Geiser, 2010). Alternatively, macrophages can break down endocytosed material via the mechanism of internal lysosomes or clearance can occur via

the lymphatic system (Stuart, 1984). This mechanism of clearance would be most important when designing an inhaled formulation for systemic delivery as the clearance of particles by phagocytosis could reduce the duration of action of the inhaled drug.

1.2.3.3 Pulmonary metabolism

The cytochrome P450 enzymes, known for their ability to metabolize drug molecules, are also found in the lung but at a much lower concentration than in the liver (Olsson et al., 2011). Because of this the drug metabolizing capability of the lungs is minimal for most small molecules. There are however several drug molecules that are known to be substrates for pulmonary metabolic enzymes, namely: budesonide, salmeterol, fluticasone propionate and theophylline (Olsson et al., 2011). Furthermore, due to the presence of proteases in the lung, inhaled doses of proteins and peptides could be affected by metabolism (Labiris and Dolovich, 2003a). Although local metabolism could cause short residence times for therapeutics in the lung, it can also be taken advantage of, for example by the use of prodrugs (Section 1.3.1) (Olsson et al., 2011).

1.2.3.4 Drug absorption

Soluble particles that are not cleared by any of the processes described above will be absorbed across the pulmonary epithelium. The mechanisms by which this occurs has been described in detail in Section 1.2.2.6, however it is crucial to highlight absorption again as a mechanism of drug clearance from the lungs. Rapid absorption of drug molecules and metabolism elsewhere in the body can lead to a short duration of action for therapeutic agents and necessitate frequent dosing (Patton and Byron, 2007). This highlights the problems faced when attempting to create an inhaled formulation for prolonged therapeutic action, as a balance between avoiding the clearance mechanisms

of the lungs and limiting the rate of drug absorption to create a reservoir of drug that can continue to act over a prolonged period of time is essential. The methods that have been previously used in an attempt to overcome this problem and create a formulation that prolongs drug action will be discussed in the next section.

1.3 Methods of prolonging drug action in the lung

Despite the routine use of aerosols in the clinic, many inhaled medicines suffer from the same limitations: a short duration of action owing to the drug's rapid clearance from the lungs. Sufferers of chronic respiratory diseases, such as asthma, are often required to take their inhaled medication up to four times daily (Loira-Pastoriza et al., 2014b). This inconvenience increases the risk of poor patient compliance, as well as the potential for fluctuating drug levels in the blood causing more unwanted side effects (Liang et al., 2015). There are a number of strategies that are being investigated as prospective methods of extending drug action in the lungs including the use of liposomes as drug carriers (Section 1.3.3) or chemical modification of the active compound (Section 1.3.1). Despite this, there are currently no controlled delivery aerosol formulations on the market (Cook et al., 2005). It is clear that the development of a formulation for inhalation with prolonged drug action could improve the therapeutic efficacy of many drugs as well as the safety profile.

1.3.1 Microparticles

Modifications to formulations on the micro scale can be used as a strategy for achieving prolonged drug action in the lungs. Large porous particles (LPP) are particles with a large geometric diameter (> 5 μm) but low density (< 0.4 g/cm^3), and as such their aerodynamic

diameter is low (Loira-Pastoriza et al., 2014b). This allows the particles to penetrate deep in to the lung on inhalation, bypassing much of the mucociliary escalator to prolong retention in the airways. Furthermore, due to their large geometric size they may be able to escape phagocytosis by alveolar macrophages (Loira-Pastoriza et al., 2014b). They are commonly made from polymer carriers such as PLGA and are prepared with porogen agent such as ammonium bicarbonate, which give the particles their porous structure (Liang et al., 2015). Recently rifampicin has been loaded into an LPP formulation and administration via inhalation achieved a higher systemic concentration than oral administration, and sustained a high local concentration in guinea pigs (Garcia Contreras et al., 2015). Despite the promising nature of LPPs there are still many limitations. Mainly, there is not yet a method for their fabrication that achieves high drug loading and predictable release profiles for all drug molecules and the porous nature of these particles calls in to question their physical stability and the potential difficulty for large scale manufacture (Liang et al., 2015).

Swellable microparticles are another aerosol formulation strategy that has the potential to achieve prolonged drug action. These particles are in the inhalable size range when dry, but after deposition and contact with the fluid in the lungs they swell to a larger size (Ni et al., 2017). The swelling of the particles limits the amount of phagocytosis by macrophages, and so the particles have a longer lung retention time to release the active agent (Liang et al., 2015). Furthermore, natural polymers such as chitosan are often used to generate the swelling particles, and so they are biocompatible and biodegradable (Ni et al., 2017). Gaspar *et al.* produced chitosan microspheres crosslinked with glutaraldehyde and containing levofloxacin. He showed that the microparticles had a high drug loading efficiency, acceptable drug release profile, and equivalent antibacterial properties to the

free drug (Gaspar et al., 2015). However, there is still an issue of how to incorporate hydrophobic drug molecules in to these microspheres, especially if chitosan is used as the swelling polymer. Low drug loading, and uneven drug distribution are problems that must be overcome if swellable microparticles are to become a suitable delivery system for all inhaled medicines (Ni et al., 2017).

1.3.2 Nanoparticles

Nanoparticles can be used as drug carriers by either adsorbing the active agent to the surface of the particle, or by encapsulating the agent within (Sung et al., 2007). A nanoparticle refers to a solid particle in the size range of 1 to 1000 nm, however the term can sometimes be used to refer to particles in the 1 – 200 nm size range (Sung et al., 2007).

Several studies have shown that nanoparticle formulations can provide a method of extending drug action in the lungs. Yamamoto *et al*. created PLGA nanoparticles of elcatonin, modified with chitosan to give them mucoadhesive properties. They showed that the elimination of the particles compared with regular nanoparticles was prolonged and this resulted in an extended therapeutic effect in guinea pigs (Yamamoto et al., 2005). Das *et al*. showed that delivering a dry powder formulation of voriconazole loaded poly(lactic-co-glycolic acid) (PLGA) nanoparticles to mice generated a sustained release profile in comparison with the intravenous (IV) route of administration (Das et al., 2015). Vaughn *et al.* explored delivering itraconazole in a formulation of nanoparticles made from polysorbate 80 and poloxamer 407 for the treatment of *Aspergillus fumigatus* fungal infections in mice, he found that the nano-formulation was able to generate and sustain the high lung concentration required compared to oral administration (Vaughn et al., 2006).

Although there have been numerous studies highlighting the potential use of nanoparticles in delivering drugs to the lungs, there are also potential shortcomings that require further investigation. A major concern when administering nanomaterials to the body is their potential for increased toxicity. Nanoparticles are developed for their surface functionalities which enhance their utility, however with such a small particle size there is a greatly increased surface area between these functional groups and the body's tissue (De Jong and Borm, 2008). Furthermore, nanoparticles can migrate from the lung into systemic circulation and their bodily distribution and ability to cross biological barriers such as the blood-brain barrier is unknown (De Jong and Borm, 2008, Bailey and Berkland, 2009). Various *in vivo* and *in vitro* studies have shown that nanoparticles can cause pulmonary inflammation, cause platelet aggregation or accelerate vascular thrombosis (De Jong and Borm, 2008, Bailey and Berkland, 2009). Additionally, nanoparticles can be unstable in storage. Solutions of nanoparticles for nebulization have been shown to lose the encapsulated drug over time due to polymer hydrolysis, and agglomeration can lead to poor aerosolization (Sung et al., 2007). Dry powders of nanoparticles will also be susceptible to agglomeration during storage, or conversely, particles that do not agglomerate run the risk of not being deposited into the lung at all, and instead being exhaled. As a result of this microparticle formulations that release the nanoparticle upon administration are being investigated, however this might be considered to be adding another layer of complexity to an already difficult problem (Sung et al., 2007).

1.3.3 Liposomes

Liposomes have also been investigated as carriers for drug delivery to the lungs. Liposomes are self-assembling colloidal structures that are formed from phospholipids and can be in the size range of 20 nm to 10 μm (Taylor and Newton, 1992, Willis et al., 2012). They can be unilamellar or multilamellar: containing many lipid bilayers separated by an aqueous core (Taylor and Newton, 1992). Due to their nature liposomes are capable of encapsulating a wide range of drug molecules. Hydrophilic drugs can be trapped within the aqueous regions of the structure, whilst hydrophobic molecules can associate with the lipid bilayers (Taylor and Newton, 1992).

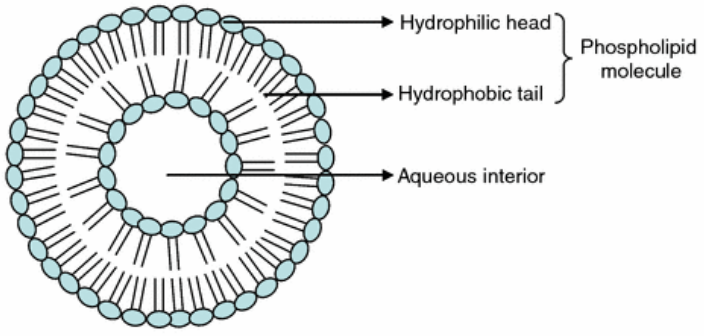

Figure 1.5 - The structure of a unilamellar liposome. From (Swaminathan and Ehrhardt, 2011)

Liposomes have been successfully incorporated in nebulized, pMDI and DPI formulations for inhalation and have been shown to be able to extend drug action. In animals liposomal formulations of compounds such as cytarabine and orciprenaline sulphate have been shown to possess a prolonged period of therapeutic activity and a minimized amount of distribution around other bodily tissues (Taylor and Newton, 1992). More recently, a

liposomal amikacin formulation (Arikace®) has been shown to enhance and sustain the activity of the aminoglycoside antibiotic against *pseudomonas aeruginosa*, and is currently in phase III clinical trials for treatment of infections in cystic fibrosis patients (Elhissi, 2017). Liposomes are attractive drug delivery systems as they are made from compounds that are endogenous to the lungs, such as the primary component of lung surfactant dipalmitoylphosphatidylcholine (DPPC) and therefore do not have any toxicity related side effects (Willis et al., 2012). There are, however, also some drawbacks with the use of liposomal formulations for pulmonary drug delivery. Formulations of liposomes for nebulization can be unstable, and even the process of nebulization can result in premature release of the encapsulated drug (Loira-Pastoriza et al., 2014b).

1.3.4 Chemical modification

Modification of the chemical structure of therapeutic agents, conjugation with a polymer or the development of a prodrug are all strategies that could be employed to create a formulation with prolonged drug action. An example of this is the modification of the short acting β2- agonist salbutamol to give the long acting salmeterol. This modification increased the molecular weight and lipophilicity of the original molecule and as a result increased the duration of action from 4 to around 12 hours (Kips and Pauwels, 2001). Conjugation of drug molecules with polyethylene glycol (PEG) also has been investigated as a means of creating prolonged drug action. PEG has a high molecular weight and creates steric hindrance around the drug molecule that slows absorption and protects from metabolic enzymes and phagocytosis (Loira-Pastoriza et al., 2014b). PEGylated insulin and calcitonin have both been shown to have increased stability in rat lungs while retaining the ability to be absorbed in to systemic situation, and PEGylated small drug molecules

such as prednisolone have been shown to have a reduced absorption rate (Loira-Pastoriza et al., 2014b). Prodrugs have also been shown to have some efficacy in the lung. A prodrug approach involves modification of a drug molecule with a moiety that will be enzymatically cleaved in the lung giving the original drug molecule that can then act. An example of this is ibuterol, a prodrug of terbutaline, was absorbed more rapidly than the parent drug but created a reservoir, releasing the parent drug over time, and was three times as effective (Zeng et al., 1995). Although chemical modification provides a potential route for creating a medicine with prolonged drug action, it only does so for an individual drug molecule at a time, and can require a large investment of time and money to create an appropriate formulation and take it to market. As such, it would be preferable to create a formulation strategy that could be applied to a range of drug molecules. One such form of chemical modification that could be applied to numerous inhaled drug molecules is the use of ion-pairs, this strategy will be discussed in the next section.

1.4 Ion-pairs as a strategy for prolonging drug action of inhaled medicines

1.4.1 Ion-pair definition

Another formulation strategy that has the potential to create an inhaled medicine with prolonged drug action is the use of ion-pairs. An ion-pair is a pair of oppositely charged ionic molecules that is held together via non-covalent interactions, such as Coulombic attraction and hydrogen bonding (Samiei et al., 2013). The general energies of these types of non-covalent interactions is around – 20 kj/mol, although the strength of the bonds can change depending on the dielectric constant of the surrounding environment (Wermuth,

2011). As a result, these interactions more readily dissociate in water, as preferential binding to water occurs. Therefore, the aim of an ion-pair is to create a stronger binding interaction between the two charged molecules so that a greater proportion of the ion-pair remains whilst in solution. In the lab this concept is often used, for example in the separation of difficult molecules by high performance liquid chromatography (HPLC) (Qiao et al., 2016). However, in a pharmaceutical sense ion-pairing refers to the binding of a charged drug molecule and a counter ion. In order to promote binding of the species on administration the counter ion is often present as an excess. The ion-pair species behaves as a single unit on dissolution and absorption across the epithelium and then dissociates in to the separate ions when diluted in the blood (Samiei et al., 2013). This differs from active agents that are formulated as salts, as they are prepared in a stoichiometric ratio. Previous studies have shown that increasing the ratio of counter ion can increase the concentration of bound species in solution, whereas a salt formulation would immediately dissociate when dissolved (Patel et al., 2009a). It is therefore important when creating a pharmaceutical ion-pair, to choose a biocompatible counter ion as it will be presented to the epithelium in a relatively high concentration.

1.4.2 Use of ion-pairs in drug delivery

The main advantage to forming ion-pairs is that it allows manipulation of a drug's physical and biopharmaceutical properties without having to alter the chemical structure of the molecule. Depending on the counter ion used an ion-pair can be more hydrophilic or more lipophilic than the drug molecule alone, so processes such as dissolution or absorption across the epithelium can be modified. Previously, the ion-pairing strategy has been used to alter the properties of drugs for transdermal, ocular and oral administration.

Song *et al.* generated adhesive patches for the administration of bisoprolol ion-pairs. They found that a bisoprolol maleate ion-pair (figure 1.6) showed the most promise as it successfully controlled the drug's flux through rabbit skin, the mechanism of action was proposed to be due to both the change in logP and molecular weight of the ion-pair when compared with the free drug (Song et al., 2012). Megwa *et al.* studied the effect of ion-pairing salicylic acid with various quaternary ammonium compounds on the penetration of the drug across human skin. They found that the bioavailability of salicylic acid could be improved by ion-pairing when the complex formed was more hydrophobic than the drug molecule, but that the degree of effect was inconsistent depending on the counter ion chosen. They hypothesized that this was due to steric hindrance of some of the chosen counter ions increasing the distance between the two ions and therefore limiting the strength of the coulombic interaction (Megwa et al., 2000). This highlights the importance of choosing suitable counter ions for use in an ion-pairing formulation.

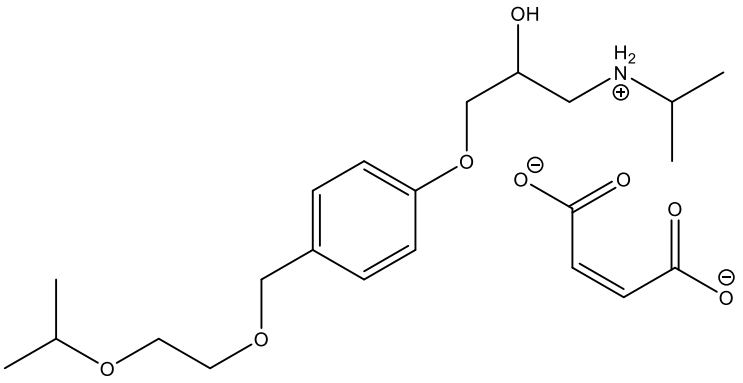

Figure 1.6 - Chemical structure of bisoprolol maleate ion-pair

In ocular formulations ion-pairing with sorbic acid was shown to generate a 2-fold increase in timolol permeation across intact rabbit corneas in a study completed by Higashiyama *et*

al.. They found that the timolol – sorbic acid ion-pair did not affect the diffusion coefficient of the drug in to the epithelium, but that it did significantly increase the partition coefficient, and so proposed that the increased permeation was as a result of enhanced partitioning of the ion-pair in to the epithelium (Higashiyama et al., 2004). In a more recent study, Li *et al.* found that ion-pairing pirenzepine with sorbic acid greatly increased the drug's absorption across the cornea, increased the drug's loading in to a liposomal delivery system and improved the penetration of the liposomes across the cornea (Li et al., 2017).

Oral absorption of amifostine was greatly improved by ion-pairing with succinic acid in a study by Samiei *et al.* in rats, reaching similar drug plasma levels after 20 minutes as an intravenous dose (Samiei et al., 2013).

In all of these examples of the use of ion-pairs to modify a drug's pharmacokinetic profile, permeation has been enhanced by creating a more hydrophobic complex. A formulation for the lungs could employ ion-pairs to create a more hydrophilic or a more hydrophobic complex. A hydrophilic complex could lower the rate of drug absorption in to the respiratory epithelium, slowing clearance by absorption. On the other hand, a more hydrophobic complex could lower the rate of dissolution, creating a drug reservoir in particle form which could be subject to clearance mechanisms, or could increase the tissue retention of the drug, creating a reservoir in the epithelial cells.

1.5 Aims and scope of the PhD

Despite the literature highlighting the potential of ion-pairs to modify a drug's pharmacokinetic profile, there has been surprisingly little investigation into their incorporation in an inhaled formulation (Patel et al., 2016) . The lung could be an ideal site

for ion-pairs to act due to the relatively low volume of fluid, which could limit the dissociation of the drug molecule and counter ion. Reviewing the literature presented in the introduction there are several considerations that need to be made when developing an ion-pair formulation for inhalation. Charged, inhaled medicines would have to be able to form ion-pairs with suitable, biocompatible counter ions, and both species would have to be able to be incorporated into an aerosol formulation so that the ion-pair is intact at the site of action. The ion-pair would then modify either the dissolution of the drug or its absorption across the respiratory epithelium in order to avoid the lungs rapid clearance mechanisms to deliver a therapeutically effective dose of the drug molecule for a prolonged duration. The desired effect of the ion-pair could change with the intended site of deposition. Locally acting drug molecules may benefit from rapid dissolution to avoid clearance via the mucociliary escalator, and therefore prolonged drug action would be a product of slow absorption of the ion-pair or tissue retention. Whereas for systemic drug delivery, ion-pairs could decrease the rate of dissolution of particles to limit the speed at which the drug enters circulation. Ion-pairs could potentially be formulated in to a nebulized, pMDI, or dry powder formulation. However, storing the drug and counter ion in a solution could increase the chances of complex dissociation and potential binding of the drug or counter ion to other excipients present in the formulation.

The aim of this project, therefore, was to assess the feasibility of ion-pairs to be used in a formulation for inhalation intended to prolong drug action. It was hypothesized that a dry powder formulation containing an ion-pair could be delivered to the lungs and be used to generate a prolonged duration of therapeutic action.

The following objectives were set in order to test this hypothesis:

- To assess the ion-pair formation of a charged inhaled model drug with a range of suitable counter ions
- To investigate the effect of ion-pair formation on the physical and biopharmaceutical properties of the drug molecule
- To create an inhalable dry powder formulation incorporating the ion-pairs
- To study the ability of the ion-pair formulations to prolong drug efficacy in an animal model

Chapter 2

Characterization of Salbutamol Ion-pairs

2.1 Introduction

There are many reasons why it might be desirable to temporarily alter a drug's physicochemical characteristics during formulation and/or administration including: to increase solubility; to modify dissolution; or to control cell uptake of the drug molecule at the administration site (Desai et al., 2015, ElShaer et al., 2014, Lozoya-Agullo et al., 2016). Forming ion-pairs could be an advantageous method to induce a temporary change in a drug's physicochemical properties as it does not modify the chemical structure of the drug molecule itself, but can modify its properties (Lozoya-Agullo et al., 2016). There have been a number of published studies that have shown forming ion-pairs between hydrophilic APIs and hydrophobic counter ions can improve permeability via oral, parenteral, ocular and transdermal routes (Lozoya-Agullo et al., 2016, Trotta et al., 2003, Tan et al., 2009). However, there are very few studies on how the fate of inhaled medicines can be changed by utilizing the ion-pairing strategy (Zhou et al., 2002, Patel et al., 2016).

Ion-pairs are formed from 2 oppositely charged species which associate to behave as one unit prior to dissociating upon dilution in to a larger body of liquid such as the blood (Lozoya-Agullo et al., 2016). The airways of the lung are an ideal site for an ion-pairing approach to control drug delivery due to the very small volumes of fluid that line the lungs which will reduce the speed of dissociation (Forbes et al., 2000). Hence forming an inhaled medicine using a drug ion-pair could improve the uptake and duration of action of both topical and systemic medicines.

In order to investigate the effect of ion-pairing on the behavior of drugs that could form inhaled medicines a model drug that is ionized at the correct (physiological) pH is needed.

For the purpose of the work in this thesis salbutamol was chosen as the model drug. Salbutamol is a β2-adrenergic receptor agonist used in the treatment of asthma as a bronchodilator (Imboden and Imanidis, 1999, Jashnani et al., 1993). At physiological pH its secondary amine is charged (figure 2.1). The structure of the drug also includes a benzene ring, and a primary, secondary and phenolic alcohol (figure 2.1).

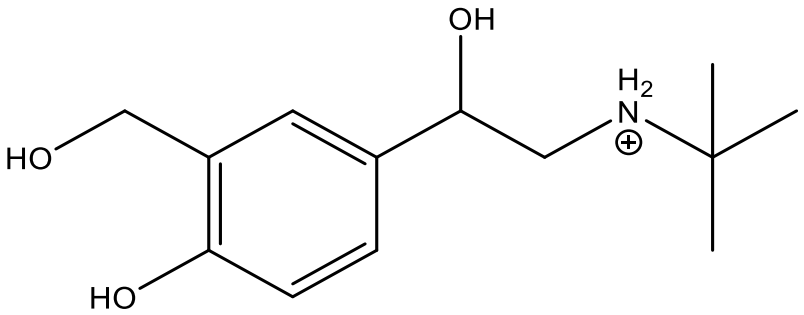

Figure 2.1 – Chemical structure of salbutamol at pH 7.4

The duration of action of salbutamol following inhalation is relatively short, around 4 hours (Jashnani et al., 1993). The frequency and severity of the symptoms of asthma peak at around 4 am due to a circadian rhythm (Hetzel and Clark, 1980, Imboden and Imanidis, 1999) and so a prolonged effect of the drug following an evening dose would be beneficial.

In an attempt to prolong the action of salbutamol its chemical structure was altered to create salmeterol and formoterol (Santus et al., 2015). However, these agents can have serious side effects, in 1993 a study Castle *et al*. published a study showing there was a threefold increase in mortality in patients prescribed with salmeterol vs salbutamol (Castle et al., 1993). Previous work has shown that salbutamol does form an ion-pair species with the sulfate and 1-hydroxy-2-naphthoate counter ions and that the 1-hydroxy-2-naphthoate

ion-pair significantly increased the percentage reversal of airway obstruction in guinea pigs when compared to salbutamol base (Patel et al., 2016). However, in this study salbutamol and its ion-pairs were administered by way of an intravenous injection and so it is possible that the effects of the ion-pair had been reduced due to its dilution and dissociation in the blood. Furthermore, IV administration does not allow for an ion-pair to alter solubility or dissolution of the drug molecule which could have a large effect on the action of the drug. Therefore administering an ion-pair as a solid dosage form might allow for the maximum effect to be observed.

The aim of the work presented in this chapter was to investigate whether salbutamol formed ion-pairs with counter ions at physiological pH, and if an ion-pair was formed to assess the strength of the complex. In order to achieve this Fourier Transform Infrared spectroscopy (FTIR) and high performance liquid chromatography (HPLC) methods were established. Other techniques can be used to analyze the binding of an ion-pair such as fluorescence spectroscopy and nuclear magnetic resonance (NMR) (Tan et al., 2009), however FTIR and HPLC were chosen due to ease of use and availability. Using results from these experiments, speciation software was used to predict the amount of drug bound in the form of an ion-pair at different ratios of drug to counter ion. Furthermore, the effect of ion-pairing on the lipophilicity and solubility of the drug was analyzed. Due to the surfactant nature of the octanoate counter ion, its ability to form micelles at the concentrations employed in other experiments was also examined using photon correlation spectroscopy.

The choice of counter ion for an ion-pair formulation is extremely important as the behaviour of the complex *in vitro* and *in vivo* is likely to change depending on how strongly the drug and counter ion associate and what chemical groups are presented to the

environment (Patel et al., 2016). In order to achieve a greater understanding of the role the counter ion might play in the physicochemical properties of an ion-pair, a range of pharmaceutically relevant anionic counter ions were chosen for investigation. Typically, in the literature, only hydrophobic counter ions have been used in order to improve transport of drugs across membranes (Zhou et al., 2002, Trotta et al., 2003), however for the purpose of this study counter ions were chosen with a range of logP values. In addition the chemical groups of the counter ions were taken in to consideration. Salbutamol possesses hydroxyl groups which could from hydrogen bonds and a benzene ring which has the potential for a π-stacking interaction. The formation of multiple non-Coulombic interactions between the drug and chosen counter ion could improve ion-pair formation and the stability of the complex. The counter ions chosen for this study are shown in figure 2.2.

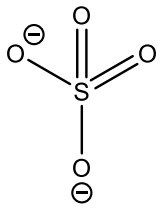

Sulfate
Log P = - 2.43

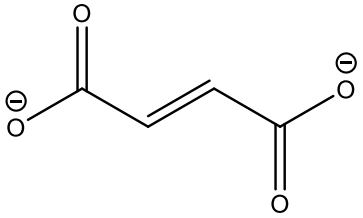

Fumarate
LogP = - 0.27

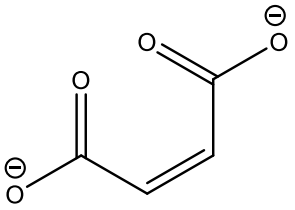

Maleate
LogP = -0.02

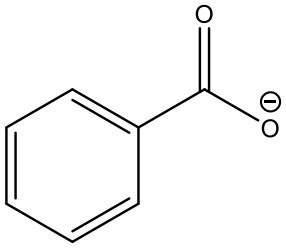

Benzoate
LogP = 1.29

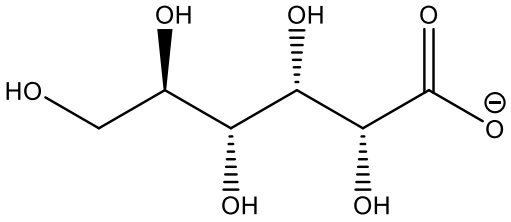

Gluconate
LogP = -2.06

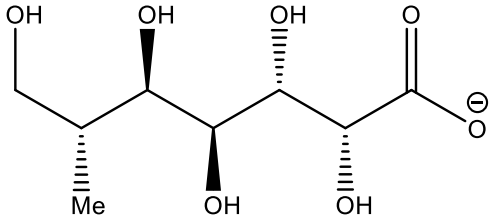

Glucoheptonate
LogP = -1.60

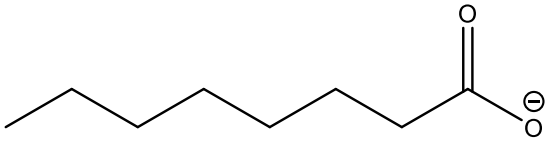

Octanoate
LogP = 3.15

Figure 2.2 – Chemical structures (at pH 7.4), names and predicted logP values of all chosen counter ions. LogP values were predicted using ALOGPS software

2.2 Materials and Methods

2.2.1 Materials

Lactohale 300 (Friesland foods, Netherlands) was used as a source of lactose. Salbutamol base was from Cipla Ltd, India and used without further purification (BN. H80619). Sodium sulfate, sodium fumarate and sodium benzoate were purchased from Alfa Aesar, UK. Sodium octanoate, sodium maleate dibasic, deuterated water, PBS and HBSS were obtained from Sigma Aldrich (Dorset, UK). Sodium gluconate and sodium glucoheptonate were purchased from Santa Cruz Biotechnology (USA). For HPLC analysis, phosphate buffered saline was from Oxoid Ltd (Hampshire, UK), ammonium acetate was purchased from VWR (Leicestershire, UK). N-octanol, HPLC grade methanol and water were supplied by Fisher ltd (Leicestershire, UK).

2.2.2 *Fourier Transform Infrared Spectroscopy (FTIR) ion-pair binding assay*

A universal transmission cell system (Omni-Cell system, Specac Ltd., Orpington, Kent, U.K.) with CaF_2 windows and Mylar spacer (25 µm path length) was used for the transmission measurements. All samples were made up in D_2O and the pH adjusted to 7.4 (± 0.2) with 1 M HCl or NaOH in D_2O as needed. Blank solutions were prepared using the same amount of D_2O and acid or base without the salbutamol. The spectra of 7 different concentrations of ionized salbutamol (ranging from 80 – 160 mM) were taken to assess if any changes in the transmission intensity of peaks occurred with increasing concentration. The spectra were recorded within the range of 4000 – 450 cm^{-1}. The resolution was set at 4 cm^{-1} and 32 scans were performed for each measurement. All spectra were baseline

corrected and differentially subtracted with the spectra of the baseline corrected blank solutions. Data was recorded using a Spectrum One spectrometer and analyzed with Spectrum software (Perkin Elmer Ltd., Beaconsfield, UK). A 100 mM concentration was chosen to investigate the effect of ion-pairing with salbutamol as this was the lowest concentration at which all peaks were clearly visible. Sodium sulfate, sodium gluconate, sodium glucoheptonate and sodium octanoate were the counter ions used. Blank solutions for these experiments consisted of an equal volume of D_2O, acid and base and an equal weight of counter ion as in the sample. The FTIR spectra of 100 mM salbutamol with increasing concentrations of each of these counter ions were obtained as before.

2.2.3 High Performance Liquid Chromatography (HPLC) ion-pair binding assay

An HPLC machine (Agilent 1100, Agilent Technologies, California, USA) was used to determine the retention time of salbutamol in a pure H_2O (pH 7.4 ± 0.2) mobile phase. The flow rate was set to 0.3 $mLmin^{-1}$ and the UV detection wavelength was 278 nm. The stationary phase consisted of a biphenyl 100 A250 x 4.6 mm column (Phenomenex, UK). For each sample 2 injections of a 1 mM salbutamol solution were performed (n=3). Binding to counter ions was assessed by the change in retention time with increasing concentration of counter ions in the mobile phase. When the increase in counter ion concentration did not result in a difference in retention time 100% salbutamol was thought to be bound.

2.2.4 Calculation of salbutamol – counter ion speciation curves

The Hyperquad Simulation and Speciation software (Hyss 2009, Protonic Software, UK) (Alderighi et al., 1999) was used to predict the percentage of salbutamol ion-pair species. The concentration of salbutamol was set to 0.00209 M (corresponding with the concentration used in cell transport experiments in Chapter 5). The binding was calculated for each counter ion at a 20:1 and 10:1 ratio assuming 1:1 binding occurred between drug and counter ion.

2.2.5 Distribution coefficient assay

PBS and octanol were equilibrated for 48 hours before use. Salbutamol base was dissolved in PBS saturated with n-octanol at a concentration of 0.2 mM for use. Counter ion was added to the drug solution at a ratio of 20:1. The drug containing PBS was pH adjusted to 7.4 (± 0.2) before an equal volume of n-octanol was added to the sample. The sample was shaken at 37^{o}C for 48 hours. After this time the aqueous layer was taken to be analyzed by UV/VIS spectroscopy using a wavelength of 278 nm (Lambda 2 UV/VIS spectrometer) and data was analyzed using Lambda 25 software (Perkin Elmer Ltd., Beaconsfield, UK). The values obtained were compared to a calibration curve of salbutamol base made up in the PBS saturated with n-octanol and any difference in the concentration found to the initial concentration was assumed to be in the octanol layer. $LogD_{7.4}$ was calculated using the following equation:

$$\mathbf{LogD_{7.4} = log\ [octanol]\ /[aqueous]} \qquad \textbf{[Equation 2.1]}$$

2.2.6 Photon correlation spectroscopy

The potential for self-assembly of sodium octanoate in to micelles was investigated using PCS (Zetasizer Nano, Malvern Instruments, Worcestershire, UK). Serial dilutions of solutions of 20:1 salbutamol sulfate (control) and salbutamol octanoate in PBS were pH adjusted to 7.4 (± 0.2) before analysis. Concentrations of the samples ranged from 0.042 – 21 mM. The derived count rate was analyzed for each concentration and where the value of the count rate was greater than 1000 the particle size was obtained from the size-intensity distribution. All measurements were carried out using a scattering angle of 173 ^{o} using water as the dispersant (refractive index 1.33, viscosity 0.8872 cP at 25°C) and at room temperature.

2.2.7 Spray drying of salbutamol ion-pair powders

Spray drying was performed on a B-191 spray dryer (Buchi, Switzerland). The optimized conditions were as follows: a total concentration of 3 g/100 mL water was used, with an inlet temperature of 180^{o}C. The aspirator was set at 80% (machine setting), the pump speed was 5 mL/min and the air flow rate was 800 l/h. A salbutamol lactose powder was generated using 1% w/w drug concentration. Ion-pair powders were generated for all counter ions in a 20:1 ratio.

2.2.8 Ion-pair solubility

HBSS (0.5 mL) was warmed to 37^{o}C using a shaking water bath. After 1 hour salbutamol spray-dried powder was added (200 mg). The pH of the suspension was measured at the beginning of the experiment and adjusted to pH 7.4 (± 0.2) with 1 M HCl/NaOH as needed.

The suspension was shaken at 150 strokes per minute and 37^{o}C for 24 hours. The pH was recorded once more at the end of the experiment. The solid material was separated from the liquid via centrifugation (Biofuge pico, Heraeus, Germany) at 2000 rpm for 5 min and an aliquot of the resulting clear solution was diluted (1:100) for HPLC analysis.

2.2.9 High performance liquid chromatography (HPLC)

An HPLC machine (Agilent 1100, Agilent Technologies, California, USA) was used to determine the concentration of salbutamol, separation was achieved using a SphereClone^{TM} ODS2 (250 x 4.6 mm, particle size: 5 µm) column (Phenomenex® Ltd., Cheshire, UK). The mobile phase for HPLC analysis was an 80:20 mixture of 1 g/L ammonium acetate solution: methanol, that had been adjusted to pH 4.5 using 1 M HCl, filtered through a 0.2 µm nylon membrane, and degassed by sonication. The run time was set at 8 min, with a flow rate of 1 mLmin^{-1} and 6 injections of 20 µL per vial. The UV detection was set at 226 nm. The amount of salbutamol in the samples was determined by comparison with a calibration curve. To generate a calibration curve an aliquot of 10 mg salbutamol was weighed out and added to a 100 mL volumetric flask and made up to volume with PBS to give a 100 µgmL^{-1} solution. A set of serial dilutions was performed using glass pipettes and volumetric flasks to prepare 7 standards (100, 80, 50, 20, 10, 5, 1 µgmL^{-1}).

2.2.10 Data analysis

Data was obtained from 3 experiments and have been expressed as a mean ± standard deviation, unless otherwise stated. Sigmoidal curves were fitted to the binding data in SigmaPlot and the value at 50% was taken as the ion-pair binding constant. One-way

Analysis of Variance (ANOVA) with a Shapiro-Wilkins normality test was performed with a probability limit of 0.05 set to indicate significant differences.

2.3 Results

2.3.1 The binding of salbutamol with negatively charged counter ions

The full FTIR spectra of salbutamol base at a concentration range from 80 – 160 mM were analyzed in order to identify the main peaks associated with the drug (figure 2.3). It was found that the main peaks associated with salbutamol occurred in the range of 1350 – 1650 cm^{-1}. The peaks found in this region were assigned to chemical groups in salbutamol based on the literature (Sharma, 2013, Paluch et al.). These peaks occurred at 1385 cm^{-1} (CH_3), 1413 cm^{-1} (COH), 1507 cm^{-1} (CH_2-N), 1596 cm^{-1} (N-H), and 1617 cm^{-1} (C=C) (figure 2.4).

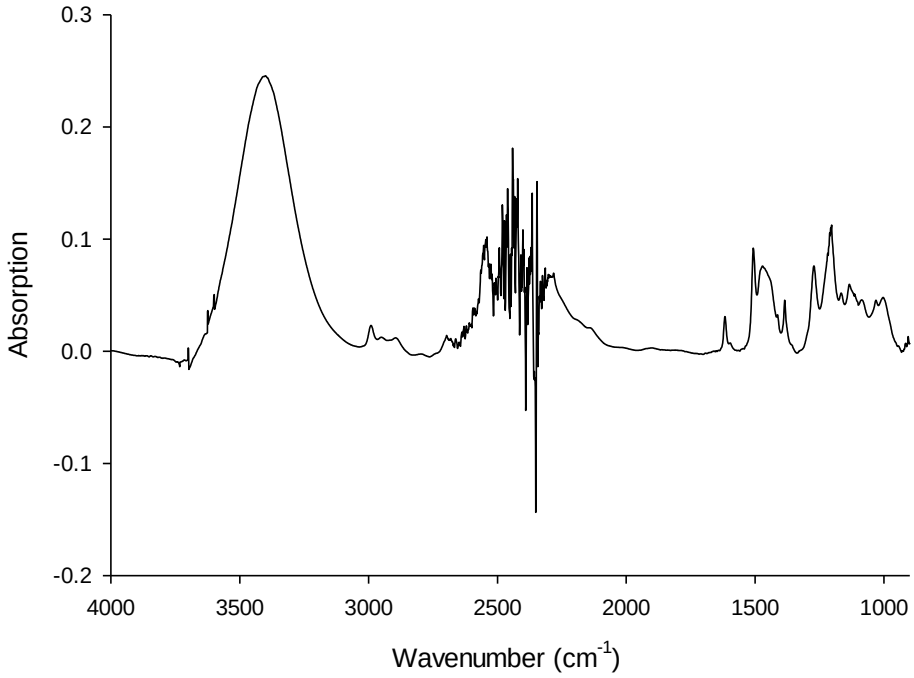

Figure 2.3 – Fourier transformed infrared spectrum of salbutamol base (120 mM, pH 7.4 (± 0.2)) in range of 800 – 4000 cm^{-1}

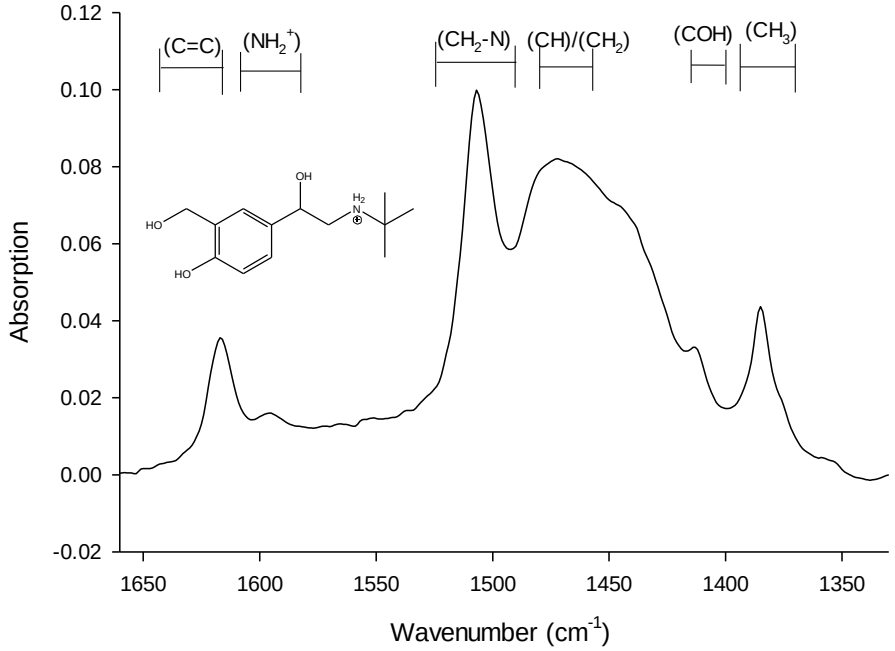

Figure 2.4 – Fourier transformed infrared spectrum of salbutamol sulfate (120 mM, pH 7.4 (± 0.2)) in the region of 1330 – 1670 cm^{-1} with chemical assignments for each peak

The changes in intensity were assessed for 3 main peaks in the spectra which were at 1617, 1507 and 1385 cm^{-1}. It was found that the absorption for these peaks increased linearly with concentration of salbutamol from 100 – 160 mM (figure 2.5) and so it was determined that changes in the ratio of one peak to another with added counter ion could be used to determine the amount of ion-pairing occurring in the system.

FTIR was only used to assess the binding between salbutamol and the sulfate, gluconate, glucoheptonate, and octanoate counter ions as the remaining molecules exhibited a strong peak in the region of 1300 – 1600 cm^{-1} making accurate reading of the salbutamol peaks very difficult.

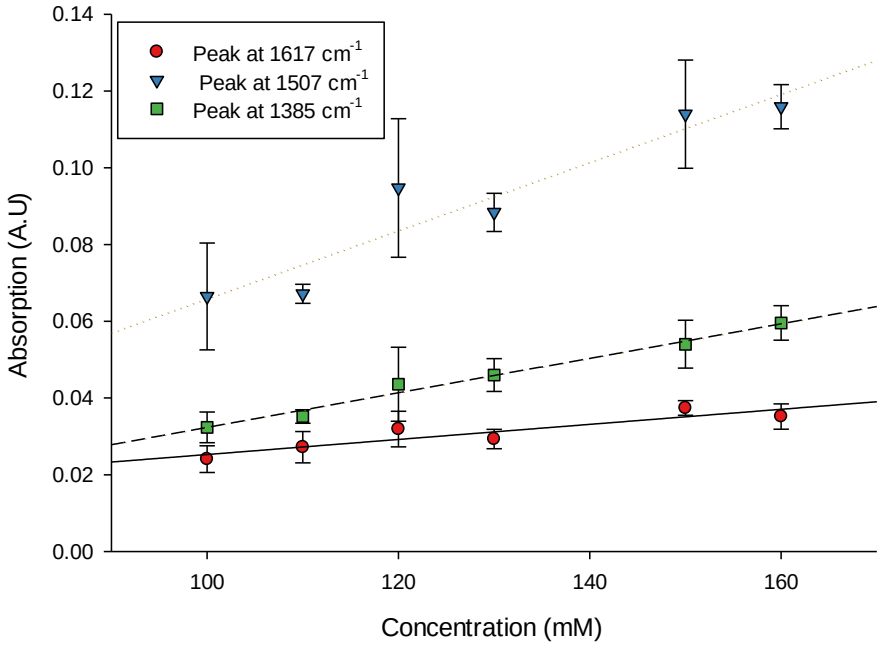

Figure 2.5 – Change in absorption of salbutamol base Fourier transformed infrared spectroscopy peaks found at 1617 cm^{-1} (C=C, red circle, R^2 = 0.831), 1507 cm^{-1} (CH_2-N, blue triangle, R^2 = 0.905), and 1385 cm^{-1} (CH_3, green square, R^2 = 0.984) over a concentration range of 100 – 160 mM. Data represents a mean ± standard deviation (n=3).

The addition of the sulfate, gluconate and glucoheptonate counter ions all resulted in an increase in the N-H peak at 1596 cm^{-1} in comparison to the inert peaks found at 1617 cm^{-1} and 1385 cm^{-1} (C=C and CH_3, respectively). On addition of the octanoate counter ion an increase in the methyl peak at 1385 cm^{-1} in relation to the benzene peak at 1617 cm^{-1} was observed. If increases in counter ion concentration no longer lead to a change in peak absorption it was assumed that 100% of salbutamol was bound in ion-pair form (figure 2.6). This data was replotted as percentage salbutamol bound vs. – log free counter ion and fitted with a sigmoidal curve to give the ion-pair association constant at 50% salbutamol bound (figure 2.7).

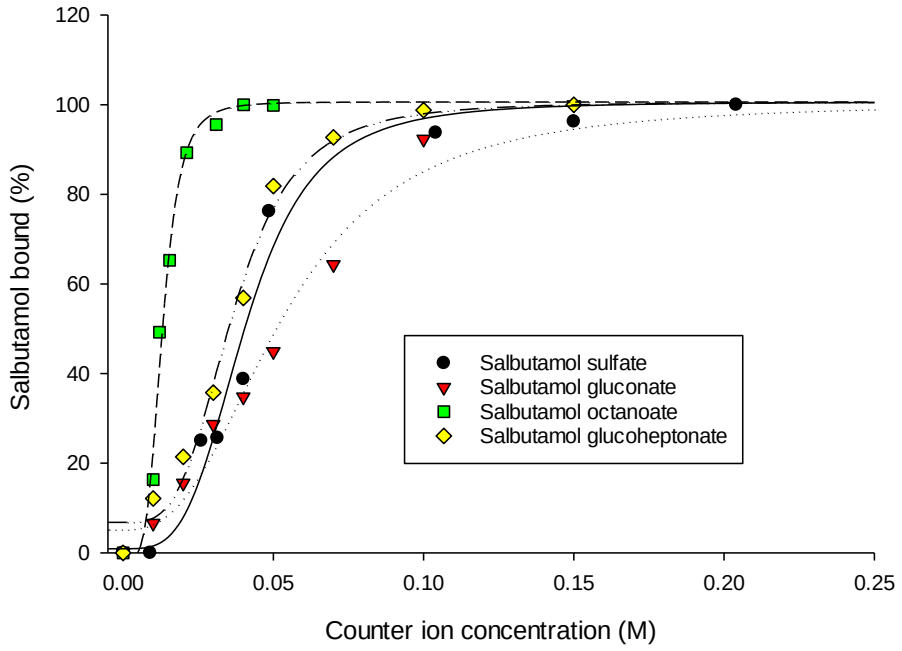

Figure 2.6 - The relationship between the concentration of counter ion and percentage of salbutamol found in ion-pair form for the following ion-pairs: Salbutamol sulfate (black circle), salbutamol gluconate (red triangle), salbutamol octanoate (green square), and salbutamol glucoheptonate (yellow diamond) (n=1).

The association constants calculated from these plots were 1.57, 1.70, 2.27 and 2.56 for salbutamol sulfate, glucoheptonate, gluconate and octanoate ion-pairs respectively (table 2.1).

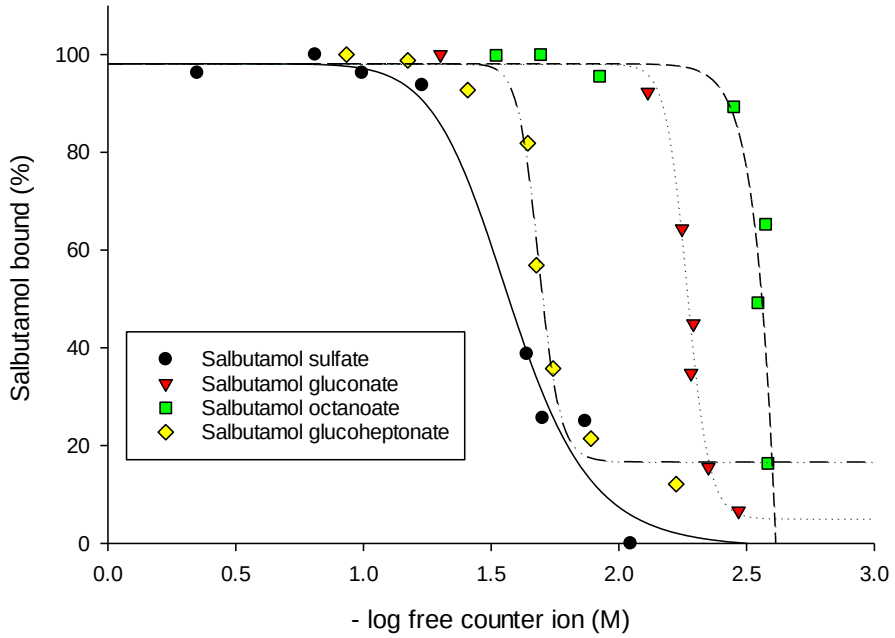

Figure 2.7 – Affinity binding plot for salbutamol sulfate (black circle), salbutamol gluconate (red triangle), salbutamol octanoate (green square) and salbutamol glucoheptonate (yellow diamond) ion-pairs (n=1)

The binding of salbutamol with anionic counter ions was also investigated using an HPLC technique. Samples of 1 mM salbutamol were analyzed by HPLC using a water mobile phase that had been pH corrected to 7.4 (± 0.2) with a flow of 0.3 $mLmin^{-1}$ and a biphenyl column. It was found that in pure water salbutamol had a retention time of 5.47 min (± 0.078). The mobile phase was then changed to a solution of counter ion at a known

concentration, corrected to pH 7.4. The change in retention time of salbutamol with increasing concentration was thought to indicate the percentage of ion-pair formation. The addition of all the counter ions studied resulted in an increase in the retention time of salbutamol (figures 2.8 – 2.10).

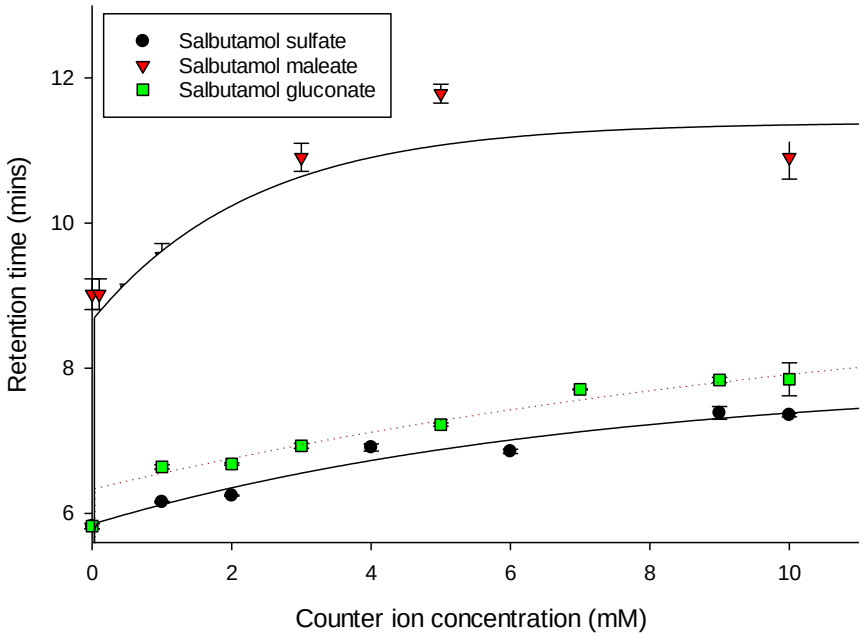

Figure 2.8 – Relationship between the retention time of salbutamol and the counter ion concentration for sulfate (black circle), maleate (red triangle) and gluconate (green square). Data represents a mean ± standard deviation (n=3)

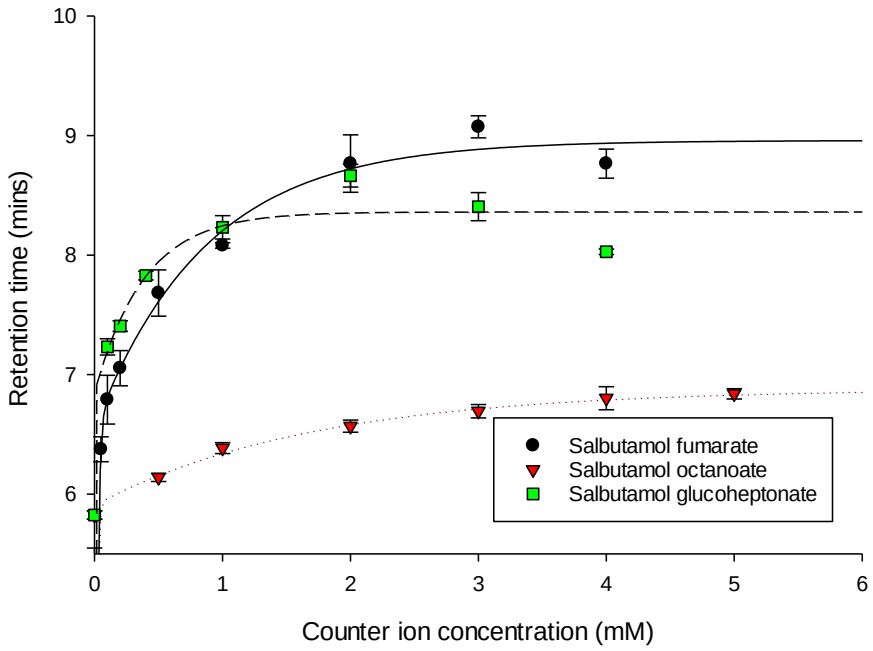

Figure 2.9 – Relationship between the retention time of salbutamol and counter ion concentration for fumarate (black circle), octanoate (red triangle) and glucoheptonate (green square). Data represents a mean ± standard deviation (n=3)

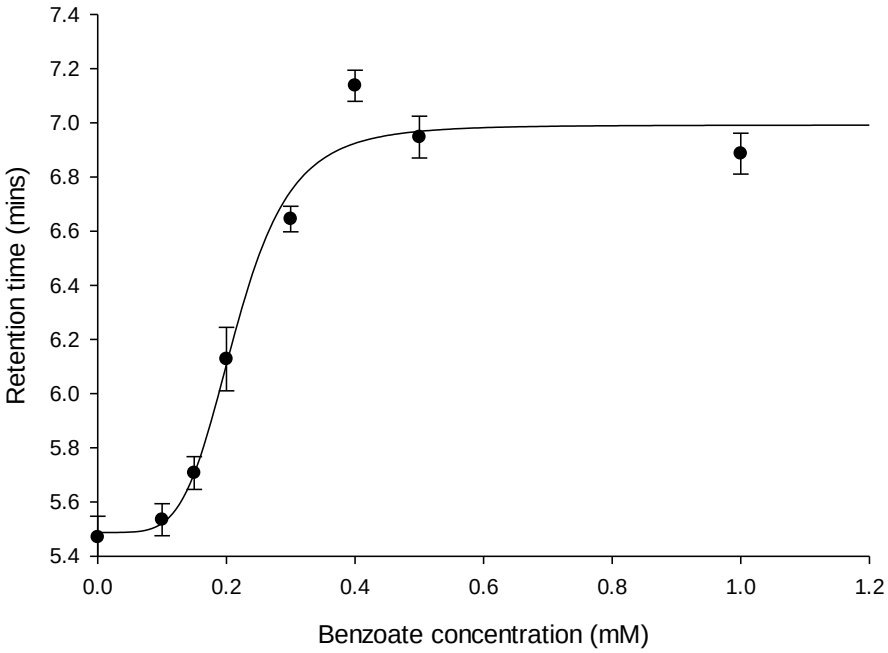

Figure 2.10 – Relationship between retention time of salbutamol and benzoate concentration. Data represents a mean ± standard deviation (n=3)

As with the FTIR data, salbutamol was assumed to be 100% in ion-pair form when an increase in counter ion concentration no longer resulted in a change in retention time. The data was used to plot percentage salbutamol bound vs. –log free counter ion concentration and fitted with a sigmoidal curve, with the 50% bound value giving the association constant for each ion-pair (figure 2.11 – 2.13, table 2.1). The association constants for the sulfate, gluconate, glucoheptonate and octanoate counter ions which were also analyzed via FTIR were 2.37, 2.62, 4.56 and 3.40, respectively (table 2.1). The exact values for association differ between the 2 techniques; however 3 of the counter ions (sulfate, gluconate and octanoate) show the same order of strength of binding. The calculated association constant for the glucoheptonate counter ion varied significantly between the 2 techniques used to calculate it. The association constants for the benzoate, fumarate and maleate counter ions were 3.82, 3.70 and 2.61 respectively (table 2.1). There was a significant increase in the association constant for salbutamol glucoheptonate ion-pair in comparison with the sulfate ion-pair ($p < 0.05$), however there was no significant difference between the other ion-pairs after HPLC binding analysis ($p > 0.05$).

.

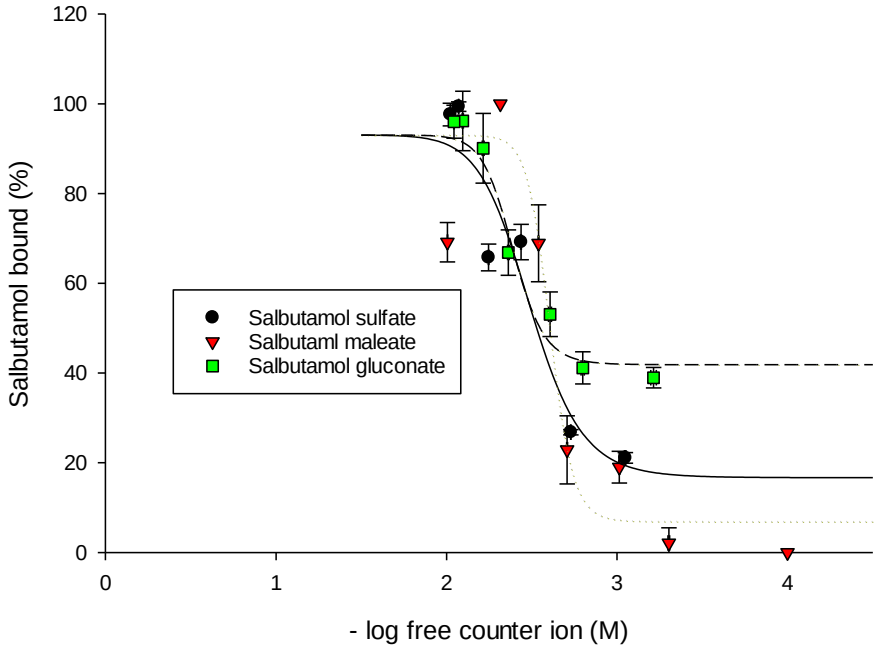

Figure 2.11 – Affinity binding plot from HPLC data for salbutamol sulfate (black circle), salbutamol maleate (red triangle) and salbutamol gluconate (green square). Data represents a mean ± standard deviation (n=3)

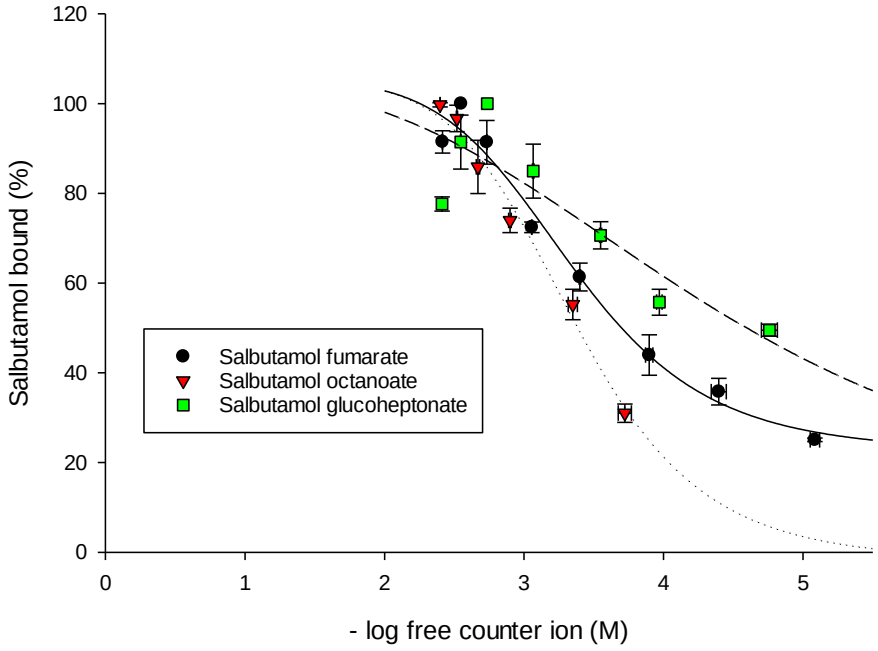

Figure 2.12 – Affinity binding plot from HPLC data for salbutamol fumarate (black circle), salbutamol octanoate (red triangle) and salbutamol glucoheptonate (green square). Data represents a mean ± standard deviation ± (n=3)

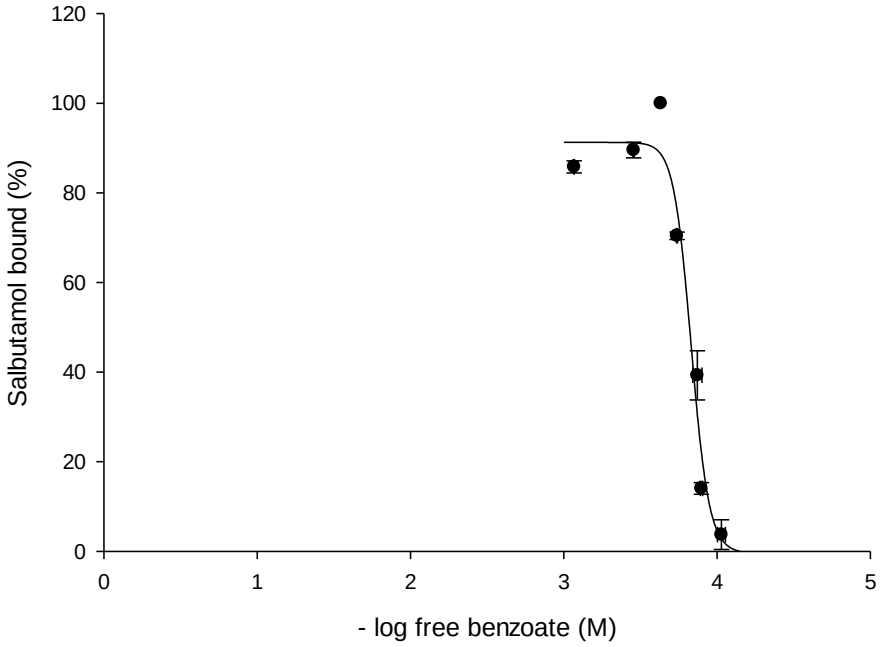

Figure 2.13 – Affinity binding plot from HPLC data for salbutamol benzoate. Data represents a mean ± standard deviation ± (n=3)

The association constants calculated from the HPLC binding study were used in Hyss speciation software to predict the amount of salbutamol thought to be in ion-pair form at a concentration of 0.00209 M and a ratio of either 10:1 or 20:1 counter ion to drug. The values from the HPLC study were used rather than the FTIR as association constants were calculated for all counter ions using this method. The resultant plots show across a pH range of 1 – 14 which form salbutamol is likely to be found in. For each of these calculations a binding ratio of 1:1 was assumed as the excess of counter ion used would primarily facilitate this binding structure (figure 2.14). The speciation curve also shows the percentage of salbutamol H^{-1} and salbutamol H^{-2} which refer to the possible charged species of salbutamol base. At a 10:1 ratio the percentage of salbutamol found in ion-pair form at pH 7.4 ranges from around 80% for the sulfate counter ion, to around 100% for the

glucoheptonate, octanoate, benzoate and fumarate molecules. At a ratio of 20:1 counter ion to drug at the same pH, 90 – 100% of the salbutamol in the system is found in ion-pair form.

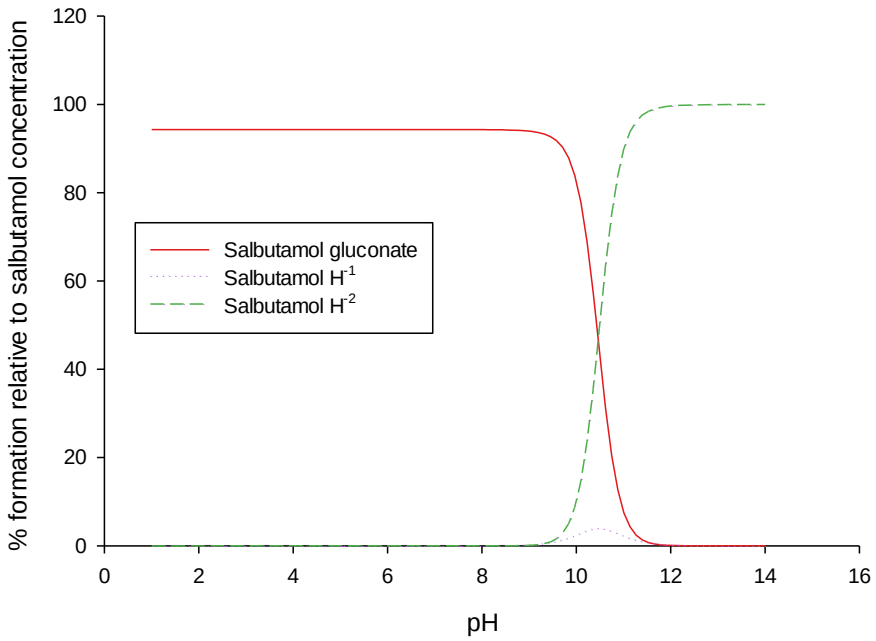

Figure 2.14 – Representative binding graph of 20:1 salbutamol gluconate at a pH range of 1 -14

Table 2.1 – Calculated pKa values from fourier transformed infrared spectroscopy (FTIR) and high performance liquid chromatography (HPLC) studies, and percentage of salbutamol found in ion-pair form at a concentration of 0.00209 M (pH 7.4) as calculated by speciation software for all counter ions. Where NA is shown a value could not be calculated.

Counter ion	FTIR pKa	HPLC pKa	Salbutamol bound at 10:1 ratio (%)	Salbutamol bound at 20:1 ratio (%)
Sulfate	1.57	2.37 (± 0.025)	81.72	90.25
Gluconate	2.27	2.62 (± 0.080)	88.72	94.23
Glucoheptonate	1.70	4.56 (± 0.274)	99.83	99.92
Octanoate	2.56	3.40 (± 0.047)	97.89	98.95
Benzoate	NA	3.82 (± 0.018)	99.15	99.58
Fumarate	NA	3.70 (± 0.106)	98.90	99.48
Maleate	NA	2.61 (± 0.039)	88.48	94.13

2.3.2 The effect of ion-pairing on the partitioning of salbutamol

In order to investigate the effect of ion-pairing on the partitioning of salbutamol a PBS – octanol system was used. Salbutamol base was dissolved in PBS that had been saturated with octanol and the system was corrected to pH 7.4 (± 0.2). Initially, a series of salbutamol concentrations ranging from 0.01 – 1 mM was analyzed in an attempt to ascertain a suitable salbutamol concentration for further experiments. To achieve a true partitioning value it was important to establish that neither of the phases was saturated with drug to ensure free movement. It was found that in the concentration range used the

relationship between absorbance and concentration was linear, suggesting that the aqueous phase was not saturated (figure 2.15). Also, very little of the salbutamol in this system moved to the organic layer.

This experiment was repeated using a 20:1 ratio of the hydrophobic counter ion octanoate, in an attempt to drive more drug in to the organic phase and determine the suitability of these concentrations of salbutamol in terms of the saturation of the octanol layer. It was found that more of the salbutamol was found in the octanol layer after shaking for 48 hours in the presence of the octanoate counter ion. Furthermore, at the concentration range tested, the relationship between the amount of salbutamol found in the organic phase and concentration appeared to be exponential (figure 2.16).

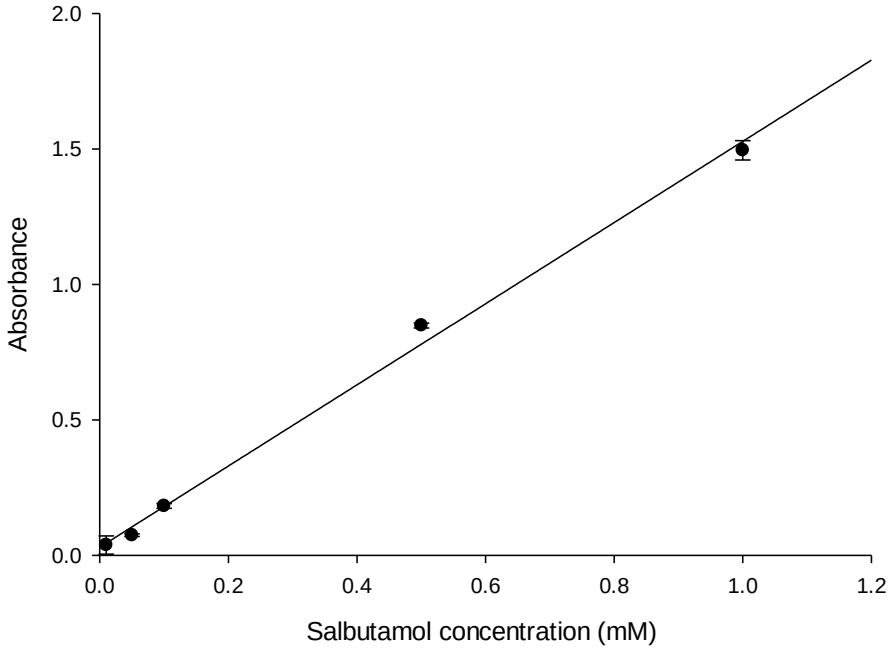

Figure 2.15 – Absorbance values of salbutamol found in aqueous layer after shaking for 48 hours with octanol at a concentration range of 0.01 – 1 mM. Data represents a mean ± standard deviation (n=3)

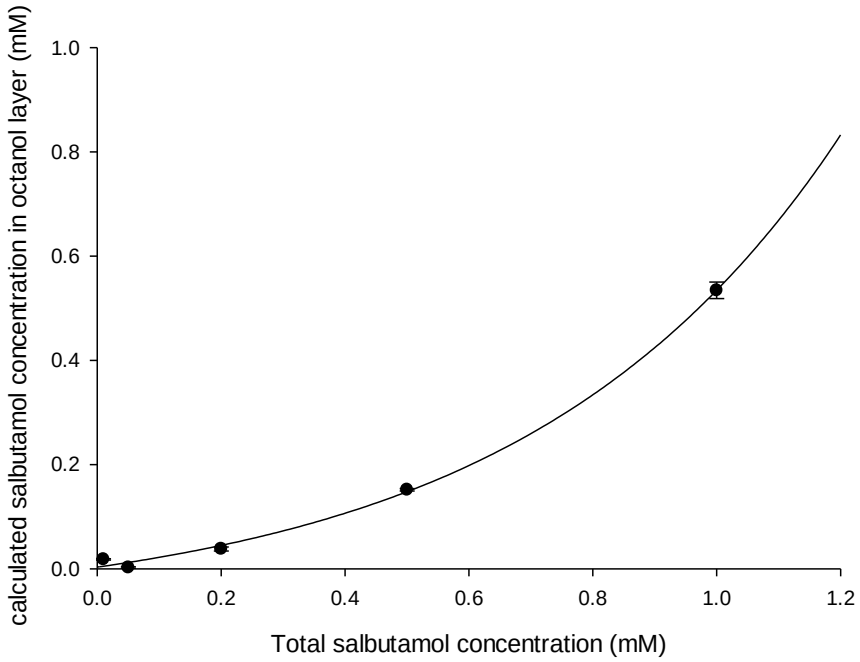

Figure 2.16 – Calculated concentration of salbutamol in octanol layer after shaking in presence of 20:1 octanoate for 48 hours (pH 7.4 (±0.2)). Data represents a mean ± standard deviation (n = 3)

In some systems the overall ionic strength of a solution can influence partitioning results. Differing amounts of acid and base were required to correct the pH of the systems to physiological pH so the ionic strength of the lowest concentration of salbutamol would greatly differ from the highest concentration. To test if the partitioning of salbutamol ion-pairs would be affected by this the previous experiments were repeated for the lowest and highest concentrations of the drug and an amount of NaCl was added to the lowest concentration such that the ionic strength of the solution would be equal to the highest concentration. It was found that there were no significant differences in the results after correcting the ionic strength and so all further experiments were performed without correction (figure 2.17 and 2.18).

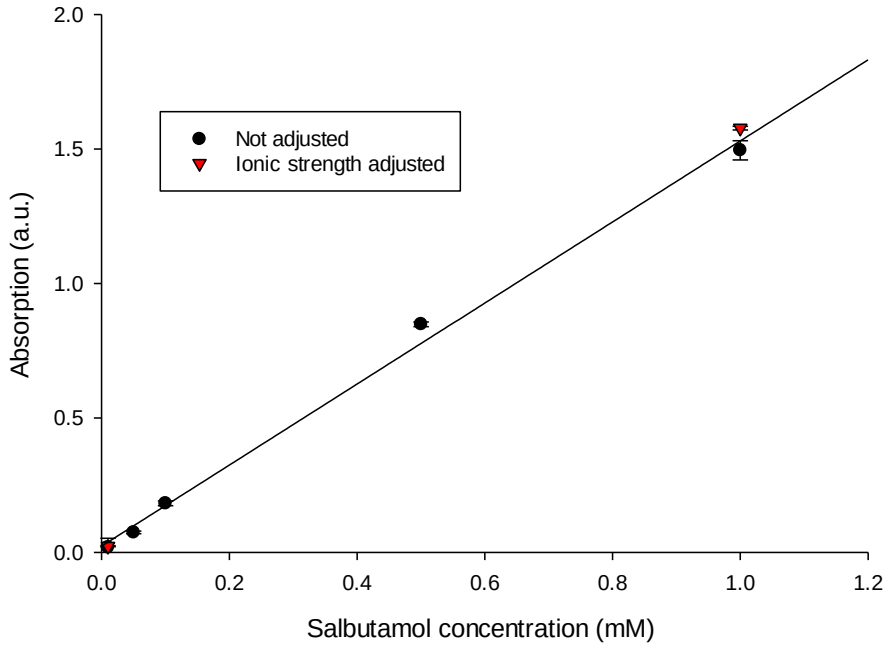

Figure 2.17 - Absorbance values of salbutamol found in aqueous layer after shaking for 48 hours with octanol at a concentration range of 0.01 – 1 mM when the solution had not been corrected for ionic strength (black circle) and when the lowest concentration was corrected with NaCl (red triangle). Data represents a mean ± standard deviation (n=3)

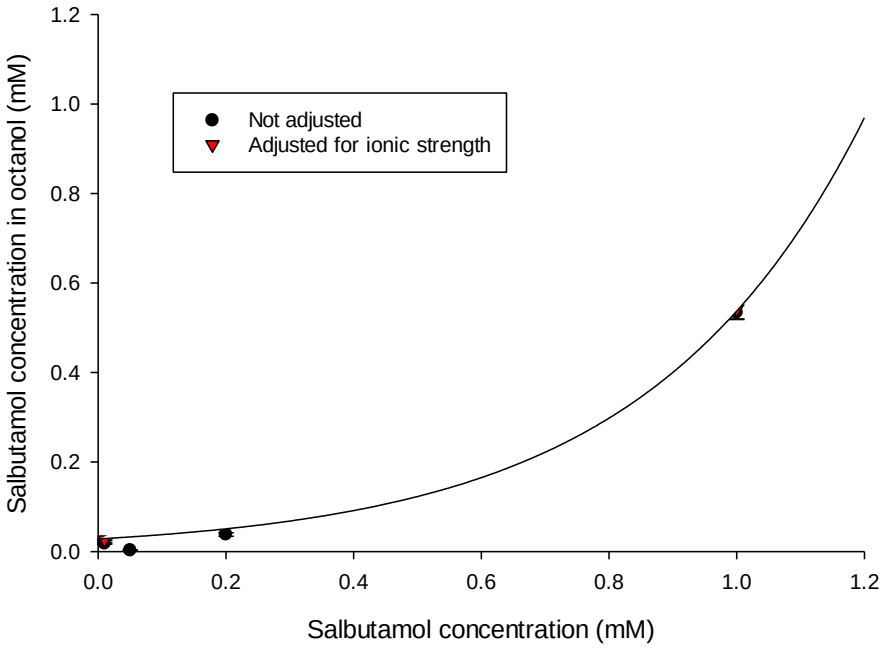

Figure 2.18 - Calculated concentration of salbutamol in octanol layer after shaking in presence of 20:1 octanoate for 48 hours (pH 7.4 (±0.2)) without correction for ionic strength (black circle) and after correction with NaCl (red triangle). Data represents a mean ± standard deviation (n = 3)

A salbutamol concentration of 0.2 mM was chosen to assess the partitioning of salbutamol ion-pairs in this system as this concentration allowed for accurate assaying of the drug and neither the aqueous or organic phase was near saturated at this concentration. Each of the counter ions were dissolved in the aqueous layer with salbutamol at a ratio of 20:1 counter ion to drug and shaken for 48 hours with octanol. The subsequent concentration of salbutamol found in the aqueous phase by UV/vis spectroscopy was used to calculate the partitioning of the drug in ion-pair form between the phases.

$LogD_{7.4}$ values could not be calculated for the benzoate, fumarate or maleate ion-pairs due to a large UV absorption peak from the counter ions that overlapped and obscured the salbutamol peak. It may have been possible to separate these overlapping peaks using

HPLC, however this was not performed as any octanol present in the sample could have been damaging for the column. For the remaining counter ions only 2 significantly changed the partitioning of salbutamol. The glucoheptonate counter ion resulted a significantly lower $logD_{7.4}$ value for salbutamol (-1.845 vs -1.386 for glucoheptonate ion-pair and salbutamol base, respectively, $p<0.05$) and the octanoate counter ion caused a significantly higher $logD_{7.4}$ value (-0.630 vs. -1.386 for octanoate ion-pair and base, respectively, $p<0.05$) (table 2.2).

Table 2.2 – Calculated logD 7.4 values for salbutamol base and all ion-pairs after shaking for 48 hours with a phosphate buffered saline:octanol system, pH 7.4 (± 0.2). Values shown are a mean ± standard deviation (n=3).

Counter ion	Average calculated $LogD_{7.4}$
None	-1.386 (± 0.036)
Sulfate	-1.405 (± 0.265)
Gluconate	-1.241 (± 0.228)
Glucoheptonate	-1.845 (± 0.118)
Octanoate	-0.630 (± 0.055)

The salbutamol octanoate ion-pair was investigated using photon correlation spectroscopy to examine whether the surfactant counter ion was forming micelles. A concentration range of 0.042 – 20.90 mM 20:1 salbutamol octanoate in PBS (pH 7.4) was compared to the same concentrations of 20:1 salbutamol sulfate. The derived count rate was observed

for each of the concentrations, and where this value was found to be over 1000, a size was generated.

It was found that there was no difference between the derived count rate values for salbutamol octanoate and salbutamol sulfate solution up to 0.42 mM ($p > 0.05$). At 2.1 and 4.2 mM concentration there was an increase in the derived count rate for salbutamol octanoate, with the highest values for 4.2 mM reaching around 2000 kcps (figure 2.19). However, a drop in the count rate was then observed for the 21 mM concentration and this value did not significantly differ from the salbutamol sulfate control. There was no significant difference between the results for salbutamol octanoate and salbutamol sulfate at the concentration used in the partitioning results (0.2 mM) ($p > 0.05$).

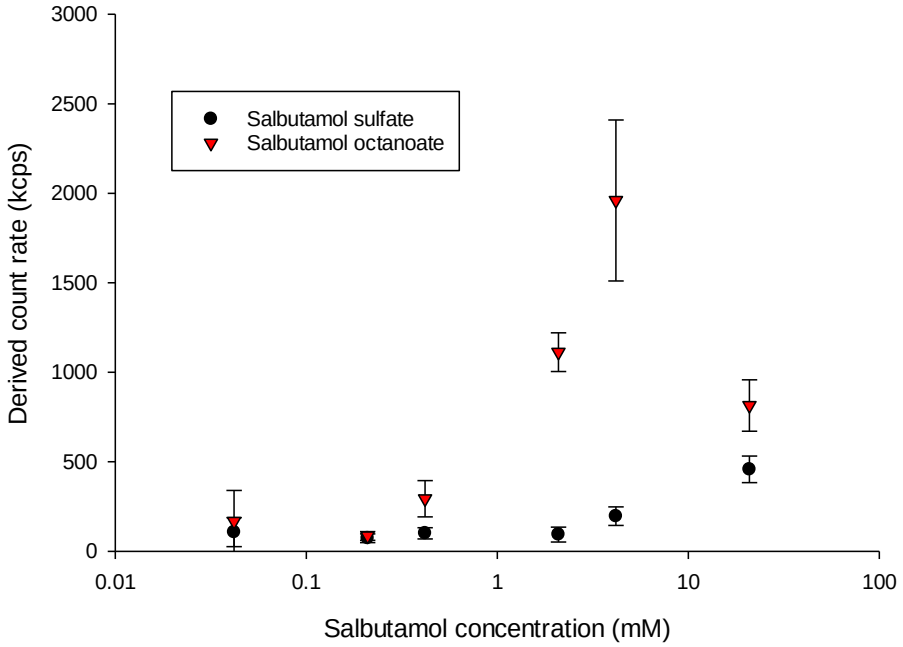

Figure 2.19 - Comparison of the derived count rates for 20:1 salbutamol sulfate (black circle) and salbutamol octanoate (red triangle). Data represents a mean ± standard deviation (n=3)

2.3.3 The effect of ion-pairing on the solubility of salbutamol

It was found that the solubility of salbutamol in the majority of the ion-pair powders was lower than that of base alone. The solubility of salbutamol in the base powder was 5.37 mg/mL. The solubility of salbutamol in the fumarate or sulfate ion-pair powders did not significantly differ from the base ($p > 0.05$). However there was a significant difference between all other ion-pair powders and the base ($p < 0.05$). The lowest concentration of salbutamol was found in the gluconate ion-pair powder, with a solubility of 3.53 mg/mL.

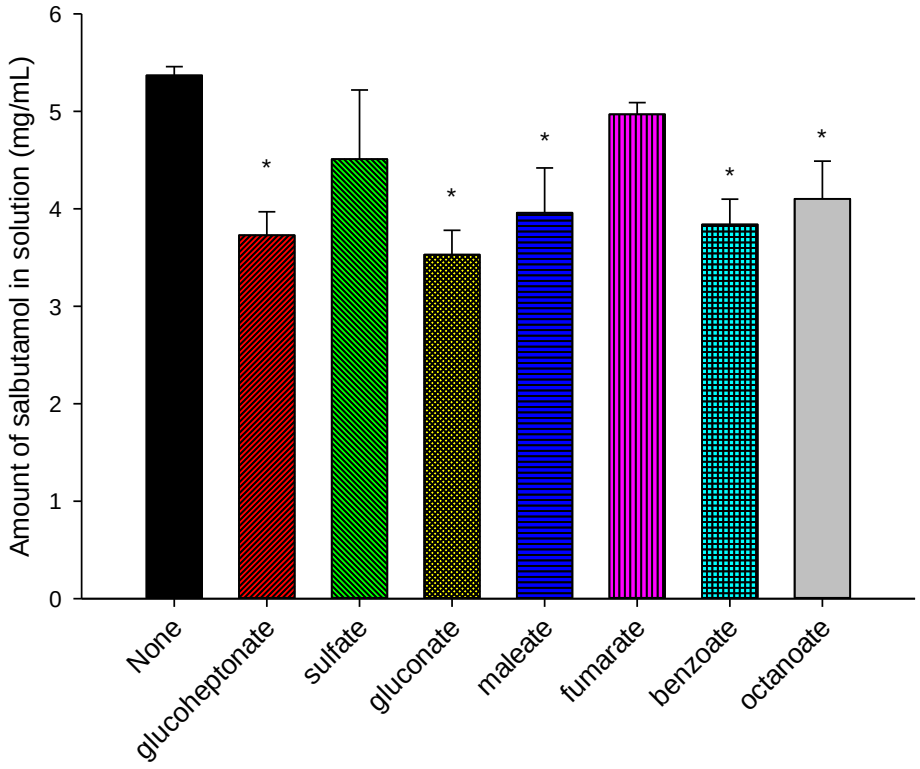

Figure 2.20 – Solubility of salbutamol in base and ion-pair lactose formulations in Hanks balanced salt solution after stirring for 24 hours with a magnetic bar in a water bath at 37°C. Data represents a mean ± standard deviation (n=3). * denotes a significant difference in comparison to the salbutamol base powder.

2.4 Discussion

Both the FTIR and HPLC ion-pair binding analysis methods showed that salbutamol forms an ion-pair with each of the counter ions. The absolute values for association constants differed by up to 2.86 between the 2 methods. This is not surprising given the different methods by which the analytical methods act to determine the ion-pair association. FTIR spectroscopy works by passing infra-red radiation through a sample and determining the radiation that is absorbed at specific frequencies (Wartewig and Neubert, 2005). This allows the analysis of complex molecular vibrations and rotations within a molecule (Schmitt and Flemming, 1998). These vibrational bands are specific for the molecules involved in the bond and their orientation and so can be used to identify functional groups in a molecule (Schmitt and Flemming, 1998, Wartewig and Neubert, 2005). Thus changes in the FTIR spectrum of salbutamol on the addition of counter ion must result from a change to the conformation of that bond or its environment. Upon addition of the sulfate, gluconate and glucoheptonate counter ions to the salbutamol solution an increase in the peak assigned to the N-H functionality (1596 cm^{-1}) of the drug was observed. This could indicate the presence of the electrostatic attraction between the 2 ions, as ionic bonding would potentially limit the movement of the N-H bond. Conversely, the addition of the octanoate counter ion to the salbutamol solution caused an increase in the absorption of the peak assigned to the methyl groups of salbutamol, found at 1385 cm^{-1}. This would indicate that the binding between salbutamol and the octanoate counter ion occurred in a different way to the previous 3 counter ions or potentially that the conformation of the ion-pair with this hydrophobic counter ion affected the movement of the methyl groups.

Chromatography entails the separation of components of a mixture by use of an adsorbent material. During the HPLC process a liquid mobile phase is pumped through a column containing a stationary phase to achieve this separation (Weston and Brown, 1997). In this study a biphenyl stationary phase was used, meaning that the functional group presented to any molecules from this phase were hydrophobic biphenyl and trimethylsilyl groups. As such it would be expected that more hydrophobic molecules have a longer retention time, due to the increased interactions with the stationary phase. The retention time of salbutamol base in this system was 5.47 min, and this was increased with the addition of each of the counter ions. This would suggest that each of the ion-pairs is more hydrophobic than the base itself but could also be caused by a conformational change of the salbutamol molecule or an overall reduction of the charge on the salbutamol in ion-pair form that favours these interactions, and this may not result in an overall increase in log P.

The rank order of binding strength between ion-pairs was similar after analysis with the HPLC and FTIR techniques. The relatively small sulfate ion had the weakest binding with salbutamol, with a conditional association constant of 1.57 in the FTIR study and 2.37 in the HPLC study. Whereas the larger and more hydrophobic octanoate counter ion displayed stronger binding to salbutamol with association constants of 2.56 and 3.40 from FTIR and HPLC, respectively. The one counter ion that did not follow the same ranking of strength of binding between the two techniques was the glucoheptonate counter ion. The salbutamol glucoheptonate ion-pair had a dissociation constant of 1.70 when studied by FTIR, making it the second weakest. However when studied by HPLC the ion-pair displayed the strongest binding of all the counter ions investigated, with a dissociation constant of 4.56. This indicates the possibility of a large disparity in results between different techniques when attempting to quantify the binding of an ion-pair.

Out of the 2 techniques used in this study, the FTIR would provide the most accurate information about the binding between the drug and the counter ion as it provides information on the changes in specific functional groups of the drug on association. The FTIR method is observing the primary interaction between the 2 counter ions, whereas the HPLC method is measuring a secondary interaction after further binding to a stationary phase. However, the HPLC method was able to provide information on salbutamol binding to all of the counter ions and so it was also very useful. Further techniques that could be used to study the association of ion-pairs include UV/vis spectroscopy and nuclear magnetic resonance (NMR) spectroscopy (Nie et al., 2015, Dezhampanah and Chokami, 2014). The counter ions chosen for this study had a range of log P values and functional groups that could bind to the salbutamol molecule, the results show that ion-pairs form with both lipophilic and hydrophilic molecules and that the strength of the interaction may increase with the amount of binding sites on the counter ion.

Although the 2 methods of ion-pair binding analysis gave differing results for the same ion-pair, they both showed that the binding of each ion-pair was sufficient for the purpose of an ion-pairing drug delivery system. All the association constants calculated were in the order of 1.5 – 5. To put this in to perspective, the association constant for the binding of the 2 ions in LiOH is 0.36, whereas the binding between a hydroxide ion and proton to give water has an association constant of 13.98 (Smith and Martell, 1989). This shows that the association between ions in the ion-pairs is stronger than that of small inorganic ions, but is also likely to dissociate when diluted in larger volumes of liquid as expected.

The partitioning of salbutamol base between PBS and octanol gave a partition coefficient of – 1.386. This differs from the reported values of water/octanol partition coefficients for

salbutamol base which range from -0.79 (Lin et al., 2005) to 0.11 (Forbes et al., 2003), but is very similar to the predicted value at pH 7.4 which is -1.32 (Patel et al., 2016). The calculated Log P from Lin et al was reached after experimentation at room temperature, whereas the experiment in this study was conducted at 37^{o}C, and so it is difficult to conclude whether the ions present in PBS, the control of pH or the difference in temperature could have led to the dissimilarity in results. PBS was used in this study instead of water in an attempt to create an environment that is a better mimic of the liquid in the lungs than pure water due to the physiological level of ions present (Pelfrêne et al., 2017). It has been shown in the literature that ion-pairing a drug molecule with a counter ion can significantly increase or decrease the logP of the drug molecule (ElShaer et al., 2014, Samiei et al., 2014) however residual charges on the ion-pair species can minimize the change in partition coefficient (Hatanaka et al., 2000). The partitioning study showed that the log$D_{7.4}$ of the sulfate and gluconate ion-pairs did not significantly differ from that of salbutamol base. The partition coefficient found in this study (- 1.405) does not significantly differ from literature values for the hemisulfate (-1.58) (Lin et al., 2005). However the lack of difference in partitioning between the base and sulfate ion-pair was unexpected, as this is often hypothesized to be the cause of the difference in cellular transport rates between the base and hemisulfate (Haghi et al., 2012). The hydrophilic counter ion glucoheptonate caused a significant decrease in the log$D_{7.4}$ value of the base, and the hydrophobic octanoate counter ion caused a significant increase. However, all ion-pairs still displayed a negative partitioning coefficient and all fall within a relatively narrow range, which could suggest that the differences in cell transport between these complexes would not be significant (Forbes et al., 2003, Foster et al., 2000).

The potential for the octanoate counter ion to form an organized structure, such as micelles, was investigated using PCS. The critical micellar concentration (CMC) of sodium octanoate is reported to be 300 mM (Stanley et al., 2009), however it was unknown whether ion-pairing or the presence of salbutamol would effect this. Therefore the effect of increasing octanoate concentration on the light intensity (derived count rate) was examined. In the concentration range studied there was not a significant enough increase in the derived count rate to assume that any form of micelle had been formed.

The solubility of salbutamol base in a lactose formulation was calculated as 5.37 mg/mL. This was significantly reduced in each of the ion-pair formulations apart from salbutamol fumarate. The glucoheptonate ion-pair had the lowest solubility at 3.53 mg/mL; this is contradictory to what would be expected when looking at the partition coefficient as the significant decrease seen would indicate that the ion-pair is more hydrophilic than the base itself and therefore should be more soluble. Possible explanations for this include that hydrophilic functional groups that were previously involved in the dissolution of salbutamol are now preferentially involved in the ion-pairing and that the ion-pair species negates the charge of the salbutamol molecule (Song et al., 2016).

2.5 Conclusion

Salbutamol was shown to form ion-pair complexes with a range of counter ions at differing strengths. The binding constants gained from HPLC studies were used to predict the percentage of salbutamol found in ion-pair form at physiological pH. It was found that at a 20:1 ratio of counter ion to drug that at least 90% of salbutamol (0.00209 M) would be in ion-pair form for each counter ion. The $logD_{7.4}$ for salbutamol base and ion-pairs was examined with significant changes to $logD_{7.4}$ being achieved for the glucoheptonate and

octanoate ion-pairs. The solubility of each of the ion-pairs except for salbutamol sulfate and salbutamol fumarate was found to be lower than salbutamol base in a lactose formulation after 24 hours. The sulfate, gluconate and octanoate counter ions were chosen to take forward to ion-pair formulation development in Chapter 4. The gluconate and octanoate counter ions were chosen because of their differences in functionalities, gluconate is a hydrophilic counter ion with multiple sites for hydrogen bonding whilst octanoate is hydrophobic, and their binding strength with salbutamol (2.27 and 2.56 association constants for salbutamol gluconate and octanoate, respectively, in the FTIR assay). Salbutamol sulfate was chosen as a comparison as it is the most widely known form of salbutamol and yet appeared to be the most weakly bound ion-pair (association constant is 1.57 by FTIR). The next chapter will explore the potential of salbutamol to form ion-pairs with novel pharmaceutical counter ions derived from phytic acid.

Chapter 3

Development of Phytic Acid as a Novel Ion-pair Agent

3.1 Introduction

Phytic acid, or *myo*-inositol hexakisphosphate (IP_6), is a compound found abundantly in plants, it makes up between 1 and 5% of weight of many cereals, legumes, nuts and pollen (Graf et al., 1987, Graf and Eaton, 1990, Gupta et al., 2015). It accounts for around 70% of the total phosphorous content of plants (Gupta et al., 2015, Zhou and Erdman Jr, 1995) and is also found and synthesized in animal cells (Letcher et al., 2008). Its structure comprises a central cyclohexane with phosphoric ester linkages present from each carbon (figure 3.1). Phytic acid has been found to have many advantageous interactions with the body: it has been shown to reduce blood glucose levels and improve insulin sensitivity in normal and diabetic rats (Kim et al., 2014); it has antioxidant properties, binding to Fe^{3+} and preventing the formation of hydroxyl radicals (Graf et al., 1987, Hawkins et al., 1993); and it has even been shown to have anticancer properties (Vucenik and Shamsuddin, 2003, Barahuie et al., 2017).

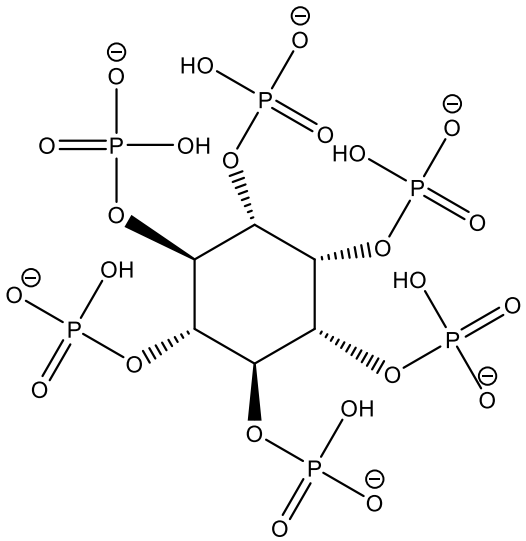

Figure 3.1 - Chemical Structure of Phytic acid at pH 7.4

Despite the numerous beneficial properties of the molecule, Phytic acid is often thought of as an anti-nutrient due to its inhibitory effect on the bioavailability of minerals such as zinc (Zhou and Erdman Jr, 1995, Hurrell, 2003). Phytic acid has a strong chelating capacity and forms complexes with minerals when ingested which are often soluble in the acidic pH of the stomach, but insoluble in the higher pH of the intestines, preventing uptake of the mineral (Zhou and Erdman Jr, 1995).

However, it is this strong chelating ability that could make phytic acid an ideal candidate for an ion-pairing strategy. As well as minerals, phytic acid has the potential to form strong complexes with organic drug compounds, and due to the presence of multiple phosphate groups present on the acid, it could also bind to several drug molecules at once. Coupled with the fact that phytic acid is known to be found in the body, and is therefore predicted to be biocompatible, it is an extremely interesting molecule and its use in an ion-pairing formulation deserves further investigation.

The drawback of using phytic acid in an ion-pair formulation with salbutamol is the size of the molecule. Phytic acid has a molecular weight of 660.03 $gmol^{-1}$. A complex with one or multiple salbutamol molecules would result in a complex with a much larger molecular weight than the salbutamol ion-pairs studied in Chapter 2, and also larger than the long acting β2-agonists formoterol and salmeterol, which have molecular weights of 344.41 and 415.57 $gmol^{-1}$, respectively. It is well known that smaller molecules are absorbed through epithelial layers more rapidly (Jitendra et al., 2011) and so it is crucial that the transport of the drug across the bronchial epithelium is not hindered in such a way as to lengthen the onset of action.

Phytic acid is metabolized by the phytase enzyme in to smaller inositol phosphates (IP_1 – IP_5) which are also found in plants and in the body (Steer and Gibson, 2002). Both phytic acid and its metabolites may be suitable to form an ion-pair with salbutamol to control its release as it could form a large hydrophilic complex that would slowly pass through respiratory epithelial cell. Of the metabolites, D-*myo*-inositol-1,4,5-trisphosphate (IP_3) was chosen as a second suitable candidate for an ion-pairing strategy with salbutamol (figure 3.2). The molecular weight of this compound is much lower than phytic acid, at 420.10 $gmol^{-1}$, but it retains multiple phosphate groups that could facilitate binding with the salbutamol molecule and the generation of a hydrophilic complex

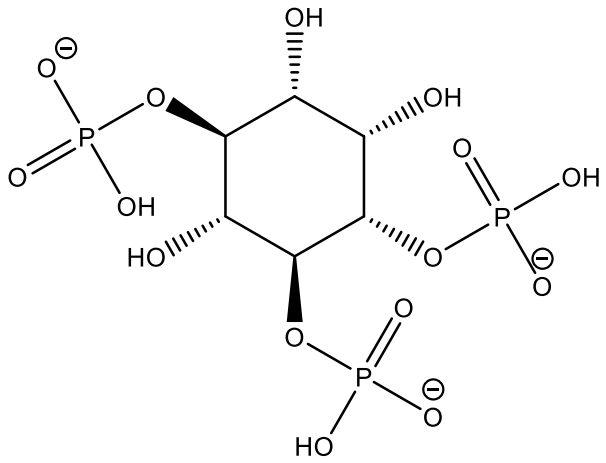

Figure 3.2 - Chemical structure of D-*myo*-inositol-1,4,5-trisphosphate (IP_3) at pH 7.4

IP_3 is commercially available, however it is also extremely expensive, and so a new synthetic method to generate the molecule *in situ* was thought to be required for its use in an ion-pairing formulation to be viable. The aim of this chapter, therefore, was to establish a synthetic method to generate D-*myo*-inositol-1,4,5-trisphosphate in sufficient quantities

to investigate its binding with salbutamol. This molecule and phytic acid would then be investigated as counter ions for an ion-pairing strategy with salbutamol using the methods established in Chapter 2. The effect of these ion-pairs on the lipophilicity of salbutamol was analyzed.

There are 2 potential ways in which to generate the IP_3 molecule, from a top-down or a bottom-up approach. The top-down approach would involve hydrolyzing the phytic acid molecule with a phytase enzyme and purifying the IP_3, whereas the bottom-up approach would be to chemically synthesize the molecule. Preliminary studies showed that the dephosphorylation process was long and resulted in a mixture of many different inositol phosphates that were difficult to identify and separate, this correlates with findings that the rate and order of hydrolysis of phosphate groups by phytase enzymes are inconsistent (Konietzny and Greiner, 2002). It was therefore decided that a chemical synthesis method of IP_3 from *myo*-inositol would be employed for the purpose of the work in this chapter.

Synthesis of inositol phosphate compounds is reportedly very difficult due to the chiral nature of the molecules and the difficulties associated with phosphorylation (Meek et al., 1988, Durantie et al., 2016). Chemical syntheses with expensive or difficult to produce chiral precursors would not be suitable for production of IP_3 for a ion-pairing formulation. Therefore a synthetic route with a limited number of synthetic steps that utilized cheap, readily available starting materials was chosen. The method chosen reportedly produced IP_3 in a high yield and so it was thought to be an ideal route to IP_3 for ion-pairing (Meek et al., 1988).

3.2 Materials and Methods

3.2.1 Materials

Salbutamol base (BN. H80619) was from Cipla Ltd, India and used without further purification. *Myo*-inositol, silicone oil, p-toluenesulfonic acid (p-TSA), trimethylamine (Et_3N), dimethyl chlorophosphate, pyridine, diethyl ether, acetone, N,N-dimethylformamide (DMF), N,N-diisopropylethylamine, deuterated chloroform, deuterated water, HPLC grade water and PBS were all purchased from Sigma Aldrich (Dorset, UK). 2,2-dimethoxypropane, deuterated dimethyl sulfoxide (DMSO) and acetonitrile were purchased from Thermo Fisher Scientific (Geel, Belgium). N-octanol, hexane and ethyl acetate were from Fisher Scientific (Leicestershire, UK). Benzoyl chloride and phytic acid dipotassium salt were both from Santa Cruz Biotechnology (USA). Deuterated methanol and , hydrobromic acid 45% w/v solution in acetic acid were acquired from Cambridge Isotope laboratories (Massachusetts, USA) and 4-dimethylaminopyridine (4-DMAP) and acetyl chloride were purchased from Fluka Analytical (Durban Kwuzulu Natal, South Africa).

3.2.2 Synthesis of D- *myo*-inositol-1,4,5-trisphosphate

The synthesis of D-*myo*-inositol-1,4,5-trisphosphate (IP_3, compound 5) was attempted by following protocols found in the literature (Khersonsky and Chang, 2002, Meek et al., 1988). The complete synthetic route is shown in figure 3.3. The synthesis and analysis of products were completed by MPharm students Evgenia Kyriakopoulou and Amir Khosravi-Nik under the careful supervision of Bridie Dutton.

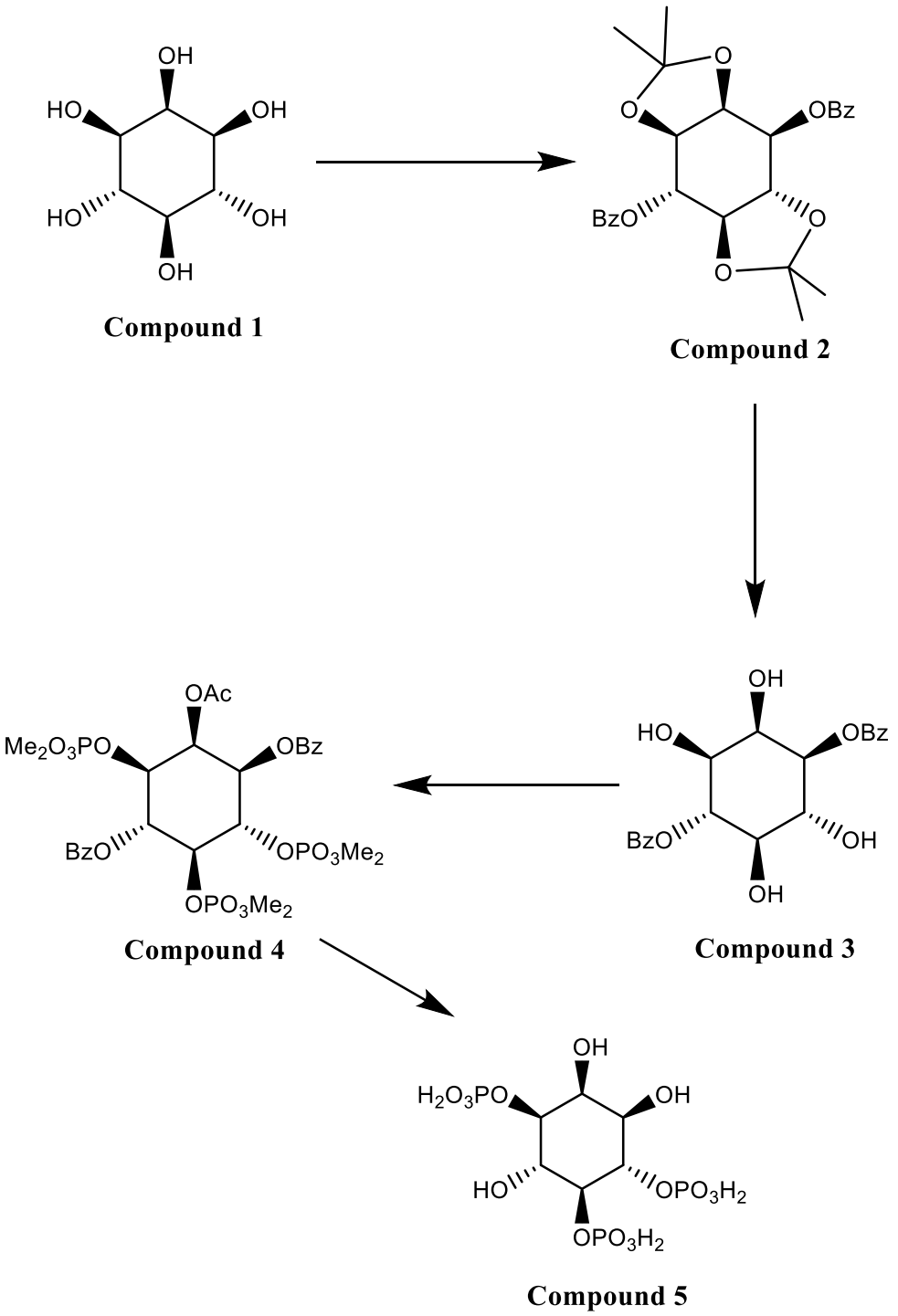

Figure 3.3 - Planned synthetic route from myo-inositol to D- myo-inositol-1, 4, 5-trisphosphate

3.2.2.1 Synthesis of 1,2:4,5-di-O-isopropylidene-3,6-di-O-benzoyl-inositol

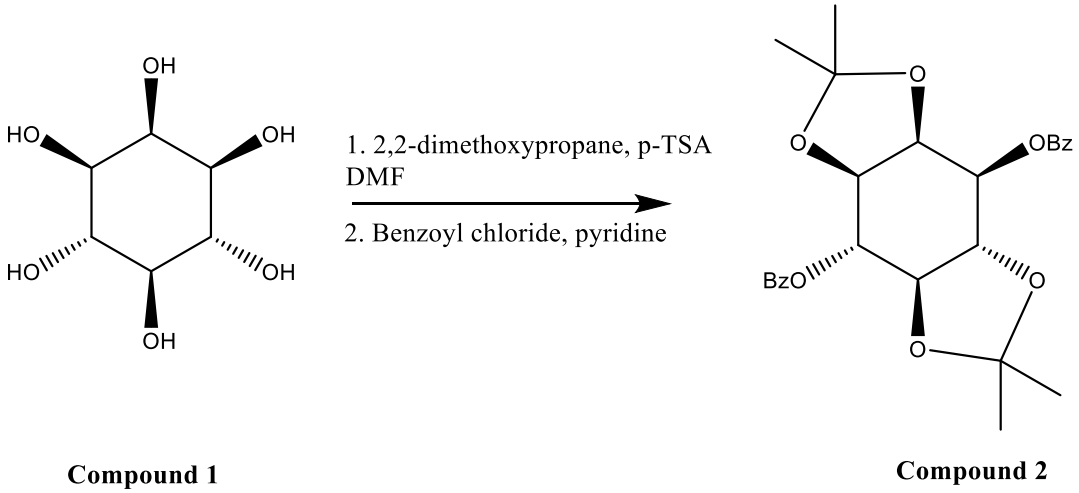

Figure 3.4 - Synthetic route for synthesis of *1,2:4,5-di-O-isopropylidene-3,6-di-O-benzoyl-inositol (compound 2)*

A mixture of *myo*-inositol (25 g, compound 1), p-TSA (0.5 g) and 2,2-dimethoxypropane (75 mL) in DMF (100 mL) was heated to 120^{o}C for 3 hours before being rotary evaporated to dryness. To the residual oil was added Et_3N (0.36 mL) and ethyl acetate (100 mL). The mixture was rotary evaporated with silica (40 g) to complete dryness. The silica powder was put in a column (5 x 9 cm) and washed thoroughly with ethyl acetate (700 mL). The solvent was removed *in vacuo* and the residual oil was cooled to 0^{o}C before pyridine (70 mL) and benzoyl chloride (50 mL) were added to it. The reaction mixture was stirred for 3 hours at room temperature. The precipitate was filtered and washed with pyridine (50 mL), water (150 mL), acetone (40 mL) and diethyl ether (50 mL). After vacuum drying, 1,2:4,5-di-O-isopropylidene-3,6-di-O-benzoyl-inositol (compound 2) was collected as a white solid (16.8 g, 27% yield).

A melting point test of the collected powder was performed by filling a capillary tube with a small amount of the product, placing the tube in a melting point apparatus (1A9000 Series; Electrothermal Cat, Bibby Scientific Limited, Staffordshire, UK) and recording the temperature at which the product melted. The product was dissolved in deuterated chloroform and analyzed by ^{1}H NMR (Bruker Advance DRX 400 MHz NMR Spectrometer).

3.2.2.2 Synthesis of 1,4-Di-O-benzoyl-<u>myo</u>-inositol

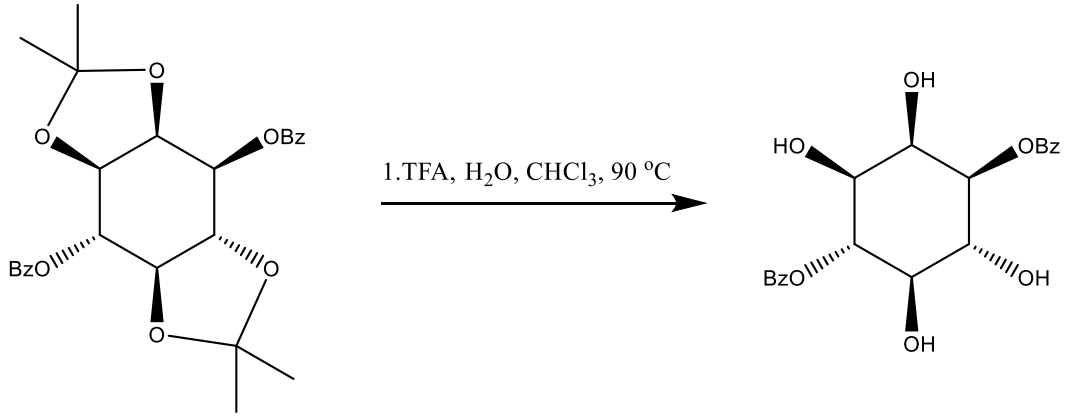

Compound 2 **Compound 3**

Figure 3.5 - Synthetic route for synthesis of 1,4-Di-O-benzoyl-myo-inositol (compound 3)

TFA (23 mL) and H_2O (2.3 mL) were added to a suspension of 1,2:4,5-di-O-isopropylidene-3,6-di-O-benzoyl-inositol (compound 2) (15 g) in boiling chloroform (210 mL). The mixture was refluxed for 1 hour and then cooled to 0^{o}C for 1 hour. A precipitate formed which was filtered and washed with diethyl ether (100 mL). After vacuum drying, 1,4-Di-O-benzoyl-myo-inositol (compound 3) was collected as a white solid (9.3 g, 75% yield). Melting point analysis and ^{1}H NMR were carried out as previously described, using DMSO-d_6 as the NMR solvent. Thin layer chromatography (TLC) was performed using

chloroform-methanol (9:1) as the solvent. The retention factor (R_f) was calculated and compared to that in the literature (Meek et al., 1988).

3.2.2.3 Synthesis of 2-O-Acetyl-3,6-di-O-benzoyl-myo-inositol-1,4,5-triphosphate

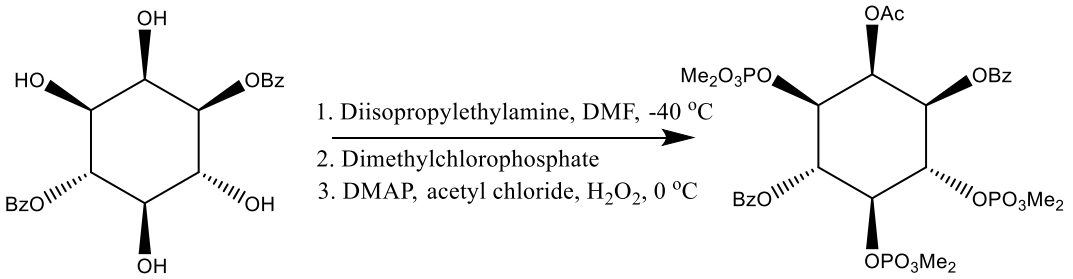

Compound 3 **Compound 4**

Figure 3.6 - Synthetic route for synthesis of *2-O-Acetyl-3,6-di-O-benzoyl-myo-inositol-1,4,5-triphosphate (compound 4)*

Dry diisopropylethylamine (14 mL) was added to a solution of 1,4-Di-O-benzoyl-myo-inositol (compound 3) (5.4 g) in dry DMF (54 mL) and the solution was cooled to -40°C. Dimethyl chlorophosphate (5 mL) was added dropwise to the solution, ensuring that the temperature stayed at -40°C and the mixture was stirred for 30 minutes before it was allowed to warm to room temperature. 4-DMAP (134 mg) and acetyl chloride (1.9 mL) were added and the solution was stirred for a further 30 minutes. Hydrogen peroxide 27.5% (18 mL) was added dropwise and the solution was cooled to 0°C and left at this temperature overnight. The solution was dried *in vacuo* before the addition of DCM (50 mL) and H_2O (100 mL). The organic layer was collected using a separating funnel and to it

was added anhydrous sodium sulfate (40 g). This was filtered and the filtrate was rotary evaporated to dryness. The product was recrystallized by dissolution in DCM (5 mL) and addition of hexane (50 mL). The resulting crystals were filtered and dried under vacuum to give 2-O-Acetyl-3,6-di-O-benzoyl-myo-inositol-1,4,5-triphosphate (compound 4) as a white solid (1.8 g, 17% yield). This melting point and ^{1}H NMR in $CDCl_3$ of this product were performed as described previously.

3.2.2.4 Synthesis of D- myo-inositol-1, 4, 5-trisphosphate

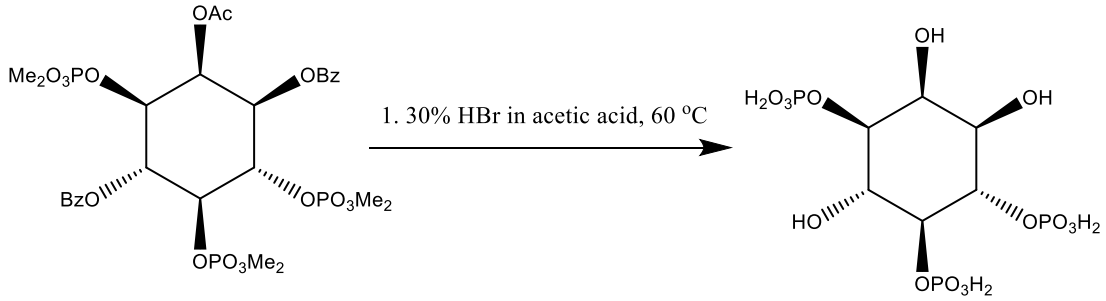

Compound 4 **Compound 5**

Figure 3.7 - Synthetic route for *D- myo-inositol-1, 4, 5-trisphosphate (compound 5)*

Hydrolysis of 2-O-Acetyl-3,6-di-O-benzoyl-myo-inositol-1,4,5-triphosphate (compound 4) (1.2 g) was attempted by heating a mixture with 30% HBr in acetic acid to 60^{o}C for 1 hour as described by Meek et al (Meek et al., 1988). However, this produced a yellow oil instead of the white powder described and so the reaction was deemed to have failed. ^{1}H NMR was performed on the oil in $CDCl_3$ as described above.

3.2.3 Fourier Transform Infrared Spectroscopy (FTIR) ion-pair binding assay

An FTIR binding study was performed for salbutamol and phytic acid as described in Chapter 2. Phytic acid concentrations of 0.1, 0.2, 0.5, 1, 5 and 100 mM were used to achieve this.

3.2.4 High Performance Liquid Chromatography (HPLC) ion-pair binding assay

An HPLC binding assay was completed for salbutamol (100 mM) and phytic acid as described in chapter 2. Phytic acid concentrations of 0.001, 0.005, 0.01, 0.025, 0.05, 0.1, 0.4 and 0.5 mM in HPLC water were used to achieve this.

3.2.5 Calculation of salbutamol – counter ion speciation curves

A speciation curve and percentage bound drug levels at 20:1 and 10:1 counter ion to drug ratios were calculated for the salbutamol phytate ion-pair as described in Chapter 2.

3.2.6 Distribution coefficient assay

The partitioning of the salbutamol phytate ion-pair made by a 1:1 mixture of drug to counter ion was performed as described in Chapter 2.

3.2.7 Data Analysis

Data was obtained from 3 experiments and have been expressed as a mean ± standard deviation, unless otherwise stated. Sigmoidal curves were fitted to the binding data in SigmaPlot and the value at 50% was taken as the ion-pair binding constant. One-way Analysis of Variance (ANOVA) with a Shapiro-Wilkins normality test was performed with a probability limit of 0.05 set to indicate significant differences.

3.3 Results

3.3.1 Synthesis of D- myo-inositol-1, 4, 5-trisphosphate (IP_3)

A white powder was collected at the end of the first reaction stage in 27% yield (16.8 g). Its identity as the reaction product 1,2:4,5-di-O-isopropylidene-3,6-di-O-benzoyl-inositol (compound 2), was confirmed with a melting point test and NMR analysis. The melting point of the powder was measured as 319 – 320^{o}C, which is close to the reported value in the literature (322 – 324^{o}C) (Khersonsky and Chang, 2002).

Integration of the 1H NMR spectrum for the isolated compound gave a total of 29 protons being detected, compound 2 has 28 protons, however the extra detected proton could be due to an impurity and is found in the region of 1 – 2 ppm (figure 3.8). Assignments were made for each peak according to the structure of the molecule and its predicted ^{1}H NMR.

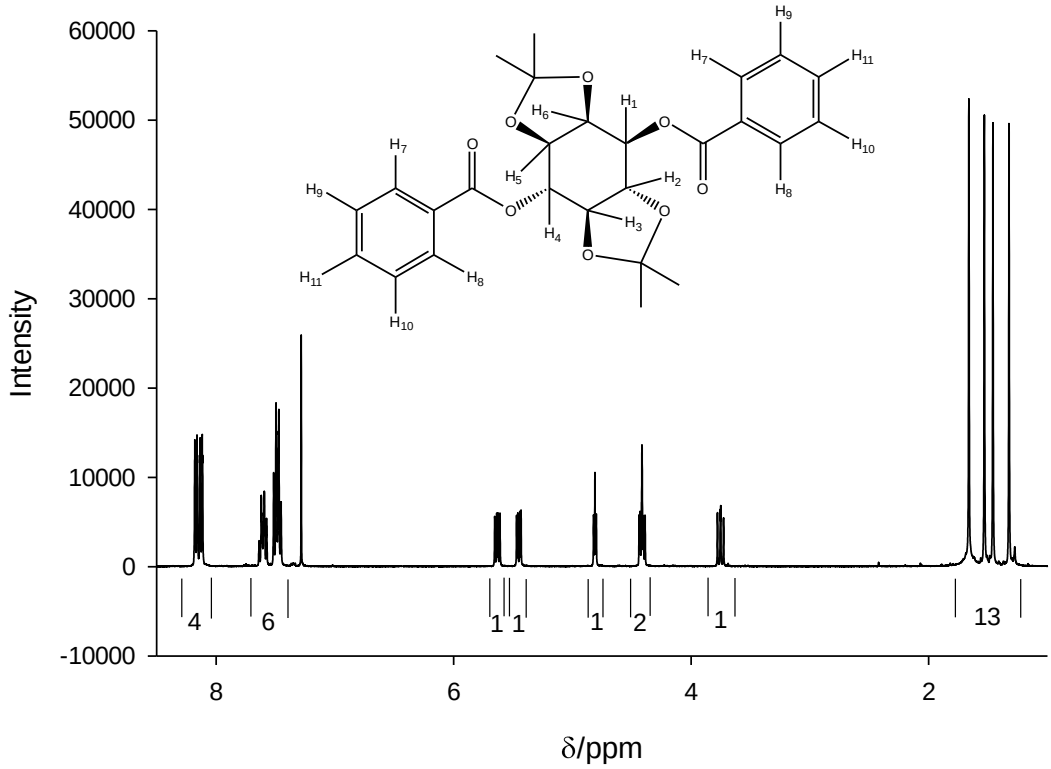

Figure 3.8 - ^{1}H NMR spectrum of 1,2:4,5-di-O-isopropylidene-3,6-di-O-benzoyl-inositol. Numbers shown underneath each peak are the calculated integral values

^{1}H NMR ($CDCl_3$): 1.32 (s, 3H, Me), 1.46 (s, 3H, Me), 1.53 (s, 3H, Me), 1.66 (s, 3H, Me), 3.74 (dd, 1H, H2 or H3), 4.41 (m, 2H, H5 and H6), 4.81 (dd, 1H, H2 or H3), 5.45 (dd, 1H, H1 or H4), 5.63 (dd, 1H, H1 or H4), 7.48 (dd, 4H, H9 and H10), 7.61 (dd, 2H, H11), 8.15 (m, 4H, H7 and H8). The chemical shifts found are similar to predicted at reported values (Khersonsky and Chang, 2002).

1,4-Di-O-benzoyl-myo-inositol (compound 3) was collected as a white powder in a 75% yield (9.3 g). The melting point of this powder was 219 – 224^{o}C which is lower than the reported literature value for the product (251 – 253^{o}C) (Meek et al., 1988). TLC analysis showed that the collected product has an R_f value of 0.55 which conformed with the

literature value for 1,4-Di-O-benzoyl-myo-inositol (Meek et al., 1988). Integration of the 1H NMR spectrum of compound 3 calculates the structure as having 24 protons, whereas the actual structure contains 20. The 4 extra protons are found in the integral of the broad hydroxyl peak, however, and so could be as a result of proton exchange with water in the sample. This could be investigated by addition of D_2O to the NMR sample, to allow for hydrogen/deuterium exchange (Dyson et al., 2008).

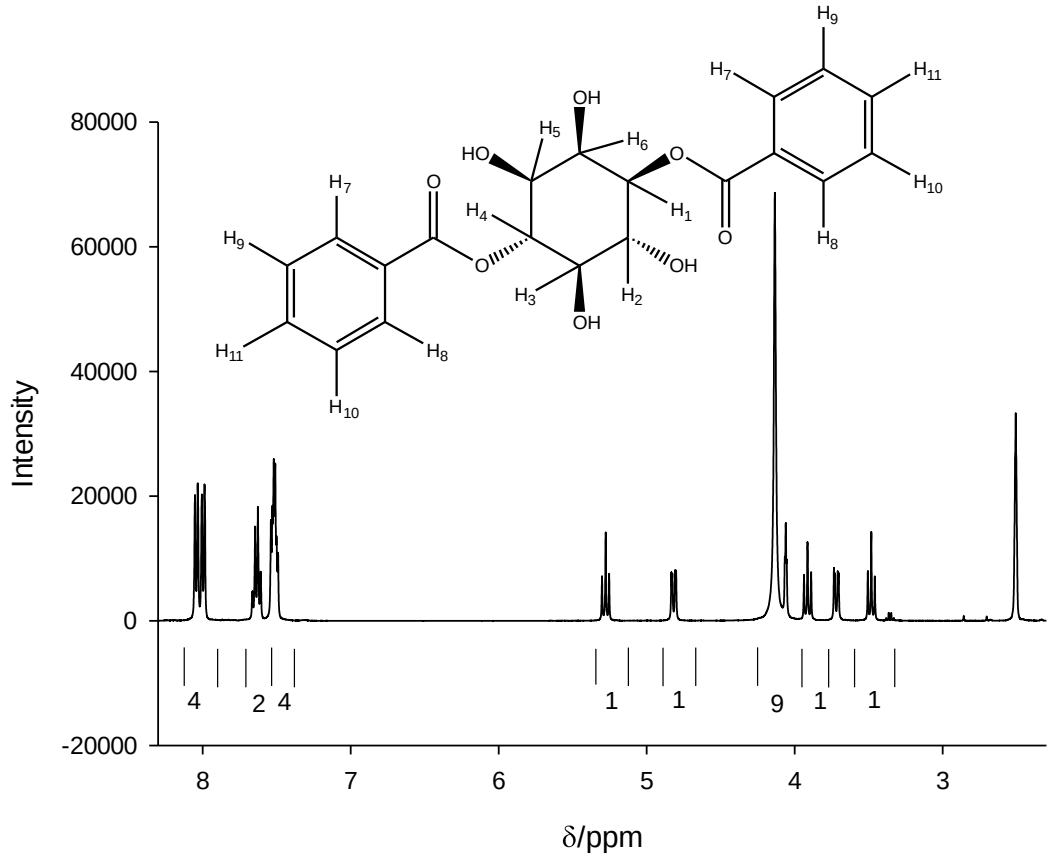

Figure 3.9 - 1H NMR spectrum of 1,4-Di-O-benzoyl-*myo*-inositol. Numbers under each of the peaks correspond with calculated integral values

The peaks were assigned as follows: 3.48 (t, 1H, H2 or H3), 3.72 (dd, 1H, H5 or H6), 3.91 (t, 1H, H5 or H6), 4.06 (t, 1H, H2 or H3), 4.13 (broad, 8H, OH), 4.82, (dd, 1H, H1 or H4), 5.28 (t, 1H, H1 or H4), 7.51 (m, 4H, H9 and H10), 7.64 (dd, 2H, H11), 8.02 (dd, 4H, H7 and H8). These values are in partial agreement with the literature values (Meek et al., 1988).

2-O-Acetyl-3,6-di-O-benzoyl-myo-inositol-1,4,5-triphosphate (compound 4) was isolated as crystals after the phosphorylation reaction in a 17% yield (1.8 g), however the properties of these crystals did not match those reported in the literature. The melting point recorded (127^{o}C) was significantly lower than the literature value for 2-O-Acetyl-3,6-di-O-benzoyl-myo-inositol-1,4,5-triphosphate (227 – 230^{o}C) and the R_f value on a TLC plate was 0.83, which was higher than the literature value (0.73) (Meek et al., 1988). Furthermore, the weak signals found by ^{1}H NMR make identification difficult (figure 1.10). Strong peaks at δ2.8 – 3.0 indicate that the dimethyl phosphate groups have been incorporated into the product (compound 4), however the uneven baseline indicates that the isolated compound is impure. Use of compound 4 in the final stage of the synthesis gave a yellow oil instead of the reported white powder and so the hydrolysis was deemed to have failed and the synthesis abandoned.

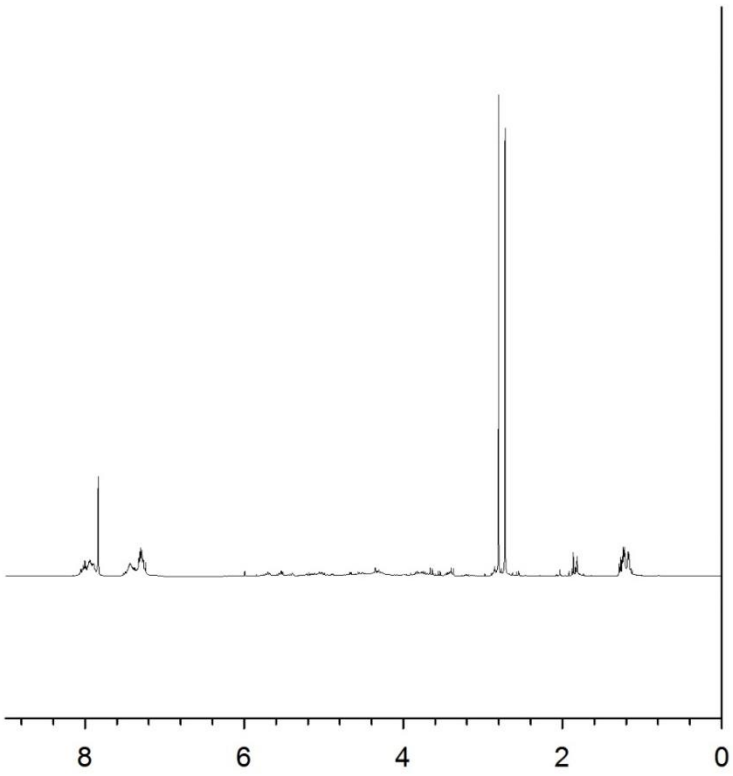

Figure 3.10 - 1H NMR spectrum of isolated compound after treatment of compound 3 with dimethyl chlorophosphate

3.3.2 The binding of salbutamol with phytic acid

Addition of phytic acid (IP_6) to solutions of salbutamol resulted in an increase in the N-H peak for the drug at 1596 cm^{-1} in comparison with the benzyl peak at 1616 cm^{-1}. It was shown that 100% salbutamol was found in ion-pair form at a phytate concentration of around 0.005 M (figure 3.11).

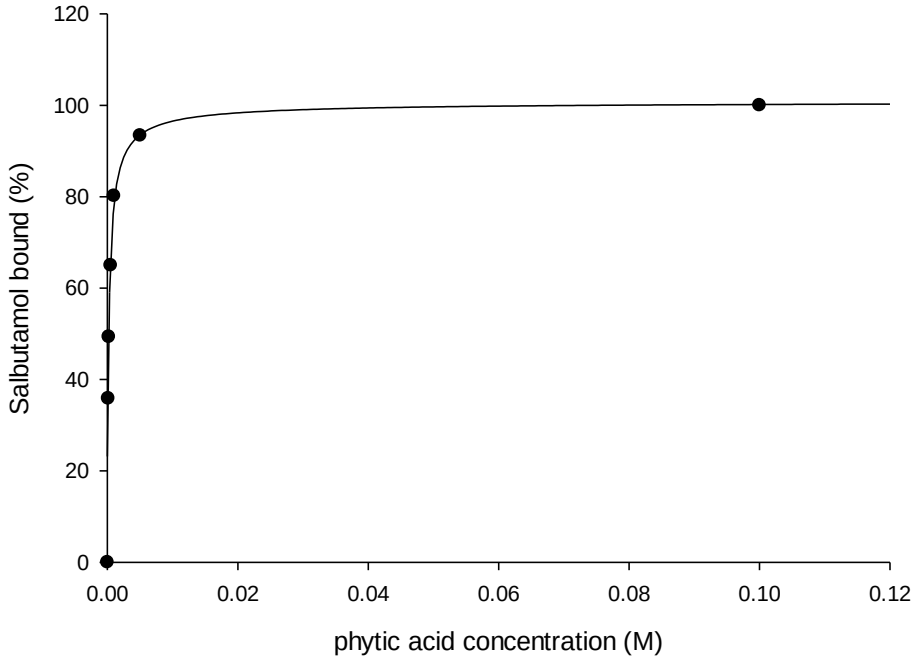

Figure 3.11 - Relationship between phytic acid concentration and percentage of salbutamol bound by FTIR (n=1)

This data was used to plot a binding affinity curve as with the counter ions in Chapter 2 and an association constant of 4.15 for the salbutamol phytate ion-pair was calculated (figure 3.12).

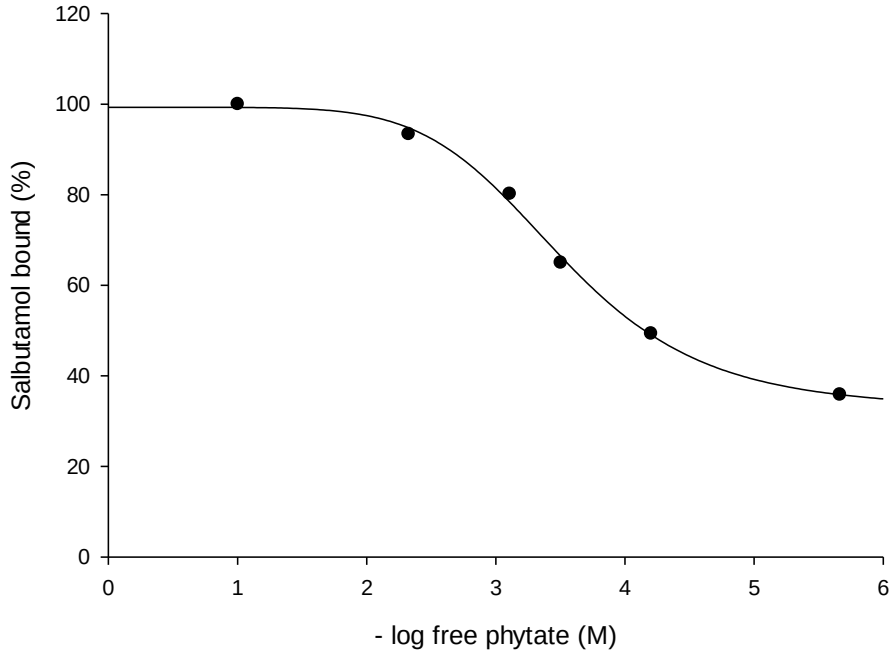

Figure 3.12 - Salbutamol phytate binding affinity curve calculated from FTIR binding data (n=1)

Addition of phytic acid to an aqueous mobile phase resulted in an increase in the retention time of salbutamol (figure 3.13).

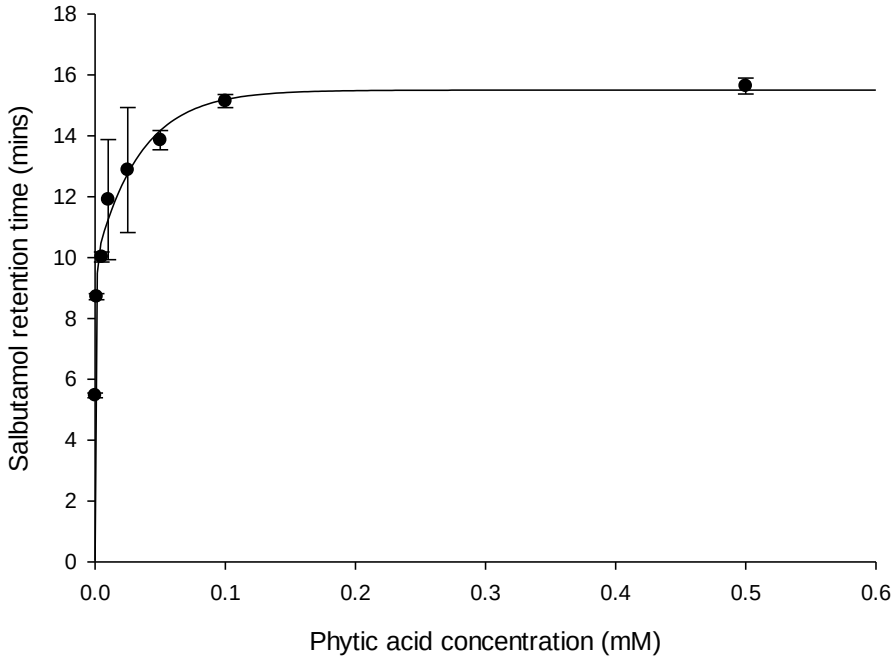

Figure 3.13 - Relationship between salbutamol retention time and phytic acid concentration in mobile phase of HPLC binding assay. Data represents a mean ± standard deviation (n=3)

This data was used to create a binding affinity curve as previously described, which gave an association constant for the salbutamol phytate ion-pair of 5.38 (± 0.16) (figure 3.14).

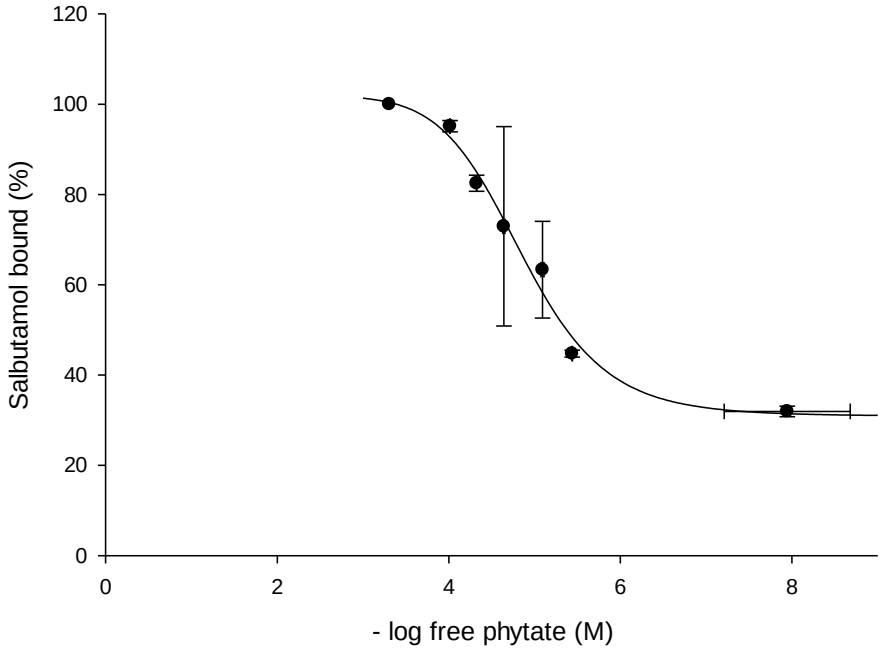

Figure 3.14 - Affinity binding plot for salbutamol phytate ion-pair calculated from HPLC binding assay data. Data represents a mean ± standard deviation (n=3)

The association constant calculated from HPLC ion-pair binding studies was used to plot speciation curves for a 10:1 and 20:1 ratio of phytic acid:salbutamol with a salbutamol concentration of 0.00209 M (figure 3.15). A 1:1 binding ratio was assumed and the percentage of salbutamol found in ion-pair form at pH 7.4 was found to be 99.98% for both the 10:1 and 20:1 counter ion-drug ratios.

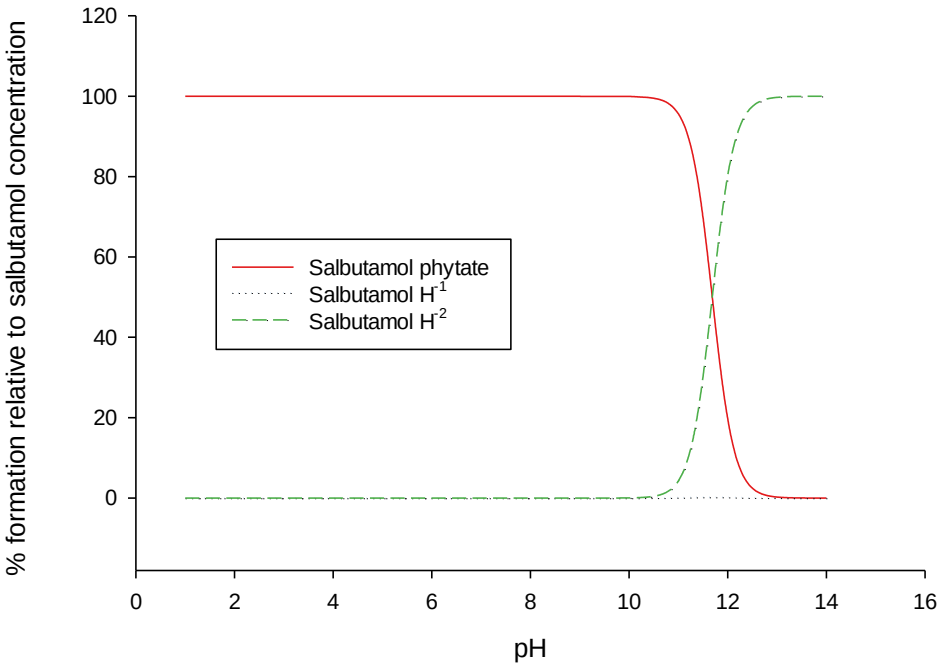

Figure 3.15 - Speciation curve for 10:1 salbutamol phytate from pH 1 - 14

3.3.3 The effect of ion-pairing with phytic acid on the partitioning of salbutamol

The octanol-water partitioning study showed that there was no significant difference in the partitioning of the salbutamol phytate ion-pair in comparison with salbutamol base alone ($p > 0.05$). The calculated $logD_{7.4}$ value for salbutamol phytate was -1.211 (± 0.181) compared with -1.386 (± 0.036) for salbutamol base.

3.4 Discussion

Preparation of D-*myo*-inositol-1, 4, 5-trisphosphate from *myo*-inositol was a complicated procedure as it required reactions to occur selectively with specific hydroxyl groups on the starting molecule and/or precise purification of the correct stereoisomer. The first reaction step, preparation of 1,2:4,5-di-O-isopropylidene-3,6-di-O-benzoyl-inositol (compound 2), is known to generate 3 separate isomers with the correct isomer being preferentially isolated due to its highly crystalline nature in comparison with the other 2 (figure 3.16) (Khersonsky and Chang, 2002, Gigg et al., 1985). ^{1}H NMR of the isolated compound 2 was in accordance with the literature, however the melting point obtained of the crystals was lower than the reported value, and so it is possible that the product still contained traces of these other isomers as impurities.

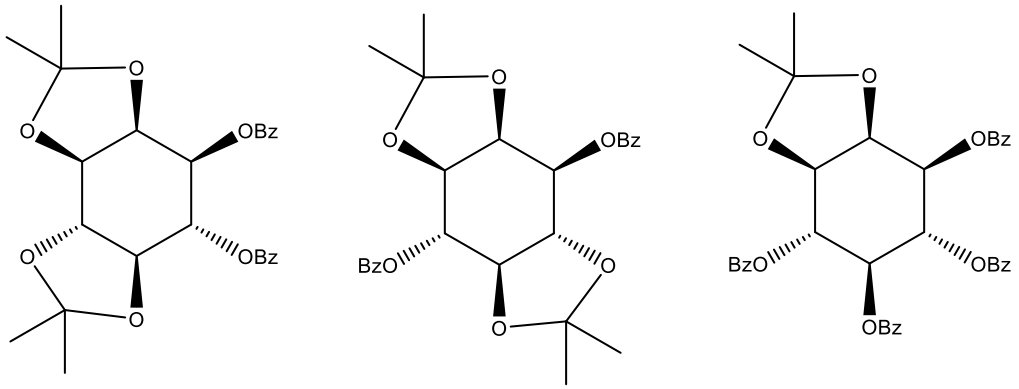

Compound 2

Figure 3.16 - 3 stereoisomers generated after reaction of *myo*-inositol with 2,2-dimethoxypropane and benzoyl chloride

Deprotection of 1,2:4,5-di-O-isopropylidene-3,6-di-O-benzoyl-inositol (compound 2) gave 1,4-Di-O-benzoyl-myo-inositol (compound 3) in good yield (75%). The TLC R_f corroborated that the correct compound had been isolated, and ^{1}H NMR showed that it was the major product (Meek et al., 1988). However, there were also trace impurities visible in the NMR and there was a stark difference between the melting point of the generated product and that found in the literature for 1,4-Di-O-benzoyl-myo-inositol (compound 3), indicating that isolated product was not pure and the impurities were likely to be stereoisomers A or C (figure 3.16) without the acetonide protecting groups (Meek et al., 1988).

Phosphorylation or phosphitylation of *myo*-inositol derivatives and isolation of an enantiomerically pure product also presented numerous difficulties. Under acidic conditions the phosphate groups have a tendency to migrate to other free hydroxyl groups on the molecule, and attempts to resolve this problem using chiral precursors or chiral resolution can be tedious and low-yielding (Meek et al., 1988, Durantie et al., 2016). Due to these problems and the trace impurities in the precursor, 1,4-Di-O-benzoyl-myo-inositol (compound 3), the isolated product of 2-O-Acetyl-3,6-di-O-benzoyl-myo-inositol-1,4,5-triphosphate (compound 4) did not have a melting point or R_f value that matched the literature. The ^{1}H NMR showed that although the phosphitylation had occurred, a mixture of compounds were present. The literature method that was followed for the preparation of D-*myo*-inositol-1, 4, 5-trisphosphate also reported a small quantity of a tetrakis(dimethyl phosphate) and an unknown tris(dimethyl phosphate) in the product after phosphitylation (Meek et al., 1988). In the previous work these did not negatively impact the final deprotection step however in the present work it seemed like there was a higher quantity of impurities from the earlier stages of the synthesis and this caused the final step to fail. Recently, studies have been published that employ chiral peptide catalysts or chiral

phosphorous sources that allow for synthesis of enantiomerically pure inositol phosphates (Durantie et al., 2016, Sculimbrene and Miller, 2001, Jordan et al., 2010, Duss et al., 2015). However, these require expensive and difficult to synthesize reagents and so would not be suitable to create an inositol phosphate counter ion for ion-pairing, as a large quantity of pure compound would be required in any final ion-pair product.

The larger, commercially available compound, phytic acid, was shown to form ion-pairs with salbutamol in both the FTIR and HPLC ion-pair binding studies. Furthermore, the concentration of phytic acid at which binding was detected was 100 fold lower than for any of the counter ions studied in Chapter 2, indicating that the binding between salbutamol and phytic acid was much stronger. The association constants generated from these studies were 4.15 M by FTIR, and 5.38 by HPLC which is significantly higher than the constants for any of the counter ions in Chapter 2 ($p < 0.05$). Previous studies quantifying the binding of phytic acid such as that by Graf who investigated the binding to calcium *via* titration also found that at pH 7.2 the apparent association constants for phytate and calcium were relatively strong (22.7 mM^{-1}) (Graf, 1983). Previous work has also found that maximum binding for phytic acid occurred at pH 8.4 when the phytic acid displayed a more negative charge (Graf, 1983, Heighton et al., 2008). Heighton *et al.* investigated the binding of phytic acid to iron *via* NMR spectroscopy in D_2O. He found that ferrous phytate had a formation constant of 0.84 and a dissociation constant of 1.19, while ferric phytate had a formation constant of 0.90 and a dissociation constant of 1.11 (Heighton et al., 2008). Comparison of these values with the association constants obtained in this study suggest that binding between phytic acid and salbutamol is stronger than that of phytic acid and mineral ions. This would be expected as salbutamol has functional groups that have the potential to interact with the phytic acid in addition to the electrostatic interaction.

There was no significant difference in the partitioning of salbutamol base and salbutamol phytate ion-pair. Both the base and ion-pair were very hydrophilic with calculated $logD_{7.4}$ values of -1.386 and -1.211, respectively. This is likely due to phytic acid having several negatively charged moieties at pH 7.4 (Heighton et al., 2008), so even though the charge of salbutamol is hidden, the ion-pair complex will still have an overall negative charge. This result could provide important information on the mechanism of action of the phytate ion-pair, should it show any differences *in vitro* or *in vivo* these can likely be attributed to the size of the ion-pair complex compared to the salbutamol parent drug, as the lipophilicity of the complex doesn't change upon ion-pairing (Ma and Hadzija, 2012).

3.5 Conclusion

Chemical synthesis of D-*myo*-inositol-1, 4, 5-trisphosphate was attempted from *myo*-inositol, however this method was abandoned due to the difficulty in separating stereoisomers. Salbutamol was shown to form an ion-pair complex with phytic acid that had a significantly higher association constant in comparison with the ion-pairs studied in Chapter 2. Ion-pairing was shown to have no significant effect on the partitioning of salbutamol between octanol and water. The next chapter will explore the incorporation of salbutamol ion-pairs using phytate and the chosen counter ions from Chapter 2 in to a dry powder formulation. Phytic acid was chosen to take forward due to the strength of binding with salbutamol and also to assess how the ion-pairing to increase molecular weight might influence salbutamol delivery. The suitability of these formulations for inhalation and stability of the powders will also be investigated.

Chapter 4

Respirable Powder Formulations of Ion-paired Salbutamol

4.1 Introduction

There are 3 main devices employed to administer drug formulations to the lung: nebulizers, pressurized metered dose inhalers (pMDI), and dry powder inhalers (DPI). For many years the pMDI was the most widely used type of inhaler due to its advantages such as ease of handling and reliability (Malcolmson and Embleton, 1998). However, the pMDI was also found to have shortfalls. One such shortfall is that many patients find the hand-lung coordination necessary to achieve optimal actuation of the device difficult (Newman, 2004). As such, DPIs are becoming more and more popular. They are breath-actuated, meaning that the patient's breath is the driving force used to deliver the powder to the lungs. They also do not need to use a propellant and could be used to deliver locally or systemically acting proteins or peptides, which is becoming increasingly important in the pharmaceutical field (Malcolmson and Embleton, 1998, Uchenna Agu et al., 2001).

The particle characteristics are a major factor in the delivery efficacy of a DPI. It is essential that the production method for creating the powders has tight control over particle size and particle size distribution as these properties determine the aerodynamic properties of the particles (Chapter 1). Many of the DPI products currently available commercially are produced by micronization, where the crystalline form of the drug is broken down via a milling technique, such as jet-milling, to a desirable particle size (Chow, 2007). However, this process can be time-consuming and inefficient as well as producing particles that carry high amounts of electrostatic charge, meaning that they are highly cohesive (Chow, 2007, Malcolmson and Embleton, 1998). In order to combat this problem, micronized particles are usually blended with a coarse carrier particle such as lactose. Drug particles are distributed over the surface of the larger carrier molecules to allow

sufficient segregation of the particles, when the particles are delivered to the lungs the drug molecule releases from the carrier to deposit in the airways (Malcolmson and Embleton, 1998).

An inhaled ion-pair formulation would need to contain the drug and counter ion in a heterogeneous, stable mixture of the correct particle size so that the majority of drug in the formulation is in ion-pair form upon deposition and dissolution. When attempting to deliver ion-pairs to the lung, the use of a DPI formulation is the most attractive option for a number of reasons. Primarily, delivery to the lung in powder form could allow the ion-pair to affect the dissolution of the drug in the lung fluid as a mechanism of prolonging drug action. In addition, although a pMDI formulation could theoretically be used to deliver ion-pairs, the storage of the drug, counter ion, and other excipients in a solution or suspension increases the likelihood of dissociation of the ion-pair before inhalation. Dissolution is a driving force for the dissociation of ion-pairs, and so a high concentration presented by a dry powder formulation would give the best chance for the drug to be presented to the lung in ion-pair form upon administration (Samiei et al., 2013).

When creating a dry powder ion-pair formulation there are many things that need to be considered. Creating particles with an excess of ions present increases the likelihood of the particles having a charged surface, which can have great effects on the inhaler retention and aerosol performance of a powder (Wong et al., 2014). It has been found in previous studies that deposition of inhaled particles in the lung can be enhanced by an electrical surface charge (Yu et al., 2017). However there is also a link between the charge of particles and their hygroscopicity which could negatively affect the stability of the powder formulation (Kwok and Chan, 2008).

Therefore, the aim of this chapter was to understand the effect that the inclusion of excess ion has on a dry powder formulation that aims to deliver an ion-pair to the lung in terms of the physical characteristics, surface morphology and aerosolization.

For the purpose of the work in this thesis, spray drying was chosen as the method of particle engineering. The spray drying process involves the spraying of a liquid feed solution in to a heated chamber where droplets are formed, quickly dried and separated from the air in a cyclone (Louey, 2004, Chow, 2007). This technique allows very precise control over the size of the particle generated compared with micronization and should also be able to create a heterogeneous mixture of drug, counter ion and excipients (Louey, 2004).

Lactose was used as the bulk of the powder due it being extremely well documented and widely accepted as a pharmaceutical excipient for inhaled formulations, as well as readily available and inexpensive (Pilcer and Amighi, 2010a). However, the issue with using lactose in a spray dried formulation is that the technique often results in an amorphous form of the sugar. Crystalline lactose is normally preferred in a formulation for inhalation due to its inherent stability. Amorphous lactose will undergo crystallization over time depending on the temperature and humidity of the storage conditions and this process can render a powder unsuitable for inhalation (Naini, 1998, Malcolmson and Embleton, 1998).

Other excipients that were investigated as to their suitability in a dry powder ion-pair formulation were polyvinylpyrrolidone (PVP) and l-leucine. The most widely studied group of excipients used for stabilizing amorphous lactose is polymers, particularly PVP (Mahlin et al., 2006). PVP is a popular choice as it has already been approved by the Food and Drug Administration (FDA) for use in a variety of routes of drug administration, including

use in a pMDI (Sou et al., 2016, Berggren and Alderborn, 2003b). Amino acids, such as leucine, have been shown to reduce hygroscopicity and improve the *in vitro* deposition of powders, they can also be used as stabilizers for certain biomolecules (Pilcer and Amighi, 2010a, Chen et al., 2016). Leucine is the most widely studied amino acid incorporated in to DPI formulations. Spray drying powders with leucine increases the dispersion of fine particles and may also have some protective ability against the crystallization of amorphous materials (Chen et al., 2016, Mangal et al., 2015).

The powders formed were analyzed for particle size, drug uniformity, surface morphology and chemical stability. The *in vitro* deposition of the powders was also assessed. These experiments were repeated after one month in different storage conditions in order to assess the stability of the powders.

4.2 Materials and Methods

4.2.1 Materials

Lactohale 300 (Friesland foods, Netherlands) was used as a source of lactose. Salbutamol base (BN. H80619) was from Cipla Ltd, India and used without further purification. Sodium sulfate was purchased from Alfa Aesar, UK. Sodium octanoate, polyvinylpyrrolidone (10k) and l-leucine were obtained from Sigma Aldrich (Dorset, UK). Sodium gluconate and dipotassium phytate were purchased from Santa Cruz Biotechnology (USA). For HPLC analysis, phosphate buffered saline was from Oxoid Ltd (Hampshire, UK), ammonium acetate was purchased from VWR (Leicestershire, UK). HPLC grade methanol and water were supplied by Fisher ltd (Leicestershire, UK).

4.2.2 Spray Drying

The following formulations were generated *via* spray drying using the method described in Chapter 2:

Table 4.1 -Salbutamol ion-pair formulations generated via spray drying

Formulation	*1*	*2*	*3*
Salbutamol base	99% Lactose with 1% salbutamol **base**		
Salbutamol sulfate	99% Lactose with 1% salbutamol 20:1 counter ion to drug **sulfate**	98.5% Lactose with 1% salbutamol 20:1 counter ion to drug 0.5% 10k PVP **sulfate^{P}**	93.5% Lactose with 1% salbutamol 20:1 counter ion to drug 0.5% 10k PVP 5% l-leucine **sulfate^{PL}**
Salbutamol gluconate	99% Lactose with 1% salbutamol 20:1 counter ion to drug **gluconate**	98.5% Lactose with 1% salbutamol 20:1 counter ion to drug 0.5% 10k PVP **gluconate^{P}**	93.5% Lactose with 1% salbutamol 20:1 counter ion to drug 0.5% 10k PVP 5% l-leucine **gluconate^{PL}**
Salbutamol octanoate	99% Lactose with 1% salbutamol 20:1 counter ion to drug **octanoate**	98.5% Lactose with 1% salbutamol 20:1 counter ion to drug 0.5% 10k PVP **octanoate^{P}**	93.5% Lactose with 1% salbutamol 20:1 counter ion to drug 0.5% 10k PVP 5% l-leucine **octanoate^{PL}**
Salbutamol phytate	99% Lactose with 1% salbutamol 1:1 counter ion to drug **phytate**	98.5% Lactose with 1% salbutamol 1:1 counter ion to drug 0.5% 10k PVP **phytate^{P}**	93.5% Lactose with 1% salbutamol 1:1 counter ion to drug 0.5% 10k PVP 5% l-leucine **phytate^{PL}**

The generated powders were stored in a sealed container with phosphorous pentoxide dessicant at either room temperature or 4^{o}C.

4.2.3 Particle Sizing

The spray dried powders were sized using a Helos/Rodos laser diffraction particle-size analyzer (Sympatec, Germany). The equipment was verified using a silicone carbonate P600 – 09 standard provided by the manufacturer. Approximately 100 mg of powder was used to obtain each size distribution. The R1 lens was used (size range 0.1 µm – 35 µm), the dispersion pressure was set at 6.00 bar and the vacuum was set at 30 - 32 mbar. Particle size distribution (PSD) was characterized using Fraunhofer theory and analyzed using WINDOX 4.0 software. The PSD was reported as x_{10}, x_{50}, x_{90} and volume mean diameter. x_{50} represents the median particle volume diameter and x_{10} and x_{90} are the 10^{th} and 90^{th} percentile, respectively.

4.2.4 Scanning Electron Microscopy (SEM)

The spray dried particles were visualized within a week of being generated. The sample was deposited with a brush on a carbon disc stuck to an aluminum stub. The stub was then coated with platinum for 60 seconds. SEM images were obtained using a Zeiss Supra 25 SEM (Carl Zeiss AG, Germany).

4.2.5 High Performance Liquid Chromatography (HPLC)

Concentrations of salbutamol were calculated using the HPLC method established in Chapter 2.

4.2.6 Content uniformity

The spray dried powder (10 mg) was weighed out 5 times and dissolved in 80% (v/v) water-methanol (10 mL). The samples were analyzed by HPLC. Data were represented as a percentage of the loaded dose of 100 µg of salbutamol per 10 mg of powder.

4.2.7 In Vitro Drug Deposition

The *in vitro* drug deposition was analyzed using a Next Generation Impactor (NGI; Copley Scientific, UK) and a Phoenix Monodose dry powder inhaler (Plastiape, Italy). A total of 3 assessments were carried out for each spray dried formulation and 5 capsules were used per assessment. Capsules were prepared by manually loading 12.5 (± 0.5) mg of spray dried powder in to a size 3 hard gelatin capsule (Meadow Laboratories Ltd, Essex, UK). The NGI was set up according to the USP (Pharmacopeia). The NGI collection cups were coated with 19.25% PEG200 in acetone, 4 mL for stage 1, and 2 mL for all other stages. The formulations were tested at 100 L/min for 2.5 seconds. After testing, the throat, all stages and the external filter paper were washed with 80% (v/v) water-methanol mixture. HPLC was used to quantify the amount of salbutamol deposited at each stage.

4.2.8 Data Analysis

Data obtained for each experiment were expressed as a mean ± standard deviation (SD) unless otherwise stated, n = 3. One-way Analysis of Variance (ANOVA) with a Shapiro-Wilkins normality test was performed with a probability limit of 0.05 set to indicate significant differences. Graphs were created using Sigmaplot software (Sigmaplot 12.5, Systat Software, Inc) and error bars show SD.

In vitro deposition data were represented as a mass median aerodynamic diameter (MMAD), geometric standard deviation (GSD), emitted dose (ED), and fine particle fraction (FPF).

The calculated average MMAD value for each formulation was compared to the average Volume mean diameter (VMD) using the following formulation:

$$d_a = \sqrt{\rho_p d_v^2 / \chi} \qquad \textbf{[Equation 4.1]}$$

where:

d_a = aerodynamic diameter, ρ_p = true density of the particle, d_v = diameter of equivalent volume sphere, χ = dynamic shape factor.

The ED of the formulation was calculated as the mass deposited in the throat and stages 1-8 of the NGI as a percentage of the mean content of salbutamol found in the content uniformity analysis. The FPF was determined as the percentage of the ED that has a particle size less than 5 μm. MMAD and GSD were calculated from the inverse normal of the cumulative percentage under the stated aerodynamic diameter versus the log effective cut off diameter.

4.3 Results

4.3.1 The effect of counter ions on the spray dried formulation

Spray drying the salbutamol - counter ion formulations resulted in a white powder in at least 20% yield (table 4.2). There was no difference in the yield or size of the particle between the base and sulfate formulations ($p > 0.05$). However the gluconate, octanoate and phytate formulations all resulted in a significantly smaller particle size ($p < 0.05$) (table 4.2). The yield of the spray drying process reduced as the particle size reduced.

Table 4.2 - Spray drying and laser diffraction particle size results for formulations (base, sulfate, gluconate, octanoate, and phytate). X_{50} is the median particle volume diameter and VMD is the volume mean diameter.

Formulation	Yield (%)	x_{50} (µm)	VMD (µm)
Base	51 (±2.00)	3.68 (± 0.26)	3.96 (± 0.30)
Sulfate	49 (± 9.02)	3.61 (± 0.28)	3.88 (± 0.25)
Gluconate	20 (± 2.31)	2.57 (± 0.35)	2.82 (± 0.36)
Octanoate	36 (± 1.53)	3.28 (± 0.06)	3.60 (± 0.06)
Phytate	40 (± 6.43)	3.26 (± 0.27)	3.56 (± 0.28)

SEM pictures showed that the particles were smooth and spherical. The particles also appeared to be agglomerated. The particle size range in the SEM images was from 1 – 15 µm. It is shown that the octanoate and gluconate formulations have slightly smaller particles on average, but they also seem to show more agglomeration (figure 4.1).

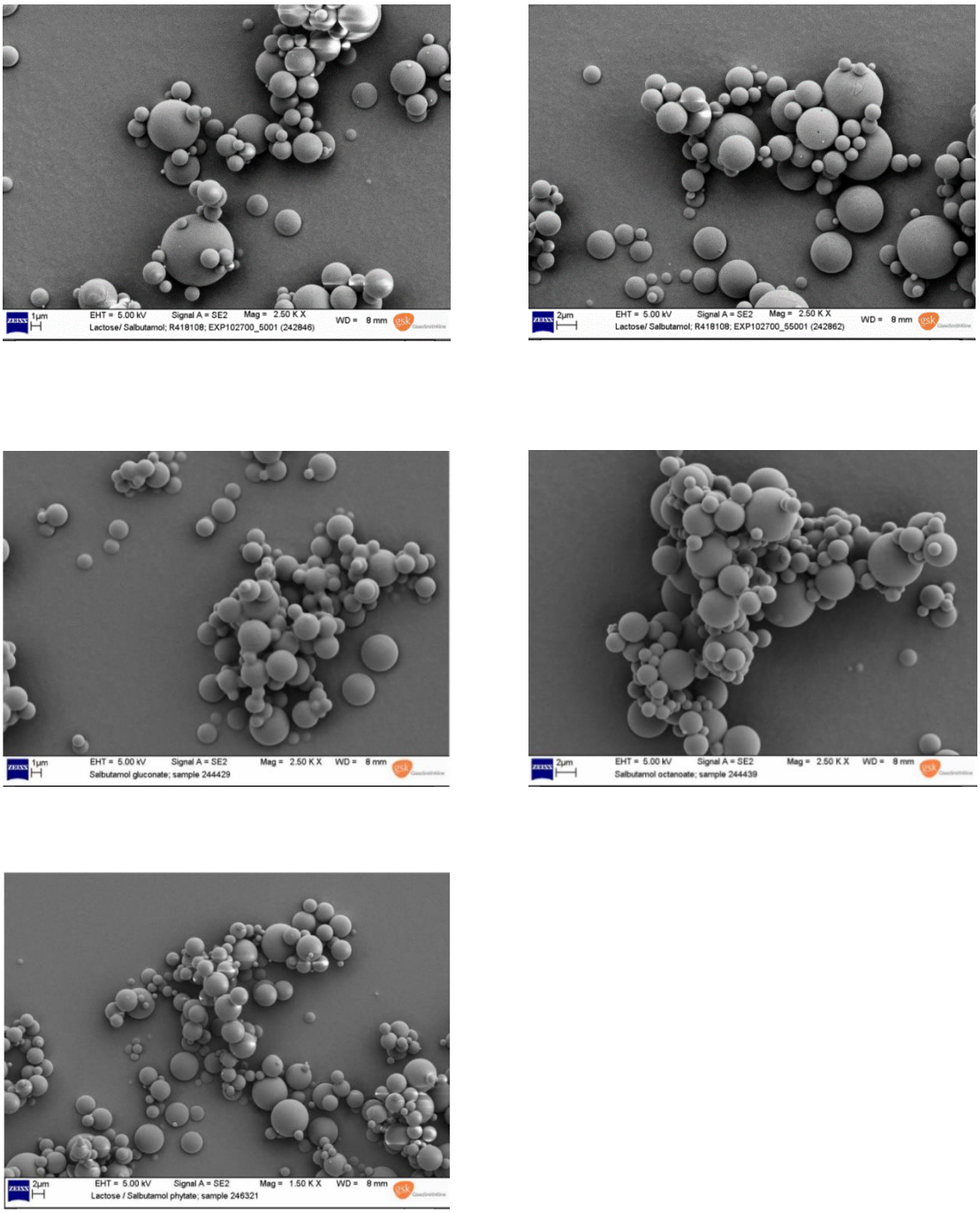

Figure 4.1 – Scanning electron microscopy images of salbutamol ion-pair formulations. Top left = base, top right = sulfate, middle left = gluconate, middle right = octanoate, bottom left = phytate)

To investigate the content uniformity of the spray dried powder five 10 mg samples were analyzed via HPLC. Powders were considered homogenous when no more than one of the samples fell outside of 85 – 115 % of the mean content, and no samples fell outside of 75 – 125% of the mean (Pharmacopoeia, 2011). The salbutamol - counter ion formulations show that some of the drug was lost during the spray drying procedure, with around 75 – 80% of the amount added in to the original feedstock being incorporated in to the final powder (table 4.3). All of the powders in these formulations were considered to be homogeneous.

Table 4.3 – Percentage of salbutamol from spray drying feedstock that was incorporated in to the powder for formulations base, sulfate, gluconate, octanoate, and phytate

Formulation	Salbutamol content (%)
Base	85.63 (± 7.27)
Sulfate	77.04 (± 0.91)
Gluconate	75.54 (± 4.52)
Octanoate	84.79 (± 3.43)
Phytate	79.78 (± 7.69)

In vitro deposition of salbutamol was assessed using an NGI with a throat, stages 1 – 8 and an external filter. The addition of the sulfate counter ion to the powder had no effect on the drug's deposition within the system and as such the formulation had the same MMAD and FPF as the control ($p > 0.05$) (figure 4.2, table 4.4). The gluconate formulation which had a smaller particle size had a reduced deposition in stage 1 of the NGI, and a greater amount of the drug was deposited in to the later stages ($p < 0.05$) (figure 4.2). The changes in deposition resulted in a significantly smaller MMAD and higher FPF value for

this formulation ($p < 0.05$) (table 4.4). The octanoate and phytate formulations had a higher deposition of drug in the throat, and a much lower deposition in stage 1 when compared with the base formulation ($p < 0.05$). However this did not appear to have a detrimental effect on the deposition in the lower stages (figure 4.2). As these formulations appeared to have better deposition in to the later stages compared with the control, they also had a significantly smaller MMAD value ($p <0.05$) (table 4.4). There was no difference in the FPF values for the octanoate or phytate formulations in comparison with the base formulation ($p > 0.05$).

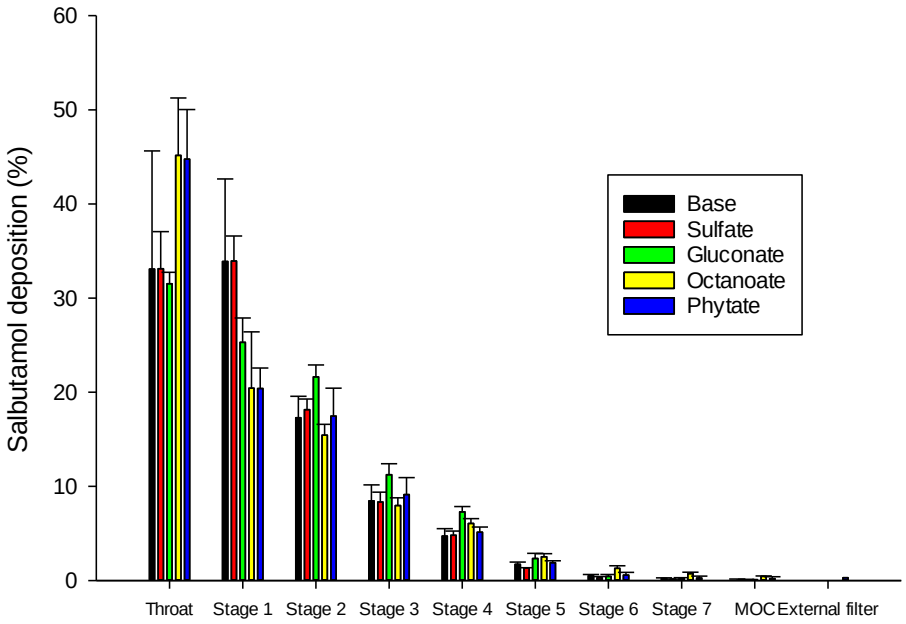

Figure 4.2 – Deposition of salbutamol on all stages of the Next Generation Impactor as a percentage of the total emitted dose for ion-pair formulations. Data shown represents the mean ± standard deviation (n=3)

Table 4.4 - Parameters derived from the stage by stage Next Generation Impactor deposition data for formulations base - phytate. Emitted dose (ED), mass median aerodynamic diameter (MMAD), geometric standard deviation (GSD), and fine particle fraction (FPF).

Formulation	ED (%)	MMAD (μm)	GSD (μm)	FPF (%)
Base	74.24 (± 2.14)	6.30 (± 0.71)	2.31 (± 0.04)	25.34 (± 4.08)
Sulfate	74.28 (± 1.35)	6.24 (± 0.36)	2.20 (± 0.09)	25.14 (± 1.42)
Gluconate	76.57 (± 1.71)	4.85 (± 0.35)	2.09 (± 0.01)	33.52 (± 3.24)
Octanoate	79.00 (± 3.06)	4.85 (± 0.73)	2.39 (± 0.18)	27.83 (± 2.84)
Phytate	71.38 (± 6.96)	4.93 (± 0.36)	2.16 (± 0.11)	26.96 (± 3.74)

The calculated MMAD values for each formulation were compared to the VMD values found in particle sizing to assess how the aerosol performed using the equation shown in part 4.2.8. As the SEM pictures show that the particles are spherical a dynamic shape factor of 1 was used.

For each formulation the calculated aerodynamic diameter (d_a) is lower than the calculated MMAD value, suggesting that the aerosolization of the powders was not complete. The octanoate and phytate formulations appear to be the ones that are better aerosolized (table 4.5).

Table 4.5 – Comparison of average mass median aerodynamic diameter (MMAD) from next generation impactor data, volume mean diameter (VMD) from laser diffraction, and aerodynamic diameter (d_a) calculated from laser diffraction VMD data for ion-pair formulations

Formulation	MMAD (μm)	VMD (μm)	Calculated d_a (μm)
Base	6.30 (± 0.71)	3.96 (± 0.30)	4.88
Sulfate	6.24 (± 0.36)	3.88 (± 0.25)	4.79
Gluconate	4.85 (± 0.35)	2.82 (± 0.36)	3.48
Octanoate	4.85 (± 0.73)	3.60 (± 0.06)	4.43
Phytate	4.93 (± 0.36)	3.56 (± 0.28)	4.38

4.3.2 The effect of PVP on performance and stability

PVP was added to the formulations as a stabilizing agent for the amorphous lactose. It was added as 0.5% of the overall powder weight and so the amount of lactose in the formulation was slightly lower than for the previous powders. The result of the addition of PVP was a slight increase in the yield of spray drying process. There was no significant difference in the size of the particles when compared with the equivalent formulation without PVP ($p > 0.05$). The octanoate^P and phyate^P had a significantly smaller particle size in comparison with the base formulation ($p < 0.05$) (table 4.6).

Table 4.6 – Spray drying and laser diffraction particle size results for polyvinylpyrrolidone formulations (base, sulfate^{P}, gluconate^{P}, octanoate^{P}, phytate^{P}). X_{50} is the median particle volume diameter and VMD is the volume mean diameter.

Formulation	Yield (%)	x_{50} (µm)	VMD (µm)
Base	51 (±2.00)	3.68 (± 0.26)	3.96 (± 0.30)
Sulfate^{P}	59 (± 1.53)	3.92 (± 0.07)	4.14 (± 0.07)
Gluconate^{P}	36 (± 6.66)	3.36 (± 0.13)	3.61 (± 0.29)
Octanoate^{P}	32 (± 6.11)	3.06 (± 0.12)	3.39 (± 0.12)
Phytate^{P}	35 (± 3.27)	3.23 (± 0.07)	3.46 (± 0.06)

The SEM pictures of the salbutamol ion-pair formulations with PVP showed that the addition of the PVP had an effect on the surface of the particles compared to the formulations without PVP. While the particles remain spherical, an uneven surface can be observed (figure 4.3).

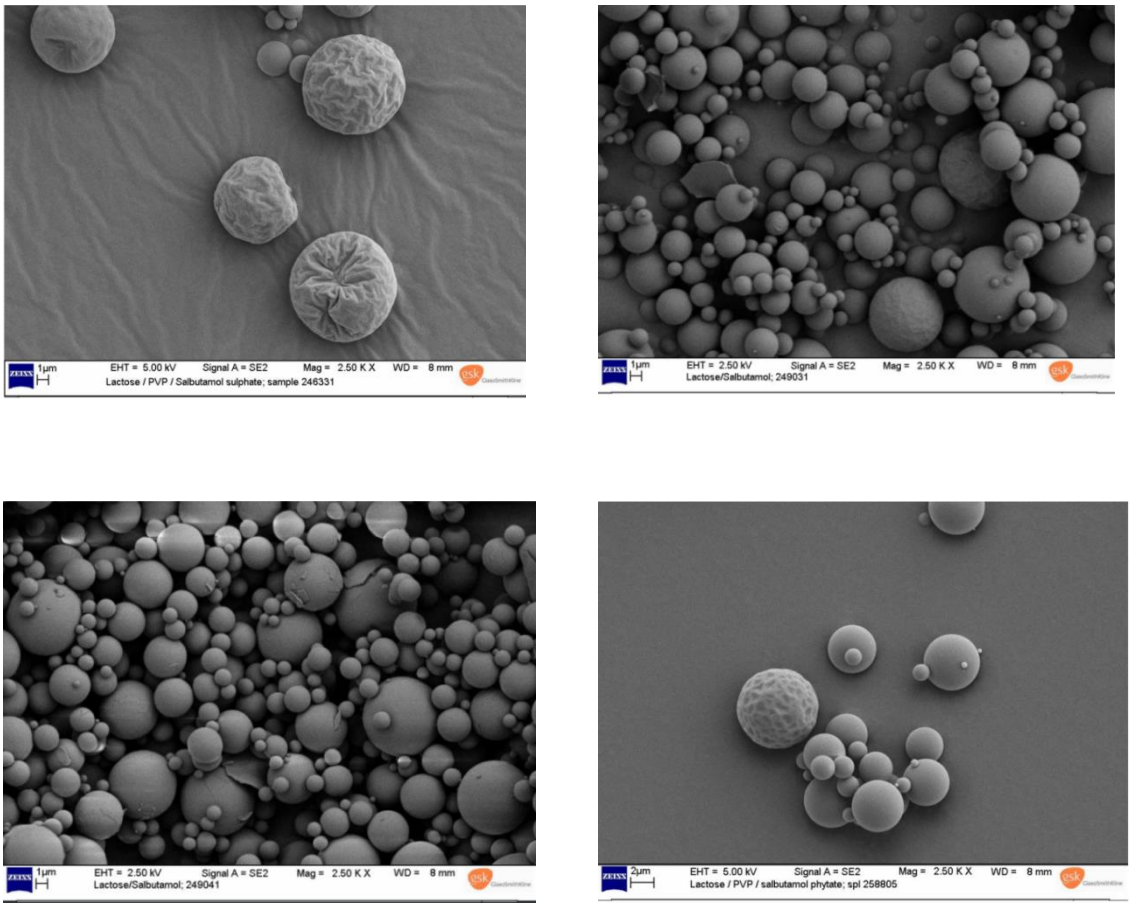

Figure 4.3 – Scanning electron microscopy images of polyvinylpyrrolidone formulations (top left = sulfate^{P}, top right = gluconate^{P}, bottom left = octanoate^{P}, bottom right = phytate^{P})

After the addition of PVP the spray dried formulations demonstrated 1 – 3 samples that fell outside the 75 – 125% of the mean uniformity range. The gluconate^{P} formulation was the most homogeneous of the PVP formulations, with 1 sample having a result of 126% of the average, and the rest falling within 94 – 101% (table 4.7).

Table 4.7 – Percentage of salbutamol from spray drying feedstock that was incorporated in to the powder for formulations base, sulfate^{P}, gluconate^{P}, octanoate^{P}, and phytate^{P}

Formulation	Salbutamol content (%)
Salbutamol Base	85.63 (± 7.27)
Sulfate^{P}	101.05 (± 25.38)
Gluconate^{P}	85.36 (± 6.62)
Octanoate^{P}	88.41 (± 17.55)
Phytate^{P}	85.15 (± 13.57)

The sulfate^{P} and gluconate^{P} had a much larger deposition of powder in the throat of the NGI compared with the sulfate and gluconate formulations ($p < 0.05$). As a result of this there is a significantly decreased amount of sulfate^{P} and gluconate^{P} powder deposited in stage 1 ($p < 0.05$); however the deposition in the later stages is very similar to the base formulation (figure 4.4).

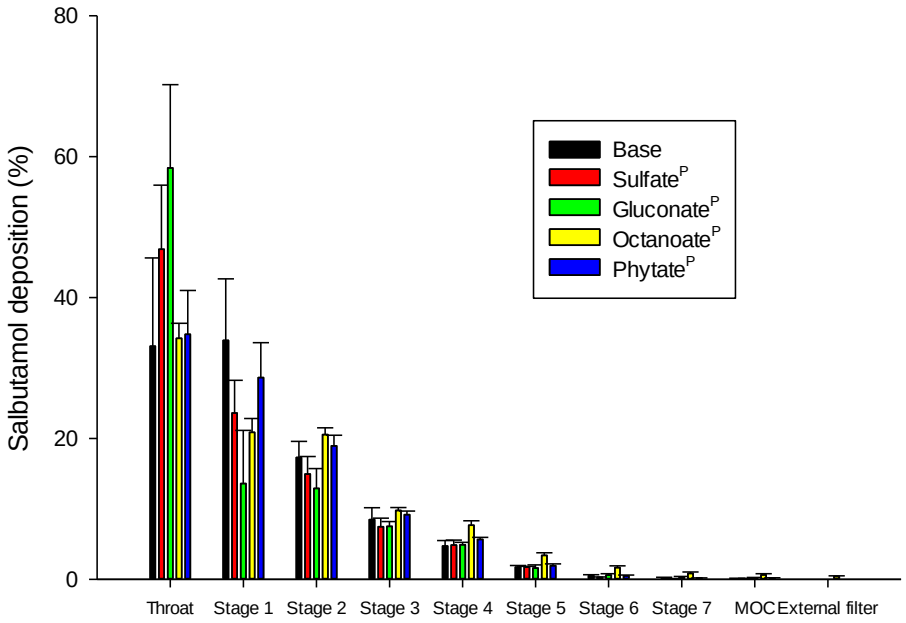

Figure 4.4 – Deposition of salbutamol on all stages of the Next generation impactor as a percentage of the total emitted dose for base formulation and formulations sulfate^P, gluconate^P, octanoate^P and phytate^P. Data shown represents the mean ± standard deviation (n=3)

The results show that significantly less of the sulfate^P and octanoate^P formulations emitted from the inhaler ($p < 0.05$), even though both of these formulations have a lower MMAD value than their counter ion only equivalents ($p < 0.05$). The calculated FPF for gluconate^P was almost 10% lower than the gluconate formulation. The FPF for the octanoate^P formulation was significantly higher than the previous value ($p < 0.05$) (table 4.8).

Table 4.8 - Parameters derived from the stage by stage Next Generation Impactor deposition data for formulations base, and sulfate^P, gluconate^P, octanoate^P, and phytate^P. Emitted dose (ED), mass median aerodynamic diameter (MMAD), geometric standard deviation (GSD), and fine particle fraction (FPF).

Formulation	ED (%)	MMAD (μm)	GSD (μm)	FPF (%)
Base	74.24 (± 2.14)	6.30 (± 0.71)	2.31 (± 0.04)	25.34 (± 4.08)
Sulfate^P	68.78 (± 2.41)	5.50 (± 0.11)	2.24 (± 0.03)	22.87 (± 3.41)
Gluconate^P	73.91 (± 3.79)	5.15 (± 0.62)	2.30 (± 0.16)	25.74 (± 3.44)
Octanoate^P	64.10 (± 3.54)	4.41 (± 0.21)	2.30 (± 0.11)	36.23 (± 1.45)
Phytate^P	83.63 (± 5.07)	5.51 (± 0.40)	2.22 (± 0.02)	28.19 (± 1.01)

For all PVP formulations the calculated aerodynamic diameter is lower than the experimental MMAD. Again the octanoate^P formulation appears to be the best aerosolized of the PVP powders, with less than 0.25 μm difference between the two values (table 4.9).

Table 4.9 – Comparison of average mass median aerodynamic diameter (MMAD) from next generation impactor data, volume mean diameter (VMD) from laser diffraction, and aerodynamic diameter (d_a) calculated from laser diffraction VMD data for ion-pair PVP formulations

Formulation	MMAD (μm)	VMD (μm)	Calculated d_a (μm)
Sulfate^P	5.50 (± 0.11)	4.14 (± 0.07)	5.10
Gluconate^P	5.15 (± 0.62)	3.61 (± 0.29)	4.45
Octanoate^P	4.41 (± 0.21)	3.39 (± 0.12)	4.18
Phytate^P	5.51 (± 0.40)	3.46 (± 0.06)	4.26

The stability of the powders with and without PVP was tested after storage for 1 month with dessicant, either at room temperature or 4^{o}C. Repetition of the content uniformity study of the formulations containing only counter ion after this time suggested that these powders were unstable as samples fell outside 75 – 125% of the mean. Although there was no change in the mean drug concentration, there was a great increase in the variability of the results for all formulations (table 4.10).

Table 4.10 – Comparison of the percentage of salbutamol from spray drying feedstock that was incorporated in to the powders for the salbutamol counter ion formulations prior to storage (T0) and after 4 weeks (T28) storage with dessicant at room temperature and 4^{o}C

Formulation	Salbutamol content at T0 (%)	Salbutamol content at T28 after storage at RT (%)	Salbutamol content at T28 after storage at 4^{o}C (%)
Base	85.63 (± 7.27)	104.24 (± 18.02)	97.36 (± 15.27)
Sulfate	77.04 (± 0.91)	79.93 (± 14.88)	80.12 (± 11.14)
Gluconate	75.54 (± 4.52)	83.56 (± 15.08)	78.71 (± 12.92)
Octanoate	84.79 (± 3.43)	86.70 (± 9.55)	82.27 (± 9.69)
Phytate	79.78 (± 7.69)	74.80 (± 11.72)	79.25 (± 11.08)

The *in vitro* drug deposition study of the base formulation after 4 weeks showed that there was a greater deposition of powder in the throat, and reduced deposition in stages 1 and 2 ($p < 0.05$). The deposition in the later stages did not significantly differ, and there was no difference in the results between the two storage conditions (figure 4.5). The same deposition pattern was observed for the sulfate formulation after storage (figure 4.6).

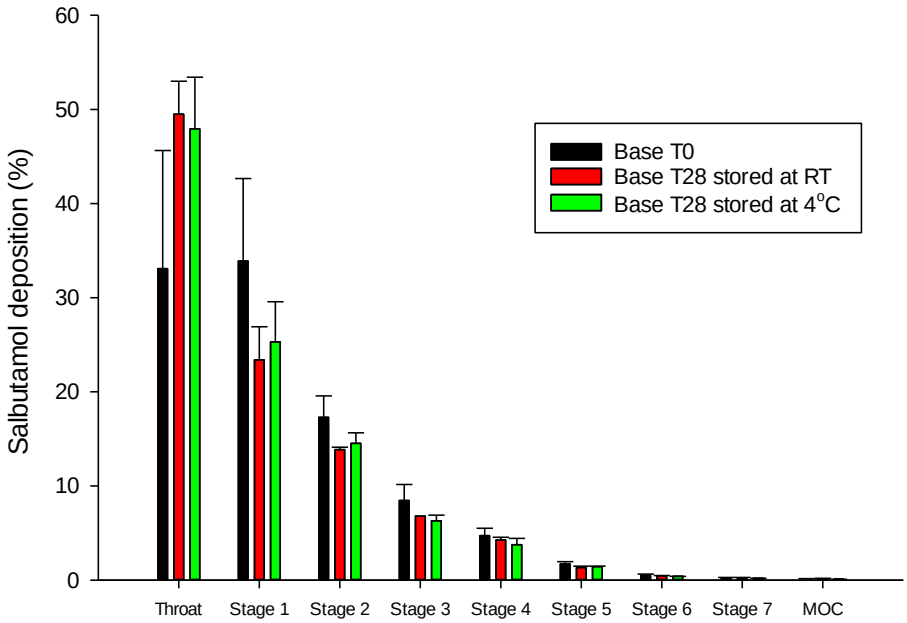

Figure 4.5 - Deposition of salbutamol in base formulation in next generation impactor (NGI) prior to storage (T0) and after 1 month storage (T28) after storage with dessicant at room temperature and 4°C. Data represents a mean± standard deviation (n=3)

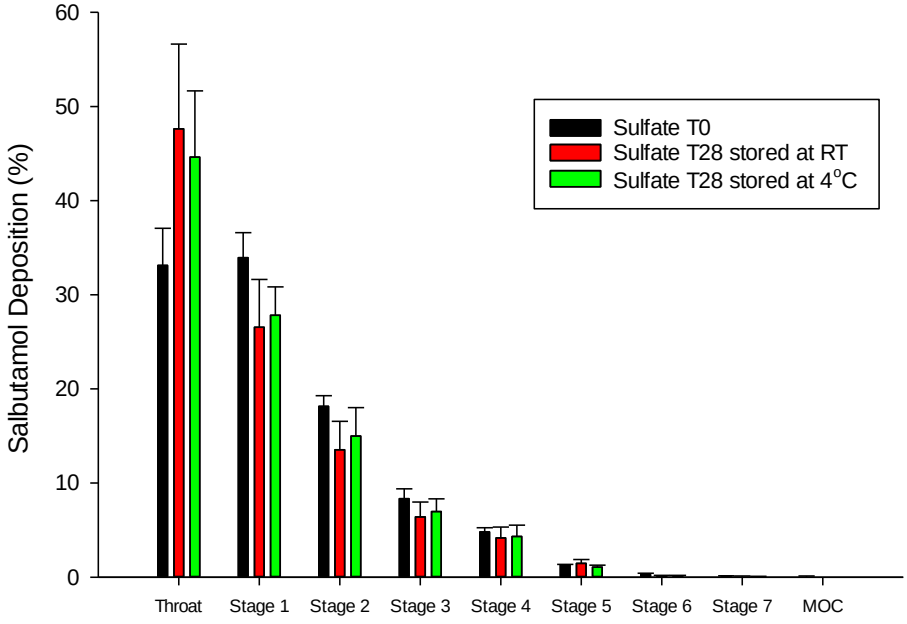

Figure 4.6 – Deposition of salbutamol in sulfate formulation in next generation impactor (NGI) prior to storage (T0) and after 1 month storage (T28) after storage with dessicant at room temperature and 4°C. Data represents a mean ± standard deviation (n=3)

There was no significant difference in the deposition of the gluconate or octanoate formulations kept in either storage condition (figure 4.7, 4.8).

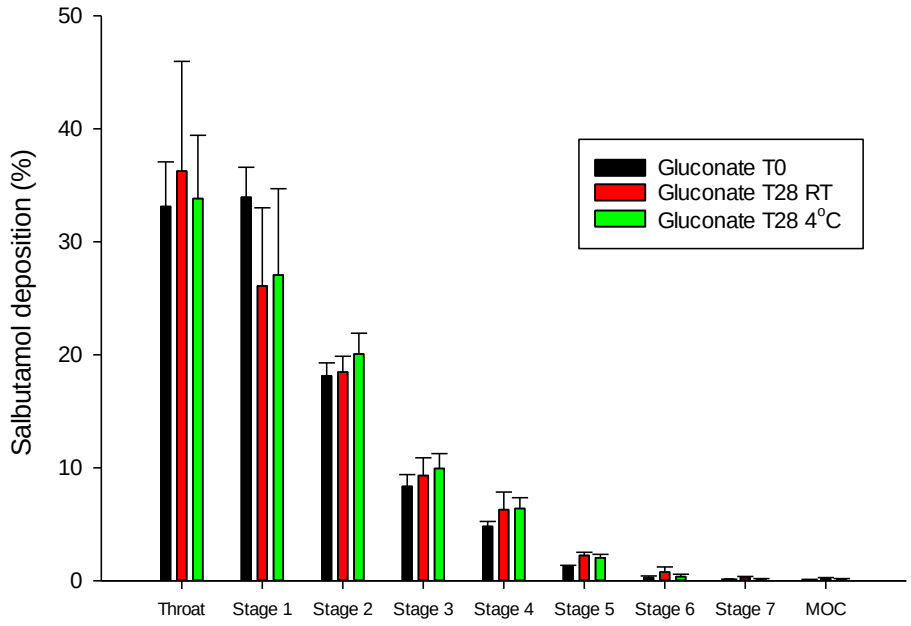

Figure 4.7 – Deposition of salbutamol in gluconate formulation in next generation impactor (NGI) prior to storage (T0) and after 1 month storage (T28) after storage with dessicant at room temperature and 4°C. Data represents a mean ± standard deviation (n=3)

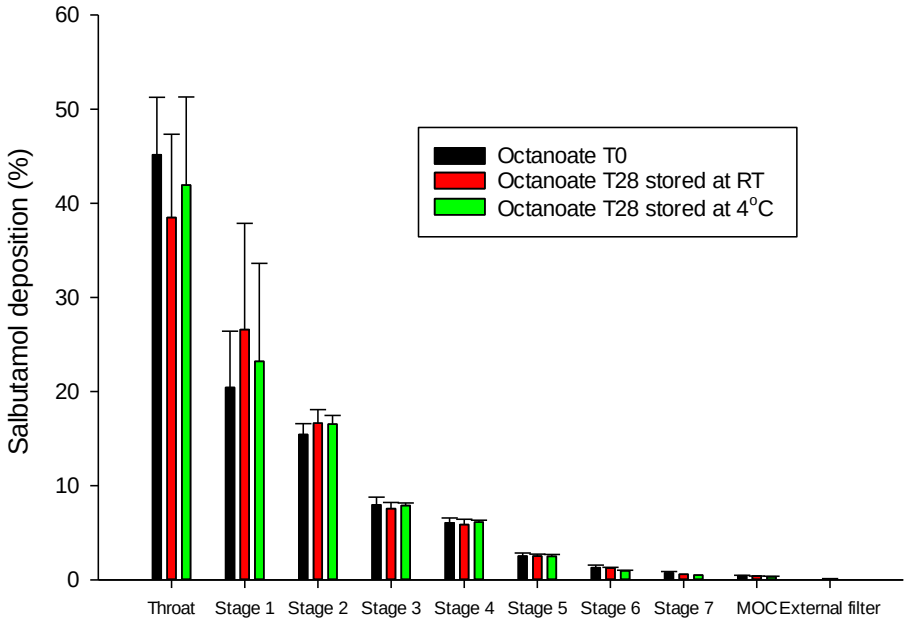

Figure 4.8 – Deposition of salbutamol in octanoate formulation in next generation impactor (NGI) prior to storage (T0) and after 1 month storage (T28) after storage with dessicant at room temperature and 4°C. Data represents a mean ± standard deviation (n=3)

After 1 month the deposition of the phytate formulation showed an increased deposition in stage 1 of the NGI ($p < 0.05$). (figure 4.9).

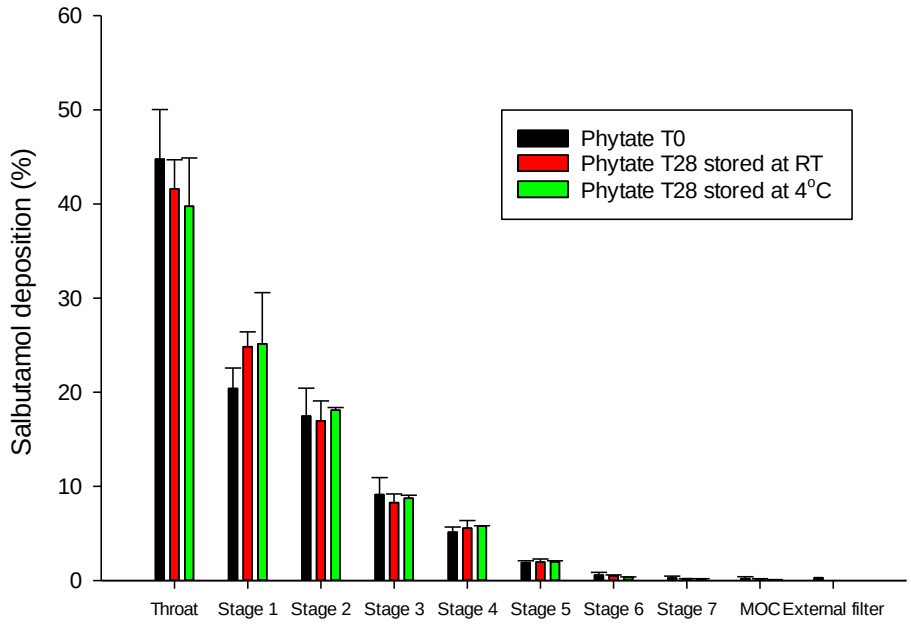

Figure 4.9 – Deposition of salbutamol in phytate formulation in next generation impactor (NGI) prior to storage (T0) and after 1 month storage (T28) after storage with dessicant at room temperature and 4°C. Data represents a mean ± standard deviation (n=3)

The variance in the original content uniformity results for the PVP containing formulations was generally decreased after storage for 1 month, and formulations that initially failed the homogeneity criteria were found to pass. There was no significant difference in the salbutamol content for any of the PVP ion-pair formulations ($p > 0.05$). There was a significant increase in the variation of the results for the gluconate^{P} powder that was stored at RT, suggesting that this formulation was more stable under the 4°C conditions ($p < 0.05$) (table 4.11).

Table 4.11 – Comparison of the percentage of salbutamol from spray drying feedstock that was incorporated in to the powders for the salbutamol-counter ion-polyvinyl pyrrolidone formulations prior to storage (T0) and after 4 weeks (T28) storage with dessicant at room temperature and 4°C

Formulation	Salbutamol content at T0 (%)	Salbutamol content at T28 after storage at RT (%)	Salbutamol content at T28 after storage at 4°C (%)
Base	85.63 (± 7.27)	104.24 (± 18.02)	97.36 (± 15.27)
Sulfate^{P}	101.05 (± 25.38)	97.87 (± 11.04)	98.02 (± 16.05)
Gluconate^{P}	85.36 (± 6.62)	70.35 (± 17.91)	73.75 (± 8.39)
Octanoate^{P}	88.41 (± 17.55)	84.23 (± 4.65)	85.70 (± 6.83)
Phytate^{P}	85.15 (± 13.57)	88.97 (± 11.24)	85.29 (± 9.77)

The sulfate^{P} powder stored at RT displayed a significant decrease in deposition in the throat, as well as an increase in the powder found in stage 1 ($p < 0.05$) (figure 4.10). However, the powder stored at 4°C had the same deposition pattern as at the initial time point ($p > 0.05$) (figure 4.10).

For the gluconate^{P} formulation there was no difference in deposition between the powders from the 2 storage conditions ($p > 0.05$). For both, a decreased deposition in the throat and increased deposition in stages 1 and 2 were observed ($p < 0.05$) (figure 4.11).

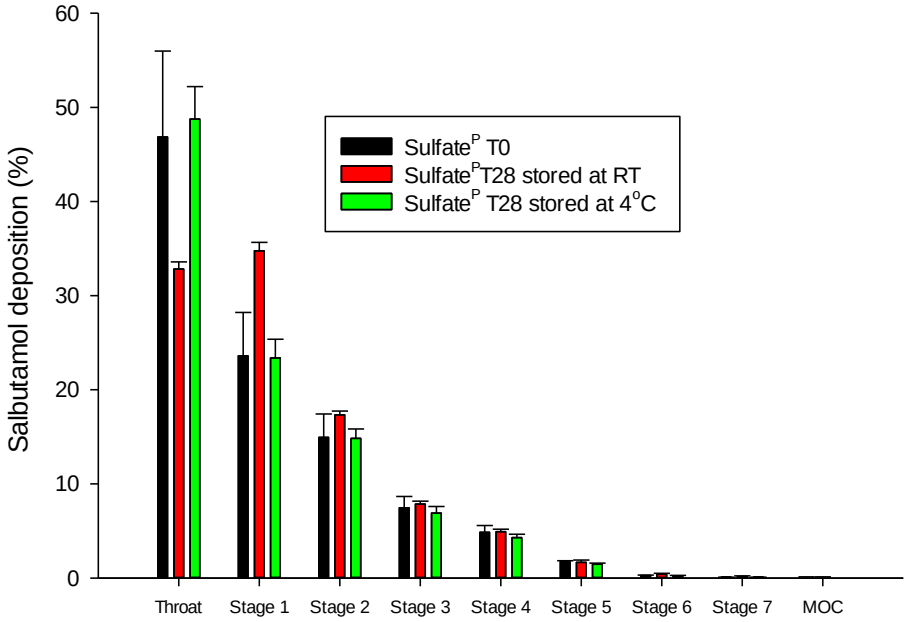

Figure 4.10 – Deposition of salbutamol in sulfate^{P} formulation in next generation impactor (NGI) prior to storage (T0) and after 1 month storage (T28) after storage with dessicant at room temperature and 4^{o}C. Data represents a mean ± standard deviation (n=3)

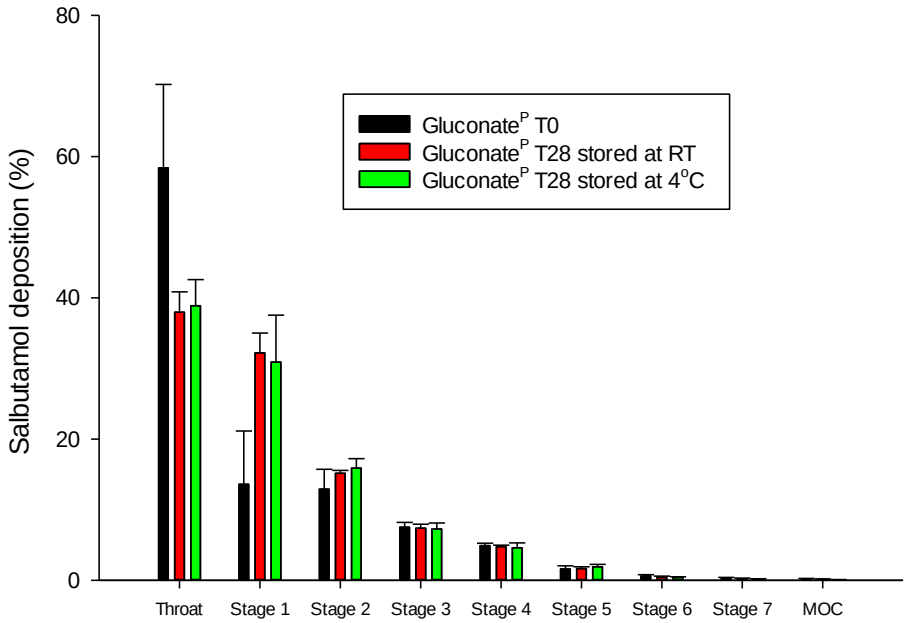

Figure 4.11 – Deposition of salbutamol in gluconate^{P} formulation in next generation impactor (NGI) prior to storage (T0) and after 1 month storage (T28) after storage with dessicant at room temperature and 4^{o}C. Data represents a mean ± standard deviation (n=3)

The octanoate^{P} powder that had been stored at RT showed an increased deposition in stage 1 of the NGI ($p < 0.05$). The powder that had been stored at 4^{o}C showed an increase in deposition in the throat ($p < 0.05$) (figure 4.12).

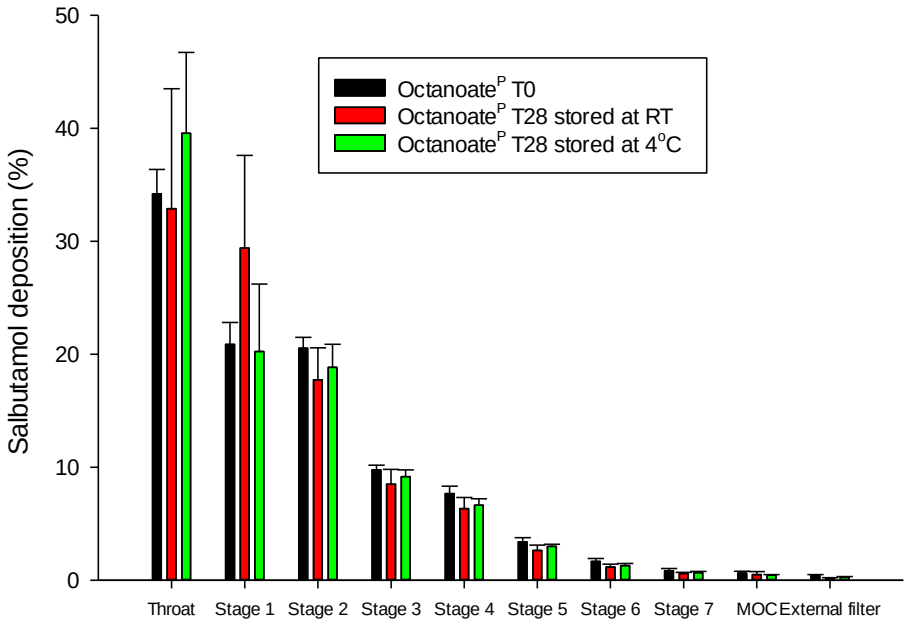

Figure 4.12 – Deposition of salbutamol in octanoate^{P} formulation in next generation impactor (NGI) prior to storage (T0) and after 1 month storage (T28) after storage with dessicant at room temperature and 4^{o}C. Data represents a mean ± standard deviation (n=3)

The phytate^{P} formulation appeared to behave similarly after storage for 4 weeks under both conditions. An increase in deposition of the powder in the throat was seen, along with a decrease of deposition in stage 1 ($p < 0.05$) (figure 4.13).

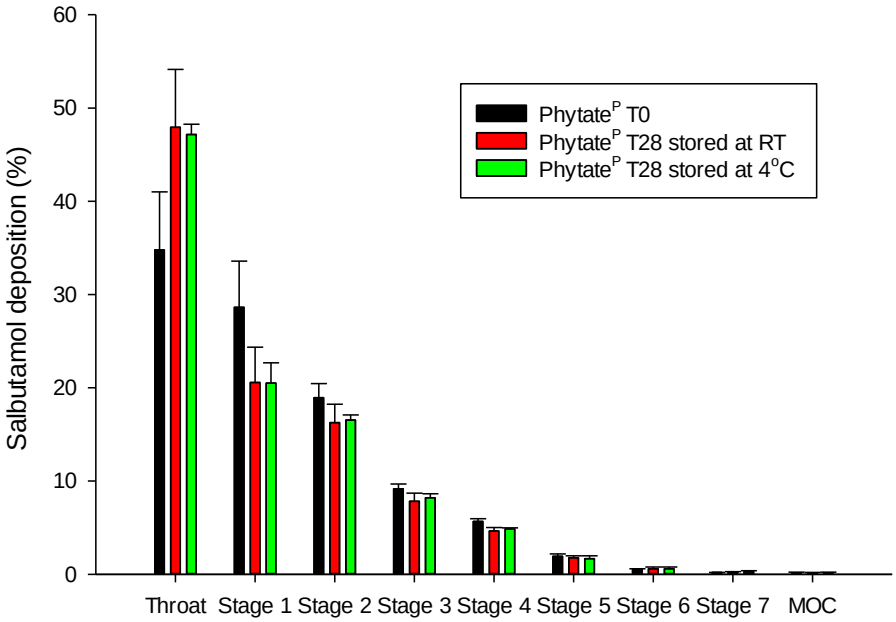

Figure 4.13 – Deposition of salbutamol in phytate^{P} formulation in next generation impactor (NGI) prior to storage (T0) and after 1 month storage (T28) after storage with dessicant at room temperature and 4^{o}C. Data represents a mean ± standard deviation (n=3)

The ED, MMAD, GSD, and FPF information from each experiment was analyzed and compared against the values at T0 to determine if they remained stable after the 4 weeks for each formulation. FDA guidance states that a 10% change in the total mass of relevant fine particles would be considered significant (Drug, 1998). Therefore, formulations were determined to be unstable if the results after 4 weeks varied by over 10% for the ED and FPF values, more than 0.5 μm for the MMAD and more than 0.2 μm for the GSD. The overall formulation was deemed unstable if more than 1 of these failed the stability check or if the one that failed did so by double the acceptable limit (table 4.12 and 4.13).

Table 4.12 – Comparison of the calculated results for ED, MMAD, GSD, and FPF for formulations Base - Phytate^{P} after storage for 4 weeks at room temperature (RT). Powders passed the stability check if the emitted dose (ED) and fine particle fraction (FPF) did not vary by over 10% the geometric standard deviation (GSD) did not vary by over 0.2 μm, and the mass median aerodynamic diameter (MMAD) did not vary by over 0.5 μm from the values prior to storage. If 2 or more of these parameters failed, or one failed by over double the acceptable limit the powder was deemed unstable.

Formulation	ED (%)	MMAD (μm)	GSD (μm)	FPF (%)	Stable?
Base	x	x	✓	✓	x
Sulfate	x	✓	✓	✓	✓
Gluconate	x	✓	✓	✓	✓
Octanoate	x	x	✓	✓	x
Phytate	x	✓	✓	✓	✓
Sulfate^{P}	x	x	✓	✓	x
Gluconate^{P}	x	x	✓	✓	x
Octanoate^{P}	✓	x	✓	✓	✓
Phytate^{P}	✓	✓	✓	✓	✓

Table 4.13 – Comparison of the calculated results for ED, MMAD, GSD, and FPF for formulations Base - Phytate^{P} after storage for 4 weeks at 4^{o}C. Powders passed the stability check if the emitted dose (ED) and fine particle fraction (FPF) did not vary by over 10% the geometric standard deviation (GSD) did not vary by over 0.2 μm, and the mass median aerodynamic diameter (MMAD) did not vary by over 0.5 μm from the values prior to storage. If 2 or more of these parameters failed, or one failed by over double the acceptable limit the powder was deemed unstable.

Formulation	ED (%)	MMAD (μm)	GSD (μm)	FPF (%)	Stable?
Base	x	✓	✓	✓	x
Sulfate	x	✓	✓	✓	x
Gluconate	x	✓	✓	✓	x
Octanoate	x	✓	✓	✓	x
Phytate	x	✓	✓	✓	x
Sulfate^{P}	x	✓	✓	✓	✓
Gluconate^{P}	✓	x	✓	✓	✓
Octanoate^{P}	✓	✓	✓	✓	✓
Phytate^{P}	✓	✓	✓	✓	✓

4.3.3 *The effect of l-leucine on aerosolisability*

The use of l-leucine in the formulation was to increase dispersity and therefore the amount of powder that would be inhaled. L-leucine was added as 5% of the total powder weight in the feed solution. The addition of the excipient further increased the yield of the powders (table 4.15). For all the formulations but the octanoate, the resultant powder was visibly much freer flowing. The particle size of the sulfate^{PL} and gluconate^{PL} formulations further increased from 3.92 and 3.36 μm, respectively, to give a size of 4.21 and 3.94 μm, respectively ($p < 0.05$) (table 4.15). Although the size of the octanoate^{PL} significantly increased from the octanoate^{P} ($p < 0.05$), there was no significant difference between that and the octanoate formulation ($p > 0.05$). There was also no significant change in the size of the particles in the phytate^{PL} formulation ($p > 0.05$) (table 4.14).

SEM pictures show that the l-leucine also affected the surface morphology of the spray dried particles. Fewer particles are seen to have the smooth appearance that was initially observed and there is an increase in uneven, “dimpled” looking particles and also broken particles (figure 4.14).

Table 4.14 – Spray drying and laser diffraction particle size results for formulations base, sulfate^{PL}, gluconate^{PL}, octanoate^{PL}, and phytate^{PL}. X_{50} is the median particle volume diameter and VMD is the volume mean diameter

Formulation	Yield (%)	x_{50} (µm)	VMD (µm)
Base	51 (±2.00)	3.68 (± 0.26)	3.96 (± 0.30)
Sulfate^{PL}	65 (± 2.52)	4.21 (± 0.05)	4.43 (± 0.07)
Gluconate^{PL}	68 (± 2.08)	3.94 (± 0.06)	4.17 (± 0.05)
Octanoate^{PL}	51 (± 1.53)	3.20 (± 0.04)	3.47 (± 0.04)
Phytate^{PL}	68 (± 1.53)	3.23 (± 0.07)	4.39 (± 0.02)

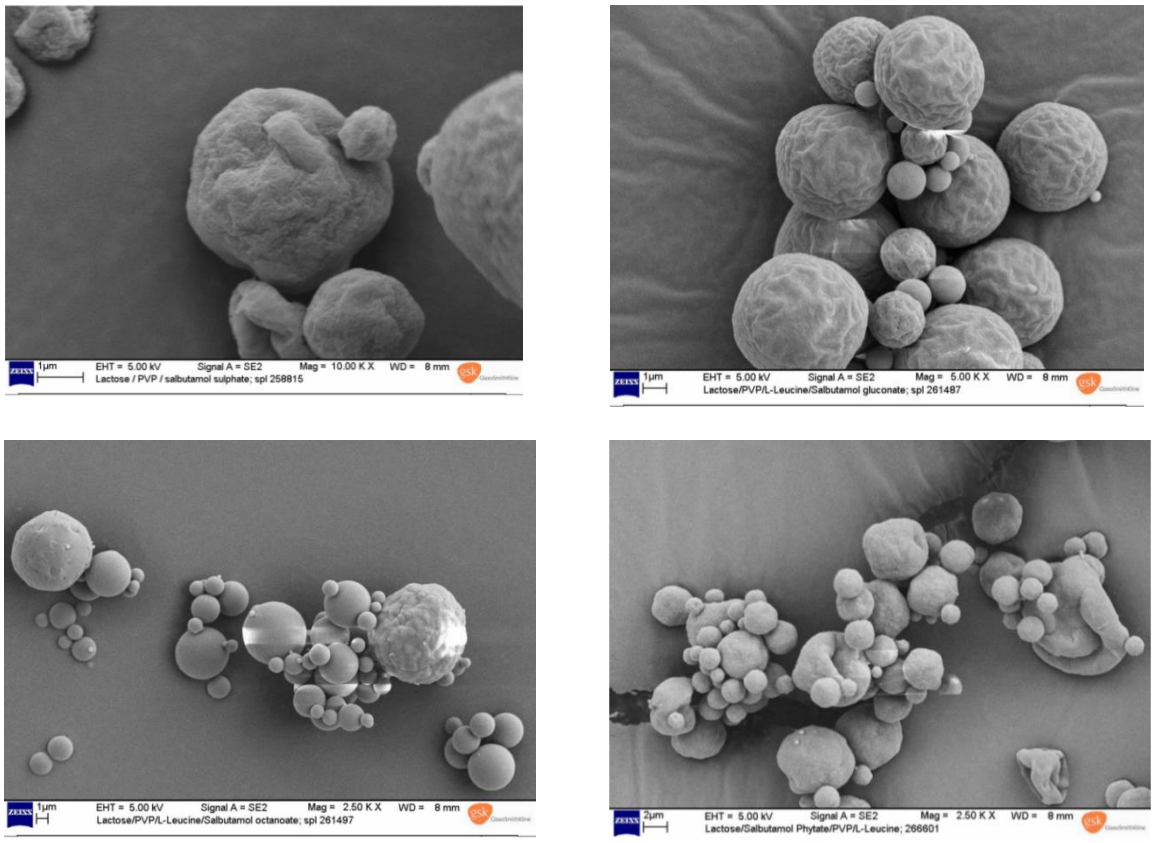

Figure 4.14 – Scanning electron microscope images of formulations sulfate^{PL}, gluconate^{PL}, octanoate^{PL}, and phytate^{PL}

The content uniformity results for the sulfate^{PL} and phytate^{PL} formulations showed that almost the entirety of the drug that was in the feedstock for spray drying was incorporated in to the resultant powder, with averages of 90 and 95% respectively (table 4.15). All of these powders apart from the octanoate^{PL} formulation were considered homogeneous according to the previously stated definition.

Table 4.15 – Percentage of salbutamol from spray drying feedstock that was incorporated in to the powder for formulations base, sulfate^{PL}, gluconate^{PL}, octanoate^{PL}, and phytate^{PL}

Formulation	Salbutamol content (%)
Base	85.63 (± 7.27)
Sulfate^{PL}	89.93 (± 5.56)
Gluconate^{PL}	73.62 (± 11.82)
Octanoate^{PL}	79.88 (± 10.41)
Phytate^{PL}	94.85 (± 3.28)

Addition of l-leucine in to the formulation was proposed to increase the dispersion efficiency of the powder; however this effect was only seen for sulfate^{PL} which has increased deposition in stages 2 -7 when compared with the base (figure 4.15). The octanoate^{PL} showed an increased MMAD value when compared to its PVP only equivalents ($p < 0.05$) (table 4.16). The phytate^{PL} formulation showed a decreased MMAD value in comparison to the phytate^{P} formulation ($p < 0.05$), but there was no difference when compared with the phytate formulation ($p > 0.05$).

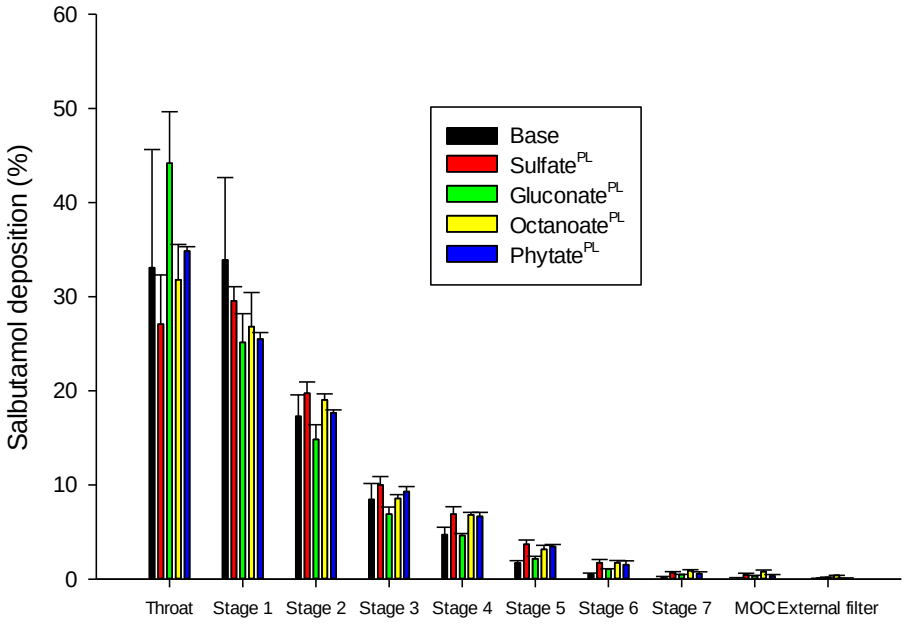

Figure 4.15 – Deposition of salbutamol on all stages of the Next Generation Impactor as a percentage of the total emitted dose for base formulation and formulations sulfate^{PL}, gluconate^{PL}, octanoate^{PL} and phytate^{PL}. Data shown represents the mean ± standard deviation (n=3)

The addition of l-leucine did increase the amount of powder emitted from the inhaler for all formulations, with a maximum of almost 88 % being emitted for gluconate^{PL}. As a result of this the FPF for each formulation except octanoate^{PL} increased, being around 5 – 10 % higher than the PVP only formulations (table 4.16).

Table 4.16 - Parameters derived from the stage by stage Next Generation Impactor deposition data for formulations base, sulfate^{PL}, gluconatePL, octanoatePL and phytate^{PL}. Emitted dose (ED), mass median aerodynamic diameter (MMAD), geometric standard deviation (GSD), and fine particle fraction (FPF).

Formulation	ED (%)	MMAD (μm)	GSD (μm)	FPF (%)
Base	74.24 (± 2.14)	6.30 (± 0.71)	2.31 (± 0.04)	25.34 (± 4.08)
Sulfate^{PL}	79.38 (± 1.12)	5.19 (± 0.15)	2.51 (± 0.03)	34.93 (± 3.36)
Gluconate^{PL}	87.58 (± 2.74)	5.30 (± 0.26)	2.44 (± 0.22)	29.96 (± 5.08)
Octanoate^{PL}	84.42 (± 2.09)	5.09 (± 0.38)	2.56 (± 0.04)	33.39 (± 1.21)
Phytate^{PL}	80.44 (± 3.24)	4.99 (± 0.14)	2.48 (± 0.08)	32.01 (± 1.13)

The calculated aerodynamic diameters for the sulfate^{PL} and phytate^{PL} powders were greater than the experimental MMAD, suggesting that the addition of l-leucine enhanced the aerosolization of these powders (table 4.17).

Table 4.17 – Comparison of average mass median aerodynamic diameter (MMAD), volume mean diameter (VMD) and calculated aerodynamic diameter (d_a) values for formulations sulfate^{PL}, gluconate^{PL}, octanoate^{PL} and phytate^{PL}

Formulation	MMAD (μm)	VMD (μm)	Calculated d_a (μm)
Sulfate^{PL}	5.19 (± 0.15)	4.43 (± 0.07)	5.46
Gluconate^{PL}	5.30 (± 0.26)	4.17 (± 0.05)	5.14
Octanoate^{PL}	5.09 (± 0.38)	3.47 (± 0.04)	4.27
Phytate^{PL}	4.99 (± 0.14)	4.39 (± 0.02)	5.41

The stability of the leucine formulations was tested in the same way as the PVP and counter ion formulations.

The content uniformity results after 4 weeks of storage seem to indicate that the leucine formulations are more stable than the PVP and counter ion ones, especially when stored at RT. The results for each of the leucine powders stored at RT do not significantly differ from the initial results, and there is no significant increase in variability ($p > 0.05$). This is also true of the octanoate^{PL} and phytate^{PL} powders stored at 4^{o}C (table 4.18).

Table 4.18 – Comparison of the percentage of salbutamol from spray drying feedstock that was incorporated in to the powders for the salbutamol-counter ion-polyvinyl pyrrolidone-leucine formulations prior to storage (T0) and after 4 weeks (T28) storage with dessicant at room temperature and 4^{o}C

Formulation	Salbutamol content at T0 (%)	Salbutamol content at T28 after storage at RT (%)	Salbutamol content at T28 after storage at 4^{o}C (%)
Base	85.63 (± 7.27)	104.24 (± 18.02)	97.36 (± 15.27)
Sulfate^{PL}	89.93 (± 5.56)	83.03 (± 8.83)	86.57 (± 13.11)
Gluconate^{PL}	73.62 (± 11.82)	78.94 (± 6.70)	80.01 (± 11.08)
Octanoate^{PL}	79.88 (± 10.41)	76.67 (± 6.46)	80.66 (± 6.10)
Phytate^{PL}	94.85 (± 3.28)	91.82 (± 3.24)	90.42 (± 6.04)

There was no change in the deposition profile of the sulfate^{PL} or gluconate^{PL} formulation after storage for 4 weeks under either condition ($p > 0.05$) (figure 4.16, 4.17).

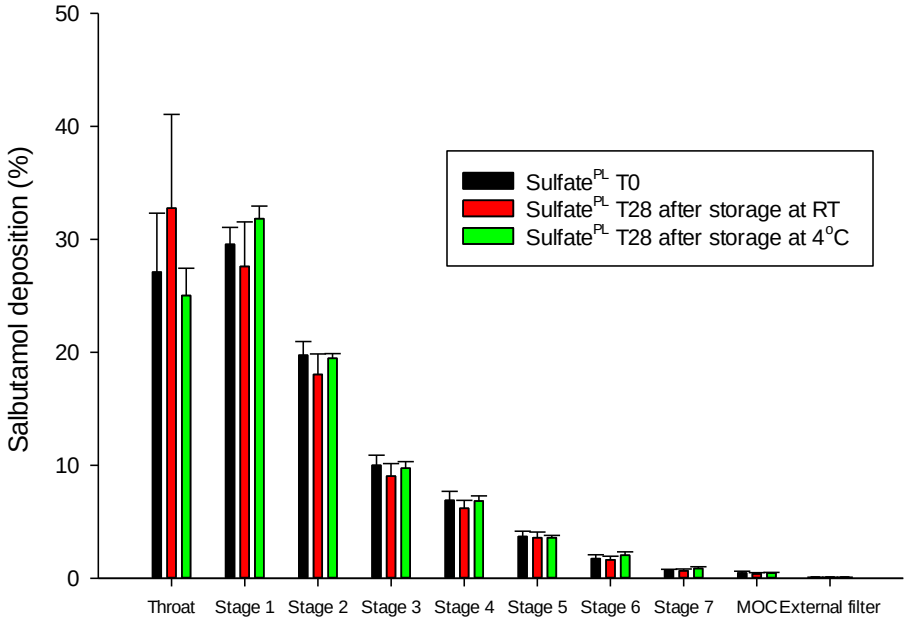

Figure 4.16 – Deposition of salbutamol in sulfate^{PL} formulation in next generation impactor (NGI) prior to storage (T0) and after 1 month storage (T28) after storage with dessicant at room temperature and 4^{o}C. Data represents the mean ± standard deviation (n=3)

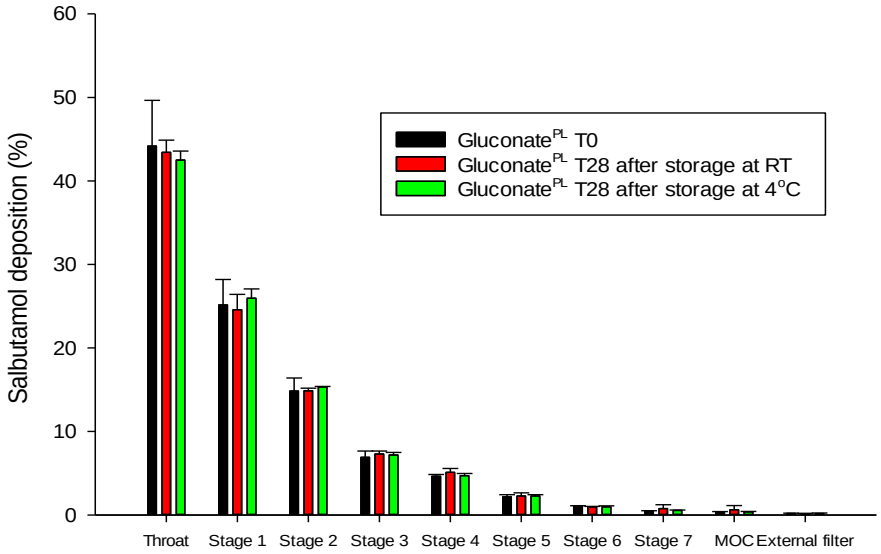

Figure 4.17 – Deposition of salbutamol in gluconate^{PL} formulation in next generation impactor (NGI) prior to storage (T0) and after 1 month storage (T28) after storage with dessicant at room temperature and 4^{o}C. Data represents a mean ± standard deviation (n=3)

Although there was no significant difference in results between the 2 storage conditions, the deposition of the octanoate^{PL} formulation after a month showed a significant increase in drug deposition in the throat ($p < 0.05$) (figure 4.18).

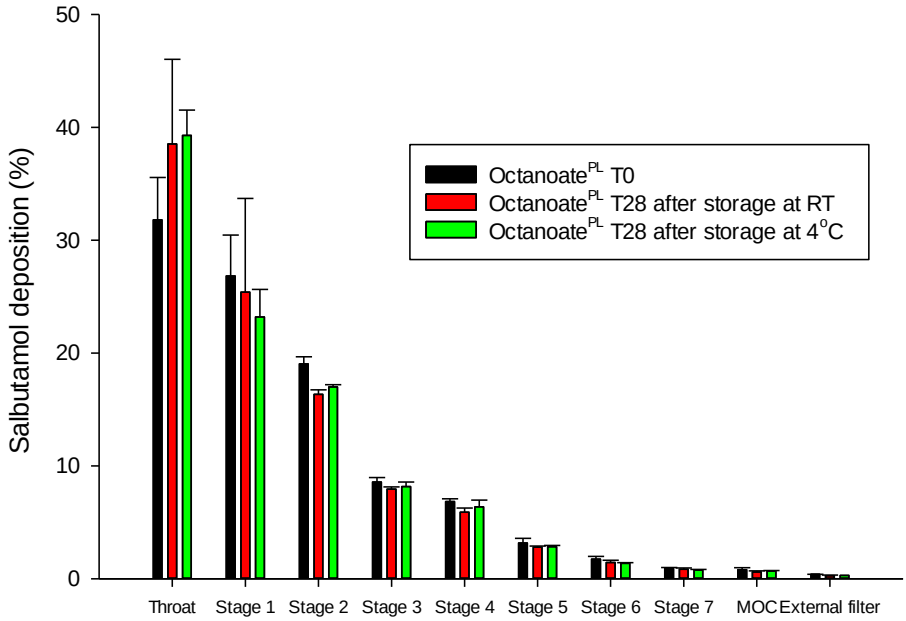

Figure 4.18 – Deposition of salbutamol in octanoate^{PL} formulation in next generation impactor (NGI) prior to storage (T0) and after 1 month storage (T28) after storage with dessicant at room temperature and 4^{o}C. Data represents a mean ± standard deviation (n=3)

The phytate^{PL} formulation also showed an increased salbutamol deposition in the throat ($p < 0.05$). However, there appeared to be no significant change in the deposition of the other stages of the NGI ($p > 0.05$) (figure 4.19).

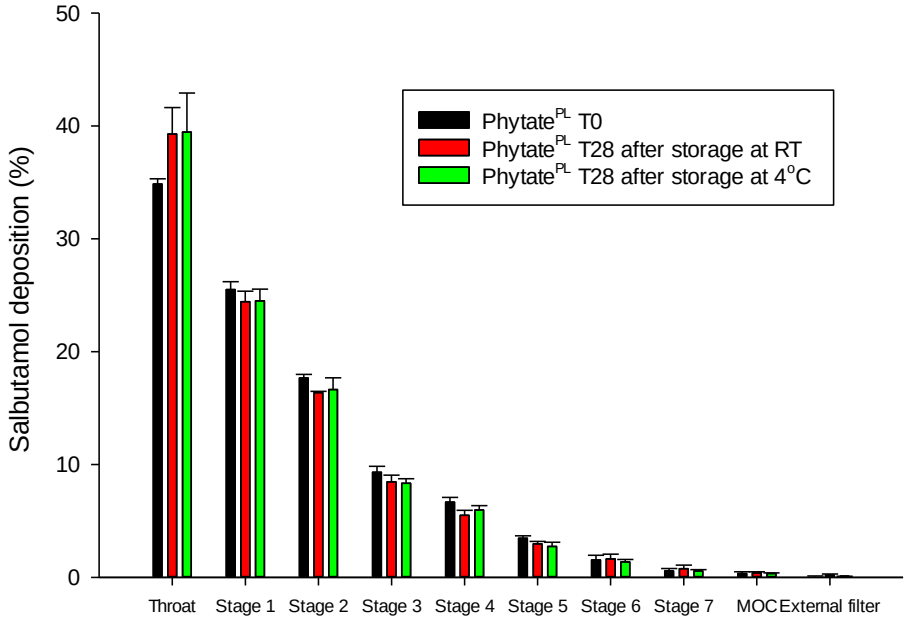

Figure 4.19 – Deposition of salbutamol in phytate^{PL} formulation in next generation impactor (NGI) prior to storage (T0) and after 1 month storage (T28) after storage with dessicant at room temperature and 4^{o}C. Data represents a mean ± standard deviation (n=3)

The ED, MMAD, GSD and FPF results were analyzed for stability using the same criteria as previously mentioned (table 4.19 and 4.20).

Table 4.19 – Comparison of the calculated results for ED, MMAD, GSD, and FPF for sulfate^{PL}, gluconate^{PL}, octanoate^{PL} and phytate^{PL} formulations after storage for 4 weeks at room temperature (RT). Powders passed the stability check if the emitted dose (ED) and fine particle fraction (FPF) did not vary by over 10% the geometric standard deviation (GSD) did not vary by over 0.2 μm, and the mass median aerodynamic diameter (MMAD) did not vary by over 0.5 μm from the values prior to storage. If 2 or more of these parameters failed, or one failed by over double the acceptable limit the powder was deemed unstable.

Formulation	ED (%)	MMAD (μm)	GSD (μm)	FPF (%)	Stable?
Sulfate^{PL}	✓	✓	✓	✓	✓
Gluconate^{PL}	✓	✓	✓	✓	✓
Octanoate^{PL}	✓	✓	✓	✓	✓
Phytate^{PL}	✓	✓	✓	✓	✓

Table 4.20 – Comparison of the calculated results for ED, MMAD, GSD, and FPF for sulfate^{PL}, gluconate^{PL}, octanoate^{PL} and phytate^{PL} formulations after storage for 4 weeks at 4^{o}C. Powders passed the stability check if the emitted dose (ED) and fine particle fraction (FPF) did not vary by over 10% the geometric standard deviation (GSD) did not vary by over 0.2 μm, and the mass median aerodynamic diameter (MMAD) did not vary by over 0.5 μm from the values prior to storage. If 2 or more of these parameters failed, or one failed by over double the acceptable limit the powder was deemed unstable.

Formulation	ED (%)	MMAD (μm)	GSD (μm)	FPF (%)	Stable?
Sulfate^{PL}	x	✓	✓	✓	✓
Gluconate^{PL}	x	✓	✓	✓	✓
Octanoate^{PL}	✓	✓	✓	✓	✓
Phytate^{PL}	✓	✓	✓	✓	✓

4.4 *Discussion*

A spray drying method for lactose and salbutamol ion-pairs was developed that generated particles below 5 μm in diameter with uniform drug content in an acceptable yield. The method was optimized for this size range as it is generally accepted that particles below 5 μm in diameter are inhalable (Elversson et al., 2003). Furthermore, the SEM pictures of all formulations showed that the particles were spherical, which indicates that they were probably amorphous (Wu et al., 2014). This was expected as it is well known that the spray drying procedure tends to generate amorphous powders (Rabbani and Seville, 2005).

Confirmation of the amorphous nature of the powders was attempted using differential scanning calorimetry (DSC) (results not shown). DSC is a technique frequently used to analyze the physical and chemical properties of a drug or formulation and how those properties change with change in temperature (Knopp et al., 2016). The recrystallization peak of lactose, the bulk of the formulations generated, is known to occur around 170^{o}C (GombÁs et al., 2002), however this could not be seen in the drug-lactose mixtures due to a chemical reaction between the two components. The Maillard reaction is the reaction of a reducing sugar, such as lactose, and amines such as salbutamol (Wirth et al., 1998). Unfortunately, this meant that the glass transition of lactose, occurring at around 115^{o}C in the base formulation was the only indicator of the physical properties of the powder. Glass transitions could not be accurately observed for any of the formulations; however the absence of noticeable T_g does not indicate that these powders are crystalline. There are drawbacks to the DSC technique when using complex mixtures in that the thermal events may overlap and weak transitions can be lost (Knopp et al., 2016). In the thermograms

acquired for this study it is possible that the T_g of lactose overlaps with the peak associated with the loss of water from the sample, and as such the T_g could not be identified. To overcome this in future experiments a powder X-ray Diffraction technique could be employed.

The addition of the sulfate counter ion in to the formulation had no significant effect on the particle size or aerosolisability of the spray dried powder. The addition of the gluconate, octanoate and phytate counter ions all resulted in a significantly lower particle size by laser diffraction. It is well documented that surfactants, such as sodium octanoate, adsorb to an air-liquid or oil-liquid interface, arranging themselves such that the hydrophilic head is in the water phase and hydrophobic tail in the non-aqueous phase (Adhikari et al., 2009, Pugnaloni et al., 2004). Low molecular weight surfactants are particularly capable of this due to their increased mobility leading to a reduction of surface tension (Pugnaloni et al., 2004). In spray-drying a reduced surface tension leads to reduced droplet size, which can explain the smaller particles size found in the octanoate formulation (Patel et al., 2009b). Similarly, in order to reduce particle size the gluconate and phytate molecules must have an effect on the properties of the feed stock solution. A reduction in surface tension, viscosity or density would all result in a smaller droplet, and therefore particle, size (Patel et al., 2009b). It has been found in studies that low molecular weight aliphatic acids, much like gluconic acid, reduce the surface tension of water (Mahiuddin et al., 2008).

The emitted dose for the base, sulfate, gluconate, octanoate and phytate formulations all ranged between 70 – 80%, showing none of the counter ions significantly affected this which could suggest that there was not a significant difference in the surface electrical charge of the particles in each of these powders (Wong et al., 2014). The MMAD value for

each of these formulations falls in to the aerosolisable range, which is up to around 7 μm for lung deposition (Maa et al., 1997, Labiris and Dolovich, 2003c). However the reduced particle size of the gluconate, octanoate and phytate powders meant these formulations also had a significantly reduced aerodynamic diameter (4.85, 4.85, 4.93 μm vs. 6.30 μm for gluconate, octanoate, phytate and base, respectively). The fine particle fractions ranged from 25 – 34%. These values are similar to the values in commercial drug – lactose mixtures without further excipients, which typically range from 20 – 30% (Hassoun et al., 2015).

Formulations were created containing PVP, as it is known to have a stabilizing effect on amorphous lactose. Although the use of amorphous materials in pharmaceutical formulations has its advantages, such as increasing the bioavailability of the active ingredient, they are inherently unstable (Mahlin et al., 2006, Berggren and Alderborn, 2003a). Amorphous powders can undergo spontaneous recrystallization, changing the physical properties of a drug formulation, and ultimately leading to a short shelf life (Berggren and Alderborn, 2003a). Incorporation of PVP in to the ion-pair formulations resulted in an increase in particle size for the sulfate^{P} and gluconate^{P} formulations. This was expected as the polymer would increase the viscosity of the feed stock solution, leading to larger droplets (Mahlin et al., 2006). Conversely, the octanoate^{P} particle size was significantly lower than the octanoate formulation. It has been shown previously that spray dried PVP enriches a particle surface and so perhaps the mixture and arrangement of octanoate and PVP molecules at the surface of the particle causes this decrease in size (Mahlin et al., 2006). There was no change in the size of the phytate^{P} particles. The SEM pictures show that the inclusion of PVP causes a dimpled appearance to some particles, this effect can also be attributed to the increase in viscosity of the feed solution containing

the polymer affecting the drying pattern of the droplets (Elversson et al., 2003). The octanoate^{P} formulation appeared to contain fewer irregularities in the surface of the particles, which might be explained by the surfactants presence at the surface of the particle (Maa et al., 1997). There was a reduction in the emitted dose and fine particle fraction of the sulfate^{P} and gluconate^{P} formulations caused by their greater particle size, although the sulfate^{P} powder had a greatly reduced MMAD in comparison to the sulfate powder. The reduction in emitted dose might also contributed to by a difference in the electrical charge of particles that have surface PVP compared with the surface composition of the none PVP particles (Wong et al., 2014). The reduction in particle size of the octanoate^{P} formulation resulted in a reduced MMAD and an increased FPF, but the formulation also suffered from a significantly reduced emitted dose which could be caused by the increased surface area and therefore contact between the particles, or a change in the charge of the surface of particles. There was an increase in the MMAD of the phytate^{P} particles, but also a significant increase in the emitted dose (83.63% phytate^{P} vs 71.38% phytate). This increase could be explained by the irregular surface of the particles increasing flowability by reducing the contact between particles (Vehring, 2008).

Both the ion-pair formulations and PVP formulations were kept with a dessicant at either room temperature or 4^{o}C for 4 weeks to test their stability over this time. Repetition of the content uniformity test showed a significant increase in the variability of salbutamol content in the ion-pair powders without PVP and therefore each of those formulations failed the homogeneity test after the storage period under either condition. Although some of the PVP formulations initially failed the homogeneity test, after one month storage the variability in salbutamol content was greatly reduced with many of the formulations now passing the test. The gluconate^{P} formulation appeared to be the least stable as under both

conditions a significant drop in salbutamol content was found (85.36% ±6.62 at T0, 70.35% ±17.91 at T28 RT, 73.75% ±8.39 at T28 4^{o}C). This formulation appeared particularly unstable after storage at room temperature as the variability in salbutamol content results was almost 20%.

The *in vitro* deposition experiments were also repeated after the storage period. All calculated values from this data were given an allowed variance (10% for ED and FPF, 0.5 μm for MMAD and 0.2 μm for GSD) and if results for a formulation fell outside of these limits they would fail. If a formulation failed in 2 or more of the 4 criteria it was deemed unstable. Of the ion-pair formulations, the sulfate, gluconate and phytate powders were the most stable as they passed the stability check after storage at room temperature. The base and octanoate powders failed the check under both of the storage conditions. The octanoate^{P} and phytate^{P} passed the stability check after storage at room temperature. It has been suggested that for stable storage of amorphous materials a temperature of at least 50^{o}C below the Tg should be used, and the Tg is reduced by any absorbed water in the material (Berggren and Alderborn, 2004). PVP is known to inhibit crystallization but the effect is increased with increasing polymer concentration and molecular weight (Berggren and Alderborn, 2003a) therefore it is possible that the concentration and molecular weight of PVP used for these formulations was not sufficient to inhibit recrystallization over 4 weeks at room temperature. However all of the ion-pair/PVP formulations passed the stability check after storage at 4^{o}C. The stabilizing action of PVP is thought to be as a result of it forming hydrogen bonds with other substances as it contains a hydrogen bond donating group (Berggren and Alderborn, 2003b, Crowley and Zografi, 2003, Taylor and Zografi, 1998).

Formulations for each ion-pair were generated containing PVP and l-leucine to assess whether a powder with improved aerosolisability could be created. The addition of l-leucine in to the spray drying feedstock greatly increased the yield of powder, with a 68% recovery for the gluconate^{PL} and phytate^{PL} formulations. It has been shown in many studies that the incorporation of l-leucine in to a spray dried powder for inhalation can improve the powder's dispersibility and aerodynamic performance (Rabbani and Seville, 2005, Li et al., 2005, Najafabadi et al., 2004). It is thought that this improved dispersibility is due to the formation of an l-leucine shell during the spray drying process. Studies have shown that pure spray dried l-leucine creates hollow crystalline leucine particles and so the amino acid has the potential to encapsulate other spray dried material in a crystalline shell (Vehring, 2008). The appearance of the generated sulfate^{PL}, gluconate^{PL} and phytate^{PL} powders were visibly freer flowing than the powders without l-leucine. This was not true for the octanoate^{PL} formulation which could be due to the octanoate molecule precipitating before l-leucine and therefore inhibiting its ability to crystallize (Vehring, 2008). This can also be seen in the SEM pictures. The sulfate^{PL}, gluconate^{PL} and phytate^{PL} all display a wrinkled appearance that has been previously seen with particles containing l-leucine (Vehring, 2008, Najafabadi et al., 2004), however the octanoate^{PL} formulation appears to contain less of these and more smooth spherical particles.

The dose emitted from an inhaler for each of the leucine containing formulations increased up to 10% in comparison with the ion-pair only formulations which could be as a result of the irregular morphology of the particles preventing excessive aggregation (Chen et al., 2012). It is thought that leucine travels to the surface of droplets in the spray-drying procedure, causing a leucine shell to form on drying. This shell causes the particle to have an irregular surface morphology, which in turn significantly decreases the contact area

between particles (Chen et al., 2016, Mangal et al., 2015). There was a significant decrease in the MMAD value for the sulfate^{PL} in comparison with the sulfate formulation (5.19 μm vs. 6.24 μm) and also a significant increase in the FPF (34.93% vs. 25.14%). However no significant difference was observed for the gluconate^{PL}, octanoate^{PL} or phytate^{PL} powders. Although the FPF value for each of the leucine formulations was higher than those without, that range was only 30 – 35% which is not significantly improved on what can be expected of simple drug – lactose powders. Previous studies have shown that incorporation of leucine in to a powder can result in respirable fractions of up to 80% of the delivered dose (Rabbani and Seville, 2005). However, these studies used initial leucine fractions of up to 10%, compared to the 5% used in this study. In addition the improved dispersion effect of leucine can be enhanced by spray drying from an ethanol-water mixture, leucine is less soluble in ethanol than water and adjusting its solubility with a co-solvent system can provide the high saturation of the molecule needed to form the crystalline shell (Rabbani and Seville, 2005, Vehring, 2008). Alternatively di- or tri-peptides, such as trileucine, can be employed to enhance aerosolisability. Trileucine is less soluble than leucine in water and such a smaller fraction is needed to improve dispersibility than the equivalent leucine formulation (Vehring, 2008).

The stability of the leucine formulations was also tested after 4 weeks storage with dessicant at either room temperature or 4^{o}C. There was no significant difference between T0 and T28 content uniformity results for any of the formulations stored at room temperature, suggesting that these powders were more stable in amorphous form than the formulations with PVP alone. This would suggest that l-leucine itself has a stabilizing effect on the amorphous bulk of the powder, inhibiting recrystallization of amorphous materials, as has been theorized previously (Sou et al., 2013). This stabilizing effect was also seen in

the repeated drug deposition data, with each of the leucine formulations meeting the set criteria for the stability check after storage under both conditions. This would indicate that with further investigation in to the concentration of l-leucine used or spray drying conditions employed to generate the powder an inhalable ion-pair formulation with high FPF that is stable over a long period of time could be created.

4.5 Conclusion

Dry powder formulations containing salbutamol ion-pairs were generated via a spray drying technique that was optimized for salbutamol and lactose. These formulations were presumed to be amorphous in nature due to being spherical and demonstrated an acceptable respirable fraction. Further ion-pair formulations were generated containing the polymer PVP. The stabilizing effects of PVP on amorphous solids are well documented and so its effect of the ion-pair formulations was investigated. It was found that the addition of PVP increased the particle size of the sulfate^{P}, gluconate^{P} formulations, thought to be caused by an increase in viscosity of the spray drying feed solution. The polymer also caused the previously spherical particles to take on a “dimpled” appearance. Conversely, the particle size of the octanoate^{P} formulation was significantly reduced, and as a result this formulation exhibited improved aerosol performance. The sulfate^{P}, octanoate^{P} and phytate^{P} formulations showed no significant change in deposition results after 4 weeks in storage at 4^{o}C, suggesting that the inclusion of PVP in to the formulation had inhibited recrystallization at this temperature. The addition of the amino acid l-leucine in to the formulations was also investigated due to its well-known ability to improve the dispersibility of powders. The generated leucine powders also had a wrinkled appearance, and displayed an amplified respirable fraction and emitted dose. L-leucine also appeared to

convey an amount of protection from recrystallization on to the powders as testing after one month showed no difference in the content uniformity or deposition results after storage at either room temperature or 4^{o}C. It was concluded that further work could improve the aerosolisability of the powders further, minimizing the particle size and therefore MMAD values to maximize lung deposition, but that the powders generated in this Chapter would be suitable to be used in the planned *in vivo* testing in Chapter 5. The specific counter ion powders that will be used in the *in vivo* work will be chosen dependent on their ability to modify salbutamol's dissolution and absorption profile which will also be explored in Chapter 5.

Chapter 5

The Effect of Ion-pairing on the *In vitro* and *In vivo* Behavior of Salbutamol

5.1 Introduction

Upon deposition in the lung, an ion-pair dry powder formulation must undergo several processes that will determine its biopharmaceutical characteristics. Given what has been shown in the previous chapters of this thesis it would be anticipated that ion-pair formation would alter the way the therapeutic agent interacts with the lung environment. The ion-pair could modify drug dissolution, tissue absorption or retention, or modify the clearance of the drug.

Ion-pair formation could modify both the drug solid state or its lipophilicity, hence it can influence dissolution. Depending on the size of the aerosolized ion-pair, the amount of lung fluid that is present for dissolution could vary from ~0.1 μm in the alveolar region to a maximum of 100 μm in the upper airways (Olsson et al., 2011, Widdicombe and Widdicombe, 1995). Therefore, it is possible that an inhaled particle will be deposited in lung fluid that has less depth than the diameter of the particle depending on where it is deposited (Olsson et al., 2011). It is generally accepted that a poorly soluble drug can show a prolonged period of therapeutic action in the lungs due to its slow dissolution (Olsson et al., 2011, Wang et al., 2014). This is due to the slow rate of dissolution preventing rapid absorption of the drug molecule, and therefore clearance in to the blood. However, undissolved particles are subject to removal from the airways via the mucociliary escalator or phagocytosis, which could greatly reduce the retention time of the therapeutic agent within the lungs (Wang et al., 2014). Thus, the use of an ion-pair strategy to limit dissolution could increase lung retention time by limiting the amount of drug that is available to be absorbed across the epithelium. On the other hand, modification of dissolution could be inappropriate for some drug molecules depending on their intended

site of action as it could lead to more efficient removal of the agent and a reduced lung retention time.

Alternatively, the ion-pair could directly modulate the absorption of the therapeutic agent across the lung epithelial cells. Absorption mechanisms can be passive or active. Passive mechanisms include the diffusion of small molecular weight lipophilic compounds through the epithelial cell, transcellular transport, or the travel of hydrophilic compounds through the intercellular space, paracellular transport (Liu et al., 2013). *In vivo* data has shown that lipophilic drugs are absorbed much more rapidly than hydrophilic drugs, so an ion-pairing strategy could be employed to create a complex with increased hydrophilicity to reduce the rate of transport into the epithelium (Olsson et al., 2011). Conversely, there have been several studies that have shown that rapidly dissolving hydrophobic molecules, such as tacrolimus, display prolonged drug action due to the molecule remaining in the epithelial cells rather than absorbing in to the systemic circulation, so creating a more hydrophobic complex could increase tissue retention (Watts et al., 2010, Thorsson et al., 2001). Finally, the rate of absorption of a compound could be altered by increasing its molecular weight. Ion-pairing with a high molecular weight counter ion could limit drug transport across the respiratory epithelium as transport rates have been shown to be inversely proportional to molecular weight (Grainger et al., 2006).

The aim of this Chapter was to investigate the effect of ion-pairing on the *in vitro* and *in vivo* behavior of salbutamol. The biocompatibility of the counter ions and excipients used in previous chapters was analyzed and the transport of salbutamol base across an airway cell monolayer assessed. The effect of the sulfate, gluconate, octanoate and phytate counter ions on the transport of salbutamol was then investigated. Following this, suitable

ion-pairs were chosen to be tested in an animal model. Dissolution studies were performed for the spray dried powders of the chosen ion-pairs containing PVP. Although the previous chapter indicated that the l-leucine containing powders appeared to be the most stable it was decided against using these powders in this study. This was as a result of l-leucines zwitterionic nature at physiological pH, which could potentially break down the salbutamol ion – pair. The bronchoprotective properties of salbutamol base and the phytate ion-pair against a histamine challenge were studied *in vivo*.

The culture of epithelial cells and cell layers is widely used and accepted in the pharmaceutical industry as a method to study the transport of inhaled medicines as well as their biocompatibility. In particular, the bronchial epithelial cell line Calu-3 has been shown to grow in to layers of columnar epithelial cells with tight junctions, making it ideal to study the transport of molecules (Forbes, 2000, Forbes and Ehrhardt, 2005). Consequently, the Calu-3 cell line was chosen as a model of the airway epithelium for use in the work in this Chapter.

This *in vitro* cell model can also be used to assess the biocompatibility of the excipients and counter ions used in the dry powder formulation. The counter ions in an ion-pair formulation are present in excess to promote the formation of the ion-pair species; as a result it is very important that they are well tolerated. For this work the effect of counter ion on cell viability using the 3-[4,5-dimethylthiazol-2-yl]-2,5 diphenyl tetrazolium bromide (MTT) assay was investigated. The MTT assay measures cell viability resulting from their mitochondrial activity (van Meerloo et al., 2011). Functioning mitochondria of the cells convert the yellow MTT compound into purple formazan crystals, and therefore the extent

to which the compound is converted can be used as a reflection of cell viability (van Meerloo et al., 2011).

Although *in vitro* cell culture models can reveal a large amount of information regarding the mechanisms and kinetics of pulmonary drug transport, animal models are still required to gain insight into the pharmacokinetic and pharmacodynamic properties of the formulation following inhalation. Ideally, the study of pulmonary medicines would be performed on humans, however the use of small animal models has many advantages including the small amount of drug sample required for experiments (Sakagami, 2006). Of the small rodents, guinea pigs are ideal models for an inhaled medicine because the guinea pig has a similar respiratory physiology to humans (Cryan et al., 2007) and the airway smooth muscle of guinea pigs is functionally similar to that of humans (Cryan et al., 2007, Canning and Chou, 2008). The use of ion-pairs to create an inhaled salbutamol formulation could lead to a prolonged duration of bronchodilation *in vivo*, or create a prolonged period of protection against bronchoconstriction. For this reason, guinea pigs were chosen as a suitable animal model to investigate the pharmacokinetic behavior of the ion-pair formulations.

5.2 Materials and Methods

5.2.1 Materials

Reagents for cell culture use were obtained from Sigma Aldrich (Dorset, UK), these included: Dulbecco's Modified Eagle's Medium/Nutrient F-12 Ham's 50/50, fetal bovine serum (FBS), non-essential amino acids, L-glutamine, gentamicin, trypsin-EDTA (0.25% trypsin, 0.05% EDTA), trypan blue, PBS, HBSS, MTT, dimethylformamide (DMF), and

Triton X. Calu-3 human bronchial cells were from ATCC (Rockville, USA). Sodium dodecyl sulfate (SDS) solution (20% w/v) was purchased from Fisher Scientific (Leicestershire, UK) and Transwell® inserts (polyester membrane, 0.4 μm pore size, 0.33 cm^2 growth surface area) were obtained from Corning Limited (Flintshire, UK). Salbutamol base (BN. H80619) was from Cipla Ltd (India) and used without further purification. Sodium sulfate was purchased from Alfa Aesar (Lancashire, UK). Sodium octanoate was obtained from Sigma Aldrich (Dorset, UK). Sodium gluconate and dipotassium phytate were purchased from Santa Cruz Biotechnology (USA). Orthophosphoric acid, HPLC grade water and acetonitrile were from Fisher Scientific (Leicestershire, UK).

5.2.2 Calu-3 cell culture

Calu-3 human bronchial cells were used between passage 10 and 50 and were kept in a humidified 5% CO_2/95% atmospheric air incubator at 37^oC. Cell culture media was made up of 50:50 Dulbecco's modified Eagle's medium F-12 Ham's (500 mL), FBS (50 mL), non-essential amino acid solution (5 mL), L-glutamine (200 mM, 5 mL), and gentamicin (0.5 mL). Medium was exchanged every 2 – 3 days and cells were passaged when they reached 80% confluency with trypsin-EDTA at a 1:3 split ratio. All cell culture work was carried out in a Class II safety cabinet.

Cells were harvested for use in experiments when they reached 80% confluency using the trypsin-EDTA solution. An aliquot of cell suspension was diluted with an equal volume of trypan blue and positioned on a haemocytometer for cell counting under a light microscope. Cells were counted from the 4 large corner squares of the haemocytometer and averaged to give a concentration of cells per mL of suspension. Non-viable cells were detected by the internalization of trypan blue and were not included in the count. The cell

suspension was diluted with the appropriate volume of cell culture medium to give the required cell seeding concentration for the experiment.

5.2.3 Biocompatibility assay

Biocompatibility of counter ions and formulation excipients was assessed using an MTT cell viability assay. Calu-3 cells were seeded at a density of 1 x 10^4 cells/well in a 96 well plate and cultured for 24 hours in cell culture medium (100 μL) with a reduced FBS concentration (2% v/v). All test samples were prepared in warmed cell culture medium (2% FBS) before use. Cells were either exposed to the test sample, cell culture medium as a negative control or 1% triton-X solution as a positive control and the cells were cultured for 24 hours. After this time the medium was removed from the cells and replaced with fresh cell culture medium (2% FBS, 200 μL) and MTT solution (5 mg/mL in PBS, 50 μL). The cells were incubated at 37^{o}C for 4 hours before the medium was removed and replaced with an SDS solution (10% w/v in 50:50 DMF:water, 100 μL). The cells were incubated with this solution for 16 hours to solubilize any formazan crystals present. Absorbance from each well was measured using a UV spectrophotometer (SpectraMax 190, Molecular Devices, USA) at 570 nm and corrected for a background reading performed at 650 nm. For each test well the absorbance value of a cell free well was subtracted and the remaining absorbance was used to determine cell viability by comparison to the positive and negative control values using the following equation:

$$\textbf{Viability}\ (\%) = \frac{\textbf{Atest} - \textbf{Apositive}}{\textbf{Anegative} - \textbf{Apositive}} \textbf{x}\ \textbf{100} \qquad \textbf{[Equation 5.1]}$$

Where Atest is the absorbance of the cell treated with sample, Apositive is the absorbance of the cell treated with the positive control and Anegative is the absorbance of the negative control (cell culture medium).

This assay was performed on the following compounds: sodium sulfate, sodium gluconate, sodium glucoheptonate, sodium fumarate, sodium maleate, sodium benzoate, sodium octanoate, dipotassium phytate, lactose, PVP.

5.2.4 Transport study

Cells were seeded on to Transwell® inserts at a density of 1.65 x 10^5 cells/well in cell culture medium in the apical (100 μL) and basolateral (500 μL) side. The cells were cultured at air liquid interface by removal of the apical medium on day 2 of culturing. The basolateral medium was replaced every 2 – 3 days. Cells were used on days 9 – 13 after seeding when cell layer barrier function is stable (Grainger et al., 2006). Transepithelial electrical resistance (TER) was measured prior to the transport assay. Cell culture medium (100 μL) was placed in the apical chamber of the well and the cells were incubated for at least 30 minutes before the TER was measured using chopstick electrodes with an EVOM voltohmmeter (STX-2 and EVOM G, World Precision Instruments, Stevenage, UK). TER was calculated by subtracting the resistance value of a cell free insert (140 Ω) and correcting for the surface area of the insert (0.33 cm^2). Cells were deemed fit for use if their TER value was over 300 Ωcm^2. Cell culture medium was removed from the apical chamber of fit for use wells and the cells were washed twice with warm HBSS (100 μL). The Transwell® insert was moved to a new well containing fresh, warm HBSS (600 μL) and HBSS was placed in the apical chamber (100 μL) before the cells were incubated for 2

hours to allow for equilibration. Test samples (salbutamol base (500 μg/mL), 20:1 salbutamol sulfate, 20:1 salbutamol gluconate, 20:1 salbutamol octanoate and 1:1 salbutamol phytate) were made up in warm HBSS before use.

At the beginning of the experiment the HBSS was removed from the apical chamber by aspiration and replaced with test solution (200 μL), a sample (100 μL) was taken immediately to verify concentration. Samples (100 μL) were removed from the basolateral chamber every 20 minutes for 2 hours and replaced with fresh warm HBSS. At 120 minutes the TER was measured again and a sample (100 μL) was also taken from the apical chamber. All samples were diluted with HBSS (1:9 dilution for apical samples, 1:2 dilution for basolateral samples) and analyzed for salbutamol concentration by HPLC.

5.2.5 High Performance Liquid Chromatography

An HPLC system consisting of a Dionex P680 pump, Dionex ASI- 100 autosampler and Dionex PDA-100 photodiode array detector (Dionex Corporation, CA, USA) was used to determine salbutamol concentration. Separation was achieved using a Gemini® (250 x 4.6 mm, particle size: 5 μm) column (Phenomenex® Ltd., Cheshire, UK). The mobile phase used for analysis was 96.5% water, 3% acetonitrile, 0.5% orthophosphoric acid that had been filtered through a 0.2 μm nylon membrane and degassed by sonication. The run time was set at 15 minutes with a flow rate of 1 mL/min and 2 injections of 100 μL per vial. The UV detection was set at 226 nm. The amount of salbutamol in the samples was determined by comparison with a calibration curve. To generate a calibration curve an aliquot of 10 mg salbutamol was weighed out and added to a 100 mL volumetric flask and made up to volume with PBS to give a 100 $\mu g mL^{-1}$ solution. A set of serial dilutions was

performed using glass pipettes and volumetric flasks to prepare 6 standards for comparison with the basolateral samples (150, 100, 80, 50, 30, 20 $ngmL^{-1}$) and 6 standards for comparison with the apical samples (100, 80, 50, 30, 20, 10 μg/mL).

5.2.6 Spray drying

Spray dried powders containing 1% salbutamol, 0.5% PVP, 98.5% lactose and 20:1 ratio of counter ion - drug were prepared as described in Chapter 2. The counter ions used were sodium octanoate and dipotassium phytate.

5.2.7 Dissolution study

Type 3 gelatin capsules were filled with 12.5 mg (± 0.5) of powders generated by spray drying. A total of 5 capsules were actuated per experiment to deliver powder on to the surface of a 0.45 μm pore Transwell insert (pre wetted with HBSS) using a Twin-Stage Impinger, as described by Grainger *et al.* (Grainger et al., 2012). The Transwell was transferred to a 24-well plate containing 600 μL of HBSS and at intervals was moved to a new well. The amount of salbutamol in the well at each time point was analyzed by HPLC.

5.2.8 Animals

Experiments were conducted under a project license issued by the United Kingdom Home Office in accordance with the United Kingdom Animal Scientific Procedures Act, 1986. Protocols were approved by the Local Ethical Review Committee of King's College London. All *in vivo* experiments were conducted on male Dunkin-Hartley guinea pigs (400-450 g, Charles River). Guinea pigs were housed in animal holding facilities maintained at 18 – 19 ^{o}C with a standard 12 h light cycle. A maximum of 6 guinea pigs were housed in

the same cage. The cages contained sawdust and hay, with cardboard tunnels to provide enrichment. Animals were fed ad libitum on an FD1 guinea pig diet (Special Diets Services, Essex, UK) with free access to water.

5.2.9 In vivo Bronchoprotection study

Guinea pigs (400 g) were anaesthetized (7 mL/kg of 25% w/v urethane in sterile saline over 4 doses) and intratracheal intubation was performed before the animals were connected to a pneumotachograph and pressure transducer. Changes in airflow were measured using a lung function recording system and were displayed in real time on a personal computer. The flow signal was integrated to give a measure of tidal volume. A cannula was inserted into the thoracic cavity between the third and fifth ribs and connected to the negative side of the pressure transducer. The positive side of the pressure transducer was connected to the side of the pneumotachograph proximal to the animal. The difference in mouth and thoracic pressure was used as a measure of transpulmonary pressure. The lung function parameter, total airway resistance (RL; cm of water per L per s), was derived from each measure of flow, tidal volume, and transpulmonary pressure by integration. Histamine (1, 2, 4 µg/kg) was injected intravenously and 10 minutes later the salbutamol base or ion-pair was administered as a nebulized solution in saline with an Aeroneb Pro device (Aerogen, Galway, Ireland). Spray dried powders were dissolved in saline to give a 1 mg/mL concentration, 1 mL was put in to the nebulizer which was actuated for 10 seconds to give a salbutamol dose of 1.5 µg/kg concentration. The Aeroneb Pro has an average flow rate of 0.4 mL/min and gives droplets in the size range of 1 – 5 µm as measured on an Andersen Cascade Impactor (average 3.1 µm) (Aerogen). Histamine was intravenously injected at 30, 60, 120 and 180 minutes post drug exposure.

5.2.10 Lung Cell Count

At the end of the bronchoprotection study a lavage was performed with 5 mL of bronchoalveolar lavage fluid. The total number of cells was counted on a Neubauer haemocytometer (Fisher Scientific, Loughborough, UK).

5.2.11 Data analysis

Data for the dissolution study was obtained from 3 experiments and was expressed as a mean ± standard deviation. The data was fitted to the following dissolution curves: first order; Baker and Londsdale; Peppas; Hixon and Crowell; and Higuchi in SigmaPlot. Data from cell culture experiments was obtained from 3 experiments, with 3 test wells per experiment, and was expressed as a mean ± standard error. Sigmoidal curves were fitted to the binding data in SigmaPlot and the value at 50% was taken as the IC_{50} value in the MTT assay. One-way Analysis of Variance (ANOVA) with a Shapiro-Wilkins normality test was performed with a probability limit of 0.05 set to indicate significant differences.

5.3 Results

5.3.1 The biocompatibility excipients used in an ion-pair formulation

A sigmoidal relationship between the concentration of each of the counter ions and excipients tested in the MTT assay and cell viability was observed (figure 5.1 – 5.3). Following 24 hour exposure, sodium octanoate was found to have the lowest half maximal inhibitory concentration (IC_{50}) with a value of 1.7 mg/mL (table 5.1). The counter ion with

the greatest IC_{50} concentration was sodium gluconate with a value of 38.1 mg/mL. The lactose and PVP excipients were shown to be well tolerated by Calu-3 cells, with IC_{50} values of 88.6 and 41.4 mg/mL, respectively (table 5.1).

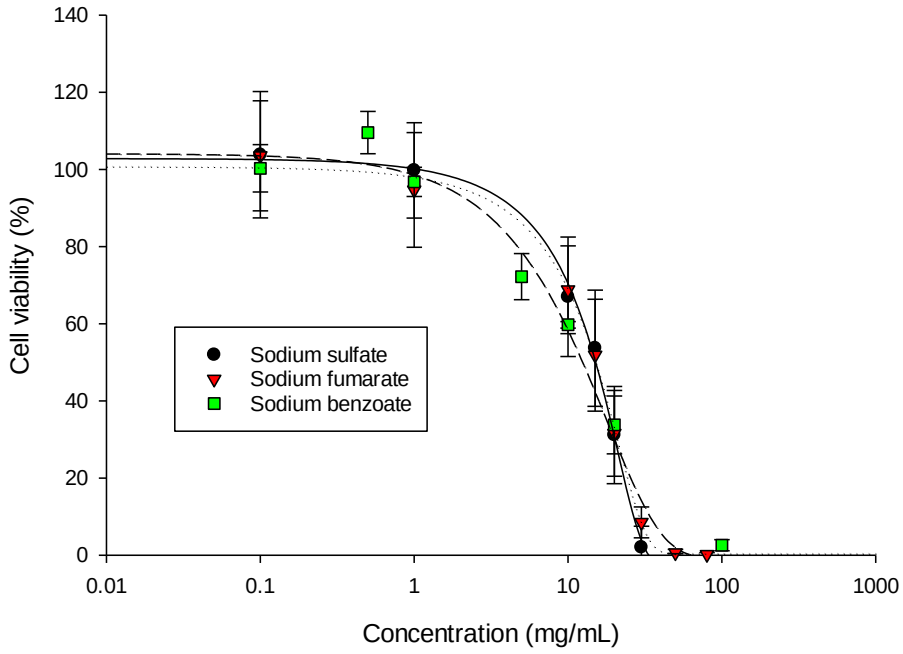

Figure 5.1 - Relationship between concentration and cell viability after 24 hour exposure for sodium sulfate (black circle), sodium fumarate (red triangle) and sodium benzoate (green square). Data is expressed as a mean ± standard error (n=3 experiments, with 3 replicates per experiment)

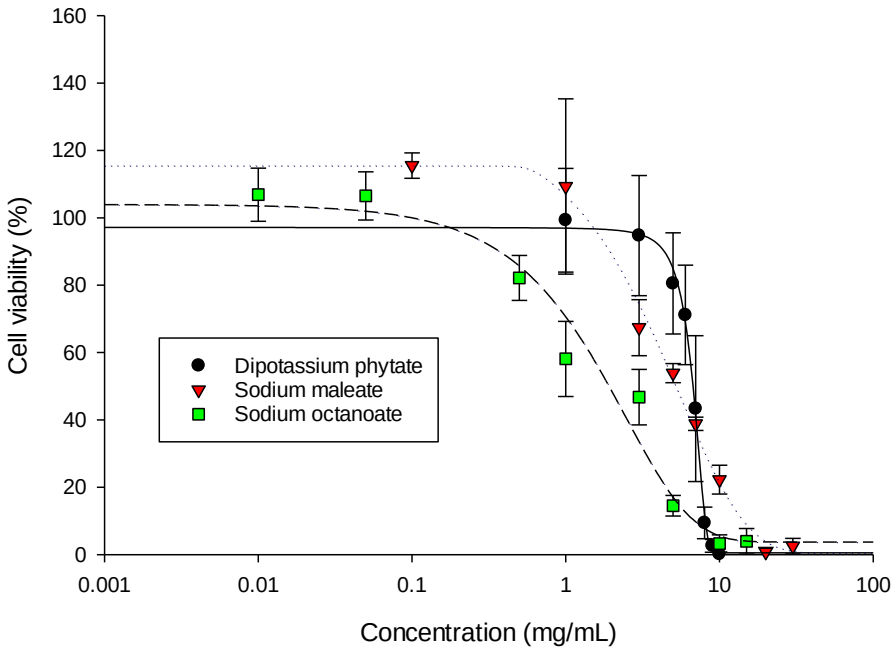

Figure 5.2 - Relationship between concentration and cell viability after 24 hour exposure for dipotassium phytate (black circle), sodium maleate (red triangle) and sodium octanoate (green square). Data is expressed as a mean ± standard error (n=3 experiments, with 3 replicates per experiment)

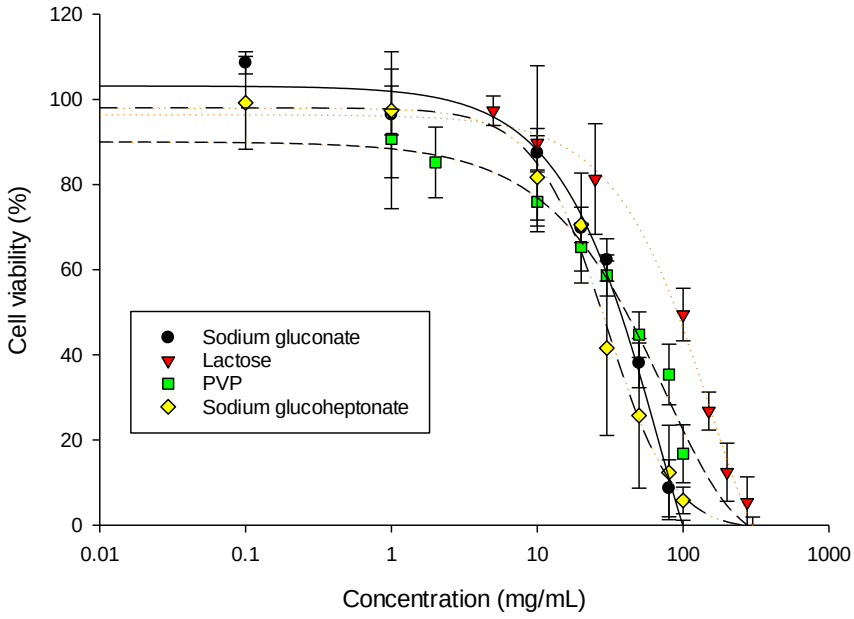

Figure 5.3 - Relationship between concentration and cell viability after 24 hour exposure for sodium gluconate (black circle), lactose (red triangle), PVP (green square) and sodium glucoheptonate (yellow diamond). Data is expressed as a mean ± standard error (n=3 experiments, with 3 replicates per experiment)

Table 5.1 – Half maximal inhibitory concentration (IC_{50}) values for each excipient after 24 hour incubation with Calu-3 cells

Excipient	IC_{50} (mg/mL)
Sodium sulfate	14.5 ± 3.6
Sodium gluconate	38.1 ± 3.2
Sodium glucoheptonate	27.8 ± 6.9
Sodium octanoate	1.7 ± 0.3
Sodium benzoate	11.7 ± 1.7
Sodium fumarate	14.6 ± 3.0
Sodium maleate	5.1 ± 0.9
Dipotassium phytate	6.6 ± 0.5
Lactose	88.6 ± 19.6
PVP	41.4 ± 0.8

5.3.2 Transport of salbutamol ion-pairs across the respiratory epithelium model

To be able to accurately quantify the salbutamol concentrations that had been transported through a cell monolayer, a more sensitive HPLC method compared to what was used in previous chapters was developed using 96.5% water, 3% acetonitrile and 0.5% orthophosphoric acid mobile phase and UV detection at 226 nm. This method gave a linear relationship between salbutamol concentration and UV absorption over a wide range of salbutamol values (0.02 – 100 μg/mL), with an R^2 value of 0.9998. The calculated limit

of detection value was 9.4 ng/mL and the limit of quantification was 28 ng/mL (figure 5.4, 5.5). The calculated coefficient of variation remained low, with a maximum value of 3.9% for the detection of a 20 ng/mL concentration.

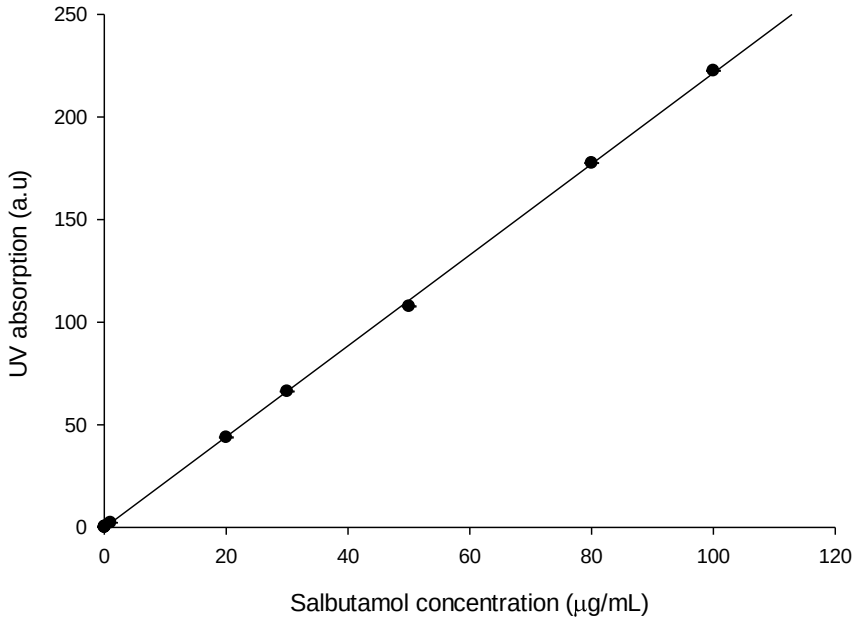

Figure 5.4 - Relationship between salbutamol concentration and UV absorption in HPLC analysis over a concentration range of 0.02 – 100 μg/mL. Data expressed as a mean ± standard deviation (n=5, R^2 = 0.9998)

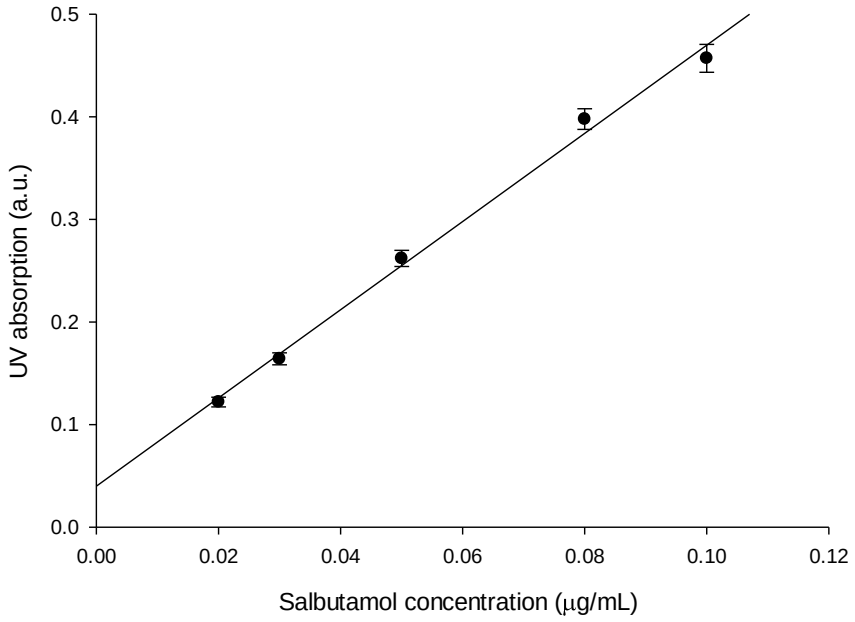

Figure 5.5 - Relationship between salbutamol concentration and UV absorption in HPLC analysis over a concentration range of 0.02 – 0.1 μg/mL. Data expressed as a mean ± standard deviation (n=5, R^2 = 0.9946)

In order to establish a suitable concentration of salbutamol to apply to cells to investigate its transport a range of concentrations (0.2 – 20 mg/mL) were tested. A linear relationship between the salbutamol concentration across the range tested and the rate of transport was observed (figure 5.6). A suitable concentration would be as close to an expected physiological concentration of salbutamol following inhalation as possible whilst also allowing for accurate analysis of the drug by HPLC. A starting concentration of 0.5 mg/mL was chosen for further experiments as it satisfied these criteria (figure 5.7).

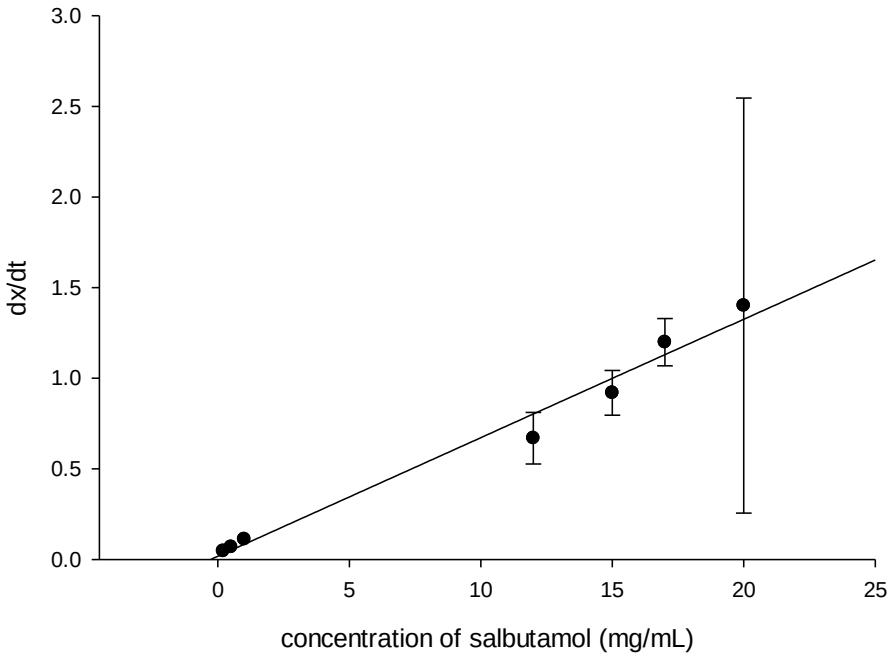

Figure 5.6 - Relationship between salbutamol concentrations applied to the apical side of Calu-3 monolayer and the rate of transport of the drug to the basolateral compartment. Data represents a mean ± standard deviation (n=3 experiments, with 3 replicates per experiment)

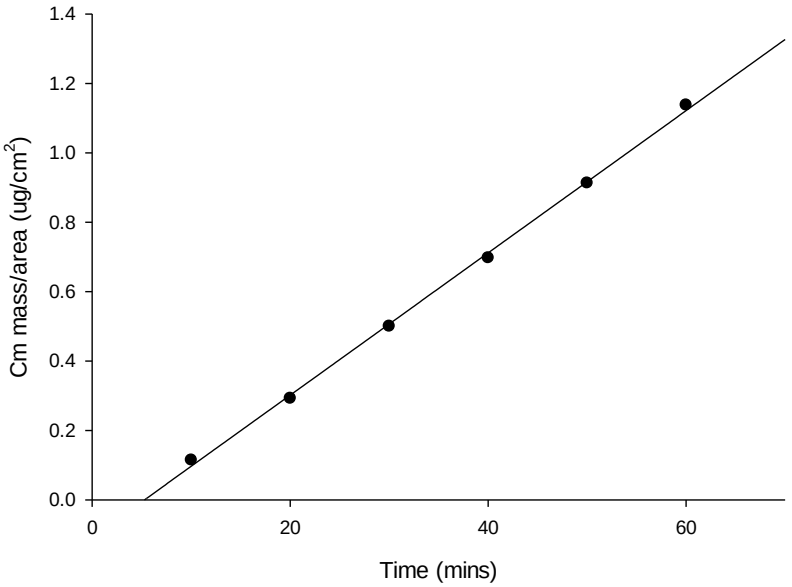

Figure 5.7 - Transport of salbutamol base (0.5 mg/mL) across a Calu-3 cell monolayer over 60 minutes (n = 1)

The rate of transport of salbutamol base (0.5 mg/mL), 20:1 salbutamol sulfate, 20:1 salbutamol gluconate, 20:1 salbutamol octanoate and 1:1 salbutamol phytate from the apical chamber of a Calu-3 monolayer grown at air-liquid interface to the basolateral chamber was therefore tested. It was found that the salbutamol sulfate, gluconate and phytate ion-pairs had a significantly lower rate of transport in comparison with the base ($p < 0.05$). The calculated apparent permeability coefficient (P_{app}) was 8.50 nm/s for salbutamol base and 4.38, 4.06, 4.32 nm/s for the sulfate, gluconate and phytate ion-pairs, respectively (figure 5.8). There was no significant difference in the rate of transport of the octanoate ion-pair (P_{app} = 10.35 nm/s) in comparison with salbutamol base ($p > 0.05$) (figure 5.8).

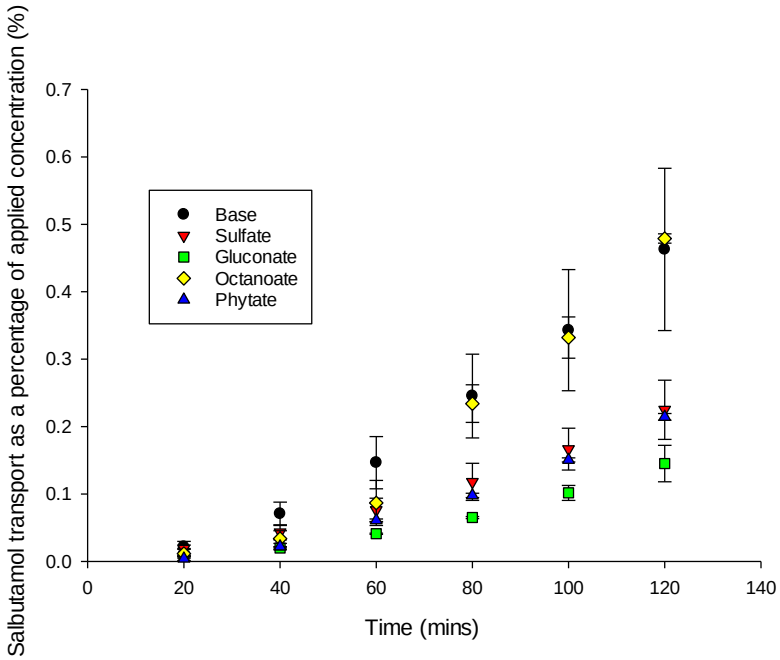

Figure 5.8 – Representative graph of the transport of salbutamol across a Calu-3 monolayer over 2 hours for salbutamol base (black circle), salbutamol sulfate (red inverted triangle), salbutamol gluconate (green square), salbutamol octanoate (yellow diamond) and salbutamol phytate (blue triangle). Data shown is expressed as a mean ± standard deviation (n=3)

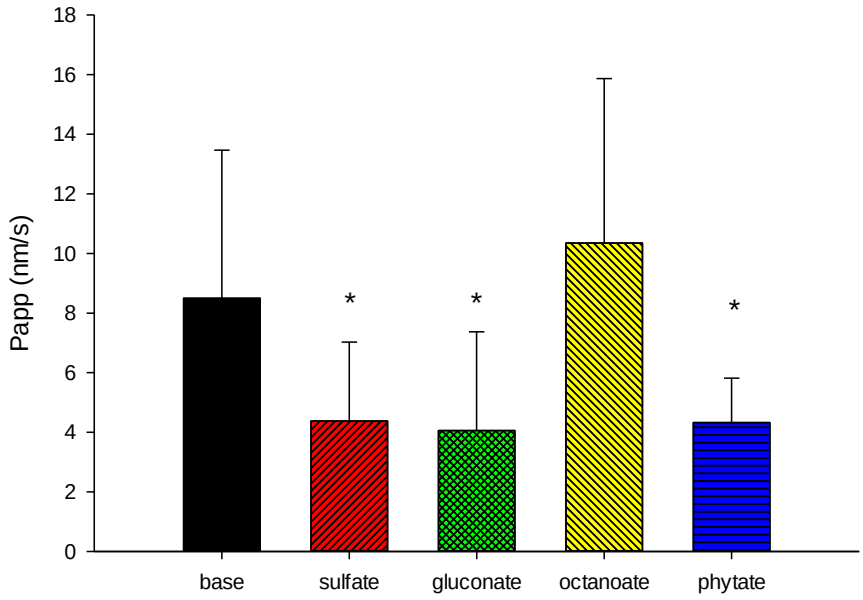

Figure 5.9 - Calculated apparent permeability coefficient (P_{app}) values for salbutamol base, salbutamol sulfate, salbutamol gluconate, salbutamol octanoate and salbutamol phytate across an air-liquid interface grown Calu-3 monolayer. Data is expressed as a mean ± standard error (n=6 experiments, with 3 replicates per experiment). * denotes a significant difference from salbutamol base.

5.3.3 Dissolution of salbutamol ion-pair spray dried powders

Salbutamol phytate and octanoate ion-pairs were chosen to take forward in to further studies to investigate whether these could be used to prolong the action of salbutamol based on the cell culture results. The dissolution profile of particles that were deposited on to a Transwell® insert in the lower chamber of a twin stage impinger was investigated. It was found that each of the powders had a rapid dissolution. A total of 31% (± 16) of salbutamol in the salbutamol base formulation, 38% (± 8) of salbutamol in the salbutamol octanoate formulation and 43% (± 3) of salbutamol in the salbutamol phytate formulation were dissolved within the first minute. There was no significant difference in the dissolution of the salbutamol base or salbutamol phytate powder ($p > 0.05$) (figure 5.10).

There was no significant difference in the dissolution of the salbutamol base and salbutamol octanoate powders in the first 15 minutes ($p > 0.05$). However there was a significant increase in the dissolution of the salbutamol octanoate powder at the 30, 45, and 60 minute time points in comparison with salbutamol base ($p < 0.05$) (figure 5.10). The salbutamol base spray dried powder reached a maximum of 77% of the total salbutamol dissolved at 60 minutes, this value was 82% for the salbutamol phytate powder and 92% for salbutamol octanoate.

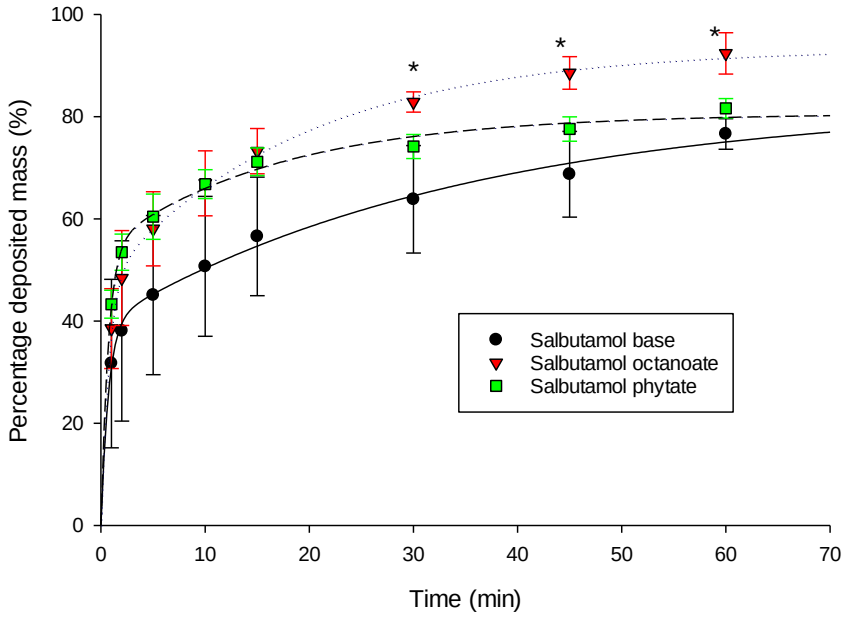

Figure 5.10 - Dissolution profile of spray dried salbutamol base, salbutamol octanoate and salbutamol phytate powders with PVP after deposition on to a Transwell insert. Data is expressed as a mean ± standard deviation (n=3). * denotes a significant difference.

The dissolution profiles were fitted with the following curves to ascertain which model best described the data: first order; Baker and Londsdale; Peppas; Hixon and Crowell; and Higuchi (figure 5.11, 5.12, 5.13). It was found that for each of the spray dried powders the

Peppas model best fit the dissolution data with R^2 values of 0.9942, 0.9927, and 0.9678 for the salbutamol base, octanoate and phytate powders, respectively.

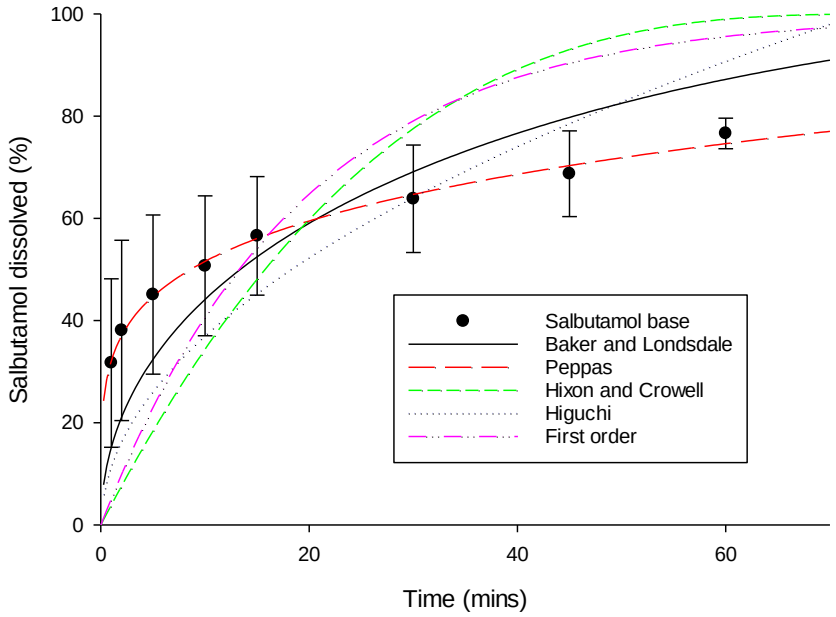

Figure 5.11 - Salbutamol base spray dried powder dissolution in PBS over 60 minutes. Data is expressed as a mean ± standard deviation (n = 3). Data is fitted with the following curves: Baker and Londsdale (black solid line, R^2 = 0.3772), Peppas (red long dashed line, R^2 = 0.9942), Hixon and Crowell (green short dashed line, R^2 = -1.408), Higuchi (blue dotted line, R^2 = -0.091), first order (pink dashed and dotted line, R^2 = -0.888).

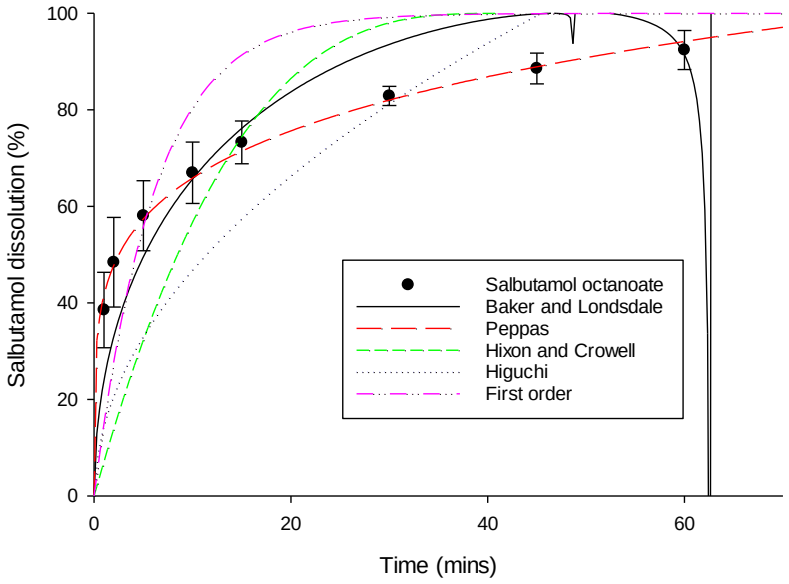

Figure 5.12 - Salbutamol octanoate spray dried powder dissolution in PBS over 60 minutes. Data is expressed as a mean ± standard deviation (n = 3). Data is fitted with the following curves: Baker and Londsdale (black solid line, R^2 = 0.704), Peppas (red long dashed line, R^2 = 0.9927), Hixon and Crowell (green short dashed line, R^2 = -0.3822), Higuchi (blue dotted line, R^2 = -0.2294), first order (pink dashed and dotted line, R^2 = 0.2571).

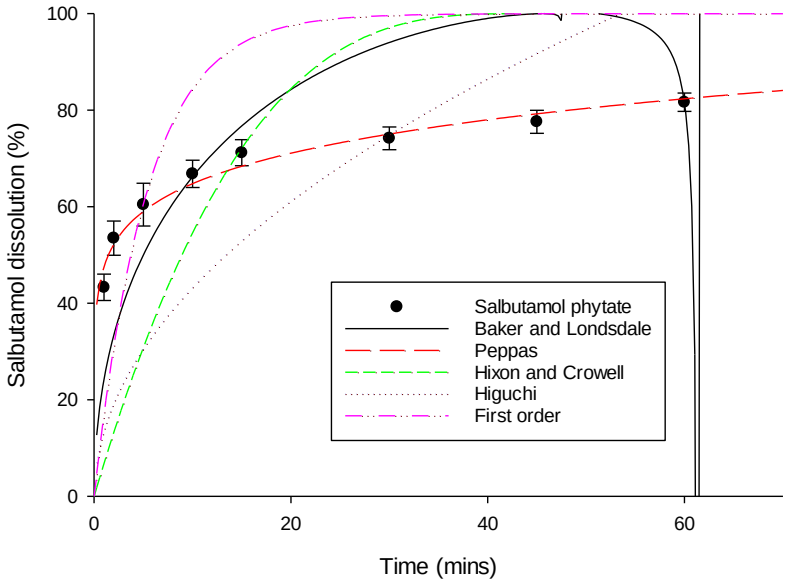

Figure 5.13 - Salbutamol phytate spray dried powder dissolution in PBS over 60 minutes. Data is expressed as a mean ± standard deviation (n = 3). Data is fitted with the following curves: Baker and Londsdale (black solid line, R^2 = -0.5313), Peppas (red long dashed line, R^2 = 0.9678), Hixon and Crowell (green short dashed line, R^2 = -3.7538), Higuchi (blue dotted line, R^2 = -2.9204), first order (pink dashed and dotted line, R^2 = -1.9782).

5.3.4 In vivo bronchoprotection efficacy of salbutamol ion-pairs

A bronchoprotection study for salbutamol base/PVP and salbutamol phytate/PVP spray dried powders as well a control of lactose/PVP/dipotassium phytate using 3 animals for each test condition. The difference in the percentage increase in maximum lung resistance was measured after a histamine challenge before administration of the test substance and then at 30, 60, 120 and 180 minutes post administration. The variation in response of each animal to the histamine challenge, as well as the test and control substances was extremely high and so statistical differences between the test substances could not be found (figure 5.14 – 5.16). As the administration of a 4 μg/kg dose of histamine gave a sufficient change in resistance for each animal before the administration of any test substances, the response to this dose for each animal was compared (table 5.2). It was found that there was a significant difference in the increase in resistance at 30, 60 and 120 minutes post salbutamol base administration when compared with the control response ($p < 0.05$, figure 5.18). The administration of salbutamol phytate resulted in a significant difference in the response to histamine challenge at 60 and 120 minutes ($p < 0.05$, figure 5.18). Response to the phytate control resulted in some animals having a higher response to histamine than at the control at 30 and 120 minutes (figure 5.18). One of the animals given the phytate control did not survive to 180 minutes.

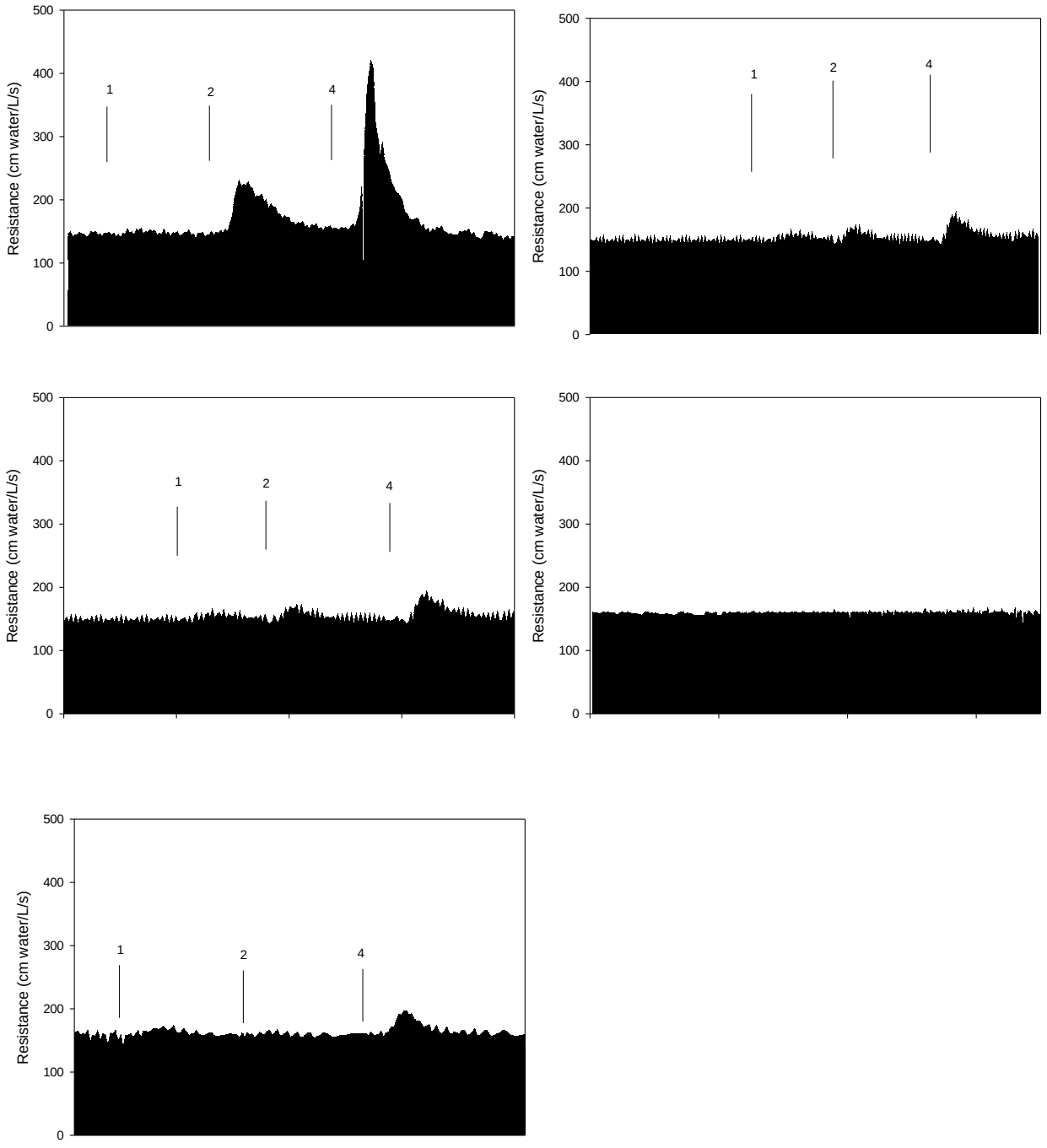

Figure 5.14 - Resistance traces for Animal 1 for salbutamol phytate. Top left = control (dose of 1, 2, 4 µg/kg histamine and nebulized dose of salbutamol base). Top right = 30 mins. Middle left = 60 mins. Middle right = 120 mins. Bottom left = 180 mins. 1, 2, and 4 markers show administration of 1, 2, and 4 µg/kg histamine.

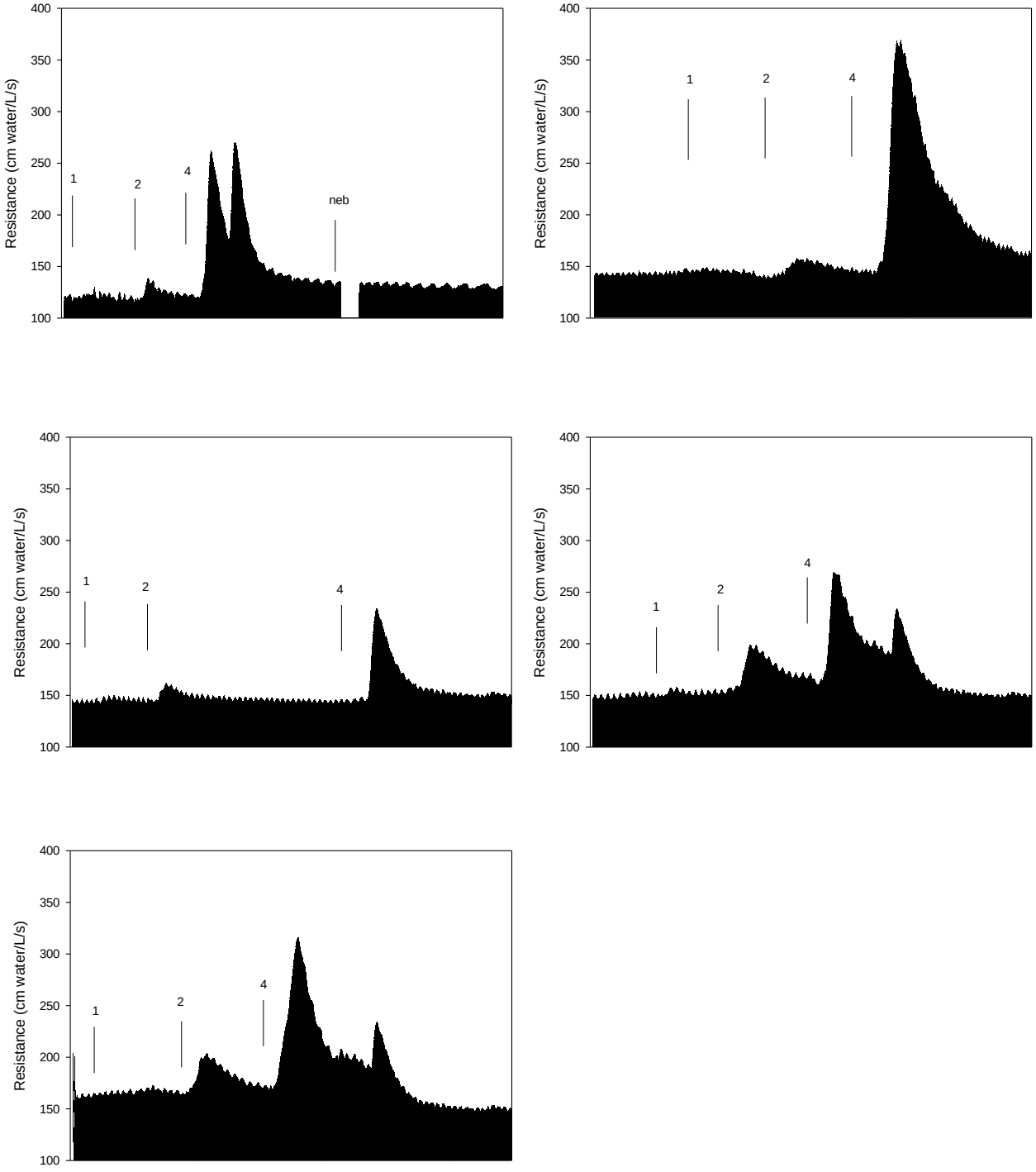

Figure 5.15 - Resistance traces for Animal 2 for salbutamol phytate. Top left = control (dose of 1, 2, 4 µg/kg histamine and nebulized dose of salbutamol base). Top right = 30 mins. Middle left = 60 mins. Middle right = 120 mins. Bottom left = 180 mins. 1, 2, and 4 markers show administration of 1, 2, and 4 µg/kg histamine.

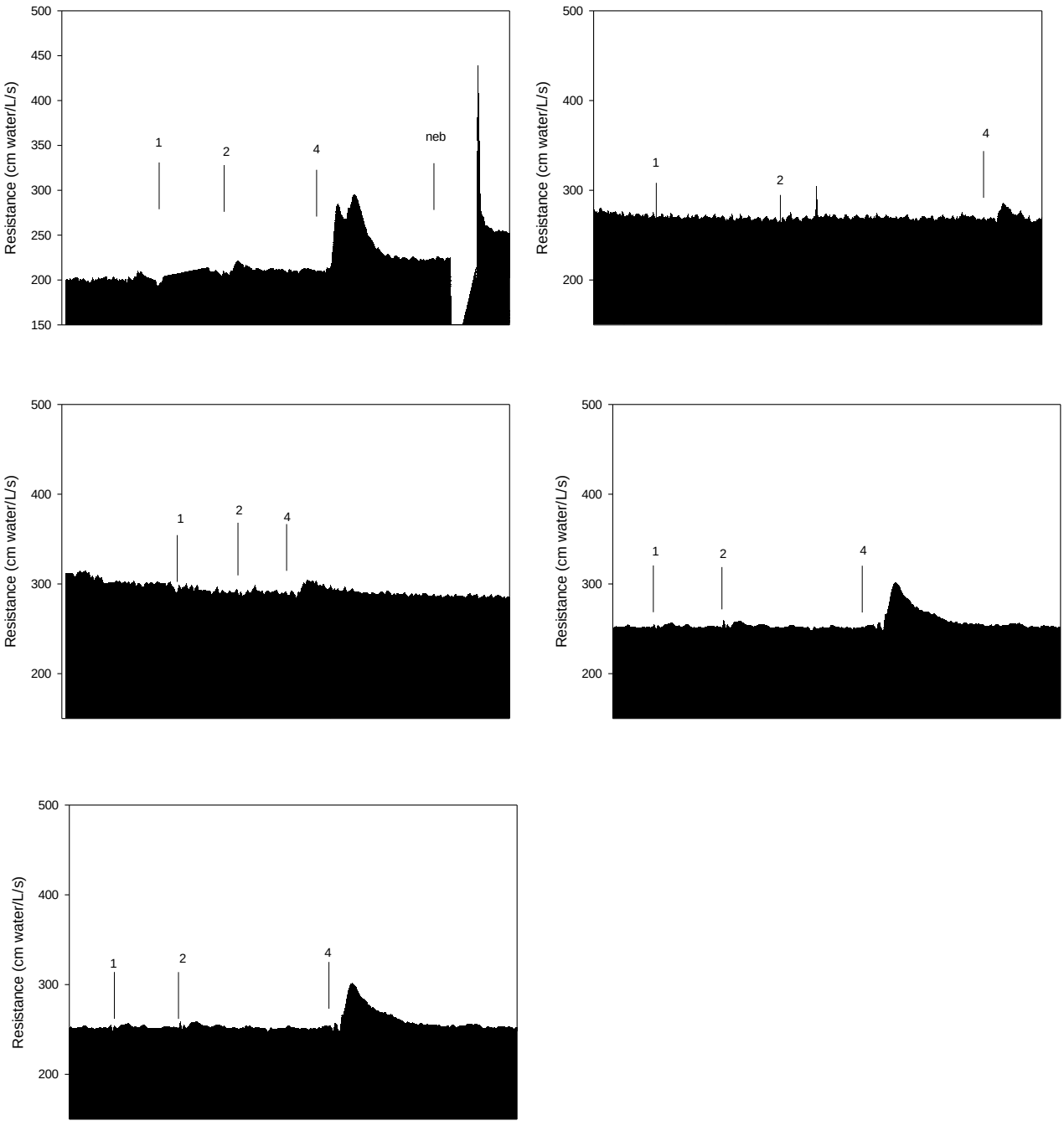

Figure 5.16 - Resistance traces for Animal 3 for salbutamol phytate. Top left = control (dose of 1, 2, 4 µg/kg histamine and nebulized dose of salbutamol base). Top right = 30 mins. Middle left = 60 mins. Middle right = 120 mins. Bottom left = 180 mins. 1, 2, and 4 markers show administration of 1, 2, and 4 µg/kg histamine.

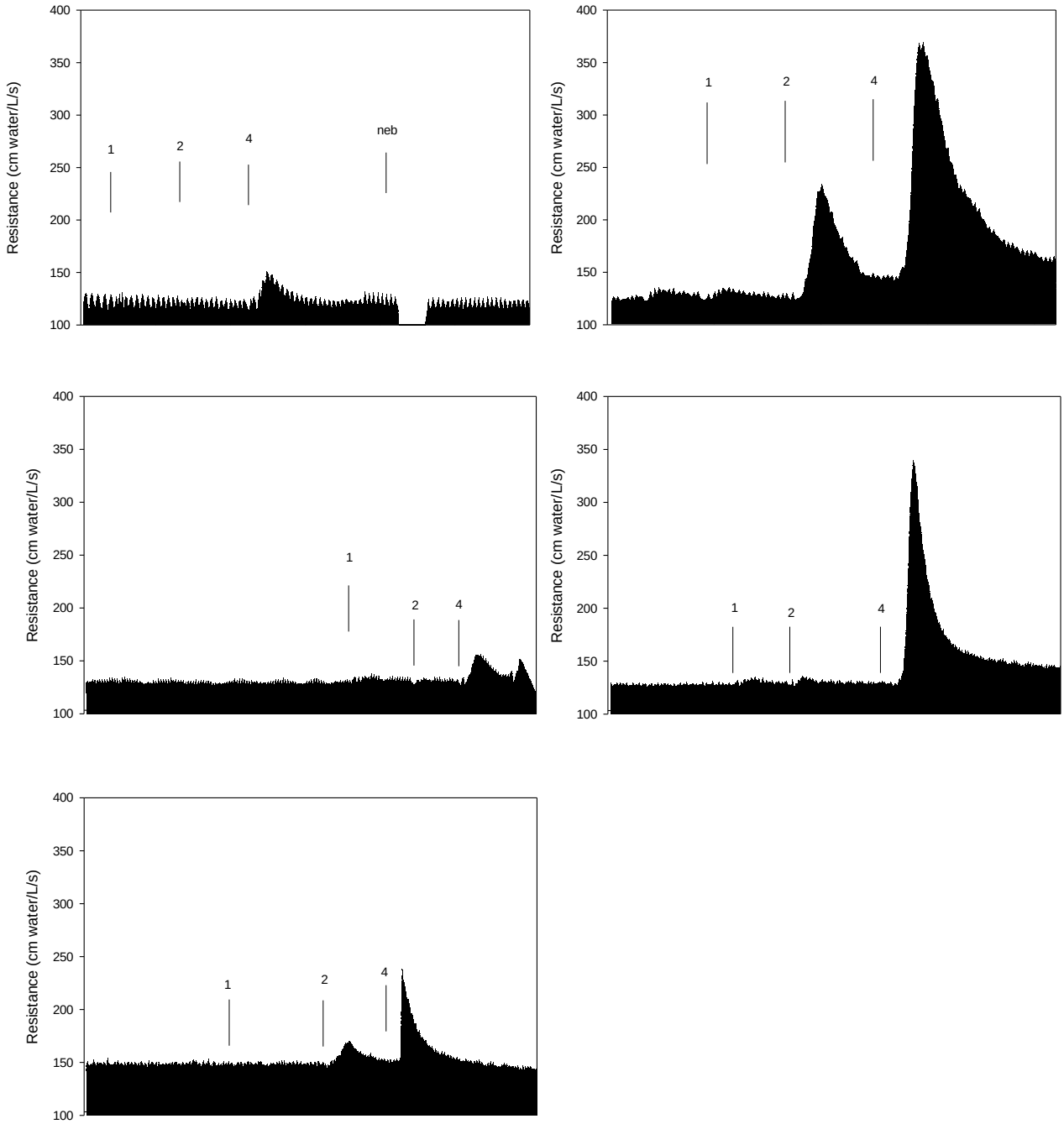

Figure 5.17 - Resistance traces after administration of dipotassium phytate control (n = 1) Top left = control (dose of 1, 2, 4 µg/kg histamine and nebulized dose of salbutamol base). Top right = 30 mins. Middle left = 60 mins. Middle right = 120 mins. Bottom left = 180 mins. 1, 2, and 4 markers show administration of 1, 2, and 4 µg/kg histamine.

Table 5.2 – Increase in lung resistance after administration of 4 μg/kg histamine at 5 min prior to and 30, 60, 120 and 180 minutes post administration of salbutamol base, salbutamol phytate or phytate control. NA is shown where there is no reading due to animal death.

Test Substance	Animal	Percentage increase in total airway resistance (%) Time (mins)					Percentage increase in resistance normalized to same animal histamine control (%) Time (mins)				
		-5	30	60	120	180	-5	30	60	120	180
Salbutamol base spray dried powder	1	105.46	42.42	7.48	43.66	79.29	100	40.22	7.093	41.40	75.18
	2	57.90	12.76	26.83	38.89	127.11	100.00	22.04	46.34	67.17	219.53
	3	101.30	10.83	3.87	41.69	33.44	100.00	10.69	3.82	41.15	33.01
Salbutamol phytate spray dried powder	1	169.09	28.87	8.95	25.02	30.60	100.00	17.07	5.29	14.80	18.10
	2	121.03	152.40	63.13	59.41	82.13	100.00	125.92	52.16	49.09	67.86
	3	34.69	6.50	4.77	20.18	36.07	100.00	18.74	13.75	58.17	103.98
Phytate control	1	43.15	13.90	49.10	93.89	2.77	100.00	32.21	113.79	217.59	NA
	2	26.99	83.63	19.50	163.44	14.60	100.00	309.86	72.25	605.56	54.09
	3	47.93	28.81	20.63	27.10	37.43	100.00	60.11	43.04	56.54	78.09

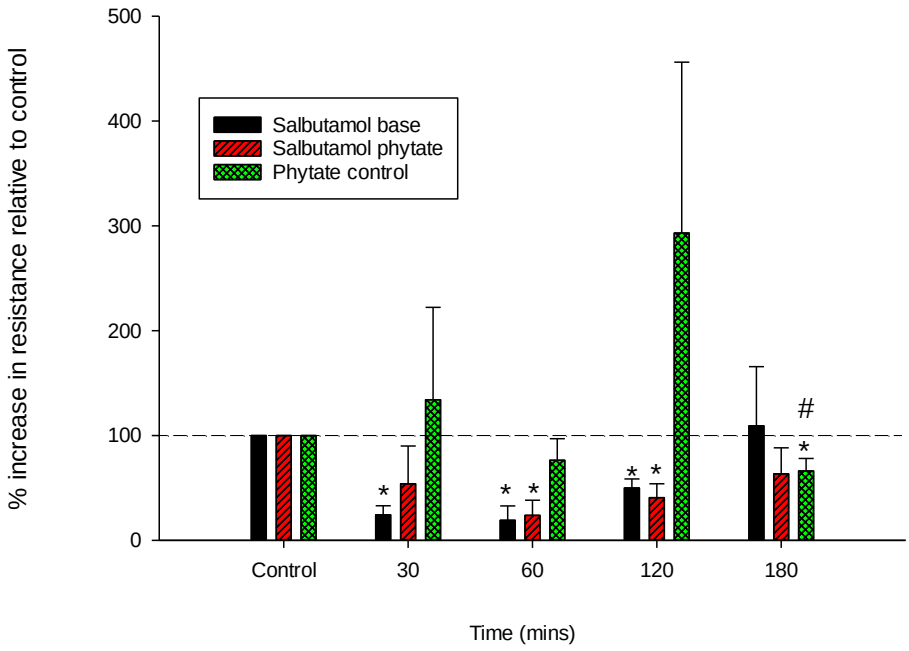

Figure 5.18 – Percentage increase in lung resistance after administration of histamine (4 µg/kg) 30, 60, 120 and 180 minutes after administration of salbutamol base (solid black bar), salbutamol phytate (red striped bar) and phytate control (green crossed bar) relative to the increase prior to administration (histamine control). Data is expressed as a mean ± standard error (n=3). Dotted line shows baseline response to histamine, * denotes a statistically significant difference to histamine control, # denotes n = 2.

The total number of cells present in the lung was counted after the experiment was concluded, although this was only performed for a small number of animals it did not indicate any differences in the total number of cells present in the lung after administration of any of the test solutions (table 5.3).

Table 5.3 – Total cell count in bronchoalveolar lavage post bronchoprotection study for salbutamol base (n = 1), salbutamol phytate (n = 2) and phytate control (n = 2).

Formulation	Cell count (x 10^4 cells/mL)
Salbutamol base	90
Salbutamol phytate	85.88 (± 12.9)
Phytate control	81.07 (± 5.5)

5.4 Discussion

The biocompatibility of excipients used in the spray dried formulations was assessed as a function of mitochondrial activity in Calu-3 cells. The desired effect of the formulations is prolonged drug action, so a 24 hour exposure to the test molecules was performed in an attempt to model an extreme situation. Lactose was extremely well tolerated in the assay with an IC_{50} value of 88.6 mg/mL, previous studies have also shown that lactose is well tolerated by the Calu-3 cell line (Scherließ, 2011). PVP was also well tolerated with an IC_{50} of 41.4 mg/mL. The counter ions showed a wide range of biocompatibility, the least tolerated was the hydrophobic octanoate counter ion (IC_{50} = 1.7 mg/mL), the most tolerated was the hydrophilic gluconate counter ion (IC_{50} = 38.1). Several studies have found that there is a negative correlation between lipophilicity of molecules and their toxicity (Chen et al., 2008, Moridani et al., 2003, Smith et al., 2002). This is thought to be because more lipophilic molecules can cross biological membranes more easily and interact with biological macromolecules such as enzymes (Chen et al., 2008). Although in general the MTT results in this chapter showed that more lipophilic compounds were less well tolerated by the Calu-3 cells, there was not a linear correlation between logP and IC_{50} values.

In order to assess whether the tested excipients are suitable for use in a powder formulation for inhalation it is important to put the biocompatibility results in to perspective. To gain maximum therapeutic efficacy salbutamol should be deposited in the middle and small airways (Tena and Clarà, 2012). A 20 mg dose of the spray dried salbutamol octanoate powder would contain: 0.18 mg salbutamol; 0.09 mg of PVP; 2.50 mg of sodium octanoate (used in this example as it has the lowest IC_{50} value); and 17.22 mg of lactose.

If this was delivered with 100% efficiency to the bronchiolar region of the lungs (generations 9 – 15) and distributed uniformly in this region the concentration of each excipient would be 3.76 x 10^{-5} mg/cm^2 for PVP, 1.04 x 10^{-3} mg/cm^2 for sodium octanoate and 7.18 x 10^{-3} mg/cm^2 for lactose (Valentin, 2002, ICRP, 1994). The experimental IC_{50} values for these excipients are 41.4 mg/mL, 1.7 mg/mL and 88.6 mg/mL for PVP, sodium octanoate and lactose, respectively, which are the equivalent of 12.94 mg/cm^2, 0.53 mg/cm^2 and 27.69 mg/cm^2, respectively, when corrected for the volume of liquid applied and surface area of the well. The theoretical deposition concentrations based on a uniform distribution are much lower than the experimental IC_{50} values. This however, is not a totally realistic view of deposition. Deposition in the lungs does not happen uniformly and instead there will be regions of higher deposition, for example at lung bifurcations where the air rapidly changes direction. The toxicity data shows that at least a 500 fold increase is needed in the concentration of sodium octanoate to reach its IC_{50} value, still presuming 100% of the dose was deposited in the bronchiolar region. It is also important to remember that toxicity assays performed in cell culture models are likely to be more sensitive than *in vivo* tissue, and so the tolerated levels in tissue would be higher (Korting et al., 1994). For these reasons each of the counter ions and excipients tested in the MTT assay were deemed suitable for use in an inhaled formulation.

The transport of salbutamol base showed a linear relationship between flux of transport and initial salbutamol concentration over a concentration range of 0.2 – 20 mg/mL. This would suggest that salbutamol base is passively transported across the Calu-3 monolayer as there appeared to be no saturation of transporters at higher concentrations. There is some discussion in the literature as to whether this is the case. Studies have shown that there is a strong correlation of the transport of salbutamol across a monolayer of

16HBE14o- cells with the transport of the paracellular marker mannitol, which suggests that salbutamol is transported via the paracellular route also (Forbes, 2000, Unwalla et al., 2012). However, contradicting studies have hypothesized that salbutamol is transported actively via an organic cation transporter (OCT) (Ehrhardt et al., 2005, Haghi et al., 2012). These studies have shown that transport of salbutamol across 16HBE14o- and Calu-3 cells, grown at both liquid-liquid interface and air-liquid interface, can be limited by an excess of another organic cation such as tetraethylammonium (TEA) (Ehrhardt et al., 2005, Haghi et al., 2012). Ehrhardt *et al.* used salbutamol concentrations of 100 μM and 5 mM and saw a significant decrease in apparent permeability coefficient at the higher concentration. This corresponds to concentrations of 24 μg/mL and 1.2 mg/mL. It is therefore possible that over the concentration range used in this study (0.2 – 20 mg/mL) that active transport due to OCT was already saturated.

The rate of transport of salbutamol across a Calu-3 monolayer was significantly reduced for the sulfate, gluconate and phytate ion-pairs. Previous studies have shown that the transport rate of salbutamol sulfate through Calu-3 cells is around half that of salbutamol base, however it was hypothesized that this was due to the difference in partition coefficients of the 2 species (Haghi et al., 2012). Partitioning studies for the salbutamol sulfate, gluconate and phytate ion-pairs in Chapters 2 and 3 show that there was no significant difference in the partition coefficient compared with the base and so this could not be the reason for the difference in transport rates. If the transport of salbutamol and the ion-pair is assumed to be passive and paracellular as indicated by the results in this chapter and literature then there may be other mechanisms that cause the reduction in transport rate. The ion-paired complex will have a high molecular weight than salbutamol base alone, however these complexes will still remain under 1000 Daltons in weight, and

so the contribution of molecular weight on transport rate is thought to be negligible (Tronde et al., 2008).

Other factors that have been shown to be extremely important to drug absorption in rat lung are the polar surface area and hydrogen bonding potential of compounds (Tronde et al., 2008). Permeability decreases with increased hydrogen bond potential due to an increase in the desolvation energy required to break hydrogen bonds with water (Conradi et al., 1996). Also in the lung the percentage polar surface area of the total molecular surface area (%PSA) has been shown to be an important factor in drug absorption. The lung has been shown to be more permeable than other biological membranes to molecules with a high polar surface area, but %PSA has still been shown to correlate to permeability (Tronde, 2002). Each of the sulfate, gluconate, and phytate counter ions have a high polar surface area and numerous sites that can form hydrogen bonds with water, and so this could be the cause of the reduced rate of ion-pair transport. The transport rate of the octanoate ion-pair did not significantly differ from that of salbutamol base even though the octanoate ion-pair did have a significantly increase $logD_{7.4}$ value in the partitioning studies in Chapter 2 (-1.386 for salbutamol base vs. -0.630 for salbutamol octanoate). Studies have shown that there appears to be a linear correlation between the log apparent partition coefficients of molecules and their absorption rate in the lung (Taylor, 1990) (figure 5.19). When comparing the partition coefficient values from Chapter 2 with the correlated compounds it is possible that although the increase in $logD_{7.4}$ is statistically significant, it may not be enough of an increase to see a significant difference in drug transport.

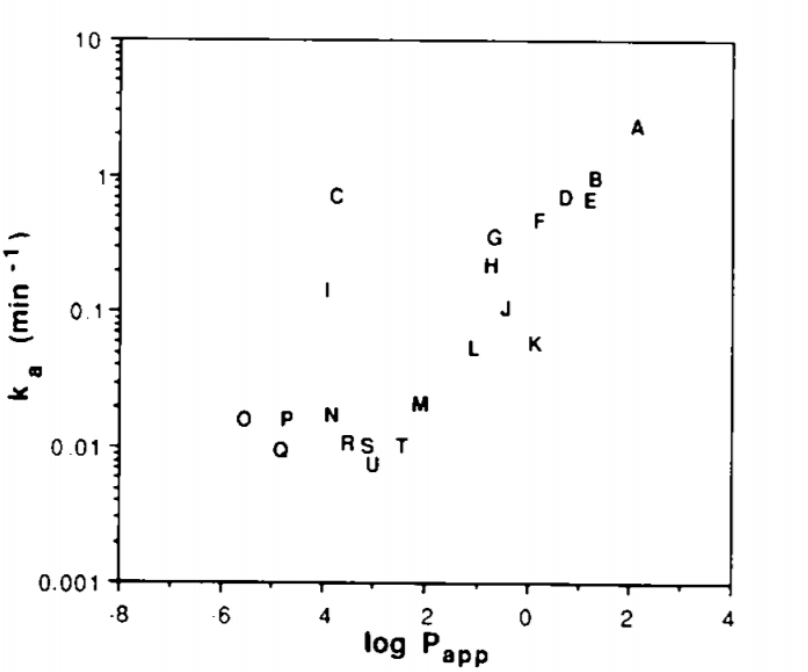

Figure 5.19 - Relationship between log apparent partition coefficient (log P_{app}) and drug absorption (k_a) from the lung for 21 compounds. Taken from (Taylor, 1990)

The dissolution of each of the salbutamol base, octanoate and phytate powders showed rapid dissolution with around 40% of the total powder being dissolved in the first minute. This could be as a result of the apparent amorphous nature of the powders. Amorphous powders have a higher Gibbs free energy, and therefore a higher dissolution and solubility than the crystalline form of the same powder (Kanaujia et al., 2015, Khadka et al., 2014). As the salbutamol octanoate had a significantly higher log$D_{7.4}$ than salbutamol base (-0.630 vs. -1.386, respectively) it was expected that the octanoate formulation might have a slower rate of dissolution, however this was not the case. The dissolution of the octanoate formulation was the same as for the base until 30 minutes, when significantly more of the total salbutamol was found in solution for the octanoate formulation. This could also be attributed to the apparent amorphous nature of the powders and might suggest that a more dramatic change in lipophilicity would be required to significantly alter dissolution of a

spray dried ion-pair formulation. Each of the powders adhered to the Korsmeyer-Peppas model (R^2 values = 0.9942, 0.9927 and 0.9678 for salbutamol base, octanoate, and phytate formulations, respectively). The Korsmeyer-Peppas model is given by the following equation:

$$\mathbf{M_t/M_\infty = Kt^n} \qquad \textbf{[Equation 5.2]}$$

Where M_t/M_∞ is the fraction of drug released at time t, K is the release rate constant, and n is the release exponent.

When dissolution data up to 60% dissolution is fitted to this equation the release exponent describes the mechanism of release (Dash et al., 2010, Carbinatto et al., 2014). For spherical particles a release exponent of less than 0.43 describes Fickian diffusion, 0.43 – 0.85 describes anomalous transport and greater than 0.85 is Case II transport (Carbinatto et al., 2014). The calculated release rate constants were 32.1034, 39.5820, and 44.7649 for salbutamol base, octanoate, and phytate, respectively. The release exponents were 0.2036, 0.2438 and 0.1949 for salbutamol base, octanoate and phytate, respectively, so each of the powders dissolved according to Fickian diffusion. Fickian diffusion can be described by a single parameter: the diffusion coefficient (Ritger and Peppas, 1987).

The variability in the *in vivo* results was unexpected. Previous studies have shown that there is significant variability in the guinea pig's response to histamine induced bronchial reactivity (DOUGLAS et al., 1973), however the use of each animal as its own control should minimize this variability in results. Therefore the variability observed in the results of this study may be due to external factors, such as changing room temperature, and therefore animal body temperature over the 3 hour experiment time.

In the animal model, administration of salbutamol base spray dried powder (1.5 μg/kg) via nebulization resulted in a diminished response to histamine at 30, 60 and 120 minutes. The protective effect of salbutamol appeared to be most pronounced at 60 minutes post administration, which would be expected as the bronchodilation effects of salbutamol following inhalation are known to peak at around 1 – 2 hours (Imboden and Imanidis, 1999). After administration of the salbutamol phytate solution there was a significant decrease in response to histamine at 60 and 120 minutes, whereas the response to histamine challenge after administration of the phytate control solution appeared to be greater than the control at 30 and 120 minutes. At 120 minutes post phytate control administration 2 of the 3 animals tested exhibited a percentage increase in lung resistance of over double what was seen prior to nebulization which would suggest that phytate is having a negative effect on the guinea pig's response to histamine. This may be caused by the action of phytic acid on other cells present in the lung as phytic acid has been shown to play a role in the respiratory burst of neutrophils (Eggleton et al., 1991). Respiratory burst is the production of reactive oxygen species that are strongly antimicrobial, but can also cause damage to surrounding lung tissue and causing the cell death of other immune cells (Dahlgren and Karlsson, 1999). Previous work has shown that although incubation of human neutrophils with phytic acid alone had no effect on the production of reactive oxygen intermediates, it caused an increased response to subsequent stimulus (Eggleton et al., 1991). Furthermore, high concentrations of histamine have been shown to act as a stimulus, causing equine neutrophils to generate the reactive oxygen species which in turn causes histamine release (Benbarek et al., 1999). It therefore might be the case that the level of histamine present in the lungs of animals that were given phytate could be higher than those who weren't, which could explain why there was no difference in the response

to histamine at 30 minutes post salbutamol phytate administration. Further testing could be completed to assess whether this is the cause of the increased response to histamine in the phytate control animals. If this was the case, it could be beneficial to use a metabolite of phytic acid as a counter ion in ion-pairing, as the smaller inositol phosphates had a greatly reduced effect on respiratory burst (Eggleton et al., 1991).

5.5 Conclusion

In conclusion, all 8 counter ions, lactose, and PVP were shown to be well tolerated by Calu-3 human bronchial cells at concentrations they might be found at after powder inhalation. The salbutamol sulfate, gluconate and phytate ion-pairs were shown to significantly reduce the rate of salbutamol transport through an air-liquid interface grown Calu-3 monolayer. There was no significant difference in the dissolution of the salbutamol octanoate or phytate spray dried powders when compared with the base and there was no significant difference in the bronchoprotective effect of salbutamol base or salbutamol phytate over a 3 hour time period. The results in this chapter indicate that ion-pairing could be used as a strategy to prolong drug action for salbutamol, but that the choice of counter ion is crucial.

Chapter 6

General Discussion

The respiratory system provides an attractive route of drug administration for both locally and systemically acting medicines. Therapeutics agents that work in the lung benefit from rapid onset of action, and high local concentrations which can minimize systemic side effects. Furthermore the large surface area and extensive network of blood vessels that serve the alveolar region allow for absorption of small molecules and macromolecules in to the systemic circulation at a therapeutically relevant concentration (Patton and Byron, 2007). With the added advantage of pulmonary drug delivery being non-invasive, the benefits of designing a medicine to be inhaled are obvious. However, there are also some challenges associated with pulmonary drug delivery. Most notably, many inhaled drug molecules suffer from a very short duration of action due to the rapid absorption and clearance from the lung tissue (Labiris and Dolovich, 2003a). The result of this is that these medicines need to be taken frequently, leading to poor patient compliance (Patton and Byron, 2007). Therefore an inhaled formulation which could avoid, but not harm, the lung's clearance mechanisms could improve the delivery of many current inhaled therapies by prolonging drug action and make the pulmonary route viable for other drug molecules.

The use of ion-pairs in an inhaled formulation is one strategy that has the potential to extend a drug's residence time in the lung. The main benefit of using an ion-pair is that the physical and biopharmaceutical properties of a drug can be altered without having to chemically modify the structure of the molecule. There have been many studies that have used ion-pairing to alter the properties of drugs given via the transdermal, ocular and oral routes; however there has been very little study of how this strategy might be used in an inhaled formulation (Song et al., 2012, Li et al., 2017, Patel et al., 2016). Furthermore, the lungs could be an ideal site for an ion-pairing strategy to work as any inhaled particles would contact with a relatively small volume of liquid, which would encourage the 2 ions in

the formulation to remain as a complex. When designing an ion-pair formulation for inhaled drug therapy there are some considerations that need to be taken in to account. Firstly, the charged drug molecule needs to bind to a counter ion with enough strength that it would not immediately dissociate when diluted in the fluid lining the lung. The chosen counter ion in the formulation needs to be highly biocompatible as it would be present in the formulation in an excess to promote the formation of the ion-pair. The ion-pair complex would need to be able to be incorporated in to a formulation that could deliver it to the correct site in the lungs, and it would need to alter the properties of the drug molecule in a way that could prolong its residence time in the lung.

The aim of the work presented in this thesis was to investigate the potential of ion-pairs to prolong drug action in the lungs. To achieve this salbutamol was chosen as the model drug, as it is known to be positively charged at physiological pH. The major findings of this work were that salbutamol formed an ion-pair with a range of hydrophilic and hydrophobic counter ions, the ion-pair complexes could be incorporated in to a dry powder formulation without adverse effects on the aerosolization of the powders, and the ion-pair complexes could alter the transport of salbutamol through an epithelial cell monolayer.

In Chapter 2, salbutamol was shown to bind to several different counter ions *via* 2 methods of analysis. The 7 counter ions that were analyzed were chosen as they had all been previously used in medical formulations, and they had a range of logP values, as well as differing numbers of sites capable of hydrogen bonding. Association constants were calculated from both the FTIR and HPLC methods of analyzing the ion-pair complex. It was found that weaker ion-pair complexes were formed between salbutamol and the small sulfate ion (pKa = 1.57 and 2.37 for FTIR and HPLC, respectively) in comparison with

molecules that had greater potential for hydrogen bonding, such as the gluconate counter ion (pKa = 2.27 and 2.62 for FTIR and HPLC, respectively), and the more lipophilic octanoate counter ion (pKa = 2.56 and 3.40 for FTIR and HPLC, respectively). The 2 methods of characterizing the ion-pairs gave different absolute values for association constants, but seemed to show the same trend. In future work the binding of salbutamol and these counter ions could be further investigated using NMR (Nie et al., 2015, Dezhampanah and Chokami, 2014). The use of multiple techniques to study an ion-pair complex could give more information on how the 2 ions bind together and how they interact with their environment.

Speciation software predicted that at a drug concentration of 0.00209 M and using 20:1 counter ion – drug ratios that at least 90% of the salbutamol would be found in ion-pair form for each of the counter ions. Under these conditions over 99% of salbutamol was predicted to be in ion-pair form for the glucoheptonate, benzoate and fumarate ion-pairs. Consequently, this ratio of drug to counter ion was chosen to assess the influence of the ion-pairs on the partitioning of salbutamol across a water-octanol interface. It was found that the $LogD_{7.4}$ value of salbutamol base was -1.386, indicating that at physiological pH the majority of the drug is found in the aqueous compartment. There was no significant difference in the $LogD_{7.4}$ value of the salbutamol sulfate ion-pair (-1.405) compared to salbutamol. This was unexpected as previous studies in to the difference in cell transport of salbutamol base and sulfate have found that the rate of sulfate transport is significantly lower and this has previously been attributed to the difference in lipophilicity (Haghi et al., 2012). There was also no significant difference in the partitioning of the gluconate ion-pair compared to the salbutamol parent molecule ($LogD_{7.4}$ = -1.241). The glucoheptonate ion-pair had a significantly lower $LogD_{7.4}$ (-1.845) and the octanoate ion-pair had a significantly

higher value (-0.630). It was therefore predicted that the glucoheptonate ion-pair would have a lower rate of transport than salbutamol and the octanoate ion-pair would have a higher rate of transport.

The presence of micelles in the salbutamol octanoate solution was investigated due to the surfactant nature of the counter ion. The concentrations of the counter ions used in the partitioning study, and in any potential formulation, were below the literature CMC value of 300 mM (Stanley et al., 2009), however it was unknown whether the ion-pairing might affect this. PCS was used to assess the difference in light intensity in comparison with a salbutamol sulfate control. There were no differences found, and so it was assumed that any octanoate would be free and available to bind to the salbutamol.

The work in Chapter 3 examined the suitability of phytic acid and its derivatives for ion-pairing with salbutamol. Phytic acid is a natural compound found in many cereals, legumes and nuts, so its potential for biocompatibility are high (Graf et al., 1987). Furthermore, it is known to be able to strongly bind to positively charged metals such as zinc (Hurrell, 2003). These properties make it an extremely interesting compound for use in an ion-pairing strategy, as it may be able to form functional ion-pairs with drug molecules. A potential method by which ion-pairing with phytic acid could decrease the rate of transport of a molecule is by increasing the molecular weight of the complex as phytic acid has a relatively high molecular weight (MW 660.04 g/mol). Enzymatic derivatives of phytic acid, such as IP_3, are smaller inositol phosphates, which should retain their chelating ability. Therefore IP_3 was chosen alongside phytic acid to compare their binding with salbutamol and how this might affect drug transport.

IP_3 is a commercially available molecule, however it is extremely expensive. Therefore in order to properly assess its binding with salbutamol, and if it were to be incorporated in to an inhaled formulation, a method of producing adequate quantities of the compound needed to be established. Synthesis of IP_3 from a myo-inositol starting material was attempted. Unfortunately, a clean sample of the IP_3 end product was not generated as the final step in the synthesis failed. Future work could look into different conditions to succeed in this final synthetic step, or another route of synthesis altogether. It might also be possible to generate IP_3 via an enzymatic degradation of phytic acid, although preliminary work suggested that chemical synthesis may have the highest potential for yielding a larger quantity of clean material.

FTIR and HPLC binding analysis of salbutamol phytate showed that the binding of salbutamol and phytate was much stronger than with any of the counter ions that had been investigated in Chapter 2 as 100% binding occurred at around a 10x lower counter ion concentration. 100% of salbutamol in salbutamol phytate was bound at 0.005 M phytate concentration, whereas 100% of salbutamol in salbutamol octanoate bound was at 0.05 M octanoate concentration by FTIR analysis. The calculated association constants (4.15 and 5.38 for FTIR and HPLC analysis, respectively) were also much higher than any calculated for the counter ions analyzed in Chapter 2. Therefore speciation software predicted that almost 100% of salbutamol would be found in ion-pair form for even a 10:1 counter ion – drug ratio.

The partitioning of the salbutamol phytate ion-pair did not significantly differ from salbutamol base alone (-1.211 vs. -1.386 for salbutamol phytate and base, respectively), therefore it was hypothesized that any change in the transport of salbutamol in the phytate

ion-pair would be due to the difference in size of the complex or its hydrogen bonding potential (Ma and Hadzija, 2012, Tronde et al., 2008).

The sulfate, gluconate, octanoate and phytate ion-pairs were incorporated in to a spray dried powder formulation with lactose (Chapter 4) and the generated particles were spherical and under 4 μm in size. The gluconate, octanoate and phytate ion-pair powders all had a significantly smaller particle size by laser diffraction (2.57, 3.28 and 3.26 μm, respectively) than the base alone or sulfate ion-pairs (3.68 and 3.61 μm respectively), which resulted in them having a smaller MMAD value and therefore being better aerosolized (MMAD values: base = 6.30, sulfate = 6.24, gluconate = 4.85, octanoate = 4.85, phytate = 4.93 μm). Furthermore all powders were homogenous in terms of salbutamol content. This suggested that a dry powder formulation could be a suitable way to deliver ion-pairs to the lung as the excess of ion present in the powder did not detrimentally affect the aerosolization or cause an increased retention of the powder in the inhaler (Wong et al., 2014). The spherical nature of the particles suggested that they are amorphous, however this could not be confirmed by DSC due to the complexity of the powders (Knopp et al., 2016). In future work this could be overcome by use of techniques such as powder x-ray diffraction (PXRD) to confirm whether the powder is amorphous or not.

Addition of PVP in to the spray dried solution resulted in significantly smaller particles for the salbutamol octanoate and phytate formulations; it also resulted in a dimpled appearance to the particles. The sulfate^{P} and octanoate^{P} formulations had a significantly lower MMAD value than their counter ion only powders, but also had a lot more powder retained in the inhaler. The stability of the powders after one month was improved by the

addition of PVP for the octanoate and phytate powders stored at RT and for all the counter ion powders stored at 4^{o}C. This work showed that successful storage, at least short-term, can be achieved for spray dried ion-pair powders. Future work could assess the use of other polymers and the optimal concentration at which they can be incorporated in to the powder for maximum stability, as well as testing the stability of the powder over 3, 6 and 12 months.

Inclusion of l-leucine in the formulations brought about a significant decrease in the MMAD and increase in FPF for the sulfate ion-pair formulation (5.19 μm and 34.93%, respectively). Unexpectedly there was no improvement in aerosolization for the gluconate, octanoate or phytate formulations. This could be as a result of leucine not presenting on the surface of the particle as has been found in other studies (Mangal et al., 2015, Chen et al., 2012). The addition of leucine also resulted in the generation of chemically stable formulations for all counter ions after 1 month at both room temperature and 4^{o}C which would indicate that its addition in to an ion-pair inhaled formulation could be beneficial even if it did not improve the aerosols dispersion.

In Chapter 5 the Calu-3 human bronchial cell line was used as a model of the pulmonary epithelium to assess the compatibility and transport of the ion-pairs (Grainger et al., 2006). Due to the counter ions being present in a great excess in the powder formulations, it was thought to be very important that they are biocompatible with the lung epithelium. All counter ions were found to be well tolerated in the study, with IC_{50} values ranging from 38.1 mg/mL for sodium gluconate to 1.7 mg/mL for sodium octanoate. The excipients were also very well tolerated with IC_{50} values of 41.4 mg/mL for PVP and 88.6 mg/mL for lactose. These data indicated that a 500 fold increase in concentration is needed to reach

the IC_{50} value of sodium octanoate based on the even distribution of a 20 mg dose of powder in the bronchiolar region. All of the counter ions and excipients tested were therefore tolerated well over the concentration that they might be found in the lung, especially considering that the toxicity test performed on discrete cells would be much more sensitive than whole tissue (Korting et al., 1994).

The sulfate, gluconate and phytate ion-pairs all significantly reduced the rate of transport of salbutamol across an air-liquid grown Calu-3 monolayer which indicated that these counter ions could be used to create a system for salbutamol that limits the transport of the drug to prevent rapid clearance whilst prolonging drug action (Patton and Byron, 2007). As none of these ion-pairs altered the partitioning of salbutamol between octanol and water (Chapter 2) it was thought that the reduction in rate of transport was due to a change in the percentage polar surface area or hydrogen bonding capability of the complex compared with the drug alone (Tronde et al., 2008). Although the octanoate ion-pair did alter the partitioning of salbutamol it did not significantly change the transport of salbutamol.

Another method of prolonging the action of salbutamol would be to limit the rate of dissolution (Borghardt et al., 2015). As the octanoate ion-pair was more hydrophobic in the partitioning study and the phytate ion-pair altered the transport and had the highest association constant of any of the ion-pairs these were chosen to assess the dissolution. There was no difference in the dissolution of these powders when compared with the salbutamol base powder. This might be expected as all the powders appear to be amorphous, and amorphous powders rapidly dissolve due to their increased Gibbs free energy (Kanaujia et al., 2015). These data could indicate that spray drying might not be an ideal method to create an inhalable powder if alteration of the dissolution of the powder is

desired as it often produces amorphous powders (Singh and Van den Mooter, 2016). The production of a crystalline inhalable ion-pair powder that could limit the rate of dissolution of a drug could be achieved by using supercritical fluid precipitation techniques or a mechanofusion process (Begat et al., 2009).

The phytate ion-pair was tested *in vivo* in a guinea pig model after administration as a nebulized solution in Chapter 5. Due to experimental limitations the formulations were not given as a dry powder. At the dose given (1.5 μg/kg salbutamol) salbutamol base gave a significantly lower response to histamine challenge at 30, 60 and 120 minutes after drug administration when compared with their response prior to the drug being given. Salbutamol phytate gave a significantly lower response at 60 and 120 minutes post drug administration. A solution of dipotassium phytate, lactose and PVP appeared to give an increased response to histamine at 30 and 120 minutes, which could have been due to a priming effect of phytate on neutrophils leading to a respiratory burst (Eggleton et al., 1991). This demonstrates the importance of counter ion choice in an ion-pairing formulation and also the importance of *in vivo* testing to know how formulations affect whole systems rather than just specific cell lines. Furthermore there was a lot of variability between animals for all 3 of the test solutions (salbutamol base, salbutamol phytate and phytate control). Because of this statistical testing for differences was difficult and further testing would be required to be able to definitively state whether there were significant differences between the test solutions or not. Future work would also administer the ion-pairs as a dry powder to the animals to fully investigate whether the high local concentration achieved by this method could affect the duration of drug action.

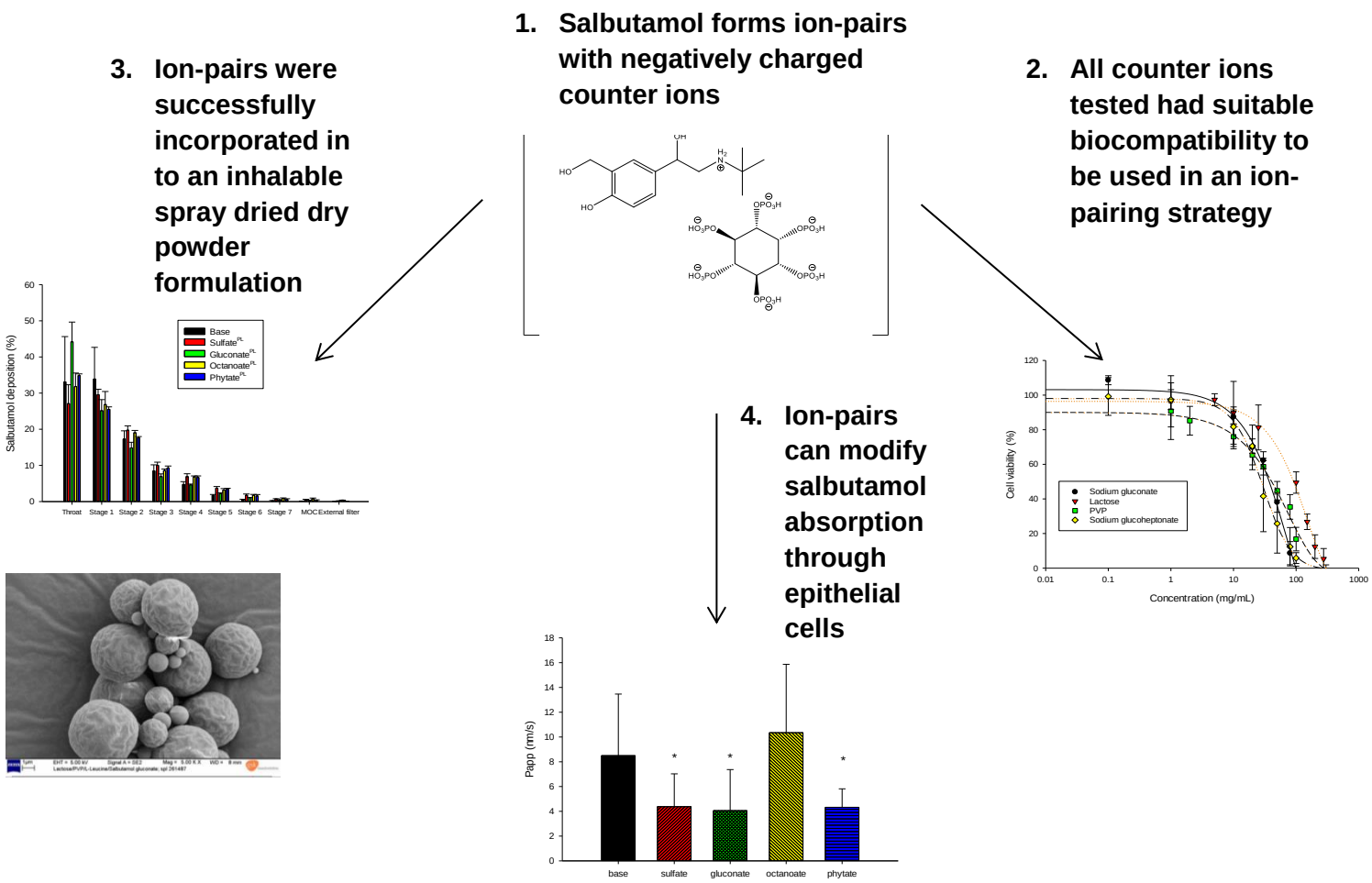

Figure 6.1 - Schematic of main findings of current work. 1. Salbutamol forms ion-pairs with negatively charged counter ions at physiological pH. 2. All the counter ions tested had suitable tolerability levels by epithelial cells. 3. Ion-pairs were incorporated in to a dry powder formulation that was in the inhalable range and stable over 4 weeks. 4. Ion-pairs can modify drug transport through an epithelial cell monolayer

6.1 Future work

The immediate area of work in this thesis that should be expanded is the *in vivo* study. The small number of animals used in the work in Chapter 5 meant that statistical differences could not be found. This was expected as there can be large inter animal variations in response to compounds, salbutamol and histamine, the challenge, and so a larger sample set is needed to fully understand the effect that the ion-pair formulation has in comparison to salbutamol base alone. Furthermore it is important to understand the increased response to histamine seen in some animals given the phytate control solution. Establishing whether this is a real reaction, perhaps due to an allergy, is essential to determining whether phytic acid is a safe and suitable compound to be used in an inhaled formulation. Furthermore, delivery of the ion-pair formulations to animals as a dry powder should be investigated. Although the work in Chapter 5 suggests that there are no differences in dissolution of the ion-pair powders when compared to the base, administration of the ion-pairs in powder form could mean that there is an increased concentration at the site of deposition and so salbutamol and the counter ion would be more likely to be found in ion-pair complex form which could accentuate any prolonged effect the ion-pair has.

In terms of the ion-pair powders, further optimization of the spray drying method could decrease the resulting particle size of the formulations which could augment the fraction of the powder that reaches the lung when inhaled. It would also be beneficial to test the powders using XRPD to confirm their amorphous nature, and stability studies carried out over 12 months could determine the effect of an excess concentration of ions in a powder intended for inhalation over a prolonged period of time. The results in Chapter 4 of this

thesis indicate that the inclusion of l-leucine in the spray dried formulation resulted in an increased stability and better powder flow for many of the ion-pairs tested, however it was excluded from the powders that were tested *in vivo* due to its zwitterionic nature at physiological pH. Further work could examine whether its inclusion in a dry powder formulation would have a deleterious effect on the action of an ion-pair, or perhaps an amino acid could be employed in an ion-pair formulation as both the counter ion for an ion-pair complex and to improve the aerosolisability of the powder.

Finally, the effect of ion-pairing on other inhaled medicines could be tested. In this study salbutamol was used as a model drug as it is a well-documented molecule with a short duration of action. However, one of the draws of an ion-pairing formulation is that physicochemical properties of drug molecules can be altered without the need to change the chemical structure, and taking that further there is a potential to find a counter ion that prolongs the duration of action of multiple different inhaled medicines. Investigation in to the ion-pairing of other inhaled medicines could establish whether the strategy can be used for useful for other molecules and whether there is one counter ion that can bind to and cause the prolonged action of numerous APIs.

6.2 Conclusion

Overall the work in this thesis has shown that ion-pairing charged drug molecules with counter ions have potential for creating a formulation that prolongs drug action in the lungs. Ion-pairs can be formed with a range of small molecules which are well tolerated by lung epithelial cells. These ion-pairs have the potential to alter physicochemical properties of drug molecules such as $logD_{7.4}$ and transport across an epithelial barrier. Ion-pairs can be incorporated in to a dry powder formulation for delivery to the lungs with no negative effects on the aerosolization of the powder. The data in this thesis has also highlighted the importance of counter ion choice, as each ion-pair complex will interact with the lung environment differently and some may not bring about the necessary changes to prolong the duration of drug action. Using ion-pairs is a promising method of prolonging drug action in the lungs and further work in a whole lung or animal model is needed to fully realize this.

References

<Maillard.pdf>.

ADHIKARI, B., HOWES, T., WOOD, B. J. & BHANDARI, B. R. 2009. The effect of low molecular weight surfactants and proteins on surface stickiness of sucrose during powder formation through spray drying. *Journal of Food Engineering,* 94**,** 135-143.

AEROGEN. *Aeroneb Pro System Instruction Manual* [Online]. https://www.aerogen.com/wp-content/uploads/2015/12/Aerogen-Pro-Instruction-Manual_ROW.pdf. [Accessed 19th September 2017].

ALDERIGHI, L., GANS, P., IENCO, A., PETERS, D., SABATINI, A. & VACCA, A. 1999. Hyperquad simulation and speciation (HySS): a utility program for the investigation of equilibria involving soluble and partially soluble species. *Coordination Chemistry Reviews,* 184**,** 311-318.

ARORA, D., SHAH, K. A., HALQUIST, M. S. & SAKAGAMI, M. 2010. In Vitro Aqueous Fluid-Capacity-Limited Dissolution Testing of Respirable Aerosol Drug Particles Generated from Inhaler Products. *Pharmaceutical Research,* 27**,** 786-795.

BAILEY, M. M. & BERKLAND, C. J. 2009. Nanoparticle formulations in pulmonary drug delivery. *Medicinal Research Reviews,* 29**,** 196-212.

BARAHUIE, F., DORNIANI, D., SAIFULLAH, B., GOTHAI, S., HUSSEIN, M. Z., PANDURANGAN, A. K., ARULSELVAN, P. & NORHAIZAN, M. E. 2017. Sustained release of anticancer agent phytic acid from its chitosan-coated magnetic nanoparticles for drug-delivery system. *International Journal of Nanomedicine,* 12**,** 2361-2372.

BECK-BROICHSITTER, M., MERKEL, O. M. & KISSEL, T. 2012. Controlled pulmonary drug and gene delivery using polymeric nano-carriers. *Journal of Controlled Release,* 161**,** 214-224.

BEGAT, P., MORTON, D. A. V., SHUR, J., KIPPAX, P., STANIFORTH, J. N. & PRICE, R. 2009. The Role of Force Control Agents in High-Dose Dry Powder Inhaler Formulations. *Journal of Pharmaceutical Sciences,* 98**,** 2770-2783.

BENBAREK, H., MOUITHYS-MICKALAD, A., DEBY-DUPONT, G., DEBY, C., GRÜLKE, S., NEMMAR, A., LAMY, M. & SERTEYN, D. 1999. High concentrations of histamine stimulate equine polymorphonuclear neutrophils to produce reactive oxygen species. *Inflammation Research,* 48**,** 594-601.

BERGGREN, J. & ALDERBORN, G. 2003a. Effect of Polymer Content and Molecular Weight on the Morphology and Heat- and Moisture-Induced Transformations of Spray-Dried Composite Particles of Amorphous Lactose and Poly(vinylpyrrolidone). *Pharmaceutical Research,* 20**,** 1039-1046.

BERGGREN, J. & ALDERBORN, G. 2003b. Effect of Polymer Content and Molecular Weight on the Morphology and Heat- and Moisture-Induced Transformations of Spray-Dried Composite Particles of Amorphous Lactose and Poly(vinylpyrrolidone). *Pharmaceutical research,* 20**,** 1039 - 1046.

BERGGREN, J. & ALDERBORN, G. 2004. Long-term stabilisation potential of poly(vinylpyrrolidone) for amorphous lactose in spray-dried composites. *European Journal of Pharmaceutical Sciences,* 21**,** 209-215.

BISGAARD, H., O'CALLAGHAN, C. & SMALDONE, G. C. 2001. *Drug Delivery to the Lung*, CRC Press.

BORGHARDT, J. M., WEBER, B., STAAB, A. & KLOFT, C. 2015. Pharmacometric Models for Characterizing the Pharmacokinetics of Orally Inhaled Drugs. *The AAPS Journal,* 17**,** 853-870.

CANNING, B. J. & CHOU, Y. 2008. Using guinea pigs in studies relevant to asthma and COPD. *Pulmonary pharmacology & therapeutics,* 21**,** 702-720.

CARBINATTO, F. M., DE CASTRO, A. D., EVANGELISTA, R. C. & CURY, B. S. F. 2014. Insights into the swelling process and drug release mechanisms from cross-linked pectin/high amylose starch matrices. *Asian Journal of Pharmaceutical Sciences,* 9**,** 27-34.

CASTLE, W., FULLER, R., HALL, J. & PALMER, J. 1993. Serevent nationwide surveillance study: comparison of salmeterol with salbutamol in asthmatic patients who require regular bronchodilator treatment. *BMJ : British Medical Journal,* 306**,** 1034-1037.

CASTRANOVA, V., RABOVSKY, J., TUCKER, J. H. & MILES, P. R. 1988. The alveolar type II epithelial cell: A multifunctional pneumocyte. *Toxicology and Applied Pharmacology,* 93**,** 472-483.

CHEN, K.-H., MUEANNOOM, W., GAISFORD, S. & KETT, V. L. 2012. Investigation into the effect of varying l-leucine concentration on the product characteristics of spray-dried liposome powders. *Journal of Pharmacy and Pharmacology,* 64**,** 1412-1424.

CHEN, L., OKUDA, T., LU, X.-Y. & CHAN, H.-K. 2016. Amorphous powders for inhalation drug delivery. *Advanced Drug Delivery Reviews,* 100**,** 102-115.

CHEN, P.-J., MOORE, T. & NESNOW, S. 2008. Cytotoxic effects of propiconazole and its metabolites in mouse and human hepatoma cells and primary mouse hepatocytes. *Toxicology in vitro,* 22**,** 1476-1483.

CHOW, A. H. L., TONG, H. H. Y., CHATTOPADHYAY, P. & SHEKUNOV, B. Y. 2007. Particle Engineering for Pulmonary Drug Delivery. *Pharmaceutical Research,* 24**,** 411-437.

CHOW, A. H. L., TONG, H. H. Y., CHATTOPADHYAY, P., SHEKUNOV, B. Y. 2007. Particle Engineering for Pulmonary Drug Delivery. *Pharmaceutical research,* 24**,** 411 - 437.

CLARKE, S. W. & PAVIA, D. 2015. *Aerosols and the Lung: Clinical and Experimental Aspects*, Elsevier Science.

CONRADI, R., BURTON, P. & BORCHARDT, R. 1996. Physico-Chemical and Biological Factors that Influence a Drug's Cellular Permeability by Passive Diffusion. *Lipophilicity in drug action and toxicology***,** 233-252.

COOK, R. O., PANNU, R. K. & KELLAWAY, I. W. 2005. Novel sustained release microspheres for pulmonary drug delivery. *Journal of Controlled Release,* 104**,** 79-90.

CRIPPS, A., RIEBE, M., SCHULZE, M. & WOODHOUSE, R. 2000. Pharmaceutical transition to non-CFC pressurized metered dose inhalers. *Respiratory Medicine,* 94**,** S3-S9.

CROWLEY, K., J. & ZOGRAFI, G. 2003. The Effect of Low Concentrations of Molecularly Dispersed Poly(vinylpyrrolidone) on Indomethacin Crystallization from the Amorphous State. *Pharmaceutical research,* 20**,** 1417 - 1422.

CRYAN, S.-A., SIVADAS, N. & GARCIA-CONTRERAS, L. 2007. In vivo animal models for drug delivery across the lung mucosal barrier. *Advanced Drug Delivery Reviews,* 59**,** 1133-1151.

DAHLGREN, C. & KARLSSON, A. 1999. Respiratory burst in human neutrophils. *Journal of Immunological Methods,* 232**,** 3-14.

DAS, P. J., PAUL, P., MUKHERJEE, B., MAZUMDER, B., MONDAL, L., BAISHYA, R., DEBNATH, M. C. & DEY, K. S. 2015. Pulmonary Delivery of Voriconazole Loaded Nanoparticles Providing a Prolonged Drug Level in Lungs: A Promise for Treating Fungal Infection. *Molecular Pharmaceutics,* 12**,** 2651-2664.

DASH, S., MURTHY, P. N., NATH, L. & CHOWDHURY, P. 2010. Kinetic modeling on drug release from controlled drug delivery systems. *Acta Pol Pharm,* 67**,** 217-23.

DAVIES, N. M. & FEDDAH, M. R. 2003. A novel method for assessing dissolution of aerosol inhaler products. *International Journal of Pharmaceutics,* 255**,** 175-187.

DE JONG, W. H. & BORM, P. J. 2008. Drug delivery and nanoparticles: applications and hazards. *International journal of nanomedicine,* 3**,** 133.

DECARLO, P. F., SLOWIK, J. G., WORSNOP, D. R., DAVIDOVITS, P. & JIMENEZ, J. L. 2004. Particle Morphology and Density Characterization by Combined Mobility and Aerodynamic Diameter Measurements. Part 1: Theory. *Aerosol Science and Technology,* 38**,** 1185-1205.

DEKHUIJZEN, P. N. R., VINCKEN, W., VIRCHOW, J. C., ROCHE, N., AGUSTI, A., LAVORINI, F., VAN AALDEREN, W. M. & PRICE, D. 2013. Prescription of inhalers in asthma and COPD: Towards a rational, rapid and effective approach. *Respiratory Medicine,* 107**,** 1817-1821.

DESAI, D., WONG, B., HUANG, Y., YE, Q., GUO, H., HUANG, M. & TIMMINS, P. 2015. Wetting Effects Versus Ion Pairs Diffusivity: Interactions of Anionic Surfactants with Highly Soluble Cationic Drugs and Its Impact on Tablet Dissolution. *Journal of Pharmaceutical Sciences,* 104**,** 2255-2265.

DEZHAMPANAH, H. & CHOKAMI, K. R. 2014. Thermodynamic study of ion-pair interaction between sertraline and eosin Y by spectrophotometry and spectrofluorimetry. *Biomedican Spectroscopy and Imaging,* 3**,** 63 - 71.

DOLOVICH, M. B. & DHAND, R. 2011. Aerosol drug delivery: developments in device design and clinical use. *The Lancet,* 377**,** 1032-1045.

DOUGLAS, J. S., DENNIS, M. W., RIDGWAY, P. & BOUHUYS, A. 1973. AIRWAY CONSTRICTION IN GUINEA PIGS: INTERACTION OF HISTAMINE AND AUTONOMIC DRUGS. *Journal of Pharmacology and Experimental Therapeutics,* 184**,** 169-179.

DRUG, D. P. I. D. 1998. Guidance for industry. *Center for Drug Evaluation and Research (CDER),* 1000.

DURANTIE, E., HUWILER, S., LEROUX, J.-C. & CASTAGNER, B. 2016. A Chiral Phosphoramidite Reagent for the Synthesis of Inositol Phosphates. *Organic Letters,* 18**,** 3162-3165.

DUSS, M., CAPOLICCHIO, S., LINDEN, A., AHMED, N. & JESSEN, H. J. 2015. Desymmetrization of myo-inositol derivatives by lanthanide catalyzed phosphitylation with C2-symmetric phosphites. *Bioorganic & Medicinal Chemistry,* 23**,** 2854-2861.

DYSON, H. J., KOSTIC, M., LIU, J. & MARTINEZ-YAMOUT, M. A. 2008. Hydrogen-Deuterium Exchange Strategy for Delineation of Contact Sites in Protein Complexes. *FEBS letters,* 582**,** 1495-1500.

EDSBÄCKER, S., WOLLMER, P., SELROOS, O., BORGSTRÖM, L., OLSSON, B. & INGELF, J. 2008. Do airway clearance mechanisms influence the local and systemic effects of inhaled corticosteroids? *Pulmonary Pharmacology & Therapeutics,* 21**,** 247-258.

EDWARDS, D. A., BEN-JEBRIA, A. & LANGER, R. 1998. Recent advances in pulmonary drug delivery using large, porous inhaled particles. *Journal of Applied Physiology,* 85**,** 379-385.

EGGLETON, P., PENHALLOW, J. & CRAWFORD, N. 1991. Priming action of inositol hexakisphosphate (InsP6) on the stimulated respiratory burst in human

neutrophils. *Biochimica et Biophysica Acta (BBA) - Molecular Cell Research,* 1094**,** 309-316.

EHRHARDT, C. & KIM, K. J. 2007. *Drug Absorption Studies: In Situ, In Vitro and In Silico Models*, Springer US.

EHRHARDT, C., KNEUER, C., BIES, C., LEHR, C.-M., KIM, K.-J. & BAKOWSKY, U. 2005. Salbutamol is actively absorbed across human bronchial epithelial cell layers. *Pulmonary Pharmacology & Therapeutics,* 18**,** 165-170.

ELHISSI, A. 2017. Liposomes for pulmonary drug delivery: the role of formulation and inhalation device design. *Current pharmaceutical design,* 23**,** 362-372.

ELSHAER, A., HANSON, P. & MOHAMMED, A. R. 2014. A novel concentration dependent amino acid ion pair strategy to mediate drug permeation using indomethacin as a model insoluble drug. *European Journal of Pharmaceutical Sciences,* 62**,** 124-131.

ELVERSSON, J., MILLQVIST-FUREBY, A., ALDERBORN, G. & ELOFSSON, U. 2003. Droplet and particle size relationship and shell thickness of inhalable lactose particles during spray drying. *Journal of Pharmaceutical Sciences,* 92**,** 900-910.

FINK, J. B., COLICE, G. L. & HODDER, R. 2013. Inhaler Devices for Patients with COPD. *COPD: Journal of Chronic Obstructive Pulmonary Disease,* 10**,** 523-535.

FORBES, B. 2000. Human airway epithelial cell lines for in vitro drug transport and metabolism studies. *Pharmaceutical Science & Technology Today,* 3**,** 18-27.

FORBES, B. & EHRHARDT, C. 2005. Human respiratory epithelial cell culture for drug delivery applications. *European Journal of Pharmaceutics and Biopharmaceutics,* 60**,** 193-205.

FORBES, B., HASHMI, N., MARTIN, G. P. & LANSLEY, A. B. 2000. Formulation of inhaled medicines: Effect of delivery vehicle on immortalized epithelial cells. *JOURNAL OF AEROSOL MEDICINE,* 13**,** 281-288.

FORBES, B., SHAH, A., MARTIN, G. P. & LANSLEY, A. B. 2003. The human bronchial epithelial cell line 16HBE14o− as a model system of the airways for studying drug transport. *International Journal of Pharmaceutics,* 257**,** 161-167.

FOSTER, K. A., AVERY, M. L., YAZDANIAN, M. & AUDUS, K. L. 2000. Characterization of the Calu-3 cell line as a tool to screen pulmonary drug delivery. *International Journal of Pharmaceutics,* 208**,** 1-11.

FREIWALD, M., VALOTIS, A., KIRSCHBAUM, A., MCCLELLAN, M., MÜRDTER, T., FRITZ, P., FRIEDEL, G., THOMAS, M. & HÖGGER, P. 2005. Monitoring the initial pulmonary absorption of two different beclomethasone dipropionate aerosols employing a human lung reperfusion model. *Respiratory Research,* 6**,** 21.

GAC, J., SOSNOWSKI, T. R. & GRADOŃ, L. 2008. Turbulent flow energy for aerosolization of powder particles. *Journal of Aerosol Science,* 39**,** 113-126.

GARCIA CONTRERAS, L., SUNG, J., IBRAHIM, M., ELBERT, K., EDWARDS, D. & HICKEY, A. 2015. Pharmacokinetics of inhaled rifampicin porous particles for tuberculosis treatment: insight into rifampicin absorption from the lungs of guinea pigs. *Molecular pharmaceutics,* 12**,** 2642-2650.

GASPAR, M. C., SOUSA, J. J. S., PAIS, A. A. C. C., CARDOSO, O., MURTINHO, D., SERRA, M. E. S., TEWES, F. & OLIVIER, J.-C. 2015. Optimization of levofloxacin-loaded crosslinked chitosan microspheres for inhaled aerosol therapy. *European Journal of Pharmaceutics and Biopharmaceutics,* 96**,** 65-75.

GEISER, M. 2010. Update on macrophage clearance of inhaled micro-and nanoparticles. *Journal of aerosol medicine and pulmonary drug delivery,* 23**,** 207-217.

GIGG, J., GIGG, R., PAYNE, S. & CONANT, R. 1985. (±)-1,2:4,5-Di-O-isopropylidene-myo-inositol. *Carbohydrate Research,* 142**,** 132-134.

GOMBÁS, Á., SZABÓ-RÉVÉSZ, P., KATA, M., REGDON JR, G. & ERŐS, I. 2002. *Journal of Thermal Analysis and Calorimetry,* 68**,** 503-510.

GRAF, E. 1983. Calcium binding to phytic acid. *Journal of agricultural and food chemistry,* 31**,** 851-855.

GRAF, E. & EATON, J. W. 1990. Antioxidant functions of phytic acid. *Free Radical Biology and Medicine,* 8**,** 61-69.

GRAF, E., EMPSON, K. L. & EATON, J. W. 1987. Phytic acid. A natural antioxidant. *Journal of Biological Chemistry,* 262**,** 11647-11650.

GRAINGER, C. I., GREENWELL, L. L., LOCKLEY, D. J., MARTIN, G. P. & FORBES, B. 2006. Culture of Calu-3 Cells at the Air Interface Provides a Representative Model of the Airway Epithelial Barrier. *Pharmaceutical Research,* 23**,** 1482-1490.

GRAINGER, C. I., SAUNDERS, M., BUTTINI, F., TELFORD, R., MEROLLA, L. L., MARTIN, G. P., JONES, S. A. & FORBES, B. 2012. Critical Characteristics for Corticosteroid Solution Metered Dose Inhaler Bioequivalence. *Molecular Pharmaceutics,* 9**,** 563-569.

GUPTA, R. K., GANGOLIYA, S. S. & SINGH, N. K. 2015. Reduction of phytic acid and enhancement of bioavailable micronutrients in food grains. *Journal of Food Science and Technology,* 52**,** 676-684.

HAGHI, M., TRAINI, D., BEBAWY, M. & YOUNG, P. M. 2012. Deposition, Diffusion and Transport Mechanism of Dry Powder Microparticulate Salbutamol, at the Respiratory Epithelia. *Molecular Pharmaceutics,* 9**,** 1717-1726.

HASSOUN, M., HO, S., MUDDLE, J., BUTTINI, F., PARRY, M., HAMMOND, M. & FORBES, B. 2015. Formulating powder–device combinations for salmeterol xinafoate dry powder inhalers. *International Journal of Pharmaceutics,* 490**,** 360-367.

HATANAKA, T., KAMON, T., MORIGAKI, S., KATAYAMA, K. & KOIZUMI, T. 2000. Ion pair skin transport of a zwitterionic drug, cephalexin. *Journal of Controlled Release,* 66**,** 63-71.

HAWKINS, P. T., POYNER, D. R., JACKSON, T. R., LETCHER, A. J., LANDER, D. A. & IRVINE, R. F. 1993. Inhibition of iron-catalysed hydroxyl radical formation by inositol polyphosphates: a possible physiological function for myo-inositol hexakisphosphate. *Biochemical Journal,* 294**,** 929-934.

HEIGHTON, L., SCHMIDT, W. F. & SIEFERT, R. L. 2008. Kinetic and equilibrium constants of phytic acid and ferric and ferrous phytate derived from nuclear

magnetic resonance spectroscopy. *Journal of agricultural and food chemistry,* 56**,** 9543-9547.

HETZEL, M. R. & CLARK, T. J. 1980. Comparison of normal and asthmatic circadian rhythms in peak expiratory flow rate. *Thorax,* 35**,** 732.

HEYDER, J. 2004. Deposition of inhaled particles in the human respiratory tract and consequences for regional targeting in respiratory drug delivery. *Proceedings of the American Thoracic Society,* 1**,** 315-320.

HICKEY, A. J. 2003. *Pharmaceutical Inhalation Aerosol Technology, Second Edition*, Taylor & Francis.

HIGASHIYAMA, M., INADA, K., OHTORI, A. & TOJO, K. 2004. Improvement of the ocular bioavailability of timolol by sorbic acid. *International Journal of Pharmaceutics,* 272**,** 91-98.

HOUTMEYERS, E., GOSSELINK, R., GAYAN-RAMIREZ, G. & DECRAMER, M. 1999. Regulation of mucociliary clearance in health and disease. *European Respiratory Journal,* 13**,** 1177-1188.

HURRELL, R. F. 2003. Influence of vegetable protein sources on trace element and mineral bioavailability. *The Journal of nutrition,* 133**,** 2973S-2977S.

ICRP 1994. Human Respiratory Tract Model for Radiological Protection. *Ann. ICRP,* 24.

IMBODEN, R. & IMANIDIS, G. 1999. Effect of the amphoteric properties of salbutamol on its release rate through a polypropylene control membrane. *European Journal of Pharmaceutics and Biopharmaceutics,* 47**,** 161-167.

ISLAM, N. & CLEARY, M. J. 2012. Developing an efficient and reliable dry powder inhaler for pulmonary drug delivery – A review for multidisciplinary researchers. *Medical Engineering & Physics,* 34**,** 409-427.

JASHNANI, R. N., DALBY, R. N. & BYRON, P. R. 1993. Preparation, Characterization, and Dissolution Kinetics of Two Novel Albuterol Salts. *Journal of Pharmaceutical Sciences,* 82**,** 613-616.

JITENDRA, SHARMA, P. K., BANSAL, S. & BANIK, A. 2011. Noninvasive Routes of Proteins and Peptides Drug Delivery. *Indian Journal of Pharmaceutical Sciences,* 73**,** 367-375.

JORDAN, P. A., KAYSER-BRICKER, K. J. & MILLER, S. J. 2010. Asymmetric phosphorylation through catalytic P(III) phosphoramidite transfer: Enantioselective synthesis of d-myo-inositol-6-phosphate. *Proceedings of the National Academy of Sciences of the United States of America,* 107**,** 20620-20624.

KANAUJIA, P., POOVIZHI, P., NG, W. K. & TAN, R. B. H. 2015. Amorphous formulations for dissolution and bioavailability enhancement of poorly soluble APIs. *Powder Technology,* 285**,** 2-15.

KHADKA, P., RO, J., KIM, H., KIM, I., KIM, J. T., KIM, H., CHO, J. M., YUN, G. & LEE, J. 2014. Pharmaceutical particle technologies: An approach to improve drug solubility, dissolution and bioavailability. *Asian Journal of Pharmaceutical Sciences,* 9**,** 304-316.

KHERSONSKY, S. M. & CHANG, Y.-T. 2002. (±)-1,2:5,6-Di-O-isopropylidene-myo-inositol and (±)-6-O-benzoyl-1,2:4,5-di-O-isopropylidene-myo-inositol: a practical preparation of key intermediates for myo-inositol phosphates. *Carbohydrate Research,* 337**,** 75-78.

KIM, J. N., HAN, S. N. & KIM, H.-K. 2014. Phytic acid and myo-inositol support adipocyte differentiation and improve insulin sensitivity in 3T3-L1 cells. *Nutrition Research,* 34**,** 723-731.

KIPS, J. C. & PAUWELS, R. A. 2001. Long-acting inhaled β2-agonist therapy in asthma. *American journal of respiratory and critical care medicine,* 164**,** 923-932.

KNIGHT, D. A. & HOLGATE, S. T. 2003. The airway epithelium: Structural and functional properties in health and disease. *Respirology,* 8**,** 432-446.

KNOPP, M. M., LÖBMANN, K., ELDER, D. P., RADES, T. & HOLM, R. 2016. Recent advances and potential applications of modulated differential scanning calorimetry (mDSC) in drug development. *European Journal of Pharmaceutical Sciences,* 87**,** 164-173.

KONIETZNY, U. & GREINER, R. 2002. Molecular and catalytic properties of phytate-degrading enzymes (phytases). *International journal of food science & technology,* 37**,** 791-812.

KORTING, H. C., SCHINDLER, S., HARTINGER, A., KERSCHER, M., ANGERPOINTNER, T. & MAIBACH, H. I. 1994. MTT-assay and neutral red release (NRR)-assay: Relative role in the prediction of the irritancy potential of surfactants. *Life Sciences,* 55**,** 533-540.

KWOK, P. C. L. & CHAN, H.-K. 2008. Effect of Relative Humidity on the Electrostatic Charge Properties of Dry Powder Inhaler Aerosols. *Pharmaceutical Research,* 25**,** 277-288.

LABIRIS, N. & DOLOVICH, M. 2003a. Pulmonary drug delivery. Part I: physiological factors affecting therapeutic effectiveness of aerosolized medications. *British journal of clinical pharmacology,* 56**,** 588-599.

LABIRIS, N. & DOLOVICH, M. 2003b. Pulmonary drug delivery. Part II: the role of inhalant delivery devices and drug formulations in therapeutic effectiveness of aerosolized medications. *British journal of clinical pharmacology,* 56**,** 600-612.

LABIRIS, N. R. & DOLOVICH, M. B. 2003c. Pulmonary drug delivery. Part I: Physiological factors affecting therapeutic effectiveness of aerosolized medications. *British Journal of Clinical Pharmacology,* 56**,** 588-599.

LAVORINI, F. & CORBETTA, L. 2008. Achieving asthma control: the key role of inhalers. *Breathe,* 5**,** 120-131.

LETCHER, ANDREW J., SCHELL, MICHAEL J. & IRVINE, ROBIN F. 2008. Do mammals make all their own inositol hexakisphosphate? *Biochemical Journal,* 416**,** 263.

LI, H. Y., SEVILLE, P. C., WILLIAMSON, I. J. & BIRCHALL, J. C. 2005. The use of amino acids to enhance the aerosolisation of spray-dried powders for pulmonary gene therapy. *The Journal of Gene Medicine,* 7**,** 343-353.

LI, Y., ZHANG, Y., LI, P., MI, G., TU, J., SUN, L., WEBSTER, T. J. & SHEN, Y. 2017. Ion-paired pirenzepine-loaded micelles as an ophthalmic delivery system for the treatment of myopia. *Nanomedicine: Nanotechnology, Biology and Medicine,* 13**,** 2079-2089.

LIANG, Z., NI, R., ZHOU, J. & MAO, S. 2015. Recent advances in controlled pulmonary drug delivery. *Drug Discovery Today,* 20**,** 380-389.

LIN, H., YOO, J.-W., ROH, H.-J., LEE, M.-K., CHUNG, S.-J., SHIM, C.-K. & KIM, D.-D. 2005. Transport of anti-allergic drugs across the passage cultured human nasal epithelial cell monolayer. *European Journal of Pharmaceutical Sciences,* 26**,** 203-210.

LIPPMANN, M., YEATES, D. & ALBERT, R. 1980. Deposition, retention, and clearance of inhaled particles. *Occupational and Environmental Medicine,* 37**,** 337-362.

LIU, X., JIN, L., UPHAM, J. W. & ROBERTS, M. S. 2013. The development of models for the evaluation of pulmonary drug disposition. *Expert opinion on drug metabolism & toxicology,* 9**,** 487-505.

LOIRA-PASTORIZA, C., TODOROFF, J. & VANBEVER, R. 2014a. Delivery strategies for sustained drug release in the lungs. *Advanced Drug Delivery Reviews,* 75**,** 81-91.

LOIRA-PASTORIZA, C., TODOROFF, J. & VANBEVER, R. 2014b. Delivery strategies for sustained drug release in the lungs. *Advanced Drug Delivery Reviews,* 75**,** 81-91.

LOUEY, M. D., VAN OORT, M, HICKEY, A, J. 2004. Aerosol dispersion of respirable particles in narrow size distributions produced by jet-milling and spray-drying techniques. *Pharmaceutical research,* 21**,** 1200-1206.

LOZOYA-AGULLO, I., GONZÁLEZ-ÁLVAREZ, I., GONZÁLEZ-ÁLVAREZ, M., MERINO-SANJUÁN, M. & BERMEJO, M. 2016. Development of an ion-pair to improve the colon permeability of a low permeability drug: Atenolol. *European Journal of Pharmaceutical Sciences,* 93**,** 334-340.

MA, J. K. H. & HADZIJA, B. 2012. *Basic Physical Pharmacy*, Jones & Bartlett Learning.

MAA, Y.-F., COSTANTINO, H. R., NGUYEN, P.-A. & HSU, C. C. 1997. The Effect of Operating and Formulation Variables on the Morphology of Spray-Dried Protein Particles. *Pharmaceutical Development and Technology,* 2**,** 213-223.

MAHIUDDIN, S., MINOFAR, B., BORAH, J. M., DAS, M. R. & JUNGWIRTH, P. 2008. Propensities of oxalic, citric, succinic, and maleic acids for the aqueous solution/vapour interface: Surface tension measurements and molecular dynamics simulations. *Chemical Physics Letters,* 462**,** 217-221.

MAHLIN, D., BERGGREN, J., GELIUS, U., ENGSTRÖM, S. & ALDERBORN, G. 2006. The influence of PVP incorporation on moisture-induced surface crystallization of amorphous spray-dried lactose particles. *International Journal of Pharmaceutics,* 321**,** 78-85.

MALCOLMSON, R. J. & EMBLETON, J. K. 1998. Dry powder formulations for pulmonary delivery. *Pharmaceutical Science & Technology Today,* 1**,** 394-398.

MANGAL, S., MEISER, F., TAN, G., GENGENBACH, T., DENMAN, J., ROWLES, M. R., LARSON, I. & MORTON, D. A. V. 2015. Relationship between surface concentration of l-leucine and bulk powder properties in spray dried formulations. *European Journal of Pharmaceutics and Biopharmaceutics,* 94**,** 160-169.

MEEK, J. L., DAVIDSON, F. & HOBBS, F. W. 1988. Synthesis of inositol phosphates. *Journal of the American Chemical Society,* 110**,** 2317-2318.

MEGWA, S. A., CROSS, S. E., BENSON, H. A. E. & ROBERTS, M. S. 2000. Ion-pair Formation as a Strategy to Enhance Topical Delivery of Salicylic Acid. *Journal of Pharmacy and Pharmacology,* 52**,** 919-928.

MORIDANI, M. Y., SIRAKI, A. & O'BRIEN, P. J. 2003. Quantitative structure toxicity relationships for phenols in isolated rat hepatocytes. *Chemico-biological interactions,* 145**,** 213-223.

MYERS, T. R. 2013. The science guiding selection of an aerosol delivery device. *Respiratory care,* 58**,** 1963-1973.

NAINI, V., BYRON, P. R, PHILLIPS, E. M. 1998. Physicochemical stability of crystalline sugars and their spray-dried forms: dependence upon the relative humidity and suitability for use in powder inhalers. *Drug Development and Industrial Pharmacy,* 24**,** 895-909.

NAJAFABADI, A. R., GILANI, K., BARGHI, M. & RAFIEE-TEHRANI, M. 2004. The effect of vehicle on physical properties and aerosolisation behaviour of

disodium cromoglycate microparticles spray dried alone or with l-leucine. *International Journal of Pharmaceutics,* 285**,** 97-108.

NEWMAN, S. P. 1985. Aerosol Deposition Considerations in Inhalation Therapy. *Chest,* 88**,** 152S-160S.

NEWMAN, S. P. 2004. Dry powder inhalers for optimal drug delivery. *Expert opinion on Biological Therapy,* 4**,** 10.

NG, A. W., BIDANI, A. & HEMING, T. A. 2004. Innate Host Defense of the Lung: Effects of Lung-lining Fluid pH. *Lung,* 182**,** 297-317.

NI, R., ZHAO, J., LIU, Q., LIANG, Z., MUENSTER, U. & MAO, S. 2017. Nanocrystals embedded in chitosan-based respirable swellable microparticles as dry powder for sustained pulmonary drug delivery. *European Journal of Pharmaceutical Sciences,* 99**,** 137-146.

NIE, H., MO, H., ZHANG, M., SONG, Y., FANG, K., TAYLOR, L. S., LI, T. & BYRN, S. R. 2015. Investigating the Interaction Pattern and Structural Elements of a Drug–Polymer Complex at the Molecular Level. *Molecular Pharmaceutics,* 12**,** 2459-2468.

OBERDÖRSTER, G. 1988. Lung clearance of inhaled insoluble and soluble particles. *Journal of Aerosol Medicine,* 1**,** 289-330.

OLSSON, B., BONDESSON, E., BORGSTRÖM, L., EDSBÄCKER, S., EIREFELT, S., EKELUND, K., GUSTAVSSON, L. & HEGELUND-MYRBÄCK, T. 2011. Pulmonary drug metabolism, clearance, and absorption. *Controlled pulmonary drug delivery.* Springer.

PALUCH, K. J., TAJBER, L., ELCOATE, C. J., CORRIGAN, O. I., LAWRENCE, S. E. & HEALY, A. M. Solid‐state characterization of novel active pharmaceutical ingredients: Cocrystal of a salbutamol hemiadipate salt with adipic acid (2:1:1) and salbutamol hemisuccinate salt. *Journal of Pharmaceutical Sciences,* 100**,** 3268-3283.

PATEL, A., JONES, S. A., FERRO, A. & PATEL, N. 2009a. Pharmaceutical salts: a formulation trick or a clinical conundrum? *British journal of cardiology,* 16**,** 281-286.

PATEL, A., KEIR, S. D., BROWN, M. B., HIDER, R., JONES, S. A. & PAGE, C. P. 2016. Using Salt Counterions to Modify β2-Agonist Behavior in Vivo. *Molecular Pharmaceutics,* 13**,** 3439-3448.

PATEL, R., PATEL, M. & SUTHAR, A. 2009b. Spray drying technology: an overview. *Indian Journal of Science and Technology,* 2**,** 44-47.

PATTON, J. S. 1996. Mechanisms of macromolecule absorption by the lungs. *Advanced Drug Delivery Reviews,* 19**,** 3-36.

PATTON, J. S., BRAIN, J. D., DAVIES, L. A., FIEGEL, J., GUMBLETON, M., KIM, K.-J., SAKAGAMI, M., VANBEVER, R. & EHRHARDT, C. 2010. The particle has landed—characterizing the fate of inhaled pharmaceuticals. *Journal of Aerosol Medicine and Pulmonary Drug Delivery,* 23**,** S-71-S-87.

PATTON, J. S. & BYRON, P. R. 2007. Inhaling medicines: delivering drugs to the body through the lungs. *Nat Rev Drug Discov,* 6**,** 67-74.

PATTON, J. S., FISHBURN, C. S. & WEERS, J. G. 2004. The Lungs as a Portal of Entry for Systemic Drug Delivery. *Proceedings of the American Thoracic Society,* 1**,** 338-344.

PAYNE, D. K. & WELLIKOFF, A. 2012. Alveolar Structure and Function. *Colloquium Series on Integrated Systems Physiology: From Molecule to Function,* 4**,** 1-76.

PELFRÊNE, A., CAVE, M. R., WRAGG, J. & DOUAY, F. 2017. In Vitro Investigations of Human Bioaccessibility from Reference Materials Using Simulated Lung Fluids. *International Journal of Environmental Research and Public Health,* 14**,** 112.

PHARMACOPEIA, U. S. *601: Aerosols, Nasal Sprays, Metered-Dose Inhalers, and Dry Powder Inhalers* [Online]. http://www.pharmacopeia.cn/v29240/usp29nf24s0_c601_viewall.html. [Accessed 1st August 2017].

PHARMACOPOEIA, B. 2011. *Appendix XII C. Consistency of Formulated Preparations* [Online]. https://wenku.baidu.com/view/4f1b6c350b4c2e3f5727630d. [Accessed 1st August 2017].

PILCER, G. & AMIGHI, K. 2010a. Formulation strategy and use of excipients in pulmonary drug delivery. *International Journal of Pharmaceutics,* 392**,** 1-19.

PILCER, G. & AMIGHI, K. 2010b. Formulation strategy and use of excipients in pulmonary drug delivery. *International Journal of Pharmaceutics,* 392**,** 1-19.

PUGNALONI, L. A., DICKINSON, E., ETTELAIE, R., MACKIE, A. R. & WILDE, P. J. 2004. Competitive adsorption of proteins and low-molecular-weight surfactants: computer simulation and microscopic imaging. *Advances in Colloid and Interface Science,* 107**,** 27-49.

QIAO, J.-Q., LIANG, C., WEI, L.-C., CAO, Z.-M. & LIAN, H.-Z. 2016. Retention of nucleic acids in ion-pair reversed-phase high-performance liquid chromatography depends not only on base composition but also on base sequence. *Journal of Separation Science,* 39**,** 4502-4511.

RABBANI, N. R. & SEVILLE, P. C. 2005. The influence of formulation components on the aerosolisation properties of spray-dried powders. *Journal of Controlled Release,* 110**,** 130-140.

RITGER, P. L. & PEPPAS, N. A. 1987. A simple equation for description of solute release II. Fickian and anomalous release from swellable devices. *Journal of Controlled Release,* 5**,** 37-42.

SAKAGAMI, M. 2006. In vivo, in vitro and ex vivo models to assess pulmonary absorption and disposition of inhaled therapeutics for systemic delivery. *Advanced Drug Delivery Reviews,* 58**,** 1030-1060.

SAMIEI, N., MANGAS-SANJUAN, V., GONZÁLEZ-ÁLVAREZ, I., FOROUTAN, M., SHAFAATI, A., ZARGHI, A. & BERMEJO, M. 2013. Ion-pair strategy for enabling amifostine oral absorption: Rat in situ and in vivo experiments. *European Journal of Pharmaceutical Sciences,* 49**,** 499-504.

SAMIEI, N., SHAFAATI, A., ZARGHI, A., MOGHIMI, H. R. & FOROUTAN, S. M. 2014. Enhancement and in vitro evaluation of amifostine permeation through artificial membrane (PAMPA) via ion pairing approach and mechanistic selection of its optimal counter ion. *European Journal of Pharmaceutical Sciences,* 51**,** 218-223.

SANTUS, P., RADOVANOVIC, D., PAGGIARO, P., PAPI, A., SANDUZZI, A., SCICHILONE, N. & BRAIDO, F. 2015. Why use long acting bronchodilators in chronic obstructive lung diseases? An extensive review on formoterol and salmeterol. *European Journal of Internal Medicine,* 26**,** 379-384.

SCHERLIEß, R. 2011. The MTT assay as tool to evaluate and compare excipient toxicity in vitro on respiratory epithelial cells. *International Journal of Pharmaceutics,* 411**,** 98-105.

SCHMITT, J. & FLEMMING, H.-C. 1998. FTIR-spectroscopy in microbial and material analysis. *International Biodeterioration & Biodegradation,* 41**,** 1-11.

SCULIMBRENE, B. R. & MILLER, S. J. 2001. Discovery of a Catalytic Asymmetric Phosphorylation through Selection of a Minimal Kinase Mimic: A Concise Total Synthesis of d-myo-Inositol-1-Phosphate. *Journal of the American Chemical Society,* 123**,** 10125-10126.

SHARMA, D. 2013. Formulation Development and Evaluation of Fast Disintegrating Tablets of Salbutamol Sulphate for Respiratory Disorders. *ISRN Pharmaceutics,* 2013**,** 8.

SINGH, A. & VAN DEN MOOTER, G. 2016. Spray drying formulation of amorphous solid dispersions. *Advanced Drug Delivery Reviews,* 100**,** 27-50.

SMITH, C. J., PERFETTI, T. A., MORTON, M. J., RODGMAN, A., GARG, R., SELASSIE, C. D. & HANSCH, C. 2002. The Relative Toxicity of Substituted Phenols Reported in Cigarette Mainstream Smoke. *Toxicological Sciences,* 69**,** 265-278.

SMITH, R. M. & MARTELL, A. E. 1989. *Critical stability constants: second supplement*, Springer.

SMYTH, H. D. & HICKEY, A. J. 2011. *Controlled pulmonary drug delivery*, Springer.

SONG, W., CUN, D., XI, H. & FANG, L. 2012. The Control of Skin-Permeating Rate of Bisoprolol by Ion-Pair Strategy for Long-Acting Transdermal Patches. *AAPS PharmSciTech,* 13**,** 811-815.

SONG, Y. H., SHIN, E., WANG, H., NOLAN, J., LOW, S., PARSONS, D., ZALE, S., ASHTON, S., ASHFORD, M., ALI, M., THRASHER, D., BOYLAN, N. & TROIANO, G. 2016. A novel in situ hydrophobic ion pairing (HIP) formulation strategy for clinical product selection of a nanoparticle drug delivery system. *Journal of Controlled Release,* 229**,** 106-119.

SOU, T., FORBES, R. T., GRAY, J., PRANKERD, R. J., KAMINSKAS, L. M., MCINTOSH, M. P. & MORTON, D. A. V. 2016. Designing a multi-component spray-dried formulation platform for pulmonary delivery of biopharmaceuticals: The use of polyol, disaccharide, polysaccharide and synthetic polymer to modify solid-state properties for glassy stabilisation. *Powder Technology,* 287**,** 248-255.

SOU, T., KAMINSKAS, L. M., NGUYEN, T.-H., CARLBERG, R., MCINTOSH, M. P. & MORTON, D. A. V. 2013. The effect of amino acid excipients on morphology and solid-state properties of multi-component spray-dried formulations for pulmonary delivery of biomacromolecules. *European Journal of Pharmaceutics and Biopharmaceutics,* 83**,** 234-243.

SOU, T., MEEUSEN, E. N., DE VEER, M., MORTON, D. A. V., KAMINSKAS, L. M. & MCINTOSH, M. P. 2011. New developments in dry powder pulmonary vaccine delivery. *Trends in Biotechnology,* 29**,** 191-198.

STANLEY, F. E., WARNER, A. M., SCHNEIDERMAN, E. & STALCUP, A. M. 2009. Rapid Determination of Surfactant Critical Micelle Concentrations Using Pressure-Driven Flow with Capillary Electrophoresis Instrumentation. *Journal of chromatography. A,* 1216**,** 8431-8434.

STEER, T. E. & GIBSON, G. R. 2002. The microbiology of phytic acid metabolism by gut bacteria and relevance for bowel cancer. *International Journal of Food Science & Technology,* 37**,** 783-790.

STEIN, S. W. & THIEL, C. G. 2017. The History of Therapeutic Aerosols: A Chronological Review. *Journal of aerosol medicine and pulmonary drug delivery,* 30**,** 20-41.

STELLMAN, J. M. & OFFICE, I. L. 1998. *Encyclopaedia of Occupational Health and Safety: The body, health care, management and policy, tools and approaches*, International Labour Office.

STUART, B. O. 1984. Deposition and clearance of inhaled particles. *Environmental Health Perspectives,* 55**,** 369-390.

SUNG, J. C., PULLIAM, B. L. & EDWARDS, D. A. 2007. Nanoparticles for drug delivery to the lungs. *Trends in Biotechnology,* 25**,** 563-570.

SWAMINATHAN, J. & EHRHARDT, C. 2011. Liposomes for Pulmonary Drug Delivery. *In:* SMYTH, H. D. C. & HICKEY, A. J. (eds.) *Controlled Pulmonary Drug Delivery.* New York, NY: Springer New York.

TAN, Z., ZHANG, J., WU, J., FANG, L. & HE, Z. 2009. The Enhancing Effect of Ion-pairing on the Skin Permeation of Glipizide. *AAPS PharmSciTech,* 10**,** 967.

TAYLOR, G. 1990. The absorption and metabolism of xenobiotics in the lung. *Advanced Drug Delivery Reviews,* 5**,** 37-61.

TAYLOR, K. M. & NEWTON, J. M. 1992. Liposomes for controlled delivery of drugs to the lung. *Thorax,* 47**,** 257-259.

TAYLOR, L. S. & ZOGRAFI, G. 1998. Sugar–polymer hydrogen bond interactions in lyophilized amorphous mixtures. *Journal of Pharmaceutical Sciences,* 87**,** 1615-1621.

TENA, A. F. & CLARÀ, P. C. 2012. Deposition of inhaled particles in the lungs. *Archivos de Bronconeumología (English Edition),* 48**,** 240-246.

THORSSON, L., EDSBÄCKER, S., KÄLLÉN, A. & LÖFDAHL, C.-G. 2001. Pharmacokinetics and systemic activity of fluticasone via Diskus® and pMDI, and of budesonide via Turbuhaler®. *British Journal of Clinical Pharmacology,* 52**,** 529-538.

TRONDE, A. 2002. *Pulmonary drug absorption: in vitro and in vivo investigations of drug absorption across the lung barrier and its relation to drug physicochemical properties.* Acta Universitatis Upsaliensis.

TRONDE, A., BOSQUILLON, C. & FORBES, B. 2008. The isolated perfused lung for drug absorption studies. *Biotechnology Pharmaceutical Aspects VII,* 7**,** 135-163.

TROTTA, M., UGAZIO, E., PEIRA, E. & PULITANO, C. 2003. Influence of ion pairing on topical delivery of retinoic acid from microemulsions. *Journal of Controlled Release,* 86**,** 315-321.

UCHENNA AGU, R., IKECHUKWU UGWOKE, M., ARMAND, M., KINGET, R. & VERBEKE, N. 2001. The lung as a route for systemic delivery of therapeutic proteins and peptides. *Respiratory Research,* 2**,** 1-12.

UNWALLA, H. J., HORVATH, G., ROTH, F. D., CONNER, G. E. & SALATHE, M. 2012. Albuterol Modulates Its Own Transepithelial Flux via Changes in Paracellular Permeability. *American Journal of Respiratory Cell and Molecular Biology,* 46**,** 551-558.

VALENTIN, J. 2002. Basic anatomical and physiological data for use in radiological protection: reference values. *Annals of the ICRP,* 32**,** 1-277.

VAN GOLDE, L. M., BATENBURG, J. J. & ROBERTSON, B. 1988. The pulmonary surfactant system: biochemical aspects and functional significance. *Physiological Reviews,* 68**,** 374-455.

VAN MEERLOO, J., KASPERS, G. J. L. & CLOOS, J. 2011. Cell Sensitivity Assays: The MTT Assay. *In:* CREE, I. A. (ed.) *Cancer Cell Culture: Methods and Protocols.* Totowa, NJ: Humana Press.

VAUGHN, J. M., MCCONVILLE, J. T., BURGESS, D., PETERS, J. I., JOHNSTON, K. P., TALBERT, R. L. & WILLIAMS, R. O. 2006. Single dose and multiple dose studies of itraconazole nanoparticles. *European journal of pharmaceutics and biopharmaceutics,* 63**,** 95-102.

VEHRING, R. 2008. Pharmaceutical Particle Engineering via Spray Drying. *Pharmaceutical Research,* 25**,** 999-1022.

VUCENIK, I. & SHAMSUDDIN, A. M. 2003. Cancer inhibition by inositol hexaphosphate (IP6) and inositol: from laboratory to clinic. *The Journal of nutrition,* 133**,** 3778S-3784S.

WANG, Y.-B., WATTS, A. B., PETERS, J. I., LIU, S., BATRA, A. & WILLIAMS, R. O. 2014. In Vitro and In Vivo Performance of Dry Powder Inhalation Formulations: Comparison of Particles Prepared by Thin Film Freezing and Micronization. *AAPS PharmSciTech,* 15**,** 981-993.

WARTEWIG, S. & NEUBERT, R. H. H. 2005. Pharmaceutical applications of Mid-IR and Raman spectroscopy. *Advanced Drug Delivery Reviews,* 57**,** 1144-1170.

WATTS, A. B., CLINE, A. M., SAAD, A. R., JOHNSON, S. B., PETERS, J. I. & WILLIAMS, R. O. 2010. Characterization and pharmacokinetic analysis of tacrolimus dispersion for nebulization in a lung transplanted rodent model. *International Journal of Pharmaceutics,* 384**,** 46-52.

WERMUTH, C. G. 2011. *The Practice of Medicinal Chemistry*, Elsevier Science.

WEST, J. B. 2008. *Respiratory Physiology: The Essentials*, Wolters Kluwer Health/Lippincott Williams & Wilkins.

WESTON, A. & BROWN, P. R. 1997. *High Performance Liquid Chromatography & Capillary Electrophoresis: Principles and Practices*, Elsevier Science.

WIDDICOMBE, J. H. 2002. Regulation of the depth and composition of airway surface liquid. *Journal of Anatomy,* 201**,** 313-318.

WIDDICOMBE, J. H. & WIDDICOMBE, J. G. 1995. Regulation of human airway surface liquid. *Respiration Physiology,* 99**,** 3-12.

WILLIS, L., HAYES, D. & MANSOUR, H. M. 2012. Therapeutic Liposomal Dry Powder Inhalation Aerosols for Targeted Lung Delivery. *Lung,* 190**,** 251-262.

WIRTH, D. D., BAERTSCHI, S. W., JOHNSON, R. A., MAPLE, S. R., MILLER, M. S., HALLENBECK, D. K. & GREGG, S. M. 1998. Maillard reaction of lactose and fluoxetine hydrochloride, a secondary amine. *Journal of Pharmaceutical Sciences,* 87**,** 31-39.

WONG, J., KWOK, P. C. L., NOAKES, T., FATHI, A., DEHGHANI, F. & CHAN, H.-K. 2014. Effect of Crystallinity on Electrostatic Charging in Dry Powder Inhaler Formulations. *Pharmaceutical Research,* 31**,** 1656-1664.

WU, L., MIAO, X., SHAN, Z., HUANG, Y., LI, L., PAN, X., YAO, Q., LI, G. & WU, C. 2014. Studies on the spray dried lactose as carrier for dry powder inhalation. *Asian Journal of Pharmaceutical Sciences,* 9**,** 336-341.

YAMAMOTO, H., KUNO, Y., SUGIMOTO, S., TAKEUCHI, H. & KAWASHIMA, Y. 2005. Surface-modified PLGA nanosphere with chitosan improved pulmonary delivery of calcitonin by mucoadhesion and opening of the intercellular tight junctions. *Journal of controlled Release,* 102**,** 373-381.

YANG, J. Z., YOUNG, A. L., CHIANG, P. C., THURSTON, A. & PRETZER, D. K. 2008a. Fluticasone and budesonide nanosuspensions for pulmonary delivery: preparation, characterization, and pharmacokinetic studies. *Journal of pharmaceutical sciences,* 97**,** 4869-4878.

YANG, W., PETERS, J. I. & WILLIAMS, R. O. 2008b. Inhaled nanoparticles—A current review. *International Journal of Pharmaceutics,* 356**,** 239-247.

YEATES, D. B., STURGESS, J. M., KAHN, S. R., LEVISON, H. & ASPIN, N. 1976. Mucociliary transport in trachea of patients with cystic fibrosis. *Archives of Disease in Childhood,* 51**,** 28-33.

YU, J., WONG, J., UKKONEN, A., KANNOSTO, J. & CHAN, H.-K. 2017. Effect of Relative Humidity on Bipolar Electrostatic Charge Profiles of dry Powder Aerosols. *Pharmaceutical Research***,** 1-9.

ZENG, X. M., MARTIN, G. P. & MARRIOTT, C. 1995. The controlled delivery of drugs to the lung. *International journal of pharmaceutics,* 124**,** 149-164.

ZHOU, H., LENGSFELD, C., CLAFFEY, D. J., RUTH, J. A., HYBERTSON, B., RANDOLPH, T. W., NG, K. Y. & MANNING, M. C. 2002. Hydrophobic Ion Pairing of Isoniazid Using a Prodrug Approach. *Journal of Pharmaceutical Sciences,* 91**,** 1502-1511.

ZHOU, J. R. & ERDMAN JR, J. W. 1995. Phytic acid in health and disease. *Critical Reviews in Food Science & Nutrition,* 35**,** 495-508.